The role of microRNAs in T helper cell function and differentiation

Atalar, Kerem Benjamin

Awarding institution:
King's College London

The role of microRNAs in T helper cell function and differentiation

A thesis submitted to the School of Medicine at King's College London for the degree of Doctor of Philosophy

By

Kerem Benjamin Atalar

Lord Lab

Department of Experimental Immunobiology

MRC Centre for Transplantation

5th Floor, Tower Wing,

Guy's Hospital

Great Maze Pond

London SE1 9RT

February 2012

Declaration

The work presented in this thesis is my own, and all experiments, except where acknowledged in the text, were performed by myself.

Kerem B. Atalar

Abstract

microRNAs are a class of short RNA molecules that mediate post-transcriptional regulation of gene expression, thereby controlling cell fate. The importance of microRNAs in normal T helper cell function has been highlighted by recent studies in which T cells that are globally deficient in microRNAs exhibit major abnormalities of homeostasis and differentiation. However the identities of those individual microRNAs that are required for normal T cell function remain unclear, and there is a lack of data regarding the cellular processes that are regulated by microRNAs in T cells.

This thesis examines the hypothesis that specific microRNAs are of critical importance for normal T helper cell function and differentiation. microRNA expression was profiled in highly-polarised T helper cell subsets, and analysed in order to detect differentially expressed microRNAs. A candidate microRNA, mir-142, was selected on the basis of these data for further functional analysis. Novel constitutive and conditional mir-142-deficient mice were generated and systematically analysed for T cell functional defects. mir-142 deficiency was found to profoundly affect T cell homeostasis, with a significant reduction in the size of the peripheral T cell pool and impaired proliferation and survival *in vivo*. T helper cell differentiation was also affected, with default adoption of a Th1 phenotype and impaired stability of non-Th1 lineages. Analysis of predicted targets revealed that both retinoic acid receptor (RAR)-γ and T-bet are targets of mir-142 that are functionally responsible for these abnormalities. Deficiency of mir-142 in T helper cells was also found to prevent the development of disease in a T cell-mediated colitis model. In summary, this work identifies mir-142 as a critically important microRNA for normal T helper cell function and differentiation. Future

studies will continue to analyse the function of mir-142 and may investigate this microRNA as a potential therapeutic target in immune-mediated disease.

Dedication

This thesis is dedicated to my family, without whom it would not have been possible. In particular my wife, Beryl, has given me endless support and love at every stage, and our daughter, Olivia, continues to be a source of great inspiration and joy.

Acknowledgements

There are a number of people who have helped me throughout the course of my research and the writing of this thesis, without whom I would not have been able to complete it. Firstly, I would like to thank my supervisors, Professor Graham Lord and Professor Giovanna Lombardi for all their invaluable advice and guidance, and for giving me the opportunity to carry out this work. I have been privileged to study such an interesting topic with such excellent support. In addition, I am indebted to Professor Robert Lechler for his help with my fellowship application, to Professor Steven Sacks for his initial supervision of my academic placement, and to Mr. Jonathon Olsburgh, consultant surgeon at Guy's Hospital, for his advice and mentorship regarding the clinical aspects of my career during this time. I would also like to thank those individuals who assessed the progress of my PhD, namely Dr. Richard Jenner, Dr. Paul Lavender and Dr. Linda Klavinskis.

I have been fortunate to work closely with many talented and dedicated individuals in the pursuit of this project. Ian Jackson, Maria Hernandez-Fuentes and Esperanza Perucha provided many hours of teaching in various laboratory techniques and concepts. Ellen Marks, Nick Powell, Arnulf Hertweck, Refik Gökmen, Emilie Stolarczyk, Behdad Afzali, Rong Dong and Yuqian Ma all also contributed help, guidance and support with specific aspects of the project. Countless other members of the Lord, Lombardi and other laboratories also gave assistance. In addition, I am deeply grateful to Mr. David Vilanova of Cepheid Inc., for his collaboration in performing microRNA microarrays and advice regarding bioinformatics.

I would also like to thank the Medical Research Council and Kidney Research UK for their generous funding of this project through my Clinical Research Training Fellowship (grant reference G0800413).

Finally, I am forever indebted to my parents, Lynne and Tekin Atalar, my wife Beryl and our daughter Olivia, my sisters Sara, Sophie and Emily and my grandmother Vi for their love and support during this intense period of study.

Table of Contents

List of Figures

List of Tables

Standard Annotations

Conventional gene nomenclature is used throughout this thesis as follows:

Symbol	Style	Example
Human gene	Uppercase, italicised	*TBX21*
Human protein	Uppercase, normal	TBX21
Mouse gene	First letter uppercase, remaining letters lowercase, italicised	*Tbx21*
Mouse protein	Uppercase, normal	TBX21

microRNA nomenclature is as follows, based on miRBase naming guidelines:

miRNA species	Description	Example
miRNA gene	Genomic locus of a miRNA	mir-121
miRNA primary transcript	Primary RNA transcript	pri-mir-121
Precursor miRNA	Precursor transcript formed following Drosha processing	pre-mir-121
Mature miRNA	Mature miRNA following Dicer processing (where only one arm of the precursor hairpin is stable)	miR-121
Mature miRNA (where mature miRNAs arise from both 3p and 5p arms of hairpin)	Mature miRNAs following Dicer processing (where both arms of precursor hairpin are stable)	miR-121-3p miR-121-5p
Paralogous miRNA species (identical sequence)	Copies of identical miRNAs exist at multiple genomic locations	mir-121-1 mir-121-2
Paralogous miRNA species (broadly similar sequences)	miRNAs with broadly similar sequences that exist at multiple genomic locations	mir-121a mir-121b

List of Abbreviations

AhR	Aryl hydrocarbon receptor
APC	Antigen presenting cell
BSA	Bovine serum albumin
CD	Cluster of differentiation
ChIP	Chromatin immunoprecipitation
DC	Dendritic cell
DMEM	Dulbecco's Modified Eagle Medium
EDTA	Ethylene-diamine-tetraacetic acid
ELISA	Enzyme-linked immunosorbent assay
FACS	Fluorescence-activated cell sorting
FCS	Fetal calf serum
FITC	Fluorescein isothiocyanate
FoxP3	Forkhead Box P3
GATA-3	GATA-binding protein 3
GFP	Green fluorescent protein
HLA	Human leucocyte antigen
IFN	Interferon
IL	Interleukin
IRF	Interferon-regulatory factor
iTreg	Induced regulatory T cell
LB	Luria-Bertani (broth)
MHC	Major histocompatibility complex
MSCV	Murine stem cell virus
NK	Natural killer
NKT	Natural killer T cell
nTreg	Naturally occurring regulatory T cell
PBS	Phosphate-buffered saline
PCR	Polymerase chain reaction
PE	Phycoerythrin
PMA	Phorbol 12-myristate 13-acetate
qRT-PCR	Quantitative real-time polymerase chain reaction
RAG1	Recombination activating gene 1
RAR	Retinoic acid receptor
RISC	RNA-induced silencing complex
ROR	RAR-related orphan receptor
RPMI	Roswell Park Memorial Institute medium
RV	Retrovirus
SEM	Standard error of the mean
STAT	Signal transducer and activator of transcription
TAE	Tris-acetate-EDTA
T-bet	T-box expressed in T cells
TCR	T cell receptor
TGF-β	Transforming growth factor β
Th	T helper
Thp	Pluripotent naïve T helper cell
TNF-α	Tumour necrosis factor α

1. Introduction

1.1. Biology of microRNAs

MicroRNAs (miRNAs) are short non-coding RNAs that post-transcriptionally regulate the expression of target genes. During the two decades that have followed their discovery, much progress has been made in understanding both the biology of miRNA expression and some of the ways in which miRNAs function. The high inter-species conservation of miRNAs reflects their biological importance, and a large number of recent studies in human diseases have demonstrated the biomarker potential of measuring miRNA expression levels. Yet many questions still need to be addressed, not least uncovering the multiple functional roles that are likely to exist for many individual miRNAs. This thesis principally concerns the role of miRNAs in T helper cells, however the underlying mechanisms of miRNA function are generally relevant to all mammalian cell types; therefore a review of current knowledge of fundamental miRNA biology is presented here.

1.1.1. History of microRNA discovery

The first description of a miRNA was made by the Ambros and Ruvkun laboratories in 1993, who collaborated to identify *lin-4* as a critical regulator of the *lin-14* gene in the nematode worm *Caenorhabditis elegans* (Lee et al., 1993; Wightman et al., 1993). In the years prior to these reports, it had been demonstrated that null mutations of *lin-4* and *lin-14*, which are required for normal *C. elegans* larval development, produced opposite phenotypes, and that dominant mutations in *lin-14* reproduced the *lin-4* null mutant phenotype (Lee et al., 2004a). In the course of their investigations, it became clear that

lin-14 was regulated through sequences in its 3' untranslated terminal region (3' UTR), and that *lin-4* was capable of inhibiting *lin-14* protein expression (Wightman et al., 1991; Arasu et al., 1991). Meticulous cloning and sequence analysis of *lin-4* led to the unexpected discovery that this gene gave rise to two novel, short, non-coding RNA molecules. Interestingly, the ~20 nucleotide (nt), shorter fragment was generated from the longer, ~60nt fragment, which was predicted to form a hairpin secondary structure. Both groups then simultaneously noted the breakthrough observation that the *lin-4* sequence exhibits antisense complementarity to multiple regulatory sequences in the *lin-14* 3' UTR. Whilst it was not termed as such at the time, *lin-4* was the first miRNA to be described, and it is now clear that these seminal reports laid the groundwork for future understanding of miRNA biology.

Throughout the years that followed the discovery of *lin-4*-mediated suppression, the field of RNA interference (RNAi) continued to emerge and develop. In 1998, the ability of synthetic double-stranded RNA (dsRNA) molecules to specifically regulate target gene expression based on sequence complementarity was described (Fire et al., 1998). Then, in 1999, it was shown that short RNA species of approximately 25nt in length were generated from longer synthetic and viral dsRNA templates, and were capable of mediating post-transcriptional gene silencing in plants (Hamilton and Baulcombe, 1999). With time, these short dsRNA templates began to be referred to as short interfering RNAs (siRNAs).

The next miRNA to be identified was *let-7*, a 21nt miRNA that was shown in 2000 to target the *C. elegans* gene *lin-41* (Reinhart et al., 2000). Importantly, *let-7* differs from *lin-4* on account of its extensive conservation between species, including in humans (Pasquinelli et al., 2000). In light of these reports, it was hypothesized that a common

mechanism could be responsible for the processing and function of both synthetic exogenous dsRNAs and endogenous siRNAs/miRNAs, and that these mechanisms may be conserved across a range of vertebrate and invertebrate species.

While efforts continued to identify these fundamental mechanisms of RNAi, many groups embarked on a search for other examples of endogenous miRNAs. In 2001, the Ambros, Bartel, and Tuschl labs simultaneously published the details of almost 100 newly-identified miRNAs (Lee and Ambros, 2001; Lau et al., 2001; Lagos-Quintana et al., 2001). It was also demonstrated that many of these miRNAs are highly conserved between species. This established beyond doubt that *lin-4* and *let-7* were not isolated examples of endogenous RNA interference, but were members of a large class of non-coding RNAs that exists in a wide range of organisms.

In the course of these pioneering research efforts, a number of new techniques (such as small RNA Northern blotting) had been optimised for the cloning and validation of miRNAs. With these new technologies in hand, an ever-increasing number of researchers began to hunt for more members of the miRNA family. It therefore became increasingly challenging to curate and organise the growing number of validated miRNAs. This process was facilitated by improved standardisation of miRNA nomenclature and the introduction of the miRNA sequence database miRBase (http://www.mirbase.org), which developed from the Rfam miRNA Registry (Ambros et al., 2003; Griffiths-Jones et al., 2003; Griffiths-Jones, 2004; Griffiths-Jones et al., 2006). In recent years, deep sequencing technology has largely supplanted traditional cloning methods for the purpose of large-scale miRNA discovery. This has led to a rapid increase in the number of validated miRNAs being registered with the miRBase

database, while the last decade has seen an exponential rise in miRNA-related publication numbers (Figure 1.1) (Kozomara and Griffiths-Jones, 2011).

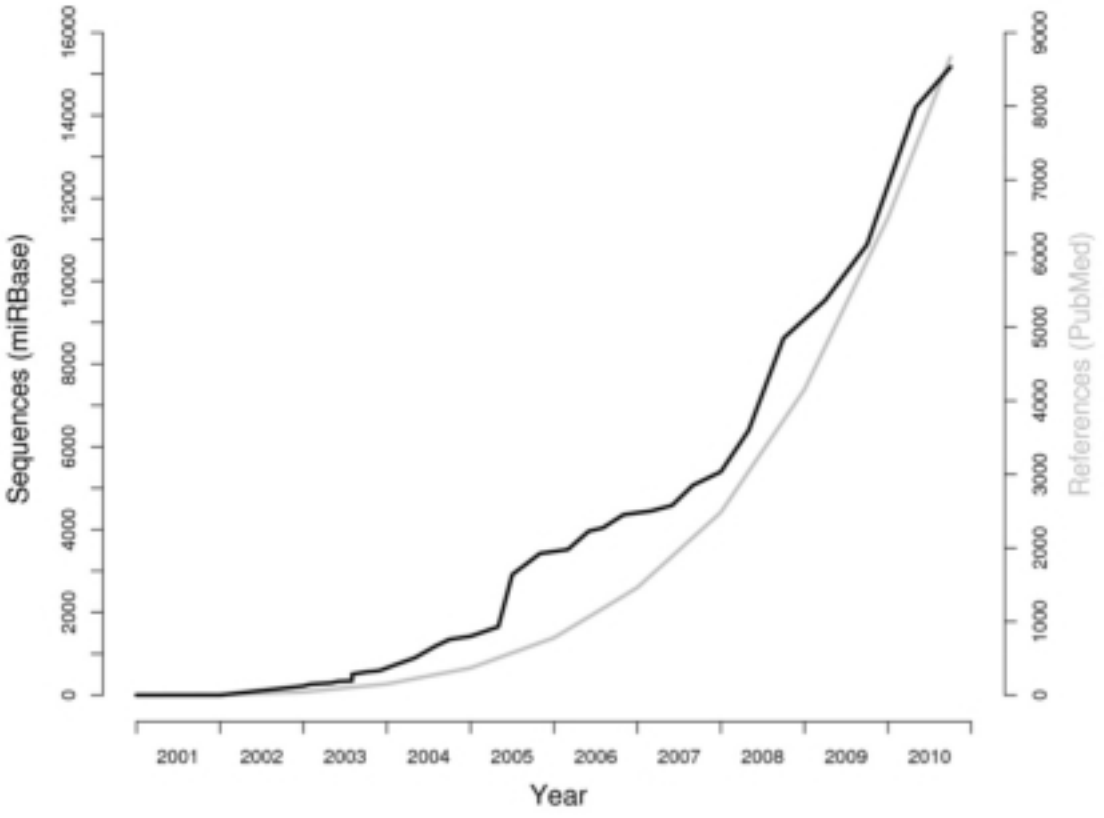

Figure 1.1 "Growth of the miRBase sequence archive (black) and the microRNA publication record (PubMed entries that reference the term 'microRNA', grey)". Reproduced with permission from Oxford University Press (Kozomara and Griffiths-Jones, 2011).

In only ten years, the research community has moved from knowledge of just two miRNAs to an expanding database of over 16,000 miRNAs in more than 150 species (miRBase release 17; April 2011). This clearly presents an enormous challenge for scientists to identify and characterise those miRNAs that are of principal interest in improving our understanding of biological processes in both health and disease.

1.1.2. Biogenesis of miRNAs

Mature miRNAs are single-stranded RNA molecules of ~22nt in length, however these short molecules are not synthesized directly. Instead they are produced by a sequence of critical enzymatic processing events that follow initial transcription (summarised in Figure 1.2).

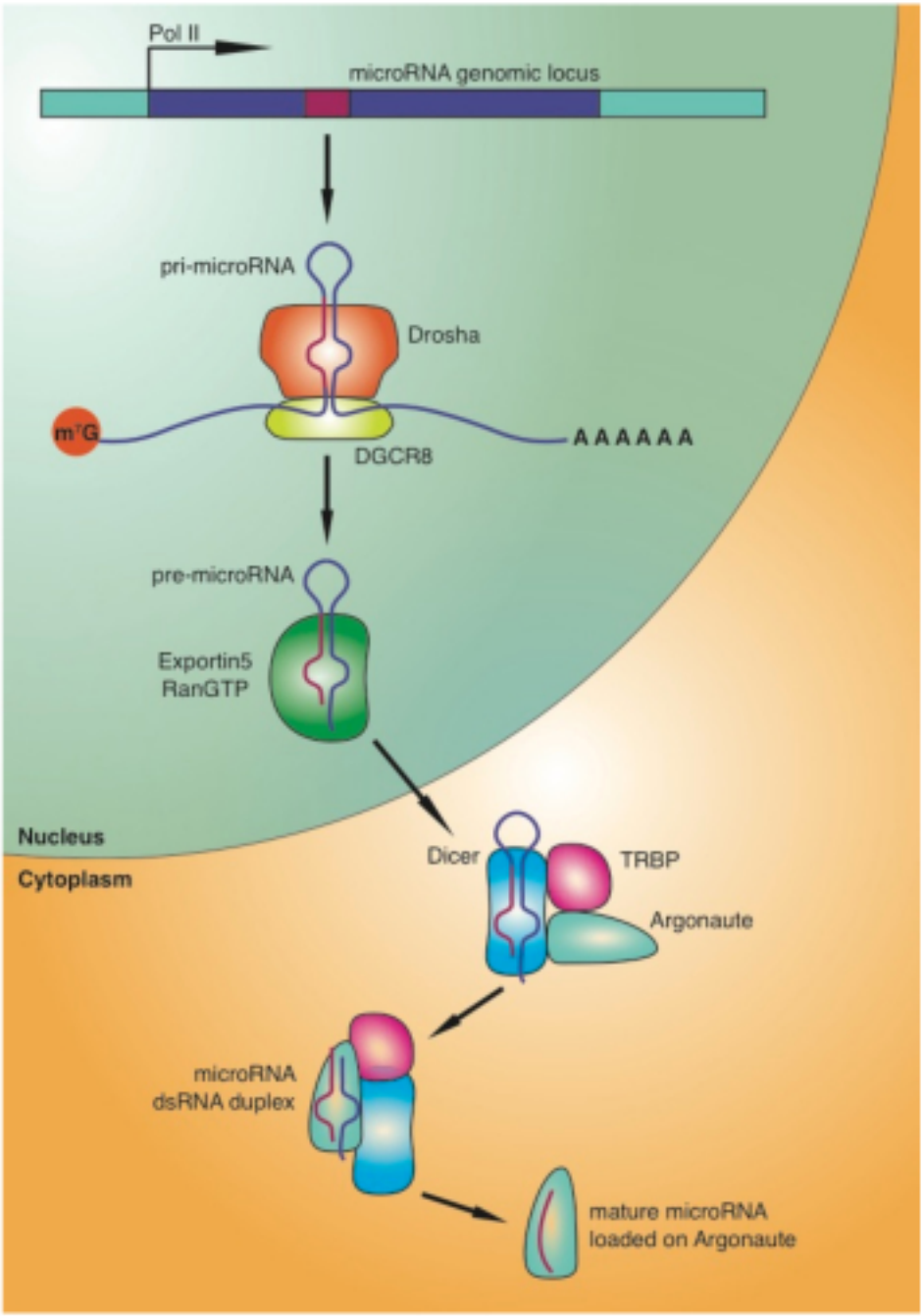

Figure 1.2 Biogenesis of typical mammalian miRNAs. Initial transcription is performed by RNA polymerase II and produces the long primary transcript (pri-miRNA). This is cropped by Drosha in the nucleus to produce a hairpin precursor (pre-miRNA), which is exported to the cytoplasm by Exportin V-Ran GTP. In the cytoplasm, the pre-miRNA is cleaved again by Dicer, which is found as part of a complex including Argonaute protein and HIV TAR RNA-binding protein (TRBP). This produces a dsRNA duplex, one strand of which is then loaded onto an Argonaute protein that goes on to form part of the RNA-induced silencing complex (RISC). Figure adapted from (Krol et al., 2010b). Reproduced with permission from Nature Publishing Group.

Transcription of the majority of miRNAs is performed by RNA polymerase II (Lee et al., 2004b; Cai et al., 2004), although a small group of miRNAs can be transcribed by RNA polymerase III (Borchert et al., 2006). Many miRNAs have been found to be encoded as multiple isoforms (paralogues) throughout the genome; these are designated by a suffixed numeral if the sequences are identical or a suffixed letter if sequences are closely related. As a result, these paralogous miRNAs can be transcribed independently and under the control of different regulatory elements. Conversely, approximately half of all mammalian miRNAs are located within clusters of multiple miRNAs (Kim et al., 2009), and these clusters may be transcribed together as part of a single polycistronic transcription unit (TU) (Lee et al., 2002). Individual miRNAs or polycistronic miRNA TUs may be derived from purely non-coding transcripts or located within protein coding genes, and can arise from both introns and exons.

Initial transcripts, termed miRNA primary transcripts (pri-miRNAs) range in length from a few hundred bases to several kilobases. As with all RNA transcripts, these molecules take on secondary and higher-order structural conformations, including the hairpin stem-loop structures that contain miRNAs. These hairpins are excised from primary transcripts by the RNAse III-type endonuclease Drosha (Lee et al., 2003). This process takes place in the nucleus, and requires as a co-factor the dsRNA-binding protein DiGeorge syndrome critical region gene 8 (DGCR8). Together these two proteins form the Microprocessor complex, which is responsible for the processing of pri-miRNAs in most cases (Gregory et al., 2004). The complex binds and cleaves the dsRNA on both the 3' and 5' ends of the stem loop, to produce a precursor miRNA (pre-miRNA) stem-loop hairpin, which is approximately 65nt in length and possesses a 2nt 3' overhang. It is worth noting here that a small group of non-coding RNAs, termed

mirtrons, are alternate miRNA precursors that do not require Drosha processing. Instead, they are found in introns and are formed by splicing and subsequent debranching of the excised lariat-shaped intron into an RNA molecule that can be trimmed to produce a dsRNA stem-loop hairpin structure (Ruby et al., 2007; Okamura et al., 2007; Berezikov et al., 2007). However, the overwhelming majority of mammalian mature miRNAs are likely to be processed from pri-miRNAs via the canonical Drosha-dependent pathway.

The pre-miRNA is exported from the nucleus to the cytoplasm by a complex consisting of exportin 5 (EXP5) and GTP-bound Ran (RanGTP) (Lund et al., 2004; Bohnsack et al., 2004; Yi et al., 2005). Hydrolysis of bound GTP then releases the pre-miRNA. This undergoes a further enzymatic cleavage step mediated by the RNAse III-type endonuclease Dicer, which excises the loop structure to produce a dsRNA duplex with 2nt 3' overhangs at both ends (Bernstein et al., 2001; Grishok et al., 2001; Hutvágner et al., 2001; Ketting et al., 2001). The result of this process is that the two strands of the dsRNA duplex have been cleaved to their final mature miRNA sequence, ready to be incorporated into the functional unit of miRNA-mediated gene silencing, the RNA-induced silencing complex (RISC).

1.1.3. Function

The term RISC encompasses a variety of molecular complexes that share certain similarities. At the heart of the RISC is a small regulatory RNA, which may be an endogenous miRNA, and which is critical for target specificity. In addition, Argonaute family proteins are required in order to bind this small RNA molecule and position it in a way that facilitates target recognition. Only single-stranded RNA molecules are loaded into the RISC, and so the dsRNA duplex generated following Dicer processing

must be separated into two strands. Typically, one strand accumulates at higher levels of abundance whilst the other may be preferentially degraded; this lower-abundance strand has been termed the passenger strand, star species or miRNA*. Whilst early cloning experiments failed to detect many of these star species, it has recently been shown that approximately 4% of all human and mouse miRNA reads generated by next-generation sequencing methods represent star species (Yang et al., 2011). Of note, a minority of miRNA duplexes give rise to two single-strand mature miRNAs with similar levels of abundance (examples include miR-142-3p/miR-142-5p and miR-17/miR-17*).

Two major mechanisms of miRNA-mediated post-transcriptional regulation were initially described, termed target degradation and translational repression. These differ with regard to the effect on target mRNA transcript expression level, with the former resulting in a reduction and the latter producing no measurable effect on transcript abundance. However, this categorization of function is an oversimplification; for example, target degradation can occur as a result of multiple mechanisms. These include target cleavage, which occurs if miRNA:mRNA sequence complementarity is perfect or near-perfect along the full length of the miRNA, resulting in complete destruction of the target transcript (Hutvágner and Zamore, 2002; Liu et al., 2004). Whilst this mechanism is common in plants, it is rare in animals (Bartel, 2009). Where miRNA:mRNA complementarity is less extensive, target destabilisation may predominate, through processes including miRNA-mediated mRNA de-adenylation and mRNA decapping, (Giraldez et al., 2006; Wu et al., 2006; Behm-Ansmant et al., 2006; Eulalio et al., 2009). Translational repression is a complex phenomenon that results in reduced target protein levels without significant reduction in target mRNA transcript abundance. This suppression of protein synthesis has been described as occurring

through various mechanisms including inhibition of both the initiation and elongation stages of translation, premature termination of translation, and protein degradation (Huntzinger and Izaurralde, 2011). Inhibition of translation can, in itself, potentially result in reduced transcript levels, demonstrating that boundaries between the various pathways are not clear-cut. These mechanisms are dependent on a large number of specific co-factors, and many of these have been noted to localise to so-called processing bodies (p-bodies) in the cytoplasm. Whilst it was initially believed that these were primarily sites of mRNA storage as part of the process of translational repression, a number of the factors present, such as GW182 proteins, mediate target degradation (Eulalio et al., 2008), indicating that multiple modes of post-transcriptional gene regulation take place here.

A number of recent studies have attempted to address whether target degradation or translational repression predominate in animals. This question is of both biological and practical importance because gene expression analysis techniques such as RT-PCR, microarray, Northern blot and next-generation sequencing are unable to detect expression changes for genes that solely undergo translational repression, as there is no measurable reduction in target mRNA levels. In 2008, the Bartel and Rajewsky groups used proteomic techniques to show that overexpression and/or knockdown of specific miRNAs in mammalian primary cells and cell lines affected both mRNA and protein levels of the majority of targets (Baek et al., 2008; Selbach et al., 2008). Hendrickson et al. subsequently determined targets of miR-124 through Argonaute immunoprecipitation in transfected HEK-293T cells, finding that mRNA levels were reduced for most targets, and that this reduction was greater than the reduction in target protein level (Hendrickson et al., 2009). In addition, these data suggested that inhibition

at or prior to the initiation of translation was the most likely mechanism of suppression. Recently, Guo et al. employed ribosome profiling in the context of specific miRNA overexpression or knockdown to demonstrate that approximately 84% of miRNA target genes were suppressed at the mRNA level in mammalian cells (Guo et al., 2010). Together these data support the notion that mRNA transcript levels can be measured in order to detect the majority of putative miRNA:mRNA interactions.

1.1.4. miRNA target specificity and prediction

The first metazoan miRNAs to be discovered were described as exhibiting partial complementarity to sequences in the 3'UTR of their target genes (Lee et al., 1993; Wightman et al., 1993; Reinhart et al., 2000). Early bioinformatic analysis revealed the importance of target complementarity toward the 5' end of the miRNA, with this observation later refined to identify nucleotide positions 2-7 of the miRNA, termed the seed sequence, as being of greatest importance (Lai, 2002; Stark et al., 2003; Enright et al., 2003; Lewis et al., 2003). Confirmatory experiments demonstrated that nucleotide substitutions had the largest effect on miRNA activity when they impaired seed sequence-target complementarity (Kloosterman et al., 2004; Doench and Sharp, 2004; Brennecke et al., 2005). These findings allowed for computational algorithms to be developed that predict miRNA targets on a genome-wide scale, by comparing the seed sequence of known miRNAs with 3'UTR sequences. An overview of some of the more commonly-encountered miRNA target prediction algorithms is shown in Table 1.1.

Algorithm/Database	Factors considered in prediction and ranking of targets
Targetscan (Lewis et al., 2005; Landgraf et al., 2007; Friedman et al., 2009) www.targetscan.org	Seed sequence pairing (stringent), number of sites, type of site, site conservation (optional). Predictions for: vertebrate (inc. human, mouse), fly, worm.
PicTar (Krek et al., 2005; Grün et al., 2005; Lall et al., 2006) pictar.mdc-berlin.de	Seed sequence pairing (stringent), number of sites, conserved sites. Predictions for: vertebrate, fly, worm.
miRanda (Enright et al., 2003; John et al., 2004; Betel et al., 2010) www.microrna.org	Seed sequence pairing (moderately stringent), number of sites, conserved sites. Predictions for: human, mouse, rat, fly, worm.
PITA (Kertesz et al., 2007) genie.weizmann.ac.il/pubs/mir07/mir07_data.html	Seed sequence pairing (variable), number of sites, conserved sites (optional), target site accessibility, flanking sequence complementarity (optional). Predictions for: human, mouse, fly, worm.
ElMMo (Gaidatzis et al., 2007) www.mirz.unibas.ch/ElMMo3/	Seed sequence pairing (moderately stringent), number of sites, conserved sites. Predictions for: vertebrate (inc. human, mouse), fly, worm.
mirWIP (Hammell et al., 2008) www.mirtargets.org	Seed sequence pairing (moderately stringent), number of sites, conserved sites, target site accessibility. Predictions for: worm.
Rna22 (Miranda et al., 2006) cbcsrv.watson.ibm.com/rna22.html	Independent identification of binding sites, seed sequence pairing (variable).

Table 1.1 Summary of selected target prediction algorithms and databases

The extent of complementarity in the seed region and beyond is important in determining the probability of suppression occurring through that site. A system for the classification of miRNA-target complementarity is summarised in Figure 1.3 (Bartel, 2009).

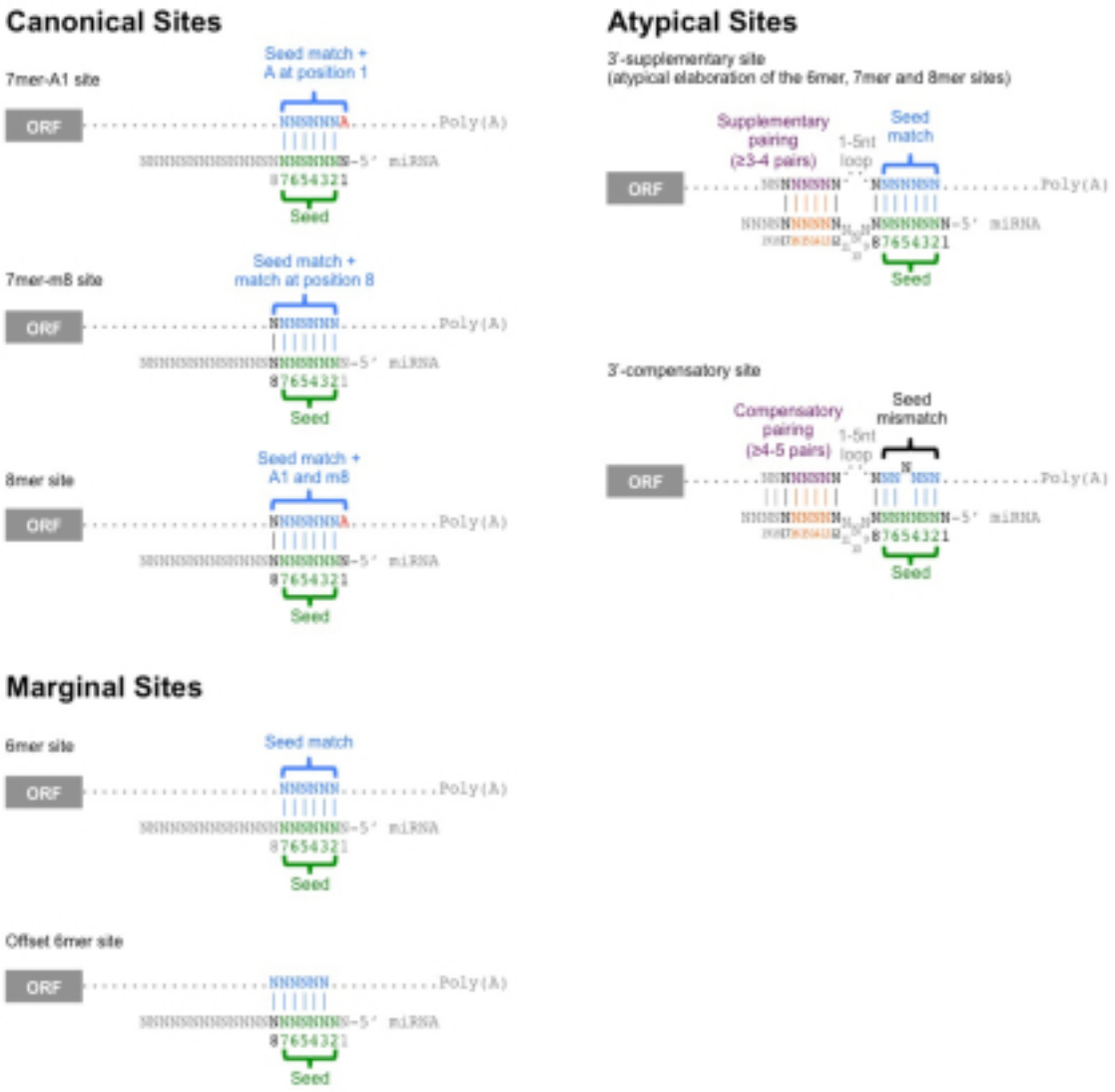

Figure 1.3 Classification of miRNA target sites. Vertical bars indicate Watson-Crick pairing. N=nucleotide, A=adenine. Figure reproduced with permission from Elsevier. (Bartel, 2009).

Where there is a perfect match at positions 2-7, these sites have been termed 'stringent' seed sites, and are classified as 8mer, 7mer-m8, 7mer-A1 and 6mer (Figure 1.3). The nucleotide complementary to position 1 of the miRNA is important, as the presence of an A residue at this point of the target sequence has been identified as increasing the likelihood of targeting (Lewis et al., 2005; Baek et al., 2008). It should be noted that target prediction algorithms such as TargetScan and PicTar differ in rewarding either an A in this position (Targetscan) or a Watson-Crick match (PicTar). Consequently the

overlap in predictions between algorithms is limited by this difference, although the majority of mammalian miRNAs begin with a U (Lewis et al., 2005; Seitz et al., 2011) and are therefore rewarded by both methods for a match in this position. 8mer and 7mer-A1 matches include an A complementary to position 1 of the miRNA, whilst 7mer-m8 matches possess a Watson-Crick match at position 8 in addition to a perfect seed-match (Figure 1.3). Seed sequence-target complementarity may also be offset such that, for example, a 6mer match at positions 3-8 of the miRNA can still result in successful targeting (Friedman et al., 2009). Mismatches within the seed-region do not necessarily preclude targeting and may be tolerated by some algorithms; these are termed 'moderately-stringent' sites. A classification system for these has also been proposed (Figure 1.4) (Gaidatzis et al., 2007).

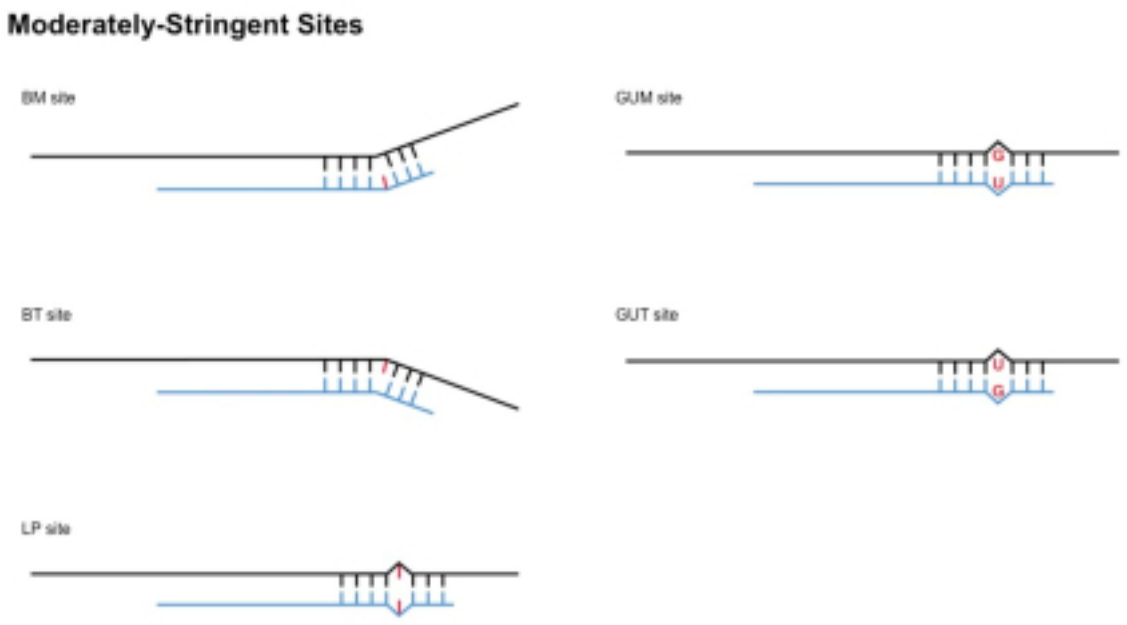

Figure 1.4 Classification of moderately-stringent sites. BM: Single bulged nucleotide on miRNA side; BT: Single bulged nucleotide on target side; LP: Single internal loop; GUM: Single GU pairing (G:U wobble) with the U on the miRNA side; GUT: Single GU pairing with the U on the transcript side. miRNA in blue, mRNA transcript in black, mismatch nucleotides in red. Note: mismatch or bulge may be located at any point in the seed region.

Correlation of predicted target datasets with experimental data quantifying the effects of miRNAs on target expression has demonstrated a hierarchy for some target-miRNA matches. For stringent seed-matches, the probability of a target being suppressed by a miRNA decreases in the order 8mer > 7mer-m8 > 7mer-A1 > 6mer (Grimson et al., 2007; Nielsen et al., 2007; Baek et al., 2008; Selbach et al., 2008; Friedman et al., 2009). The presence of a bulge, G:U wobble or loop significantly reduces the likelihood of targeting, although experimental evidence indicates that the effect on targeting is unpredictable (Brennecke et al., 2005). Stringent seed-matches are therefore more likely to be valid targets than moderately-stringent sites. Complementarity to the 3' part of the miRNA can support targeting, being defined as "3'-supplementary" pairing in the context of stringent seed-matching and "3'-compensatory" pairing when associated with moderately-stringent matching (Figure 1.3) (Bartel, 2009). Specifically, pairing centred on nucleotides 13-17 of the miRNA and consisting of 3-4 Watson-Crick matched nucleotides provides optimal support for targeting in stringent-matched miRNA-target interactions (Grimson et al., 2007). More extensive pairing of typically more than 9 Watson-Crick matches in the 3' region can compensate for mismatches, but this is a rare feature of predicted miRNA targets in mammals (Bartel, 2009). Indeed, only a small subset of targets exhibit significant conservation of complementarity to 3' miRNA sequences, indicating that both the requirement for and utilisation of this phenomenon are relatively uncommon (Bartel, 2009).

The accuracy of early target-prediction methods was sub-optimal, particularly suffering from high false-positive rates. However algorithms have been progressively refined to incorporate newly-described concepts of miRNA biology. One of the earliest refinements to be implemented was the analysis of predicted target site conservation

between species. A number of groups demonstrated in different species that predicted target sites of real miRNAs were more highly conserved, particularly in the seed region, than predicted sites of scrambled miRNA sequences; this led to improved algorithms that select for highly conserved sites and thereby reduce the false positive rate (Lewis et al., 2003; Krek et al., 2005; Brennecke et al., 2005; Lewis et al., 2005). However this process necessarily removes many non-conserved targets, which may outnumber conserved targets by as much as ten to one for 7mer matches (Farh et al., 2005). A large proportion of non-conserved targets are indeed valid miRNA targets, however genes with non-conserved sites tend not to be co-expressed in the same tissue type with the targeting miRNA (Farh et al., 2005). Hence algorithms that incorporate conservation in their scoring method tend to select for more biologically relevant interactions by concentrating on miRNAs and targets that will actually encounter each other within the cell. Nonetheless, target prediction based on conservation will always result in a significant number of functionally relevant and valid targets being missed.

The location of target sites also impacts on the likelihood of targeting. The probability of targeting via 3'UTR target sites is increased where the site is located away from the centre of the UTR, but at least 15nt downstream of the stop codon (Grimson et al., 2007). Target sites have also been described in both 5'UTRs (Jopling et al., 2005; Lytle et al., 2007; Ørom et al., 2008; Lee et al., 2009a) and open reading frames (ORFs) of mRNAs (Farh et al., 2005; Lewis et al., 2005; Lim et al., 2005; Easow et al., 2007; Grimson et al., 2007; Baek et al., 2008). However the majority of functional sites are located within the 3'UTR and this is likely to be due to the effect of active translation impeding the association of the miRNA-RISC complex with the target transcript (Gu et al., 2009). Multiple sites within the same UTR also increase the overall likelihood of

targeting (John et al., 2004), and when these sites are within close proximity to each other the suppressive effect of targeting can be amplified (Doench and Sharp, 2004; Grimson et al., 2007; Saetrom et al., 2007).

In addition to the location of target sites, the accessibility of the site affects the likelihood of targeting, and this is determined in part by mRNA secondary structure. A:U-rich areas surrounding predicted sites increase the probability of the site being active, possibly because these sites are more accessible as a result (Grimson et al., 2007; Bartel, 2009). A number of methods have attempted to integrate *in silico*-predicted mRNA secondary structures into target prediction algorithms (Robins et al., 2005; Kertesz et al., 2007; Long et al., 2007; Hammell et al., 2008). However, these fail to outperform simple scoring of A:U content in the region of the miRNA (Grimson et al., 2007; Baek et al., 2008) indicating that, at present, structural predictions are not sufficiently accurate to justify the considerable computing effort required to perform such an analysis on the genome-wide scale.

A summary of the various factors discussed here that influence the probability of targeting is presented in Table 1.2.

Factor	Summary
Seed-sequence complementarity	Seed-sequence is at positions 2-7 of miRNA; perfect seed match is major determinant of targeting probability
	Adenine across from position 1 of miRNA and Watson-Crick match at position 8 increase targeting probability independently and co-operatively
	Seed-region mismatches reduce probability but do not preclude targeting
3' miRNA-target pairing	Complementarity of 3-4nt at positions 13-16 (towards 3' end of miRNA) can augment stringent seed-matched targeting
	More extensive complementarity centred on positions 13-19 can compensate for mismatches and incomplete matches in seed region
	Both likely to be rare features of miRNA activity based on conservation and prevalence of sites
Conservation	Selective pressure results in conservation of functional sites
	Conservation scoring enhances specificity of target prediction algorithms
Target site location	Many sites in 3'UTR and ORF; few in 5'UTR
	3'UTR sites at least 15nt downstream of stop codon and away from UTR centre
Target site multiplicity	Multiple sites enhance suppression
Target site accessibility	Determines probability of targeting but difficult to accurately model

Table 1.2 Summary of factors that influence probability of miRNA targeting

1.1.5. Regulation of miRNA activity

A number of mechanisms are known to regulate miRNA activity. Indeed, virtually all points during the lifecycle of a miRNA susceptible to some form of regulation. miRNAs are transcribed in the same way as protein-coding genes and this transcription may be controlled through the same mechanisms. Specifically, transcription factors that act to promote or repress transcription may bind to genomic regulatory regions and thereby control miRNA expression. Interestingly, these transcription factors may themselves be targets of the miRNA in question, allowing for regulatory feedback loops to exist that act either to repress or powerfully upregulate miRNA expression. An example is the reciprocal repression between miR-7 and the transcription factor Yan, which ensures

appropriate miR-7 expression in photoreceptors of *Drosophila* (Li and Carthew, 2005). However, it is uncommon for a simple relationship between a single miRNA and a single transcription factor to exist in isolation, and complex networks can arise when the effects of multiple transcription factors and their many targeting miRNAs are taken into account.

Processing of miRNA primary transcripts and precursors is also a highly regulated process. Drosha cleavage of primary transcripts is regulated by its critical binding partner DGCR8, and Drosha itself can influence this process by cleaving hairpins from DGCR8 mRNA resulting in DGCR8 degradation (Han et al., 2009). The ratio of Drosha to DGCR8 is important as DGCR8 excess inhibits Drosha activity (Gregory et al., 2004). A further layer of complexity results from the finding that Drosha-mediated cleavage is not necessarily a fixed process, and that some miRNA precursors may be variably cleaved in such a way that mature miRNAs differ in their final sequence (Wu et al., 2009). As a consequence of differences at the 5' end of the miRNA, seed-target matches will be different because the seed sequence has been shifted in position, and this variation may be of importance in differential regulation of target genes. The mechanisms that govern this variability in 5' miRNA processing are not fully understood. Similar to Drosha, Dicer is directly regulated by the interaction with its binding partner TRBP, which stabilises pre-miRNA processing (Chendrimada et al., 2005). TRBP is regulated through phosphorylation of serine residues by mitogen-activated protein (MAP) kinase / extracellular regulated kinase (ERK) (Paroo et al., 2009), and these pathways are controlled in a tissue specific manner. In addition, a large number of accessory proteins have been described as acting as co-factors or regulators of miRNA processing. These act through diverse pathways such as preventing cleavage

of specific primary transcripts by Drosha, or recruiting other cofactors that enhance processing. Finally, Dicer is itself a target of the miRNA let-7, in an autoregulatory feedback loop that can globally influence miRNA levels within the cell (Forman et al., 2008).

miRNAs can also be directly subjected to sequence modifications. The most notable example of this is editing of the miRNA by ADARs (adenosine deaminase, RNA-specific). These enzymes act on dsRNA molecules to convert adenosine to inosine, a process that can have important consequences for base-pairing and transcript structure. ADARs can introduce changes to both pri- and pre-miRNAs, affecting Drosha processing (Yang et al., 2006), Dicer processing (Kawahara et al., 2007a), and seed-target interactions (Kawahara et al., 2007b). In addition, miRNAs can undergo end-modification as a result of adenylation (Katoh et al., 2009) and uridylation (Jones et al., 2009), which can have profound effects on the function of the miRNA. In particular, such modifications can affect the rate at which mature miRNAs decay, a process that may also vary depending on the rate of cell-cycling (Hwang et al., 2007). Little is known about the specific mechanisms that control miRNA degradation, but experimental studies indicate that miRNAs are likely to be highly stable RNA molecules with relatively long half-lives (van Rooij et al., 2007; Hwang et al., 2007; Gatfield et al., 2009; Krol et al., 2010a).

The function of mature miRNAs can also be controlled by the activity of the numerous proteins that interact with the RISC. Levels of Argonaute proteins are known to determine mature miRNA abundance, indicating that regulation of Argonaute expression may influence global miRNA expression (Diederichs, 2007). The ubiquitin ligase TRIM32 enhances the activity of several mammalian miRNAs through

interactions with Argonaute 1 (Schwamborn et al., 2009). RNA-binding proteins can also positively and negatively regulate miRNA-mediated repression by associating with target mRNAs under specific cellular conditions. For example, the protein HuR binds to AU-rich elements in the 3'UTR of the gene CAT-1 in human hepatoma cells undergoing stress, reducing miR-122-mediated translational inhibition and enhancing CAT-1 translation by promoting its recruitment to polysomes (Bhattacharyya et al., 2006).

miRNA activity can also be regulated independently of the miRNA processing and functional pathways through specific changes in the target mRNA. In particular, modification of the 3'UTR sequence can disrupt miRNA seed-target interaction and inhibit or prevent suppression. In proliferating $CD4^+$ T cells, 3'UTRs are shortened by increased rates of termination at upstream polyadenylation sites, with the effect that fewer miRNA target sites are present in the 3'UTRs of mRNA transcripts (Sandberg et al., 2008). The functional implication is that mRNA translation is enhanced in these proliferating cells, a process which is likely to be complementary to the demands of increased cell division.

1.1.6. Summary

The rapid expansion of miRNA research has produced numerous findings that demonstrate the importance of these small RNA molecules in virtually all biological processes. Perhaps the most significant examples of this are the genetically-modified organisms in which miRNA processing is purposely abolished by deletion of critical components such as Drosha and Dicer, causing near-total absence of mature miRNAs. Knockout of these endonucleases results in early embryonic lethality (Bernstein et al.,

2003; Fukuda et al., 2007), and deletion of the Drosha co-factor DGCR8 in mouse embryonic stem cells results in failure to silence pathways of self-renewal during differentiation (Wang et al., 2007). Clearly miRNAs are indispensible for embryogenesis, but to address their role in later stages of development, conditional Dicer and Drosha knockout mice have been developed that enable selective deletion in specific cell types. As an example, conditional deletion of either of these two endonucleases in T cells results in marked abnormalities of differentiation and function, highlighting the requirement for miRNAs even in mature, specialised cell types (Cobb et al., 2005; Muljo et al., 2005; Chong et al., 2008). Collectively, these findings provide confirmation of the general importance of miRNAs for a diverse range of cell functions, and demonstrate the complexity of the pathways involved. The challenges for the next era of miRNA research include the need to ascribe specific functionality to individual miRNAs, the continuing effort to understand the interplay of regulatory factors that govern miRNA biology, and the desire to translate this vast wealth of knowledge into tools that may be of use in the management of human disease.

1.2. T helper cell subsets

$CD4^+$ T cells are of critical importance for effective immunity. Their functions primarily involve interactions with other immune cell types, orchestrating responses of both the innate and adaptive immune system. Whilst $CD4^+$ T cells undergo a clearly defined programme of development in the thymus, their final state of differentiation in the periphery has the potential to vary widely in response to the differing stimuli that they may receive. It is this range of $CD4^+$ T cell subsets that allows for a highly specific response to individual threats, directing the immune system to act in the most

appropriate way. Through these means, $CD4^+$ T (helper) cells are able to control most classes of pathogens including viruses, intra- and extracellular bacteria, helminths and fungi. The number of recognised T helper cell subsets has expanded significantly in recent years, as has the evidence that cells may simultaneously or sequentially exhibit some features that are characteristically associated with different subsets. What once seemed to be clear-cut lineage boundaries now appear less well defined. As a result, the complexity of the mechanisms that control commitment pathways has become increasingly apparent, a change that has been amplified by recent discoveries of novel cellular processes that regulate gene expression and function, such as the role of non-coding RNAs. Driving this research is the belief, increasingly supported by evidence, that improved understanding of T helper cell biology can be exploited in a targeted manner to improve the management of a wide range of human diseases.

1.2.1. Overview of T helper subset discovery

T helper subsets were initially recognised and defined principally by the specific cytokines that they were found to produce. This section provides a summary history of the discovery of these subsets. However, in recent years it has been recognised that the expression of master regulatory transcription factors determines the differentiation of individual T cell populations, and these are increasingly used in the definition of T helper cell subsets. The identities and functions of these transcription factors are reviewed later, in section 1.2.2, along with the mechanisms that are responsible for differentiation.

1.2.1.1. The Th1/Th2 paradigm

In 1986, Mosmann and Coffman described a system for the classification of murine T cell clones into two phenotypes. These were termed T helper type 1 (Th1) and Th2 based on differences in their expression of cytokines and the antigens for which they provided B cell help (Mosmann et al., 1986). They found Th1 cells to produce interferon-γ (IFN-γ) whereas Th2 cells produced a number of T cell growth factors including IL-4. Following this report, these definitions were progressively developed and expanded to include a wider range of cytokines and surface molecules that define these cells. Th1 cells are now known to preferentially express the cytokines tumour necrosis factor α (TNF-α) and lymphotoxin α (LTα) in addition to IFN-γ (Cherwinski et al., 1987), and the cell surface chemokine receptors CCR5 (Loetscher et al., 1998) and CXCR3 (Bonecchi et al., 1998; Sallusto et al., 1998). A large number of Th2-associated cytokines including IL-4, IL-5, IL-9, IL-10, IL-13, IL-24, IL-25 and amphiregulin have been identified, whilst these cells express CCR3 (Sallusto et al., 1998), CCR4 (Bonecchi et al., 1998; Sallusto et al., 1998; D'Ambrosio et al., 1998), CCR8 (D'Ambrosio et al., 1998) and CRTh2 (Nagata et al., 1999) on the surface.

Following the identification of Th1 and Th2 cells, the pathways that result in their development from naïve T cells were systematically uncovered. T helper cell differentiation occurs following antigen-presenting cell (APC) stimulation of naïve T cells with cognate antigen, and is dependent on factors including cytokine milieu, signal strength and antigen concentration. Naïve T cells make very little cytokine of any type upon direct *ex vivo* stimulation. It was first demonstrated in 1990 that these cells could be induced to produce IL-4 in significant quantities if cultured for 2-3 days in the presence of T cell receptor (TCR) ligands and exogenous IL-4, hence becoming skewed

towards the Th2 phenotype (Le Gros et al., 1990; Swain et al., 1990). This process was observed to represent a feedback loop mechanism that ensures effective polarisation. Efficient skewing towards the Th1 phenotype was subsequently demonstrated to occur following culture of naïve T cells in the presence of TCR stimulation and IL-12 (Hsieh et al., 1993). The strength of TCR stimulus and antigen concentration were also investigated and have been found to influence differentiation, with weaker stimuli and lower antigen concentrations both favouring Th2 commitment (Hosken et al., 1995; Constant et al., 1995; Tao et al., 1997; Yamane et al., 2005).

Evidence to support the Th1/Th2 classification continued to appear during the decade that followed its initial description. Importantly, this dichotomy was soon shown to be broadly conserved between human and rodent following the isolation of Th1- and Th2-type cells from patients with inflammatory diseases (Wierenga et al., 1990; Maggi et al., 1991; Parronchi et al., 1991). It also became clear that the two subsets play different functional roles. Th1 cells help to promote B cell class-switching to IgG2a, stimulate macrophages through production of IFN-γ and respond primarily to pathogenic intracellular organisms. Th2 cells promote B cell class-switching to IgG1 and IgE subtypes, stimulate eosinophils, mast cells and basophils and direct immunity against extracellular parasites. Early studies of these T cell subsets in animal infectious disease models and human diseases provided evidence that reinforced the functional basis of this classification. Mice infected with the protozoan intracellular parasite *Leishmania major* are able to successfully clear the infection if a Th1 response is mounted, but succumb to the disease if the response is Th2-mediated (Scott et al., 1988; Heinzel et al., 1989). Interestingly, the type of response to *L. major* infection depends on the strain of mouse that is infected: C57BL/6 mice develop Th1-type responses and so are protected,

whilst BALB/c mice develop a Th2 response that actually contributes to disease progression and so do not survive (Heinzel et al., 1989). A comparable human model of the Th1 vs. Th2 response to infection can be observed in the variable pathology of *Mycobacterium leprae* infection: lepromatous leprosy is characterised be massive accumulation of intracellular parasites and is associated with a Th2 response that fails to control infection, whereas tuberculoid leprosy features a Th1 response with IFN-γ production and efficient clearance of bacteria, but significant immune-mediated tissue damage (Salgame et al., 1991; Yamamura et al., 1991). Experimental models of Th2-mediated immunity were also developed; for example, mice infected with the nematodes *Heligmosomoides polygyrus* and *Trichuris muris* require a Th2 response to clear the disease (Urban et al., 1991; Else et al., 1992). The Th1/Th2 paradigm was also supported by evidence from human and experimental inflammatory diseases. The non-obese diabetic (NOD) mouse model of autoimmune diabetes mellitus was shown to be dependent on Th1 cytokines for disease induction (Debray-Sachs et al., 1991; Campbell et al., 1991) and prevented by administration of IL-4 (Rapoport et al., 1993). Multiple sclerosis was found to be associated with increased levels of IFN-γ, TNF-α and LT-α (Rotteveel et al., 1990; Selmaj et al., 1991), and the corresponding mouse model, experimental autoimmune encephalitis (EAE), was shown to be associated with Th1 activity (Ando et al., 1989). In contrast, Th2 responses were found to be associated primarily with allergic and atopic human diseases (Parronchi et al., 1991; Robinson et al., 1992).

1.2.1.2. Th17 cells

Whilst this model of T cell differentiation was both elegant and tractable for the purpose of improving the understanding of T cell biology at that time, a number of

inconsistencies began to be reported that hinted at a deeper complexity. In particular, confusion arose when diseases that were believed to be Th1-mediated either failed to be ameliorated or were worsened by certain experimental interventions aimed at limiting Th1 responses. For example, inhibition of IFN-γ in the setting of EAE was seen to produce opposing results when compared with IL-12 inhibition, with IFN-γ knockout mice being more highly susceptible to disease (Willenborg et al., 1996) and IL-12 p40 knockouts being protected (Segal et al., 1998). An explanation for this discrepancy was provided in 2000 when it was discovered that the p40 subunit of IL-12 is also a component of the previously unrecognised cytokine IL-23 (Oppmann et al., 2000). The second element of these heterodimeric molecules differs: IL-12 is defined by the presence of the p35 subunit and IL-23 by p19. Confirmation was subsequently provided by studies comparing p40 knockout mice with p35 knockouts, which showed that p35 knockouts displayed increased sensitivity to EAE (Becher et al., 2002; Gran et al., 2002). In keeping with these findings, deletion of p19 resulted in complete protection from disease, demonstrating that IL-23 was the critical cytokine in the development of EAE, and that IL-12 was not responsible (Cua et al., 2003).

These data contradicted the existing Th1-mediated model explanation of EAE and indicated that a previously unrecognised T cell subtype might be responsible. The landmark observation that IL-23 induces IL-17 production by a subset of T helper cells (Aggarwal et al., 2003) provided the link between IL-23 and a potential mechanism for inflammation, as IL-17 had previously been demonstrated to be an inflammatory T cell-derived cytokine (Yao et al., 1995). It was later recognised that IL-23-induced, IL-17 producing $CD4^+$ T cells were highly pathogenic and responsible for inflammation in both murine EAE (Langrish et al., 2005) and collagen-induced arthritis (CIA) (Murphy

et al., 2003). In time, these IL-17-producing cells came to be described as Th17 cells, a novel subset in its own right that was readily distinguishable from Th1 and Th2 cells (Harrington et al., 2005; Park et al., 2005). The primary function of Th17 cells appears to be to direct the immune response to extracellular pathogens through the recruitment of cells such as neutrophils and the induction of cytokine expression by both immune and other cell types (Schmidt-Weber et al., 2007). As with Th1 and Th2 cells, the sources and identities of factors that regulate Th17 differentiation have been the subject of concerted investigation, with cytokines such as transforming growth factor β (TGF-β), IL-6 and IL-1β all being described as playing significant roles in the process (Bettelli et al., 2006; Mangan et al., 2006; Veldhoen et al., 2006; Sutton et al., 2006). However, numerous unresolved controversies have emerged in relation to the precise mechanisms of Th17 differentiation and there appear to be larger differences between human and mouse Th17 cells in this regard when compared with Th1 and Th2 cells. These topics are discussed further in section 1.2.2.3.

1.2.1.3. Regulatory T cells

The subsets described above are generally considered to be effector cell types whose role is to co-ordinate the most appropriate response to any threat. By the early 1990s, several decades' worth of evidence had slowly accumulated that a separate T cell population with regulatory properties existed, but many researchers had sadly abandoned their efforts along the way, in part due to confusion in the field and a lack of appropriately sophisticated tools to study this (Sakaguchi et al., 2007). However, a report in 1995 that $CD4^+$ $CD25^+$ cells possess potent suppressor function reinvigorated these longstanding research efforts (Sakaguchi et al., 1995). These cells were termed regulatory T cells (Treg), a functionally distinct subset of T cells that are capable of

suppressing the effector cell response and are of critical importance in the prevention of autoimmunity. Further characterisation identified a number of highly expressed surface molecules on these cells including cytotoxic T-lymphocyte antigen 4 (CTLA-4) (Takahashi et al., 2000; Read et al., 2000) and glucocorticoid-induced TNF receptor-related protein (GITR) (Shimizu et al., 2002; McHugh et al., 2002). In addition, it was soon recognised that these cells characteristically express the transcription factor FoxP3 (Hori et al., 2003; Khattri et al., 2003; Fontenot et al., 2003). FoxP3 expression has come to be regarded by many as the defining feature of Treg cells, and its role is discussed in more detail in section 1.2.2.4.

The primary function of Treg cells is to limit immune responses in order to prevent immune-mediated harm to self. It is recognised that the mechanisms of thymic negative selection, so-called central tolerance, are unable to prevent all self-reactive effector T cells from escaping to the periphery. Unchecked, these cells would respond to presentation of self-antigen and produce damaging autoimmune responses, but Treg-mediated peripheral tolerance acts to prevent this from occurring. Treg cells carry out their function through a number of mechanisms. These include secretion of inhibitory cytokines such as TGF-β, IL-10 and IL-35, which is a recently-described heterodimer comprising the p35 subunit of IL-12 and another subunit, Ebi3 (Collison et al., 2007). These cytokines are able to act on effector T cells and other cells of the immune system to suppress immune responses. Treg can also directly kill target cells through cytolytic activity mediated by secretion of granzyme B and perforin (Gondek et al., 2005; Zhao et al., 2006; Cao et al., 2007). In addition to this, Treg can disrupt the local microenvironment in such a way that target cell metabolism is adversely affected. A number of pathways for this have been reported, including local IL-2 consumption

leading to effector T cell IL-2 "starvation" (Pandiyan et al., 2007), elevation of local adenosine concentration with consequent inhibition of effector function (Borsellino et al., 2007; Deaglio et al., 2007; Kobie et al., 2006), and direct transfer of the inhibitory messenger cyclic AMP (cAMP) into T cells (Bopp et al., 2007). Finally, dendritic cells (DCs) are also a target of Treg suppressor function, with Tregs inhibiting co-stimulation and enhancing expression of indoleamine 2,3-dioxygenase (IDO), which catabolises the metabolism of tryptophan to immunosuppressive molecules (Fallarino et al., 2003). The precise manner in which suppressive function is achieved *in vivo* is likely to represent a combination of these and possibly other pathways.

Treg cells are not a homogeneous population and can be subdivided into categories based on differences in their development. A population of Treg cells termed natural Treg (nTreg) develops in the thymus in parallel with those T cells that will emerge into the periphery as naïve T cells. Alternatively, naïve T cells can differentiate into Treg cells under the appropriate conditions both *in vivo* and *in vitro*; these cells are described as induced Treg (iTreg). TGF-β is thought to be important for this process and *in vitro* stimulation of naïve T cells through TCR signalling in TGF-β-containing cell culture medium results in expression of FoxP3, CD25 and other surface markers expressed by Treg (Chen et al., 2003). Conversion of naïve T cells to Treg *in vivo* has been demonstrated following adoptive transfer of naïve T cells into Treg-deficient mice (Curotto de Lafaille et al., 2004). There is evidence that iTreg cells may be generated as part of the response to non-self antigens in order to prevent an excessive and potentially damaging immune reaction from occurring. Transfer of antigen-specific naïve T cells into lymphopenic hosts that constitutively express the cognate antigen results in an initial severe T cell-mediated immune response resembling graft versus host disease.

This is followed by a recovery phase in which FoxP3$^+$ CD25$^+$ iTreg cells develop and control inflammation (Knoechel et al., 2005). iTregs can also be induced in TCR-transgenic mice that lack nTregs following oral administration of the antigen (Mucida et al., 2005).

1.2.1.4. Follicular helper T cells

Follicular helper CD4$^+$ T cells (Tfh) were initially described in humans in 2000 and 2001 as tonsillar CD4$^+$ T cells that express high levels of the chemokine receptor CXCR5 (Breitfeld et al., 2000; Schaerli et al., 2000; Kim et al., 2001). These cells were found to be highly concentrated in germinal centres within the tonsil and to co-localise with B cells in these regions. Both IL-6 and IL-21 have been shown to contribute to the differentiation of Tfh cells (Suto et al., 2008; Nurieva et al., 2008), although it is likely that B cells also play an important role in this process (Crotty et al., 2010). The functions of Tfh cells include provision of help to B cells to ensure appropriate antibody isotype class-switching, and production of cytokines including IL-21 which forms a positive feedback loop to ensure Tfh polarisation. The relationship between the previously described effector subsets (Th1, Th2 and Th17) and Tfh cells remains unclear, because it has been reported that Tfh cells can display some of the features of these cells such as cytokine expression (Zaretsky et al., 2009), leading to speculation that Tfh cells are subject to an additional, secondary program of differentiation (Fazilleau et al., 2009; Awasthi and Kuchroo, 2009).

1.2.1.5. Other subsets

A number of other types of T helper cell have been identified in recent years. A subset termed Th9 has been recently reported by several groups and is defined by expression of IL-9 in the absence of the characteristic cytokines of other T helper cell subsets

(Veldhoen et al., 2008b; Dardalhon et al., 2008). IL-9 was initially described as being associated with Th2-related disease models and induced by TGF-β and IL-4 (Gessner et al., 1993; Schmitt et al., 1994). It has recently been demonstrated that IL-9 expression can be induced in Th2 and Th17 cells by culture in the presence of TGF-β (Veldhoen et al., 2008b; Beriou et al., 2010) and also in Th1 cells cultured with IL-33 (Blom et al., 2011). Th9 cells are considered to be of importance in Th2-type responses such as nematode infection and atopy (Faulkner et al., 1997; Forbes et al., 2008). However, the fact that other subsets may be directed to become Th9 cells raises the question of whether IL-9-producing cells should truly be considered a separate lineage.

The same problem arises regarding IL-10-producing cells. An IL-10-secreting regulatory cell population that has been termed Tr1 can be induced to develop from naïve T cells by a combination of the cytokines TGF-β and IL-27, and possesses potent immunosuppressive function without expressing FoxP3 (Awasthi et al., 2007). However this same cytokine combination is able to upregulate IL-10 expression in differentiated Th1, Th2 and Th17 cells (Stumhofer et al., 2007; Fitzgerald et al., 2007), suggesting that IL-10 expression may not be the defining feature of a separate subset but rather the superposition of a state of subset differentiation with regulatory capability. There is no doubt that IL-10 expression plays an important role in controlling the immune response, but at present it is unclear whether Tr1 cells truly represent a separate lineage.

Th22 cells have also been recently described in humans only (Nograles et al., 2009; Duhen et al., 2009; Trifari et al., 2009). These cells express only IL-22 and do not appear to belong to other subsets based on cytokine and transcription factor profiling. Whilst the function and differentiation mechanism of this lineage is unclear at present,

these cells were reported to preferentially home to the skin, indicating that this may represent a highly specialised T helper cell subset.

1.2.1.6. Summary

Ultimately, whilst distinct patterns of cytokine and transcription factor expression are readily observable in response to different types of disease, evidence increasingly suggests that these boundaries are not so rigidly fixed, and that significant plasticity and crossover exists in the realm of T helper differentiation (reviewed in section 1.2.3). These descriptions have been very helpful in advancing our understanding of the role of T helper cells in health and disease, but it is becoming clear that they represent an abstraction of a system capable of greater subtlety in tailoring its response to perceived threats.

1.2.2. Mechanisms of subset differentiation

The understanding of the fate-determining regulatory networks that govern T helper cell differentiation has expanded enormously in recent years. A complex interplay has been described between cell-extrinsic factors such as cytokines and co-stimulatory molecules, and cell-intrinsic mechanisms including signalling molecules, transcription factors and non-coding RNAs. A basic general schema for the induction of T cell differentiation is as follows: (1) Cytokines found in the local microenvironment bind to cytokine receptors at the time when T cells are activated by encounter with antigen-presenting cells (APCs). (2) These cytokine signals are then transduced to the nucleus via activation of specific signalling pathways, typically involving STAT proteins, which ultimately regulate the expression of subset-specific master-regulatory transcription factors through their binding to chromatin. (3) One or more feedback pathways may

then be established to promote efficient polarisation. These feedback mechanisms may be mediated by cytokines acting in an autocrine manner, transcription factors, and other molecules, and can inhibit pathways that promote differentiation to alternative subsets whilst positively reinforcing the intended phenotype. It should be noted that upregulation of master-regulatory transcription factors does not occur in the absence of TCR stimulus, indicating that signalling through TCR-dependent pathways such as NFκB (nuclear factor kappa-light-chain-enhancer of activated B cells), nuclear factor of activated T cells (NFAT) and activator protein-1 (AP-1) is of critical importance in differentiation (Zhu and Paul, 2010).

A number of the components of these pathways appear to be highly specific to individual subsets and are therefore often considered as defining features; these are summarised in Figure 1.5 and Table 1.3 and Table 1.4. The pathways and molecules responsible for differentiation are described thereafter.

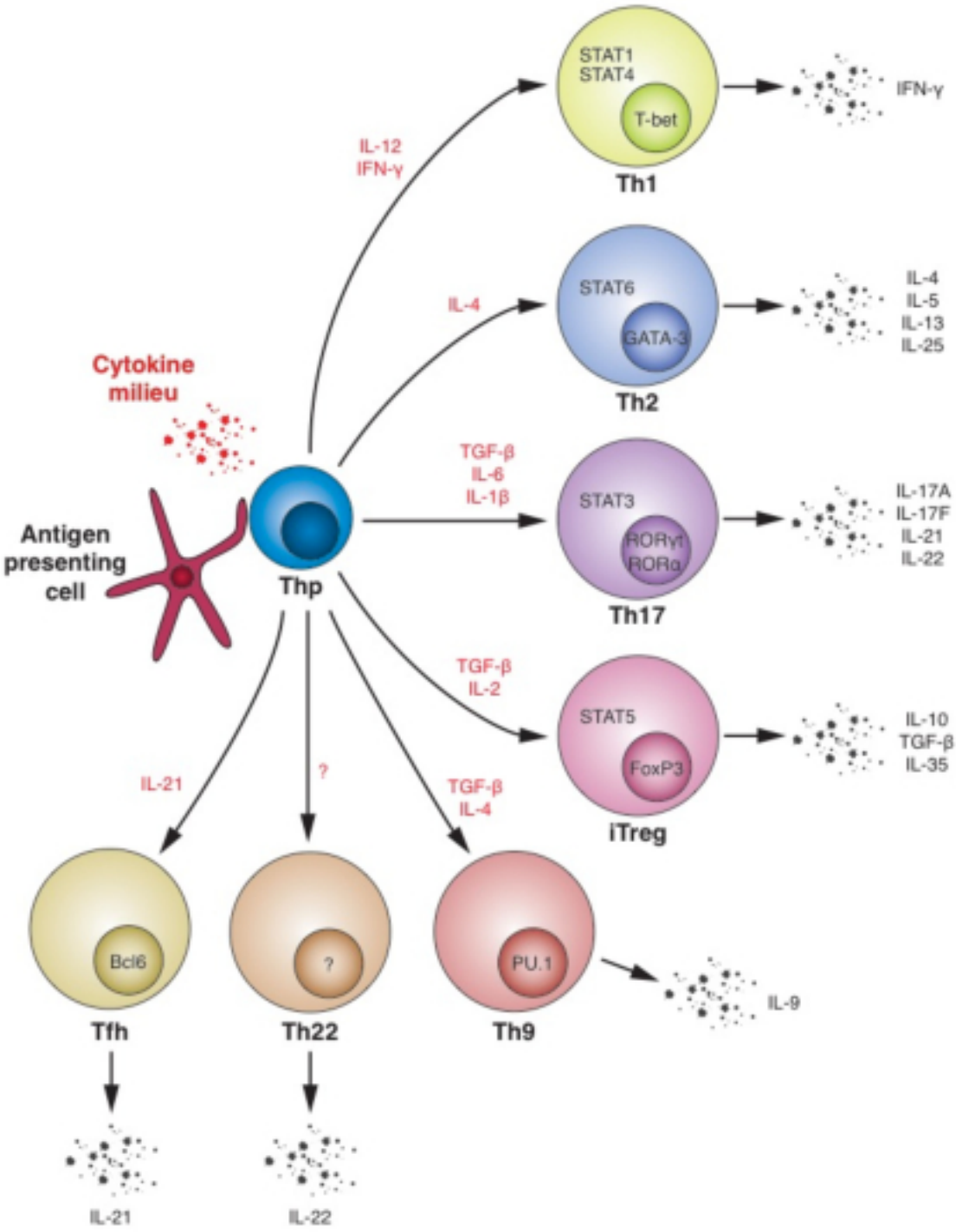

Figure 1.5 T helper cell differentiation. Key cytokines, signalling molecules and transcription factors that promote differentiation of naïve T cells to the indicated subsets are shown, in addition to the characteristic cytokines produced by each cell type. This figure is not intended to be comprehensive, hence some transcription factors and cytokines are omitted for the sake of clarity.

Subset	Transcription Factors	Notes
Th1	**T-bet**, STAT1, STAT4, Runx3, Hlx, Ets1, IRF-1	Signalling through IL-12-STAT4 and IFN-γ-STAT1 pathways promotes T-bet upregulation which controls Th1 differentiation. T-bet upregulates and co-operates with Runx3 and Hlx to promote IFN-γ production. IRF1 regulates response to IL-12.
Th2	**GATA-3**, STAT6, c-Maf, Ikaros, Gfi-1, TCF-1, Dec2, IRF-4	IL-4-induced STAT6 signalling upregulates GATA-3 expression. GATA-3 upregulates many of the other listed transcription factors to stabilise the phenotype and repress non-Th2 transcriptional programmes
Th17	**RORγt**, RORα, STAT3, AhR, Batf, IRF-4, Runx1	STAT3 signalling is critical. RORγt is the master regulator and reinforces Th17 differentiation by promoting IL-21 expression.
Treg	**FoxP3**, STAT5, Runx1	FoxP3 is master regulator, induced by TGF-β-Smad signalling and IL-2-STAT5. Runx1 suppresses ROR-γt function.
Th9	PU.1	PU.1 recently described as inducing IL-9 expression in T helper cells. Currently unclear whether master regulator of Th9.
Tfh	Bcl6	Bcl6 induces expression of CXCR5 and IL-21. Can be co-expressed with other master regulatory transcription factors.

Table 1.3 Transcription factors associated with T helper cell subset differentiation. Transcription factors considered to be "master regulatory" for the subset are indicated in bold type.

Subset	Cytokines promoting differentiation	Cytokines inhibiting differentiation	Cytokines produced
Th1	IL-12, IFN-γ	IL-4	IFN-γ, TNF-α, LT-α
Th2	IL-2, IL-4	IFN-γ	IL-4, IL-5, IL-13, IL-24, IL-25, amphiregulin
Th17	TGF-β, IL-6, IL-1β, IL-21	IFN-γ	IL-17A, IL-17F, IL-21, IL-22
Treg	TGF-β, IL-2	IL-6	TGF-β, IL-10, IL-35
Th9	TGF-β, IL-4	Unknown	IL-9
Tfh	IL-21	Unknown	IL-21

Table 1.4 Role of cytokines in T helper subset differentiation. Cytokines that have been established to promote and inhibit differentiation to the indicated lineage are listed, in addition to the cytokines characteristically produced by those cells.

1.2.2.1. Th1 differentiation

T-bet was identified in 2000 as the master regulator of Th1 differentiation, controlling Th1 polarisation and production of Th1 cytokines such as IFN-γ (Szabo et al., 2000). However T-bet is not expressed in naïve T cells. IFN-γ is able to direct Th1 differentiation via the IFN-γ receptor and STAT1 (Lighvani et al., 2001; Mullen et al., 2001; Afkarian et al., 2002), upregulating T-bet expression and thereby creating an IFN-γ-dependent feedback loop that ensures efficient polarisation. IL-12 fulfils a similar role by signalling via the IL-12 receptor and STAT4 (Kaplan et al., 1996b; Thierfelder et al., 1996), and ultimately inducing T-bet expression (Yang et al., 2007b). The exact hierarchy between IL-12 and IFN-γ in terms of their role in Th1 differentiation is unclear. Naïve T cells do not express the IL-12 receptor signalling subunit (IL-12Rβ2) until activated by TCR stimulus (Presky et al., 1996; Szabo et al., 1997), but both T-bet and IFN-γ (via STAT1) upregulate its expression (Mullen et al., 2001; Rogge et al., 1997). A recent report by Schulz et al. employs mathematical modelling to determine that Th1 differentiation is determined by sequential activity of the TCR-IFN-γ-STAT1-T-bet pathway followed by the IL-12-STAT4-T-bet pathway (Schulz et al., 2009). They suggest that the IFN-γ-dependent pathway controls initial polarization whilst the IL-12 pathway controls Th1 imprinting that allows for later IFN-γ re-expression upon antigen encounter. It is clear that these two pathways complement each other in reinforcing polarisation, but the precise relationship between them requires further study. DCs provide a source of IL-12 *in vivo*, and this can act directly on T cells or on natural killer (NK) cells which respond by producing IFN-γ, thereby promoting Th1 differentiation (Martín-Fontecha et al., 2004).

T-bet also induces expression of and/or co-operates with a number of Th1-associated transcription factors. Interferon-regulatory factor (IRF)-1 is a transcription factor whose expression is induced by IFN-γ, and which acts to upregulate the β1 subunit of IL-12R, thereby contributing to IL-12-mediated polarisation (Kano et al., 2008). Hlx is a homeobox transcription factor that is induced by T-bet expression and promotes the stable maintenance of the Th1 phenotype (Mullen et al., 2002). Ets-1 is the prototype member of the ETS family of transcription factors, has been reported to co-operate with T-bet in promoting Th1 activity, and is required for normal IFN-γ expression in Th1 cells (Grenningloh et al., 2005). Together these transcription factors impose a transcriptional program upon the cell that ensures robust differentiation to the Th1 phenotype.

One of the key functions of T-bet is to inhibit cell polarisation to non-Th1 effector lineages through effects on the expression and/or function of cytokines and transcription factors. T-bet inhibits the Th2 master regulatory transcription factor GATA-3 by direct interaction with it, leading to the sequestration of GATA-3 away from its binding sites (Hwang et al., 2005). This inhibits expression of Th2 cytokines that might otherwise promote Th2 differentiation. T-bet also induces the expression of the transcription factor Runx3 and together these two form a complex that both promotes IFN-γ expression and silences IL-4 expression (Djuretic et al., 2007). Th17 differentiation is also negatively regulated by T-bet which prevents Runx1 from transactivating the Rorc locus, thereby inhibiting expression of the Th17 master regulator ROR-γt (Lazarevic et al., 2011). In this manner, T-bet is able to restrict the expression of a range of non-Th1 subset-specific genes and thereby inhibit deviation from the Th1 programme.

1.2.2.2. Th2 differentiation

As noted above, GATA-3 has been identified as the master regulator of Th2 differentiation (Zhang et al., 1997; Zheng and Flavell, 1997; Ouyang et al., 2000). One of the earliest reports identified IL-4 signalling as a key mechanism of Th2 differentiation (Kopf et al., 1993). This is mediated via the IL-4 receptor and STAT6 (Kaplan et al., 1996a; Shimoda et al., 1996; Takeda et al., 1996a), and results in upregulation of GATA-3 (Kurata et al., 1999). STAT5 signalling, which occurs in response to cytokines including IL-2, is also of critical importance in Th2 differentiation (Zhu et al., 2003; Cote-Sierra et al., 2004); this is in addition to the general role of IL-2 in promoting the expansion and survival of other T helper subsets. This pathway is IL-4-independent, indicating that Th2 differentiation *in vivo* may not be solely IL-4-induced. A further IL-4-independent pathway has been identified, in which Notch signalling directly upregulates GATA-3 expression (Amsen et al., 2007; Fang et al., 2007). Interestingly, GATA-3 has been shown to be capable of binding to its own promoter, thereby enhancing its expression (Ouyang et al., 2000). In contrast with T-bet, naïve T cells do express GATA-3 and it has also been shown to possess many critical functions for thymic T cell development (Ho et al., 2009). The primary *in vivo* source of IL-4 for Th2 differentiation has been the subject of much investigation and discussion, but evidence suggests that both memory $CD4^+$ T cells and some innate cells, such as basophils, may provide the initial stimulus for polarisation (Tanaka et al., 2006; Sokol et al., 2008).

A number of other transcription factors have been reported to promote Th2 development. One of the earliest to be described, c-Maf, was identified as a Th2-related transcription factor that controls IL-4 expression (Ho et al., 1996). Ikaros is the

prototype member of a family of zinc finger transcription factors that was initially identified on account of its role in T cell development (Georgopoulos et al., 1992), and was recently determined to promote Th2 differentiation by regulating chromatin remodelling and expression of subset-specific transcription factors (Quirion et al., 2009). Gfi-1 plays an important role in Th2 development by promoting the IL-4-independent IL-2-STAT5 pathway of Th2 induction (Zhu et al., 2002), whilst Dec2 synergises with GATA-3 in a feed-forward loop mechanism to promote expression of Th2 cytokines and polarisation to the Th2 phenotype (Yang et al., 2009; Liu et al., 2009). IRF-4 plays a complex role in T helper differentiation and has been identified for its importance in the differentiation of both Th2 and Th17 cells. However, it was originally described as being crucial for promoting GATA-3 expression in Th2 cells and repressing IFN-γ and the Th1 phenotype (Lohoff et al., 2002). Finally, T cell factor (TCF)-1 upregulates GATA-3 expression upon TCR stimulus, and does so independently of IL-4-STAT6 signalling (Yu et al., 2009b). TCF-1 has also recently been shown to directly repress expression of IL-17 (Ma et al., 2011b). Integrating this expanding profile of transcription factors into the model for Th2 differentiation is a challenge, but despite the proliferation of regulatory genes that have been identified it remains clear that most pathways converge on GATA-3, and as a result it continues to be considered the master regulator of Th2 commitment.

1.2.2.3. Th17 differentiation

Th17 cells are one of the most recently identified subsets and as a result of this our understanding of the pathways that are responsible for Th17 differentiation is incomplete. This has been compounded by confusion in the literature regarding the cytokines that are necessary for differentiation, and by possible differences between

humans and mice. However, it is increasingly recognised that this confusion may have been provoked by the surprising degree of redundancy that exists in the systems and pathways of Th17 differentiation, and by some subtle heterogeneity amongst the populations of T helper cells that are defined by IL-17 production.

IL-23 was the first cytokine to be described as acting on T cells to induce IL-17 expression (Aggarwal et al., 2003), but naïve T cells do not express IL-23 receptor (Ivanov et al., 2006; Zhou et al., 2007). It is therefore thought that IL-23 may instead act to maintain and enhance Th17 function rather than promote differentiation, and so other cytokines have continued to be investigated for their role in the induction of Th17 differentiation. IL-6 was soon identified as a promoter of IL-17 production from T cells (Veldhoen et al., 2006; Zhou et al., 2007), but it does not induce IL-17 expression unless combined with other cytokines. One of these cytokines is TGF-β, and the combination of TGF-β and IL-6 is capable of potently inducing the differentiation of naïve T cells into Th17 cells *in vitro* (Bettelli et al., 2006; Mangan et al., 2006; Veldhoen et al., 2006). In addition to this is IL-21, which can be produced by both Tfh and Th17 cells, and is able to induce IL-17 expression in combination with other cytokines such as TGF-β (Zhou et al., 2007; Nurieva et al., 2007; Korn et al., 2007; Wei et al., 2007). In this way, an IL-21-mediated feedback loop promotes polarisation of the cell to a Th17 phenotype. Finally IL-1β has also been latterly recognised as an important inducer of Th17 differentiation when combined with other cytokines including IL-6 and IL-23, and a combination of these three cytokines efficiently induces Th17 differentiation in the absence of TGF-β (Acosta-Rodriguez et al., 2007; Ghoreschi et al., 2010).

These cytokines act via signalling molecules and transcription factors that transduce signals to the nucleus: TGF-β via Smad proteins (Malhotra et al., 2010; Martinez et al., 2010; Takimoto et al., 2010); IL-6, IL-21 and IL-23 via STAT3 (Mathur et al., 2007; Yang et al., 2007a; Laurence et al., 2007); and IL-1β via NFκB complex (Chen et al., 2010; Okamoto et al., 2010). In particular, STAT3 appears to be critical for Th17 differentiation, as mice in which STAT3 was deleted in T cells show defective Th17 response (Mathur et al., 2007; Yang et al., 2007a; Laurence et al., 2007). Ultimately, these pathways appear to converge on a pair of transcription factors – retinoid acid orphan receptor (ROR)-γt, which has been posited as the master regulator of Th17 differentiation (Ivanov et al., 2006), and ROR-α (Yang et al., 2008b). Deletion of either of these transcription factors impairs Th17 development, whilst overexpression promotes IL-17 production. STAT3 binds to the promoter of ROR-γt (Durant et al., 2010), and overexpression of active STAT3 in ROR-γt deficient cells fails to restore IL-17 production (Zhou et al., 2007), demonstrating that ROR-γt is a critical component of the differentiation pathway.

A number of other transcription factors have been implicated in Th17 differentiation. The aryl hydrocarbon receptor (AhR) is a molecule that is responsive to a wide range of natural and synthetic ligands (Esser et al., 2009), and in 2008 was demonstrated to be of direct importance in promoting Th17 function when activated with specific ligands, albeit by inducing expression of the Th17 cytokine IL-22 (Veldhoen et al., 2008a). This is of particular interest as AhR represents a tangible target for drug therapy of Th17-mediated disease, and also demonstrates an important connection between environment and immunity. Batf belongs to the AP-1 family of transcription factors but functions primarily to inhibit AP-1 activity (Schraml et al., 2009). Batf is expressed in all T cell

subsets, but Batf deficient mice are unable to generate Th17 cells despite normal Th1 and Th2 differentiation (Schraml et al., 2009). Whilst it is known that Batf binds to the promoters controlling IL-17, IL-21 and IL-22 expression, the reasons why deficiency has such profound and specific effects on Th17 differentiation remain unclear. IRF4, beyond its aforementioned role in Th2 cells, appears to play an important part in Th17 differentiation as IRF-4-deficient mice show impaired production of IL-17 following TGF-β and IL-6 stimulation (Brüstle et al., 2007). Finally, Runx1 is a transcription factor that interacts with both FoxP3 and ROR-γt, and is capable of promoting Th17 differentiation by enhancing transcription of the genes encoding ROR-γt and IL-17 (Zhang et al., 2008). However, Runx1 expression was also found to be important for the Th17-suppressing activity of the Treg master regulator FoxP3 during Treg polarisation, and so its precise role appears to be dependent on the context in which it is expressed.

1.2.2.4. Treg differentiation

FoxP3 was identified in 2003 as the master regulatory transcription factor for Treg (Fontenot et al., 2003; Hori et al., 2003), and is expressed in both nTreg and iTreg populations. FoxP3 is critical for regulatory T cell function as demonstrated by FoxP3 deficiency in humans and mice, in which fatal autoimmune pathologies spontaneously develop as a result of uncontrolled T effector cell activity (Chatila et al., 2000; Bennett et al., 2001; Brunkow et al., 2001). The mechanisms of induction of FoxP3 expression appear to centre on TGF-β and IL-2 signalling. TGF-β signalling via Smad proteins directly upregulates FoxP3 expression upon T cell stimulation (Zheng et al., 2002; Chen et al., 2003; Tone et al., 2008), but this process has been shown to be dependent on IL-2 (Zheng et al., 2007a). The role of IL-2 is interesting as IL-2 deficient mice initially puzzled researchers due to their spontaneous development of autoimmunity (Sadlack et

al., 1993). Previously it had been assumed, based on *in vitro* data, that IL-2 functioned to promote effector T cell activity and that knockout would impair immune responses. When it was discovered that Treg express the high affinity IL-2 receptor beta chain (CD25), it was suggested that IL-2 might contribute to Treg development, and this was subsequently demonstrated to be the case (Bayer et al., 2005; Fontenot et al., 2005). IL-2 signals via STAT5 which binds to the FoxP3 promoter, and the O'Shea group have demonstrated that STAT5-deficient mice have lower FoxP3 expression (Yao et al., 2007; Laurence et al., 2007). Indeed in human T cells, IL-2-STAT5 signalling alone has been shown to induce FoxP3 upregulation, although the cells were not demonstrably suppressive (Passerini et al., 2008).

A number of other factors influence Treg development. Retinoic acid signalling is able to enhance Treg differentiation in the context of TGF-β through a mechanism that may involve suppression of pathways that favour Th17 differentiation such as IL-6 and IL-23 signalling (Benson et al., 2007; Xiao et al., 2008b). Indeed, IL-6 is a potent inhibitor of Foxp3 induction (Pasare and Medzhitov, 2003; Bettelli et al., 2006; Dominitzki et al., 2007; Chen et al., 2009), acting via STAT3 (Yao et al., 2007). In addition, IL-21 and IL-27 both signal via STAT3 and both also inhibit FoxP3 induction (Korn et al., 2007; Neufert et al., 2007; Huber et al., 2007). Finally, IL-4-induced Th2 transcription factors directly repress FoxP3 expression, with this mechanism demonstrated to occur via GATA-3 in human T cells (Mantel et al., 2007), and STAT6 in mouse (Takaki et al., 2008). A number of additional transcription factors co-operate with FoxP3 in the Treg transcriptional programme including Runx1 which suppresses ROR-γt expression (Zhang et al., 2008), the Ikaros family member Eos which silences many effector genes in Tregs (Pan et al., 2009), and Foxo family proteins Foxo1 and Foxo3 which control

expression of FoxP3 and other Treg-specific genes (Ouyang et al., 2010). In a similar manner to the other subsets, a combination of the master regulator, FoxP3, with these other factors ensures that a coherent transcriptional programme is imposed upon the cell.

1.2.2.5. Differentiation of other subsets

Whilst the four previously mentioned subsets have been extensively characterised, comparatively less is known about the mechanisms of differentiation of some of the other subsets. However it has been demonstrated that Tfh differentiation is directed by expression of the transcription factor Bcl-6, with Bcl-6 deficiency resulting in failure of Tfh development and Bcl-6 overexpression causing adoption of the Tfh phenotype (Johnston et al., 2009; Nurieva et al., 2009; Yu et al., 2009a). In this sense, Bcl-6 can be considered a master regulator, but it is worth noting that its relationship with other master regulatory transcription factors such as T-bet and GATA-3 is complicated. Bcl-6 is known to suppress expression of these factors but simultaneous expression of non-Tfh subset cytokines is also possible (Nurieva et al., 2009; Crotty, 2011). The mechanism of Tfh subset induction is also unclear, with disagreement in the literature on the role of cytokines such as IL-21 and confusion about the identity of accessory and/or parent cells that are integral to Tfh development (Crotty, 2011). Our understanding of the way this important T cell subset relates to other types of T helper cell continues to improve but at present a number of questions remain.

Recently, the transcription factor PU.1 has been identified as being required for the production of IL-9 by T cells in response to both *in vitro* stimulation of naïve T cells with TGF-β and IL-4, and *in vivo* models of asthma (Chang et al., 2010). IL-9 secretion had classically been associated with Th2 response, but given recent studies demonstrating direct induction of IL-9-secreting Th9 cells, it has been speculated that

PU.1 is a key transcriptional regulator of Th9 development. It should be noted, however, that PU.1 deletion did not completely abrogate expression of IL-9, and so it remains to be seen whether this can be truly considered a master regulator.

1.2.3. Plasticity

The model in which phenotypically-pure polarised subsets are irreversibly fixed in that state has been increasingly called into question. In part, this has been as a result of data demonstrating that T cells may simultaneously exhibit features of "opposing" subsets, and evidence that some cells express combinations of multiple master regulatory transcription factors. Intertwined with these facts is the concept of plasticity, in which T cells may be susceptible to change in their phenotype over time or in response to particular stimuli. For many years, T cell subsets had been deemed to constitute true lineages, i.e. terminally differentiated cell types whose phenotype was programmed and fixed. However, evidence is growing that this is not always true, and that interconversion between certain subsets is possible.

The concept of fixed T helper cell lineage commitment was based on the initial observation that cells which were differentiated to Th1 and Th2 phenotypes continued to express subset-specific cytokines, surface receptors and transcription factors after multiple *in vitro* passages, and that cell lines committed to these phenotypes could be readily generated. This is a biologically plausible phenomenon because recalled T cell responses to previously encountered antigen would presumably be most effective if they employ the same mode of orchestrated immune activity in order to counter the pathogen. Whilst this framework was capable of incorporating the expanding number of lineages,

it became increasingly challenging to understand the precise drivers behind lineage choice.

However an increasing number of reports have emerged that describe flexibility of key lineage markers, particularly in the production of cytokines. A very prominent example of this is seen in the relationship between Th17 cells and other subsets. It is common to find cells that produce both IFN-γ and IL-17, particularly from humans (Wilson et al., 2007; Annunziato et al., 2007), and this presents challenges for our understanding of the mechanisms of Th1 and Th17 differentiation. What is more, Th17 cells can switch from being IL-17 producers to exclusive IFN-γ producers, demonstrating that differentiation is not necessarily fixed (Lee et al., 2009b; Bending et al., 2009). Another example that is of particular concern to the emerging field of cell-based therapy is the reported ability of Tregs to develop a pathogenic IL-17-producing phenotype under inflammatory conditions (Xu et al., 2007; Yang et al., 2008a). These changes are not only at the level of cytokine production. Transcription factor expression can change from predominance of one master regulator to another, for example FoxP3 expression can be downregulated in favour of ROR-γt expression under inflammatory conditions (Yang et al., 2008a). In addition, cells can simultaneously express two or more master regulatory transcription factors, such as Tregs that express both T-bet and FoxP3 (Koch et al., 2009), and Th17 cells that co-express T-bet and ROR-γt (Ghoreschi et al., 2010). Other examples include induction of IFN-γ and IL-12Rβ2 expression in Th2 cells (Hegazy et al., 2010), expression of IL-13 by Th1 cells (Hayashi et al., 2007), and expression of other cytokines such as IL-9, IL-10 and IL-21 by multiple subsets, as discussed previously.

However it is important not to generalise regarding plasticity, as some of the permutations of inter-subset conversion have not yet been supported by experimental

evidence, and the separation between Th1 and Th2 subsets appears more robust *in vivo* than others such as Th1/Th17 and Th17/Treg. Indeed a number of the examples given above occur under highly specific experimental conditions, and as such the relevance of these findings to the *in vivo* immune response remains to be fully determined.

One of the greatest immediate challenges is to understand how plasticity is controlled, and the approach to this problem will require the collaboration of multiple biological disciplines. Not least amongst these is the systems biology approach that will aim to make sense of the vast wealth of data generated regarding the factors that control differentiation. It is increasingly clear that epigenetic mechanisms are critical in control of cell phenotype, and that histone and DNA modifications are markedly different between subsets. Recently-published chromatin immunoprecipitation studies reveal the genomic loci at which master regulatory transcription factors bind and where epigenetic modifications are found (Wei et al., 2009; Marson et al., 2007; Zheng et al., 2007b). These provide an important genome-wide resource that will continue to be studied carefully for mechanistic insight into T helper cell subset differentiation. The same is true of microarray and RNA-sequencing datasets that will allow unbiased survey of the transcriptional landscape within differentiated cell types. Integrating all of these with our constantly evolving understanding of the mechanisms of genetic regulation will be a major challenge in years to come, but the potential rewards are great. The tantalising prospect of modifying harmful T cell phenotypes in the context of undesired immune responses, and greater confidence that cells used for therapy will remain as intended, are just two of the foreseeable benefits that might stem from better understanding of T helper cell plasticity.

1.3. T cell homeostasis

T cells undergo a complex programme of development in the thymus that results in a broad repertoire of antigen specificity. Following this development, naïve T cells migrate to the periphery, homing to lymphoid organs in particular, and awaiting encounter with their cognate antigen. The thymus continuously produces T cells, yet in health the number of T cells in the periphery remains relatively stable over time. A number of homeostatic mechanisms ensure that T cell numbers remain balanced between the desire to recognise a wide range of antigens, and the pressure of resource availability. One such resource is physical space, as organs such as the spleen and peripheral lymph nodes have a finite functional capacity for the provision of optimally-efficient immune function. The most well characterised mechanisms for the maintenance of T cell homeostasis are through TCR engagement with self-peptide-MHC complexes, and through cytokine stimulation, predominantly involving IL-7.

1.3.1. Role of TCR signalling in homeostasis

Naïve T cells are characterised by high expression of the secondary lymphoid organ-homing receptors CD62L and CCR7, and low expression of CD44. These cells have gone through the process of both positive and negative selection in the thymus, in which TCR response to self-peptide-MHC complex determines whether the cell is appropriate for release to the periphery. T cells at the double positive (DP, $CD4^+$ $CD8^+$) stage with low avidity responses are depleted due to neglect, which in this context means lack of TCR signalling. This process is termed positive selection. By contrast, negative selection occurs when these cells show excessive reaction to self-antigen and are therefore deleted from the T cell pool by induction of apoptosis, in order to minimise

the risk of autoimmunity. If, following positive and negative selection, T cells have an appropriate TCR response, they then transition to single positive status. These cells express exclusively either CD4 or CD8 depending on whether interaction occurs with MHC class II or class I, respectively.

Following departure from the thymus and migration to the periphery, these naïve T cells continue to encounter antigen presented in the context of MHC. If signalling reaches an appropriately high threshold, cells enter the cell cycle and expand in number as part of the adaptive immune response to a potential pathogen. Following resolution of this reactive phase, a small number of memory cells may be generated that are characterised by high expression of CD44. These signalling events typically occur in response to strong stimuli such as infection and immunization, but both germ-free mice (Huang et al., 2005) and unborn humans (Byrne et al., 1994; Szabolcs et al., 2003) possess memory cells, despite never having received such an antigenic stimulus. There is increasing evidence that some memory cells may instead develop following exposure to self-antigen-MHC complex in the periphery. It has also become clear that TCR engagement with self-peptide-MHC complex is a critically important, normal mechanism whose role is to maintain the survival of naïve T cells *in vivo*. It is therefore likely that some memory cells develop as a product of this homeostatic mechanism.

The process of positive selection ensures that cells possess a sufficient response to antigen. However, cells undergo a critical process of TCR 'tuning' during positive selection that ensures the response to self-antigen is reduced to levels below the threshold for cell activation (Grossman and Singer, 1996; Eck et al., 2006; Stephen et al., 2009). This process results from interaction with dendritic and epithelial cells within the thymic medulla (Stephen et al., 2009) and induces upregulation of genes and

pathways that suppress the TCR response such as the ubiquitin ligase Cbl-b (Huang et al., 2006), and CD5 (Perez-Villar et al., 1999). Through this means, naïve T cells are held in a quiescent state as long as only self-peptide-MHC is encountered. A number of transcription factors are also involved in the maintenance of this state, although the mechanism in general is incompletely understood. This includes forkhead transcription factors such as Foxo3a and Foxj1, which suppress NFκB activity by promoting synthesis of the inhibitory molecule IκB (Lin et al., 2004a; 2004b).

This process of desensitization is crucial because mature T cells continuously receive TCR stimulus in the periphery, and as mentioned above this is a requirement for naïve T cell survival. This phenomenon was first discovered through experiments in which T cells were prevented from contact with self-MHC, resulting in a significant reduction in their lifespan (Takeda et al., 1996b). It has also been demonstrated that inducible abrogation of TCR signalling results in reduced naïve T cell lifespan (Polic et al., 2001; Seddon and Zamoyska, 2002). Interestingly, the abundance of a particular T cell clone appears to have a major impact on survival. Transfer of large numbers of TCR-transgenic naïve $CD4^+$ T cells into normal syngeneic hosts results in a rapid decline in numbers, whereas transfer of very few cells is associated with much longer average survival (Hataye et al., 2006). This indicates that there is limited availability of self-peptide-MHC complexes of sufficient affinity to promote survival of each clone, and numbers of individual naïve T cell clones are regulated as a result. The effect of this is that diversity in the T cell repertoire is maintained. Unfortunately, the downstream mechanisms that mediate TCR-dependent survival of naïve T cells are poorly characterised at present. It has been suggested that the pathways are the same as for

normal T cell activation, but that signalling is of a lower strength than on encountering foreign antigen (Surh and Sprent, 2008), however the precise mechanisms are unclear.

1.3.2. Role of cytokines in homeostasis

Comparatively more is known about the role of cytokines in homeostasis, particularly of IL-7 signalling which is vital in promoting naïve T cell survival. IL-7 is mainly produced by haematopoietic stromal cells within the secondary lymphoid organs and thymus. Abrogation of IL-7 signalling through either the transfer of cells into IL-7-deficient lymphopenic recipients or antibody blocking experiments results in dramatically impaired cell survival (Vivien et al., 2001; Kondrack et al., 2003; Tan et al., 2001). IL-7 signalling is mediated through the IL-7 receptor, which comprises two subunits. These are IL-7Rα and the common cytokine receptor γ-chain (γ_c, CD132), which also forms part of the receptors for IL-2, IL-4, IL-9, IL-15 and IL-21. Signalling through the IL-7 receptor is via JAK-STAT pathways, as well as phosphoinositide 3-kinase (PI3K) pathway (Rochman et al., 2009). IL-7 acts to promote the expression of the pro-survival molecules B cell lymphoma (BCL)-2 and myeloid cell leukaemia (MCL)-1, whilst downregulating expression of pro-apoptotic factors such as BCL-2-interacting mediator of cell death (BIM) and BCL-2 antagonist of cell death (BAD) (Takada and Jameson, 2009). It also acts on pathways of metabolism to promote cell survival and prevent atrophy, in particular via PI3K-AKT, which acts to activate the mammalian target of rapamycin (mTOR) and promote expression of the glucose transporter protein GLUT1 (Rathmell et al., 2001; Wofford et al., 2008). In addition, IL-7 signalling can control T cell trafficking through AKT-mediated suppression of FOXO1 (del Peso et al., 1999), which is known to promote expression of chemokine receptor (CCR)-7, and the transcription factor Kruppel-like factor (KLF)-2, which in

turn upregulates CD62L and sphingosine 1-phosphate receptor 1 (S1PR1) (Kerdiles et al., 2009; Bai et al., 2007). These trafficking molecules promote recruitment of T cells to secondary lymphoid organs, and migration through these organs encourages interaction with dendritic cells presenting self-antigen in the context of MHC, thereby promoting survival through TCR signalling and enhancing the probability of T cells encountering cognate foreign antigen.

IL-7 signalling is regulated through a network of feedback and inhibitory loops that are only partly understood, and is principally controlled by availability of the IL-7Rα subunit, as the γ_c component is ubiquitously expressed on T cells (Schluns et al., 2000). IL-7 signalling in itself suppresses IL-7Rα expression (Park et al., 2004). This is mediated in part by transcription factors such as growth factor-independent (GFI)-1, which suppresses *Il7ra* expression in thymocytes and $CD8^+$ T cells (Yücel et al., 2003; Park et al., 2004). In addition, FOXO1 binds to the enhancer region of IL-7Rα and FOXO1 deficiency results in impaired IL-7Rα expression (Kerdiles et al., 2009; Ouyang et al., 2010). IL-7 receptor signalling activates AKT, which phosphorylates FOXO1 (del Peso et al., 1999) and promotes its migration from the nucleus to cytoplasm (Jackson et al., 2000), hence impairing its ability to promote IL-7Rα expression and therefore leading to IL-7Rα downregulation as part of an autoregulatory feedback loop.

Other cytokines play a role in T cell homeostasis, including IL-2 and IL-15. IL-2 signalling under physiological conditions does not appear to be necessary for homeostatic maintenance of cell types other than Treg (Surh and Sprent, 2008), for which it is critical in the process of differentiation (as discussed previously in section 1.2.2.4). However IL-15 signalling is of importance for maintenance of memory $CD8^+$

T cells, as demonstrated by IL-15 deficient mice which have a selective reduction in memory $CD8^+$ T cell numbers (Kennedy et al., 2000). However it is clear that IL-7 is the key cytokine in the control of naïve T cell homeostasis.

1.3.3. Summary

The homeostatic control of the T cell pool is dependent on both TCR signalling and cytokine signalling, but the relationship between these two mechanisms is unclear. There are some indications that there may be cross-regulation, for example in $CD8^+$ cells, IL-7 signalling results in downregulation of CD5 expression, and this may increase TCR sensitivity (Gagnon et al., 2010). In addition, IL-7 signalling upregulates CD8α expression, which also has the effect of increasing TCR sensitivity (Park et al., 2007). However, the extent of cross-regulation in $CD4^+$ T cells is unknown, and there remains much more to learn about the relationship between these two pathways and T cell homeostasis in general.

1.4. Function of microRNAs in T helper cells

In the relatively short time that miRNAs have been known about and actively investigated, most research has focused on general miRNA biology and global miRNA knockout experiments. However, functions have been discovered for a number of specific miRNA molecules in T helper cells. A number of these miRNAs are listed below, in no particular order, and briefly described within this section.

1.4.1. miR-181a

miR-181a was one of the first miRNAs to be discovered to have a role in $CD4^+$ T helper cell function. In 2004, Chen and colleagues identified miR-181a as being specifically expressed in the haematopoietic lineage and discovered that overexpression of miR-181a in haematopoietic progenitors resulted in an increase in the number of B cells and a reduction in T cell numbers (Chen et al., 2004). They also reported particularly high expression in the thymus and a differential effect on $CD4^+$ and $CD8^+$ numbers, with the latter being more severely affected. In 2007, members of the same group then went on to dissect the mechanism of miR-181a function, finding that elevated miR-181a expression augments TCR signalling strength by inhibition of multiple phosphatases and consequent increase in phosphorylated intermediate signalling molecules downstream of the TCR (Li et al., 2007). Levels of miR-181a were found to be dynamically regulated during T cell development and this was positively correlated with TCR sensitivity, indicating that miR-181a expression functions to tune TCR sensitivity. Ebert and colleagues later confirmed that miR-181a is critically important for negative selection in the thymus, and that inhibition of miR-181a activity at the DP thymocyte stage allows the survival of T cells that would be otherwise be deleted on account of elevated autoreactive potential (Ebert et al., 2009).

1.4.2. miR-155

miR-155, which is processed from an exon of the non-coding RNA transcript *bic* (Lagos-Quintana et al., 2002), has been implicated as an important component of both T and B cells. In 2007, Rodriguez and colleagues reported that miR-155-deficient mice exhibit immunodeficiency and airway inflammation (Rodriguez et al., 2007). They were

able to identify defects in B cells, DCs and T cells, with $CD4^+$ T cells exhibiting normal proliferation but increased production of Th2 cytokines such as IL-4 and reduced IFN-γ production. Microarray experiments identified a number of target genes that were overexpressed in activated, miR-155 deficient T helper cells, and luciferase reporter experiments confirmed that c-Maf was a target gene, providing a link with a known Th2-promoting transcription factor. An additional role for miR-155 in immune regulation was then reported by Lu and colleagues, who found that FoxP3 controlled miR-155 expression and that miR-155 deficiency in Treg impaired the Treg response to IL-2 (Lu et al., 2009). They demonstrated that miR-155 targets SOCS1, and that loss of this suppression results in impaired STAT5 activation, with a reduction in Treg numbers as a consequence but no significant impairment in Treg function. Kohlhass et al. published confirmatory findings soon after (Kohlhaas et al., 2009). The Reiner group then demonstrated in 2009 that miR-155 overexpression promotes Th1 differentiation and found that miR-155 targets the IFN-γ receptor α-subunit (Banerjee et al., 2009). The Baltimore group then reported that miR-155 deficient mice are resistant to EAE, and that miR-155 functions to promote both Th1 and Th17-type response (O'Connell et al., 2010). More recently, in 2011, Murugaiyan and colleagues confirmed the results of the Baltimore group and demonstrated that intravenous administration of a miR-155-specific antagonist was sufficient to ameliorate EAE disease severity (Murugaiyan et al., 2011), providing a potentially translatable, novel therapeutic modality for this disease.

1.4.3. miR-146a

A number of early gene profiling studies identified miR-146a as being highly expressed in immune cell types, and demonstrated differential expression in T helper cell subsets with particularly high expression in Treg when compared with effector subsets, and

higher expression in Th1 when compared with Th2 (Monticelli et al., 2005; Cobb et al., 2006). The earliest studies of miR-146a function reported that it is a negative regulator of myeloid cell pro-inflammatory activity through its effects on inhibiting TRAF6 and IRAK1/2 signalling (Taganov et al., 2006; Hou et al., 2009). Curtale and colleagues subsequently examined its function in T cells, showing that its expression is upregulated on TCR stimulation and that this impairs IL-2 production and AP-1 transcription factor activity (Curtale et al., 2010). In addition, they reported that overexpression of miR-146a protects T cell lines from activation-induced cell death (AICD) and that miR-146a targets the gene Fas-associated death domain (FADD). This work was followed by the report from Lu and colleagues detailing the phenotype of miR-146a-deficient mice (Lu et al., 2010). In this study, a specific role for miR-146a in Treg was identified, as evidenced by Treg hyperproduction of IFN-γ and loss of suppressive ability in the absence of miR-146a. They also demonstrated targeting of STAT1 by miR-146a and found that increased STAT1 activity in Treg was responsible for the development of spontaneous autoimmunity in these mice.

1.4.4. miR-29

Two recent reports have demonstrated a functional role for miR-29 in the regulation of T cell differentiation. Ma et al. demonstrated that miR-29 directly targets IFN-γ, and that inhibition of miR-29 results in a default switch to an IFN-γ producing phenotype (Ma et al., 2011a). In addition, they report that miR-29 deficient mice exhibit greater resistance to infection with *Listeria monocytogenes* and *Mycobacterium tuberculosis*, demonstrating that miR-29 suppresses the immune response to intracellular pathogens. Steiner et al. reported similar results, although they identified both T-bet and the related

transcription factor Eomesodermin (Eomes) as direct targets of miR-29 (Steiner et al., 2011).

1.4.5. mir-17_92 complex

The mir-17_92 complex consists of a number of co-transcribed individual miRNAs, namely miR-17-5p, miR-17-3p, miR-18a, miR-19a, miR-20a, miR-19b-1, and miR-92a, and these molecules are frequently found to be upregulated in lymphoma cells (Tagawa and Seto, 2005; He et al., 2005). Overexpression of this gene cluster in haematopoietic stem cells results in accelerated tumour development in a murine model of B cell lymphoma (He et al., 2005), and *in vivo* overexpression in lymphocytes results in spontaneous lymphoproliferative disease and autoimmunity as a result of increased targeting of the genes PTEN and Bim (Xiao et al., 2008a). Ventura et al. have also showed that deletion of mir-17_92 cluster causes lung hypoplasia that results in death shortly after birth (Ventura et al., 2008). In addition these mice expressed increased levels of Bim in B cells resulting in failure of foetal B cell development, however the effect on T cell development was not analysed.

1.4.6. mir-142

mir-142 is a haematopoietic-specific miRNA precursor that gives rise to two functional mature miRNAs – miR-142-3p and miR-142-5p (Chen et al., 2004; Landgraf et al., 2007). *In vitro* overexpression of mir-142 in haematopoietic stem cells results in increased numbers of mature T cells (Chen et al., 2004), and the expression of mir-142 is dynamically regulated in the thymus (Li et al., 2007; Landgraf et al., 2007). In T cells, miR-142-3p was described by Huang et al. as targeting the adenylyl cyclase AC9, and lower expression of miR-142-3p in nTreg was found to correlate with higher levels of

cAMP (Huang et al., 2009). This thesis studies the functional role of mir-142 in more depth through the analysis of mir-142 deficient mice.

1.4.7. miR-150

miR-150 has been extensively studied in B cells, but there is limited information on its role in T cells. Recently, Ghisi et al. reported that miR-150 expression is dynamically regulated during thymic T cell maturation, and that miR-150 targets NOTCH3 in human T cells (Ghisi et al., 2011). Notch family proteins control cell cycle progression and apoptosis in T cells, with NOTCH3 being critically important for early thymocyte maturation (Bellavia et al., 2003).

1.4.8. miR-125b

A single recent report by Rossi et al. has identified miR-125b as a key regulator of human T helper cell development (Rossi et al., 2011). Forced expression of miR-125b inhibited progression from the naïve state to differentiated effector cells, and it was found that miR-125b targets a number of molecules related to T cell differentiation including IFN-γ, IL-2Rβ subunit, IL-10Rα subunit and Blimp-1.

1.4.9. miR-126

miR-126 has recently been identified as a Th2-related miRNA by Mattes et al., as miR-126 was upregulated in a mouse model of asthma, and miR-126 antagonism suppressed disease activity (Mattes et al., 2009). Whilst a target of miR-126 was not formally identified, it was demonstrated that miR-126 antagonism resulted in increased PU.1 and

reduced GATA-3 expression, indicating a possible role for this miRNA in subset differentiation.

1.4.10. miR-326

Similarly, miR-326 was recently described by Du and colleagues as a critical regulator of Th17 differentiation (Du et al., 2009). They identified miR-326 as an upregulated miRNA in the blood of patients with multiple sclerosis and in mice with EAE, and found that silencing of miR-326 impaired Th17 differentiation. This was demonstrated to be as a result of miR-326 targeting Ets-1 which suppresses Th17 differentiation.

1.4.11. miR-182

A report by Stittrich and colleagues identifies miR-182 as a promoter of T cell clonal expansion (Stittrich et al., 2010). They report that IL-2 induces binding of activated STAT5 to miR-182, which promotes miR-182 expression in activated T cells. miR-182 is found to directly target Foxo1 at the posttranscriptional level, resulting in enhanced proliferation. Finally they demonstrate that inhibition of miR-182 activity in a mouse model of arthritis reduces disease severity.

1.4.12. miR-214

Jindra et al. used microarray analysis of activated murine T helper cells to identify differentially expressed miRNAs, and report that miR-214 expression increases on stimulation (Jindra et al., 2010). This increase in expression was found to be dependent on CD28-mediated co-stimulation. They also demonstrate that miR-214 targets PTEN

resulting in reduced PTEN expression, and that miR-214 overexpression results in increased cell proliferation.

1.4.13. let-7f

A recent report by Li et al. describes the regulation of IL-23 signalling in human T helper cells by the microRNA let-7f (Li et al., 2011). They find that let-7f is significantly reduced in memory T helper cells when compared with naïve cells, and that let-7f directly targets IL-23 receptor. They also demonstrate that exogenous let-7f downregulates IL-23 receptor expression *in vitro* and impairs IL-17 expression.

2. Hypothesis and Aims

The principal hypothesis that is tested in this thesis is that specific miRNAs are of critical importance in the function and differentiation of T helper cells. In order to address this, a number of specific objectives are set:

1. Identification of subset-specific patterns of miRNA expression, and the relationship of master-regulatory transcription factor expression and binding with miRNA expression patterns
2. Identification of candidate miRNA for functional investigation
3. Targeted analysis of the biological role of selected candidate miRNA

3. Materials and Methods

3.1. Mice

3.1.1. Source and breeding of mice

Wild-type C57BL/6 mice were purchased from Harlan Laboratories (Indianapolis, IN, USA). C57BL/6 RAG1-deficient mice were purchased from Jackson Laboratories (Bar Harbor, Maine, USA) and bred within the Biological Services Unit of King's College London (KCL) and at Charles River Laboratories (CRL; Kent, UK). mir-142 deficient mice were generated by Genoway S.A. (Lyon, France) and subsequently bred at KCL and CRL. All mice were bred and maintained in Specified Pathogen-Free (SPF) conditions and analysed between 6-12 weeks of age. All mice were handled according to both local (KCL) and national standards, and all experimental protocols involving rodents were reviewed and approved by our local ethics review committee and the UK Home Office (project license: PPL/70/6792).

3.1.2. Generation of constitutive and conditional mir-142 deficient mice

Mice were generated by Genoway S.A. as follows: A targeting vector was constructed for the purpose of homologous recombination, such that the wild-type mir-142 locus was flanked by loxP sites approximately 0.25 kilobases upstream and downstream, and a neomycin resistance cassette flanked by FRT sites was included within this region in order to allow antibiotic selection for recombination events occurring in embryonic stem (ES) cells (Figure 3.1).

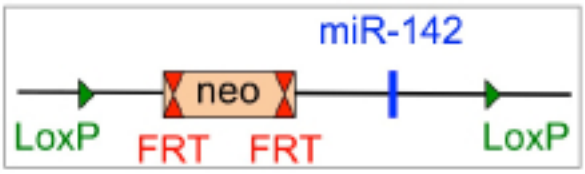

Figure 3.1 Schematic representation of mir-142 targeting construct (not to scale). Solid line represents chromosome sequence. LoxP: locus of X-over P1; FRT: flippase recombination target; neo: neomycin resistance cassette.

Following its construction, the targeting vector was linearised by restriction digest with the enzyme FseI and transfected into ES cells (129Sv background) according to Genoway's standard electroporation procedures ($5x10^6$ ES cells in presence of 40µg of linearised plasmid, 260 Volt, 500 µF). Positive selection was commenced 48hrs after transfection by culture in the presence of 200µg/ml G418. 134 resistant clones were isolated and selected to be screened for successful recombination, of which 3 were initially detected by 5' PCR to have undergone recombination (Figure 3.2). Further validation by 5' (Figure 3.3) and 3' (Figure 3.4) Southern Blot identified 2 ES cell clones in which successful recombination had occurred.

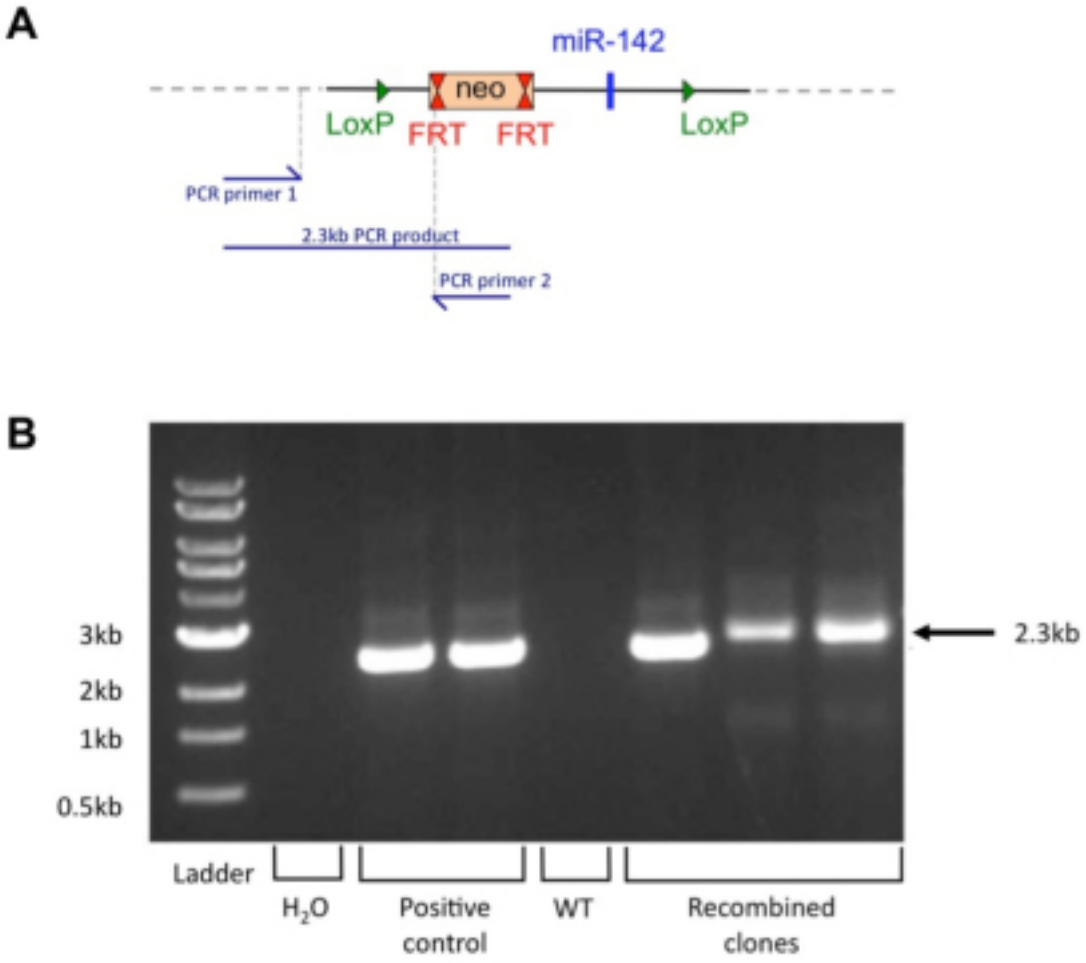

Figure 3.2 5' PCR validation of ES cell clones. A: Schematic depicting 5' PCR strategy for identification of recombination event in ES cell clones (not to scale). Solid line represents targeting vector, dashed line is flanking chromosomal DNA sequence. B: agarose gel electrophoresis of PCR products from 3 ES cell clones that were screened positive for recombination with targeting vector. Primer 1 hybridizes upstream of targeting vector homology sequence; primer 2 hybridizes within neomycin resistance cassette; positive control PCR was performed on a positive control vector designed to contain the binding site of both primers, mimicking the DNA sequence that occurs following homologous recombination between the mir-142 locus and the targeting vector. Data supplied by Genoway S.A.

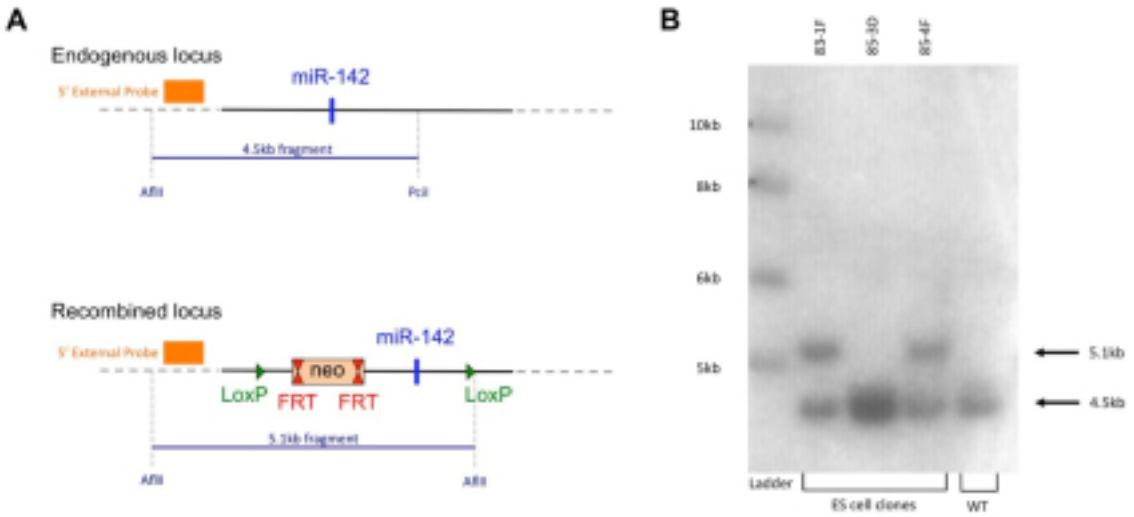

Figure 3.3 Southern Blot validation of 5' recombination. A: Schematic demonstrating expected sizes from endogenous wild-type mir-142 locus (upper panel) and recombined mir-142 locus (lower panel). Position of probe is indicated. B: Southern blot of genomic DNA from 3 selected clones, digested with AflII and PciI restriction enzymes, and probed with 5′ external probe. Successful 5′ recombination is identified in clones 83-1F and 85-4F. Data supplied by Genoway S.A.

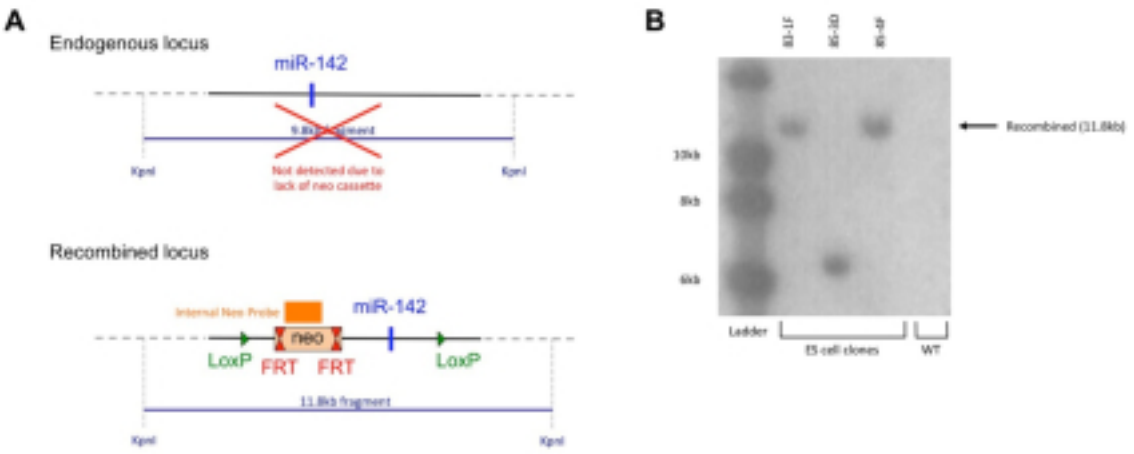

Figure 3.4 Southern Blot validation of 3' recombination. A: Schematic demonstrating expected size from recombined mir-142 locus (lower panel). Note that wild-type endogenous mir-142 locus (upper panel) is not positively identified by this assay as the neo probe is designed to hybridize with the neomycin resistance cassette. B: Southern blot of genomic DNA from 3 selected clones, digested with KpnI and probed with neo probe. Successful 3′ recombination is identified in clones 83-1F and 85-4F. Data supplied by Genoway S.A.

Recipient blastocysts were then isolated from pregnant C57BL/6 females, and recombined ES cell clones were injected into these. Injected blastocysts were then re-implanted into pseudo-pregnant OF1 mice and allowed to proceed until term. Offspring were assessed according to coat colour at 3 weeks of age, and highly chimeric males were then selected for further breeding. In order to generate constitutive mir-142 deficient mice, chimeras were bred with C57BL/6J Cre deleter mice. For the generation of conditional mir-142 deficient animals, chimeras were bred with C57BL/6J Flp deleter mice. Offspring were then assessed by PCR genotyping for occurrence of Flp or Cre mediated recombination (as appropriate). Mice heterozygous for either the constitutive or conditional mir-142 deficient allele were selected for further breeding. PCR genotyping was employed as detailed below in order to distinguish between homozygous mir-142 sufficient (mir-142$^{+/+}$, WT), heterozygous (mir-142$^{+/-}$) and homozygous mir-142 deficient (mir-142$^{-/-}$) genotypes, as well as those mice either heterozygous or homozygous for the mir-142 conditional allele (mir-142$^{fl/+}$ or mir-142$^{fl/fl}$, respectively).

3.1.3. Genotyping

Genomic DNA is isolated by overnight digestion at 56°C of ear or tail samples in 200µl of lysis buffer (5 mM EDTA, 100 mM Tris-HCl pH 8.5, 0.2% SDS, 200 mM NaCl, 1mg/ml Proteinase K). Digested samples are diluted 1:40 in nuclease-free water. PCR reaction comprises 12.5µl 2x Mango Mix (Bioline Ltd., London, UK), 10µl nuclease-free water, 1 µl each of PCR primers (diluted in nuclease-free water to 25µM), 0.5µl genomic DNA. Genotyping primers and reaction conditions are as listed in Table 3.1.

Genotype	Primers	Reaction conditions	Expected product size
Constitutive mir-142 deficient	31616bct-HOJ2: GAGGGAAGAAGGTTACA AAGAGGAAGTTGG 31617bct-HOJ2: AATAACAGAGTCAGACA AAAGCGAAACCAGTC	1: 94°C 2min 2: 94°C 30sec 3: 65°C 30sec 4: 68°C 60sec 5: Repeat steps 2-4 (35x) 6: 68°C 10min	WT: 0.7kb mir-142^{-}: 0.5kb
Conditional mir-142 deficient	31624flp-HOJ2: AGTGGCTGTGGTCTTTAC CTGAGTGTCC 31625flp-HOJ2: TTCCTTGATGTTGGAGTG GAGGACG	1: 94°C 2min 2: 94°C 30sec 3: 65°C 30sec 4: 68°C 60sec 5: Repeat steps 2-4 (35x) 6: 68°C 10min	WT: 450bp mir-142^{fl}: 541bp

Table 3.1 Genotyping PCR primer sequences, reaction conditions and expected product sizes

Sample genotyping results are shown in Figure 3.5.

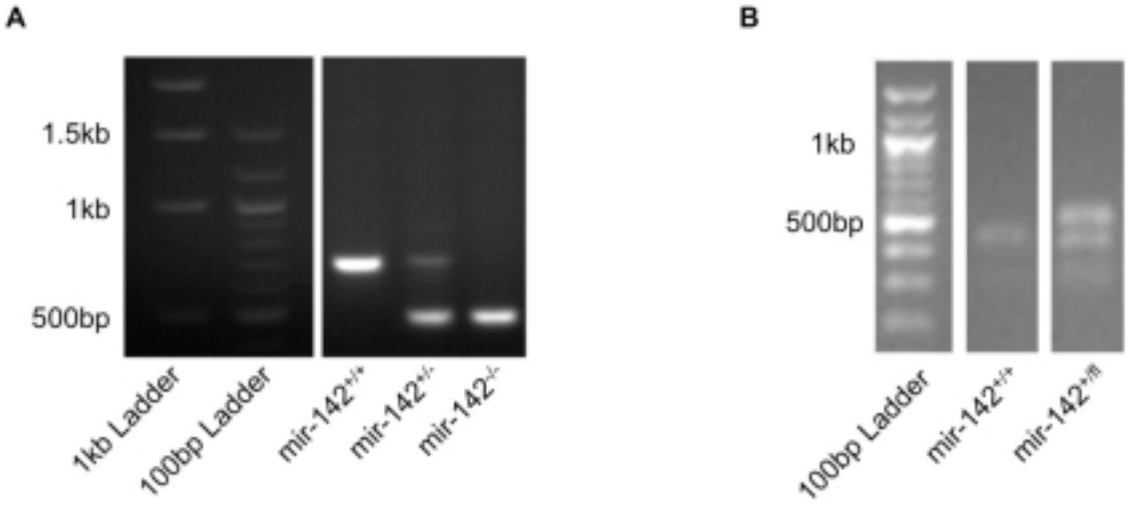

Figure 3.5 A: Agarose gel electrophoresis demonstrating representative results from PCR genotyping of constitutive mir-142 deficient mice. B: Agarose gel electrophoresis demonstrating representative results from PCR genotyping of conditional mir-142 deficient mice.

3.2. Cell isolation

3.2.1. Tissue harvest

Mice were euthanized by inhalation of a rising concentration of carbon dioxide gas, and then dissected in a laminar flow cabinet using aseptic technique. Spleen, thymus, mesenteric lymph nodes and peripheral lymph nodes (inguinal, axillary, cervical) were excised and placed in ice-cold complete cell culture medium (RPMI-1640 medium (PAA Laboratories, Pasching, Austria) supplemented with 10% (v/v) heat-inactivated fetal calf serum (FCS) "Gold" (PAA Laboratories), 10mM HEPES, 0.1mM non-essential amino acids (Gibco), 1mM sodium pyruvate (Sigma), 2μM L-glutamine (Sigma), 50μM 2-mercaptoethanol (Gibco), 50IU/ml penicillin and 50μg/ml streptomycin (Invitrogen Corp., Carlsbad, CA, USA)). Colon was excised and prepared by gentle expulsion of colonic contents, followed by flushing with ice-cold sterile PBS. Mechanical disruption of spleen, lymph node and thymus through nylon mesh was performed in order to prepare a single cell suspension suitable for further manipulation. Cell suspensions isolated from spleen were subjected to red blood cell lysis by resuspension for 2 minutes in ACK lysis buffer (0.15M NH_4Cl, 1mM $KHCO_3$, 0.1mM Na_2EDTA, pH 7.2-7.4). All cell washing and resuspension was performed with complete cell culture medium unless otherwise stated, and trypan-blue staining was used in order to assess cell viability and count live cells.

3.2.2. Magnetic cell isolation

$CD4^+$ cells were positively selected by incubation with anti-CD4 (L3T4) microbeads followed by gravity-flow separation using MACS LS columns mounted on a

quadroMACS magnet according to manufacturer's protocols (all reagents and equipment supplied by Miltenyi Biotec Gmbh, Bergisch Gladbach, Germany).

3.2.3. Flow cytometric cell sorting

Magnetically-enriched samples were incubated with the appropriate antibodies according to manufacturer's protocols. For isolation of naïve $CD4^+$ T cells, cells were stained with anti-CD4 APC-eFluor 780 (RM4-5; eBioscience), anti-CD62L Pacific Blue (MEL-14; eBioscience), anti-CD44 PE-Cy7 (IM7; eBioscience) and anti-CD25 (PC61.5; eBioscience). Samples were sorted with a BD FACS Aria II Special Order System fitted with a 70µm nozzle and running FACSDiva software version 5.0.1 (BD Biosciences, Franklin Lakes, NJ, USA). Sterile PBS was used as sheath fluid in order to maximise post-sort cell viability. Pre-sort samples were resuspended in sterile complete medium at $50x10^6$ cells/ml, and were kept at 4°C throughout. Software and machine were calibrated daily according to manufacturer's instructions, and a gating strategy was established in order to isolate desired cell populations as detailed below.

Gate sequence for isolation of naïve $CD4^+$ Cells:

1. Lymphocyte gate as defined by forward- and side-scatter area parameters
2. Doublet discrimination based on forward-scatter height and area parameters
3. $CD4^+$ cells
4. $CD62L^{high}$ $CD44^{low}$ cells
5. $CD25^-$ cells

Software was set to prioritise sample purity rather than yield. Post-sort sample purity was assessed by acquisition with identical settings and was typically greater than 98%

pure. Post-sort cell viability was assessed by trypan-blue exclusion staining and was typically greater than 95%. An example of pre- and post-sort sample phenotypes are shown in Figure 3.6.

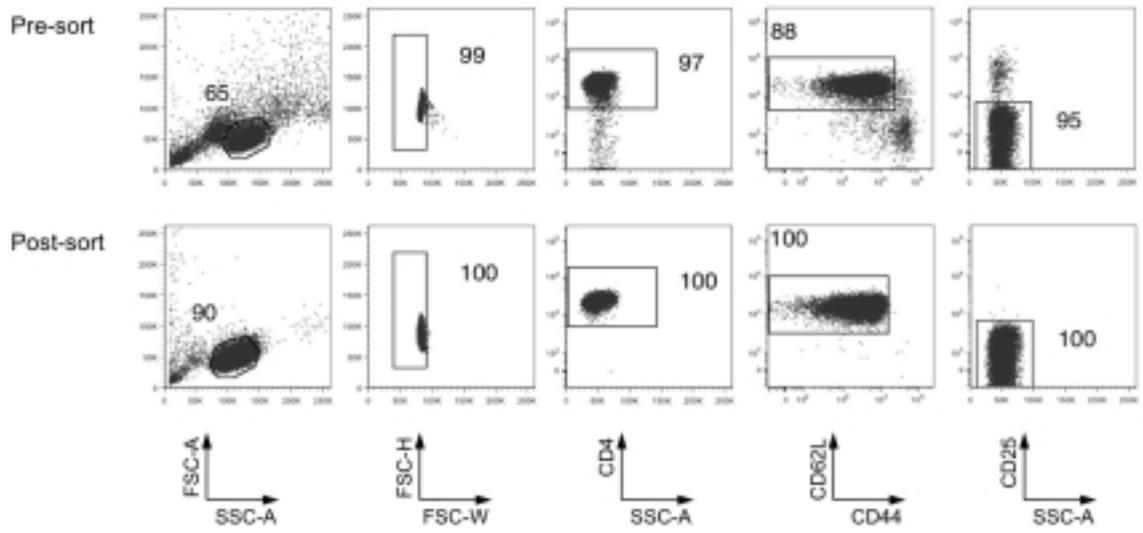

Figure 3.6 Naive CD4⁺ FACS sorting. Pre- and post-sort surface phenotypes are shown with parameters indicated below plots.

3.3. Cell culture

3.3.1. General considerations

Cells were cultured in complete cell culture medium as described in section 3.2.1., with the exception of 293T cells for which RPMI-1640 was substituted with high glucose (4.5g/L) DMEM medium (PAA Laboratories) and 2-mercaptoethanol was not supplemented. Cells were maintained at 37°C and 100% humidity in electronically regulated cell culture incubators.

3.3.2. T cell skewing

Cells were counted and plated at a concentration of $1x10^6$ cells/well of a 48 well tissue culture plate (Iwaki brand; Sterilin Ltd., Newport, UK). Plates were pre-coated overnight at 4°C with anti-CD3 antibody (2μg/ml; clone 145-2C11; BioXCell, West Lebanon, NH, USA) and anti-CD28 antibody (2μg/ml; clone 37.51; BioXCell), with the exception of Th17 cultures for which anti-CD28 antibody was omitted in favour of soluble anti-CD28 supplemented directly into the cell culture medium. Following 72hrs of activation with plate-bound antibodies, cells were removed from culture and split 1:2 into a new plate. Thereafter, cells were split 1:2 on a daily basis or as the progress of cell proliferation dictated. In order to promote cell differentiation into various subsets, a cocktail of antibodies and cytokines was supplemented into the cell culture medium as appropriate, details of which are listed in Table 3.2.

Skewing condition	Supplemented cytokine/antibody	Concentration
Th0	IL-2	20ng/ml
Th1	IL-2	20ng/ml
	IL-12	20ng/ml
	Anti-IL-4	5μg/ml
Th2	IL-2	20ng/ml
	IL-4	20ng/ml
	Anti-IFN-γ	20μg/ml
iTreg	TGF-β1	3ng/ml
	IL-2	20ng/ml
Th17	TGF-β1	2ng/ml
	IL-6	20ng/ml
	IL-1β	10ng/ml
	Anti-IFN-γ	20μg/ml
	Anti-IL-4	5μg/ml
	Anti-CD28	5μg/ml

Table 3.2 Culture conditions for skewing of $CD4^+$ T helper cell subsets.

Cytokines were obtained as follows: IL-2 and TGF-β1 (recombinant human; R&D Systems, Abingdon, UK); IL-4, IL-12, IL-6, IL-1β (recombinant murine; eBioscience). Anti-IFN-γ (clone XMG1.2) and anti-IL-4 (11B11) were purchased from BioXCell.

3.4. Cell labelling

In order to track proliferation of cells *in vitro* and *in vivo*, cells were labelled with fluorescent cell labelling dyes for certain experiments. Carboxyfluorescein succinimidyl ester (CFSE) labelling was performed by incubation of $2x10^6$ cells/ml at 37°C in a pre-warmed PBS / 2μM CFSE (Invitrogen) solution for 6 minutes. CellTrace Violet (Invitrogen) labelling was performed in the same way but with a 2μM CellTrace Violet / PBS solution substituting for the CFSE / PBS solution. Following incubation, ice-cold

complete cell culture medium of 10x the staining volume was used to quench the labelling process; cells were then washed twice, counted and assessed for viability by Trypan blue staining.

3.5. Gene Cloning

3.5.1. General methods

A number of genes and genetic sequences were cloned for the purpose of this study. Cloning PCR was performed on template DNA using the high-fidelity *Thermococcus*-derived DNA polymerase Pfx (Accuprime Pfx Supermix; Invitrogen) according to manufacturer's instructions, in order to minimise the introduction of mutations. Source templates included genomic (isolated by ethanol precipitation from digested mouse tail sample or lysed human blood from healthy volunteer) and cDNA (generated by reverse transcription of RNA isolated from cell cultures). Amplified DNA bands corresponding to the expected size were excised following agarose gel electrophoresis of PCR products and purified using the Montage gel purification kit (Millipore, Billerica, MA, USA) according to manufacturers instructions. DNA was precipitated overnight at -20°C by addition of 340µl of 100% ethanol, 40µl of 3M sodium acetate and 2µl of linear acrylamide per 100µl of purified gel slice. This was then centrifuged at 15000g for 15 minutes in order to produce a visible pellet, which was then washed with 70% ethanol and finally resuspended in 20µl of nuclease-free water. The concentration of DNA was then determined by using a NanoDrop spectrophotometer (Thermo Fisher Scientific Inc., Waltham, MA, USA). This PCR product was then blunt ligated into the pCR-BLUNT-II TOPO vector (Invitrogen) according to manufacturer's instructions, and transformed into TOP-10F ultracompetent *E. coli* bacteria (Invitrogen) to allow for

subsequent identification of successful cloning events. Bacteria were streaked onto LB Agar coated 7.5cm Petri dishes in the presence of 50μg/ml Kanamycin (Sigma-Aldrich Co. LLC, St. Louis, MO, USA) and cultured at 37°C for 16 hours in a bacterial oven. Individual colonies were inoculated into 2ml of LB broth containing 50μg/ml Kanamycin and cultured in a bacterial shaker at 37°C for 16 hours. Plasmid DNA was then isolated from individual cultures using Plasmid Miniprep kit (Qiagen Inc., Valencia, CA, USA) according to manufacturers instructions. Restriction digest was then performed using appropriate restriction enzymes (New England Biolabs Inc., Ipswich, MA, USA) according to the manufacturer's instructions. Digested plasmid DNA was analysed by agarose gel electrophoresis for the presence of bands of the expected sizes. Clones exhibiting appropriate digest patterns were selected for large-scale plasmid production and were inoculated into 250ml of LB broth in the presence of 50μg/ml Kanamycin, which was then cultured in a bacterial shaker at 37°C for 16 hours. Plasmid DNA was isolated from this culture using the Plasmid Maxiprep kit (Qiagen), and was then sent for commercial sequencing (Source Bioscience LifeSciences plc, Nottingham, UK), of the insert using the M13F and M13R primers to ensure that it corresponded with the expected sequence and to determine the presence of any mutations. Following verification of insert sequence, both the pCR-BLUNT II TOPO cloning plasmid and the desired target vector plasmid were digested using restriction enzymes corresponding to the appropriate restriction sites. Digested vector and insert were then isolated by agarose gel electrophoresis, gel band purification and ethanol precipitation as described previously. Digested gel band was then ligated into the target vector using T4 DNA ligase (New England Biolabs) according to the manufacturer's instructions, and with the quantity of insert and vector calculated using the following formula (Figure 3.7):

$$\text{insert mass (ng)} = \frac{\text{vector mass (ng)} \times \text{insert length (bp)}}{\text{vector length (bp)}} \times \text{insert:vector ratio}$$

Figure 3.7 Formula used for calculation of ligation reaction concentrations.

Typically an insert:vector ratio of 3:1 or 1:1 was used in order to optimise ligation efficiency. The product of the ligation reaction was then transformed into XL-2 Blue ultracompetent *E. coli* bacteria (Agilent Technologies Inc., Santa Clara, CA, USA) according to the manufacturers instructions. Bacteria were then streaked on LB Agar coated 10cm Petri dishes in the presence of Ampicillin at a concentration of 100µg/ml (Sigma-Aldrich), and cultured at 37°C for 16 hours in a bacterial oven. All vectors used in this study confer ampicillin resistance with the exception of pCR-BLUNT-II TOPO (confers Kanamycin-resistance). Again, individual colonies were inoculated into 2-ml ampicillin-containing LB broth and cultured in order to isolate plasmids by Miniprep processing, which were then analysed by restriction digest for the presence of the appropriately-sized insert. Verified clones were then cultured for Maxiprep processing in order to generate sufficient quantity for both final sequence verification and *in vitro* experiments such as transfection of 293T cells.

3.5.2. Methods of generation of specific constructs

A list of primers and engineered restriction sites for primary gene cloning experiments performed in the course of this study are shown in Table 3.3.

Construct Name	PCR Cloning Primers	Restriction Sites	Description
pMSCV-eGFP-mRARG	mRARGF-1: AGATCTGCCACCATGGCCACCAATAAG mRARGR-1: GAATTCTCAGGGCCCCTGGTCAGGTTG	5'BglII -> 3' EcoRI	RARγ expression construct
pCSGW-eGFP-hmir-142	hmiR142F-2: TTTGGATCCAGTCACCGCCCACAAGGCCC hmiR142R-2: ATACTCGAGAGGAAGGGCAGGAAAGCCATGGAG	5' BamHI -> 3' XhoI	hmir-142 expression construct
pSI-CHECK2-RARG-3U	RARG3U1-F: CTCGAGCCTACCCCGTTGTGGGGTT RARG3U1-R: GCGGCCGCTTGAGTTTCCATCACTTTATTTTGC	5' XhoI -> 3' NotI	RARγ 3'UTR luciferase construct

Table 3.3 PCR primers, restriction sites for ligation and description of constructs used in this work

The vectors pMSCV-GFP-mir142 and pMSCV-GFP-mir181a were generated prior to this study by Prof. Graham Lord and Mr. Ian Jackson. The vectors pMIG and pMIG-DN-T-bet were generous gifts from Prof. Steven Reiner, University of Pennsylvania, USA. The vectors pMY and pMY-Cre were generous gifts from Prof. Matthias Merkenschlager, Imperial College London, UK. Vectors were subjected to sequencing prior to use, and results were compared against published reference sequences.

3.6. Retroviral transduction

3.6.1. Production of retrovirus

In order to produce high titre retrovirus for the purpose of infecting primary T cells, HEK-293T cells (Clontech Laboratories Inc., Mountain View, CA, USA) were transiently transfected with appropriate constructs using the following calcium

phosphate-mediated method. $1x10^6$ HEK-293T cells were plated on 7.5cm tissue culture plates (Nunclon Surface; Thermo Fisher Scientific) in fully supplemented high glucose DMEM medium as described in section 3.3.1. At 48 hours following initiation of culture, and when cells had typically reached approximately 50% confluency, chloroquine was supplemented into culture medium to a final concentration of 25μM. Cells were then incubated at 37°C for 30 minutes prior to transfection. Calcium phosphate transfection was performed as follows: 200μl of 1.25M $CaCl_2$ was transferred into a sterile 50ml tube. For production of retrovirus intended for infection of murine cells, 5μg of desired expression plasmid and 5μg of pCL-Eco plasmid (Imgenex, San Diego, CA, USA), which provides the retroviral genes gag, pol and ecotropic env, were added into this mix. Sterile nuclease-free water was then added to produce a final volume of 1ml in total. After mixing thoroughly, 1ml of 2x HEPES-buffered saline (Fluka brand; Sigma-Aldrich) was slowly pipetted dropwise into this solution whilst bubbling constantly with a Pasteur pipette. This calcium phosphate-DNA mix was then added evenly onto the HEK-293T cells by dropwise pipetting, and mixed with culture medium by gently swirling the plate. Plates were returned to the incubator for 6 hours, after which time the medium was carefully removed, cells were washed once by gentle addition and removal of 10ml pre-warmed PBS, and 10ml of medium was then added to the plates. After a period of 24 hours further culture, this medium was then removed from the plates, filtered through a 45μm sterile filter, and aliquoted for storage at -80°C until it was needed for transduction. Where appropriate, a sample of HEK-239T was removed for assessment of transfection efficiency by flow cytometric evaluation of fluorescent marker (e.g. GFP) expression.

3.6.2. Transduction of T cells

T cell transduction was performed at 24 hours after the initiation of cell culture. Cells had been plated at a concentration of $1x10^6$ cells/well in a 48 well plate, in 1ml of complete culture medium. Frozen viral supernatant aliquots (prepared as described in section 3.6.1) were thawed on ice. 500µl of medium was removed from cell culture wells and carefully replaced with 450µl of this viral supernatant. A further 50µl of cell culture medium supplemented with 10X concentration skewing cytokines and antibodies was added at this stage, in addition to polybrene (hexadimethrine bromide; Sigma-Aldrich) to a final concentration of 8µg/ml. Any residual viral supernatant that was thawed but unused was discarded rather than refrozen. Plates were then centrifuged at 2500xg for 1 hour at 32°C. Cells were then incubated for a further 12 hours at 37°C, at which point the entire culture medium was carefully removed, discarded and replaced with fresh cell culture medium supplemented with the appropriate skewing cytokines and antibodies. Cell culture then proceeded as normal, with removal from activation at day 3 and splitting of cells as appropriate. A small aliquot (50µl of 1ml resuspended cells) was typically sampled for analysis of transduction efficiency at day 4.

3.7. Flow cytometry

3.7.1. Equipment and software

Samples were acquired using identically configured BD LSR II and BD LSRFortessa (BD Biosciences) flow cytometers. Sample data was recorded in FCS 3.0 data format using BD FACSDiva 6.0 software (BD Biosciences). Sample analysis was performed using FlowJo software for MacOS (Versions 8 and 9, Treestar Inc., Ashland, OR, USA).

3.7.2. Reagents

The following table lists antibodies used in flow cytometry experiments for this study.

Antigen	Clone	Conjugate(s)	Supplier
CD3	17A2	FITC, PE, eFluor450	eBioscience
CD4	RM4-5	FITC, PE, APC, APC-eFluor780, PE-Cy7	eBioscience
CD8a	53-6.7	PE	eBioscience
CD19	MB19-1	FITC	eBioscience
B220	RA3-6B2	FITC	eBioscience
CD62L	MEL-14	FITC, eFluor450	eBioscience
CD44	IM7	PE, PE-Cy7	eBioscience
CD25	7D4 / PC61.5	PE, APC, APC-eFluor780	eBioscience / BD
NKp46	29A1.4	Alexa Fluor 647	eBioscience
CD11c	N418	APC	eBioscience
MHC Class II	M5/114.15.2	PE	eBioscience
T-bet	4B10	eFluor660	eBioscience
FoxP3	FJK-16s	APC	eBioscience
IFN-γ	XMG1.2	FITC, PE, APC, PE-AlexaFluor610	eBioscience / Invitrogen
IL-4	11B11	APC	BD
IL-17A	eBio17B7	FITC, APC	eBioscience
IL-2	JES6-5H4	PE, APC	eBioscience

Table 3.4 Flow cytometry antibodies used in this study.

3.7.3. Surface antigen staining

Cells were harvested and washed once with PBS, and then counted. The following staining protocol is designed for staining a total of $1x10^6$ cells and was scaled where

appropriate for varying cell numbers. Cells were resuspended in 100µl of PBS, and then blocked by adding 100µl of 50% FCS / PBS solution, in order to reduce the degree of non-specific binding. Where appropriate (e.g. staining of whole spleen), 0.5µg of anti-CD16/32 blocking antibody (FcBlock; BD Biosciences) was also added.

3.7.4. Intracellular cytokine staining

In order to perform intracellular cytokine staining for this study, the following protocol was used. Cells were harvested, washed with PBS and counted. $1x10^6$ cells were plated per well in a 48 well plate in 1ml of complete cell culture medium. Cells were then stimulated by supplementation of 50ng/ml phorbol 12-myristate 13-acetate (PMA; Sigma) and 1µg/ml ionomycin (Sigma) for 4.5 hours. In addition, 2µM monensin (Sigma) was added for the final 2 hours in order to inhibit intracellular protein transport. Cells were then harvested, washed with PBS and then stained for surface antigens as described in section 3.7.3, and for viability as described in section 3.7.6. Following this, cells were washed once with PBS and then fixed by resuspending cells in 1ml 4% formaldehyde (Thermo Fisher Scientific) for 10 minutes at room temperature. Cells were then washed once with cold PBS, and a second time with a 0.1% Saponin (Thermo Fisher Scientific) / 1% FCS / PBS cell permeabilisation solution. Cells were then blocked with a 50% FCS / 0.1% Saponin / PBS solution for 10 minutes at 4°C in order to reduce non-specific antibody labelling, followed by staining with appropriate antibodies in 0.1% Saponin / 1%FCS / PBS solution at 4°C for 20 minutes. Cells were then washed once with cell permeabilisation solution and resuspended in PBS prior to acquisition.

3.7.5. Intranuclear staining

Cells undergoing staining for transcription factors were stimulated as described in section 3.7.4. In order to stain for T-bet, no further modification to the intracellular cytokine staining protocol was necessary. In order to stain optimally for FoxP3, the following protocol was used. Stimulated cells were washed once with PBS and stained for any surface antigens as necessary. Cells were then resuspended in 1ml of 1X FoxP3 fixation/permeabilisation buffer (eBioscience) for 16 hours. Cells were then washed twice with 1X FoxP3 permeabilisation buffer (eBioscience) and blocked with 50µl of 50% FCS / 1X FoxP3 permeabilisation buffer and 0.5µg FcBlock (where appropriate) for 10 minutes at room temperature. 0.5µg of anti-FoxP3-APC antibody (eBioscience) was then added and cells were stained for a further 30 minutes at 4°C. Cells were washed once with 1X permeabilisation buffer and then resuspended in FCS prior to acquisition.

3.7.6. Apoptosis and cell viability staining

A number of different reagents were used in this study for assessment of cell viability and apoptosis. Cell viability was typically assessed by staining with the commercial dyes LIVE/DEAD® Yellow and LIVE/DEAD® Aqua (Invitrogen). This was performed by resuspending cells in 1ml of a 1/1000 dilution of LIVE/DEAD® reagent in PBS for 15 minutes at room temperature, prior to any cell fixation or permeabilisation steps in the staining protocol. Alternatively, in some cases Propidium Iodide (PI; Invitrogen) was used as a cell viability indicator, by resuspension of unfixed, unpermeabilised cells in a 3µM PI / PBS solution immediately prior to acquisition of the sample.

Annexin V staining was used in most cases as a marker of apoptosis, and was performed as follows. Cells were isolated, washed with cold PBS, counted and stained where appropriate with cell viability reagent. $1x10^6$ cells were then washed with 1X Annexin V binding buffer (eBioscience and BD Biosciences) and then resuspended in a 100µl volume of this buffer. 5µl of Annexin V staining reagent was then added. Staining reagent was either conjugated to eFluor-450 fluorochrome (eBioscience) or PE fluorochrome (BD Biosciences). Cells were incubated for 15 minutes at room temperature, washed with 1X binding buffer and resuspended in 500µl of 1X binding buffer immediately prior to acquisition. Where appropriate, PI was added to this solution to a final concentration of 3µM. In a small number of cases, the activated caspase detection reagent CaspACE (Fitc-VAD-FMK; Promega Corp., Madison, WI, USA) was used as a marker of apoptosis. This was stained for by addition of CaspACE to a final concentration of 10µM into cell culture wells containing $1x10^6$ cells in 1ml of complete cell culture medium, for 20 minutes in a 37°C incubator. Cells were then washed and subjected to either further staining for cell viability or acquired immediately.

3.8. RNA extraction

RNA extraction was performed using Trizol reagent (Invitrogen), within a dedicated RNA work area. Equipment and surfaces were cleaned with RNaseZap solution (Ambion Inc., Austin, TX, USA) prior to use to reduce potential nuclease contamination of samples. Cells were pelleted, in some cases after 5 hours of anti-CD3/CD28 restimulation, and resuspended in a minimum of 1ml Trizol up to a maximum of $1x10^7$ cells/ml. Following thorough resuspension, cells were either processed immediately or stored at -80°C for up to 1 month prior to extraction. 200µl chloroform (Sigma Aldrich)

was first added to fresh/thawed samples, with the sample then mixed thoroughly and incubated at room temperature for 2 minutes. This was then centrifuged at 12000xg for 15 minutes at 4°C prior to allow phase separation. The upper colourless (aqueous) phase was carefully transferred to a fresh tube without disturbing the interphase, and 500µl of ice-cold isopropanol was then added. After vortex-mixing, the sample was centrifuged for 15 minutes at 4°C, at which point a pellet was observed. The supernatant was carefully removed; the pellet was then washed with 1ml 75% ethanol and centrifuged for a further 5 minutes at 7500xg. The supernatant was then removed and the pellet allowed to air dry prior to resuspension in an appropriate volume of nuclease-free water. Samples were then assessed for quality, contamination and RNA concentration by analysis with a NanoDrop spectrophotometer. RNA was then stored at -80°C pending further analysis.

3.9. Microarrays

3.9.1. microRNA microarrays

microRNA microarrays were processed by Cepheid Inc., at their research facility in Toulouse, France. Total RNA was first quantified using a NanoDrop spectrophotometer. RNA quality was then assessed using the 2100 Bioanalyzer capillary electrophoresis platform with the 6000 Nano RNA chip (both Agilent Technologies). Samples that had passed these quality control assays were then subjected to size fractionation using the FlashPAGE electrophoresis chamber (Ambion) according to manufacturer's instructions, which selectively purifies the RNA fraction with size <40nt. RNA was then 3' labelled by overnight ligation of a UUUU-Cy5 fluorescent tag. Control oligos were then spiked into samples at known concentrations in order to perform cross-chip normalisation.

Labelled RNA was hybridized overnight to pre-prepared microarray slides, and fluorescence was then measured using the GenePix 4000A scanner in conjunction with GenePix Pro Software (Molecular Devices, Sunnyvale, CA, USA). Scanned images were manually checked for errors or defects in hybridization and scanning. Microarrays were designed by Cepheid to incorporate all known miRNAs conserved between human and mouse (published in miRBase 11.0), in addition to over 2000 predicted conserved miRNAs that had been generated by computational analysis of the genome by Cepheid's proprietary algorithms.

3.9.2. Whole genome microarrays

Whole genome microarrays were processed at the Genomics Centre, King's College London (KCL). Briefly, RNA was quantified with NanoDrop spectrophotometer and subjected to Bioanalyzer quality control as described in section 3.9.1. For cDNA synthesis and labelling where total RNA quantity was greater than 50ng for all samples, sample preparation was performed using the Whole Transcript cDNA Synthesis and Labelling Kit (Affymetrix Inc., Santa Clara, CA, USA) according to the manufacturer's instructions. Where total RNA quantity was less than 50ng in at least one sample, the Ovation Pico WTA System (NuGEN Technologies Inc., San Carlos, CA, USA) was used for cDNA synthesis and amplification, followed by labelling using the Affymetrix kit. Samples were hybridized to the Affymetrix Mouse Gene 1.0 ST array according to manufacturer's protocols and then scanned for fluorescence with the Affymetrix GeneChip 3000 7G scanner. Scanned images were analysed with the Microarray Analysis Suite 5.0 algorithms incorporated into GeneChip Operating Software (Affymetrix) with default settings.

3.9.3. Microarray data analysis

A number of software platforms were used for analysis of microarray data. Affymetrix gene expression microarrays were annotated, normalised and filtered using multiple Bioconductor (http://www.bioconductor.org) libraries within the R statistical computing environment (version 2.12.1; http://www.r-project.org). The core Bioconductor set was installed, comprising the following packages: affy, affydata, affyPLM, affyQCReport, annaffy, annotate, Biobase, biomaRt, Biostrings, DynDoc, gcrma, genefilter, geneplotter, GenomicRanges, hgu95av2.db, limma, marray, multtest, vsn, and xtable. The package 'oligo' (version 1.16.0) and its dependents were installed and used to import and normalise arrays using the Robust Multiarray Average (RMA) method (Irizarry et al., 2003). The package 'annaffy' (version 1.24.0) was used to annotate array data with annotations from the 'mogene10sttranscriptcluster.db' (version 7.0.1) annotation database. Data was exported, either as the entire dataset or restricted to specific gene subsets, into tab-delimited text files suitable for import into software such as Microsoft Excel (Office 2011; Microsoft, Seattle, WA, USA). Heatmap visual representations of data and self-organising map (SOM) analysis was produced using MayDay software (http://www-ps.informatik.uni-tuebingen.de/mayday/wp/) (Battke et al., 2010).

3.10. Enzyme-Linked Immunosorbent Assay (ELISA)

Secreted protein levels were quantified by ELISA as follows. $1x10^6$ T cells were washed, plated in 1ml of complete cell culture medium and activated for 24 hours with plate-bound anti-CD3 and anti-CD28 antibody (both 2µg/ml; BioXCell). Supernatant was then carefully harvested and stored at -80°C for up to 1 month prior to ELISA

analysis. DuoSet ELISA kits (R&D Systems) were used for all ELISAs, and comprised capture antibody, biotinylated detection antibody, protein reference standard and streptavidin-HRP (horse radish peroxidase) reagent. 96 well ELISA plates (Nunc Immunosorp; Thermo Fisher Scientific) were pre-coated overnight at 4°C with 100µl 1X capture antibody / reagent diluent (0.1% bovine serum albumin (BSA) / PBS) solution as per manufacturer's instructions. Wells were washed by aspiration of coating antibody solution followed by three cycles of filling all wells with 300µl wash buffer (0.05% Tween (Sigma Aldrich) / PBS) followed by aspiration. Wells were then blocked by addition of 300µl of a 1% BSA / PBS solution for 1 hour at room temperature. Wash step was repeated. Samples and reference standard were then diluted as appropriate in reagent diluent and 100µl was added to each well. Samples were typically tested in duplicate at varying concentrations. Reference standard followed a two fold serial dilution from the top concentration suggested in the individual product literature. Samples were incubated for 2 hours at room temperature, after which the wash cycle was repeated. 100µl of 1X detection antibody / reagent diluent solution was then added per well and incubated for 2 hours at room temperature, followed by a repeated wash cycle. Diluted streptavidin-HRP was then added into each well and incubated for 20 minutes at room temperature, followed by a repeated wash cycle. 100µl Tetramethyl benzidine (TMB) chromogen solution (Invitrogen) was added to each well and incubated for 20 minutes at room temperature during which time a colour change was observed. Reaction was stopped by addition of 50µl 0.5M sulphuric acid (H_2SO_4). Optical density (OD) at 450nm wavelength was measured using a Bio-TEK EL800 plate reader (Wolf Laboratories, UK). The standard curve was computed by KCjunior software (Wolf Laboratories) using optical densities of known concentrations of

reference standard; this was then used to calculate protein concentration in individual samples.

3.11. Reverse transcription-quantitative PCR (RT-PCR)

In order to quantify RNA expression levels in individual samples, RT-PCR was used. The protocol used for the majority of genes (herein termed 'standard RT-PCR') differed from the protocol used for mature miRNA RTPCR; protocols for both are detailed here.

3.11.1. Standard RT-PCR

Following assessment of RNA quality and concentration using the NanoDrop spectrophotometer (Thermo Fisher Scientific), reverse transcription (RT) was first performed on 100ng of total RNA. The iScript Select cDNA Synthesis kit (Bio-Rad Laboratories, Hercules, CA, USA) was used according to manufacturer's instructions with oligo(dT) primers. Reaction mix was incubated at 42°C for 60 minutes followed by 5 minutes at 85°C in order to heat-inactivate reverse transcriptase. Control reactions in which reverse transcriptase was not added (-RT samples) were also performed for each sample. RT product was then either used immediately or stored at -80°C. Quantitative PCR (qPCR) was performed using Applied Biosystems (Foster City, CA, USA) TaqMan gene expression assays. An internal reference control assay specific for mouse β-actin (*Actb*) was added to each well. A final reaction volume of 10µl comprising 5µl 2X TaqMan Gene Expression Master Mix, 0.5µl TaqMan gene-specific expression assay (FAM-conjugated), 0.5µl TaqMan reference control gene assay (VIC-conjugated), sample cDNA and nuclease-free water to 10µl was added to each well of a 384-well plate (Applied Biosystems), with samples assayed in duplicate. qPCR was performed

using the 7900 HT Fast Real-Time PCR System (Applied Biosystems) running SDS version 2.3 software. Thermal cycling protocol was as follows: 95°C for 10 minutes, followed by 40 cycles of amplification (each cycle comprising 95°C for 15 seconds followed by 60°C for 60 seconds). Amplification curves were verified by manual inspection for all samples and for negative (-RT) controls. Ct (cycle threshold) values were automatically calculated by SDS software and exported to tab-delimited text files. Relative quantification of expression was calculated for further comparative analysis, by first subtracting mean Ct values of the gene of interest from mean Ct value for *Actb* to provide the ΔCt value. Relative quantification was then calculated using:

$$\text{Relative Quantification (RQ)} = 2^{-\Delta Ct}$$

3.11.2. MicroRNA RT-PCR

In order to measure miRNA expression, RT was first performed using Applied Biosystems proprietary stem-loop hairpin RT primers according to manufacturer's protocol. This required separate RT reactions for each miRNA of interest in each sample. In addition, -RT reactions were performed for each miRNA in each sample. U6 small nuclear RNA (snRNA) was used as a reference control gene for each sample since its expression is relatively stable between different samples (Mr. David Vilanova, Cepheid Inc., personal communication). 10ng of total RNA was used for each RT reaction. RT reaction was performed in a thermal cycler using the following programme: 16°C for 30 minutes, 42°C for 30 minutes, 85°C for 5 minutes, 4° hold. Quantitative PCR was then performed using a similar protocol to the standard RT-PCR detailed in section 3.11.1. The only modifications were that internal control *Actb* was not multiplexed in each well, and that 2X TaqMan Universal PCR MasterMix No

AMPErase UNG (Applied Biosystems) was used as per manufacturer's suggestion. qPCR thermal cycling, data acquisition and data analysis were all performed in the same way as in section 3.11.1.

A list of Applied Biosystems RT-PCR assay that were used in this study is shown in Table 3.5.

Gene	Assay Identifier
Tbx21	Mm00450960_m1
Gata3	Mm00484683_m1
FoxP3	Mm00475162_m1
Rora	Mm00443103_m1
Rorc	Mm01261022_m1
Ifng	Mm01168134_m1
Il4	Mm00445259_m1
Il17a	Mm00439618_m1
Il21	Mm00517640_m1
Il22	Mm00444241_m1
Actb	Mm00607939_s1
pri-mir-142 miRNA primary transcript	Mm03306331_pri
miR-142-3p mature miRNA	000464
miR-142-5p mature miRNA	002248
U6 snRNA	001973

Table 3.5 List of Applied Biosystems TaqMan Assays used in this study

3.12. Northern Blot

Northern blot was performed for the detection of miR-142-3p and miR-142-5p RNA in collaboration with Dr. Rong Dong, a member of our research group. Total RNA was isolated using the Trizol method described in section 3.8. 40μg of total RNA in RNA sample loading buffer (Sigma Aldrich) was loaded into each well of a 1% denaturing formaldehyde-agarose gel. Following electrophoresis, RNA was transferred onto Hybond-N+ membrane (GE Healthcare UK Ltd., Little Chalfont, UK). Chemiluminescent miRNA Northern Blot kits (Signosis Inc., Sunnyvale, CA, USA) specific for miR-142-3p and miR-142-5p were used for detection of miRNA, according to manufacturer's instructions. Briefly, hybridization was performed by overnight incubation under rotation at 42°C in the presence of biotin-labelled miRNA probes. After washing, membrane was incubated with streptavidin-HRP, then washed again, and finally incubated with detection substrate. Detection was performed with the Hyperfilm imaging system (GE Healthcare).

3.13. Bone marrow transfer

Bone marrow was harvested from donor animals by dissection of femur and tibia, taking care to strip associated soft tissue, followed by flushing of bone marrow content with sterile PBS. Recovered bone marrow was disrupted through sterile nylon mesh before being washed with PBS, centrifuged and counted. Bone marrow chimeric animals were generated by sublethal irradiation of RAG-1 deficient mice with 3.5Gy from a caesium-137 source. $1x10^6$ BM cells were injected intravenously in a volume of 100μl PBS into the tail vein of recipient mice on the day of irradiation. Mice were

weighed immediately prior to irradiation; weights were thereafter monitored weekly and mice were inspected daily for signs of illness or distress such as inactivity, diarrhoea, reduced grooming and postural changes. A safety cut-off point of weight loss to 80% of starting weight was imposed; if any animal reached this limit the experiment would be terminated. Otherwise, the experiment was terminated at four weeks following injection. Recipient mice were euthanized by CO_2 inhalation and dissected for harvest of lymphoid organs.

3.14. *In vivo* T cell transfer

Naïve or *in vitro*-activated T cells were harvested, washed twice and counted. Cells were resuspended in sterile PBS at an appropriate concentration, and injected intraperitoneally into RAG-1-deficient mice. For longer-term (greater than 1 week) experiments, $0.5x10^6$ naïve cells were injected, and $1x10^6$ activated T cells were injected. For short-term *in vivo* studies, $2.5x10^6$ cells were injected. As described in section 3.13, mice were weighed prior to cell transfer, and both condition and weight were monitored throughout with the same safety cut-off point (80% of initial weight). Experiments were terminated at 4 weeks following transfer in experiments in which naïve T cells were transferred and 3 weeks when activated cells were transferred. Mice were euthanized by CO_2 inhalation and lymphoid organs and colon were harvested for further analysis.

3.15. Histology

Samples were fixed for histology by immersion in pre-filled 10% neutral buffered formaldehyde specimen containers (Leica Microsystems (UK) Ltd., Milton Keynes, UK), and then embedded in paraffin wax by standard procedures. Tissue sections (5μm thickness) were cut by microtome, fixed onto glass slides and stained with haematoxylin and eosin by standard methods.

3.16. Immunohistochemistry

Fluorescent immunohistochemistry was performed by Dr. Ellen Marks as follows. Tissue samples were snap frozen in Jung tissue freezing medium (Leica Microsystems). 7 μm cryostat sections were fixed in acetone and then blocked with 20% normal horse serum (PAA Laboratories). Sections were incubated with anti-CD3-Fitc (eBioscience), anti-B220-biotin (eBioscience), followed by streptavidin-conjugated Alexa594 (Invitrogen). Nuclei were visualised by staining with 1μg/ml DAPI (Invitrogen). Images were acquired with an Olympus BX51 microscope using Micro-Manager software (Vale Laboratory, University of California San Francisco).

3.17. Luciferase Assay

Luciferase assay was used to validate targeting of specific 3'UTRs by specific miRNAs. The vector pSI-CHECK2 (Promega) was used, which contains a multiple cloning site (MCS) downstream of the Renilla luciferase gene, and a separate firefly luciferase gene on the same plasmid, which serves as an internal control for transfection efficiency.

3'UTRs of interest were cloned into the MCS and sequence-verified. HEK-293T cells were used for the assay, and were plated at a density of $1x10^4$ cells per well in a 24 well plate (Nunclon Surface, Thermo Fisher Scientific) 24 hours prior to transfection. Transfection was performed using the calcium phosphate method described in section 3.6.1, with the exception that 200µl of the transfection mix was added to each well. A total of 10ng of pSI-CHECK2 vector was used and 1µg of expression vector per well. Transfections were performed in triplicate. At 24 hours following transfection, cells were washed with PBS and lysed by gentle shaking for 15 minutes in the presence of 100µl of Passive Lysis Buffer (Promega). Lysate was analysed for firefly and renilla luciferase activity using the Dual Luciferase Reporter System (Promega), according to manufacturer's instructions; luminescence was measured with a LUMAT LB 9507 luminometer (Berthold Technologies GmbH, Bad Wildbad, Germany). Luminescence was normalised internally to firefly luciferase activity. Mean luminescence was then normalised to control vector and expressed as relative fold change.

3.18. Statistics

Statistical analysis was performed using GraphPad Prism version 5 (GraphPad Software Inc., La Jolla, CA, USA). Unpaired non-parametric datasets were tested with the Mann-Whitney U test. Paired data were assessed with the paired t test, or with the Wilcoxon signed-rank test if data were not normally distributed. p values are indicated throughout; a p value of <0.05 was chosen as indicating statistical significance.

4. microRNA expression profiling of T helper cell subsets

4.1. Introduction

miRNAs have emerged as key regulators of cell fate, functioning through their ability to post-transcriptionally control the expression of multiple specific genes. This broad range of targets encompasses a wide range of gene classes, including transcription factors, and thus miRNAs are likely to be of critical importance in determining the phenotype of many cell types. It is clear that the abundance of many individual miRNAs is dynamically regulated during T cell development. For example, miR-181a expression is markedly increased at the double positive stage of thymic development, and this contributes to the enhanced T cell receptor sensitivity that is observed at this stage (Li et al., 2007). Whilst a number of alternative mechanisms have been described that regulate miRNA function (detailed in section 1.1.5), activity is typically well correlated with changes in miRNA expression (Ritchie et al., 2009). As a result, it is generally accepted that changes in expression of specific miRNAs are directly related to changes in their functional activity. A consequence of this is that measurement of differential miRNA expression between related but distinct cell subtypes can be used to identify candidate miRNAs that may play a role in specifying the differences between cell types.

A primary aim of this study is to identify miRNAs of importance in regulating T cell subset differentiation. I therefore used miRNA expression profiling in order to determine patterns of miRNA expression within individual subsets, and to thereby identify miRNA candidates of interest. In addition, I analysed genome-wide binding

data for a number of key T cell transcription factors in order to determine any association between these master regulators and differentially expressed miRNAs.

4.2. Subset polarisation

In order to determine patterns of miRNA expression in specific subsets, naïve ($CD4^+$ $CD62L^{high}$ $CD44^{low}$ $CD25^-$) murine T helper cells were cell-sorted and cultured *in vitro* for seven days in medium containing an optimised mix of cytokines and antibodies for efficient polarisation. Following culture, cells were analysed by intracellular flow cytometry (Figure 4.1), cytokine ELISA (Figure 4.2) and qRT-PCR (Figure 4.3) to ensure that features of subset-polarisation were present where appropriate.

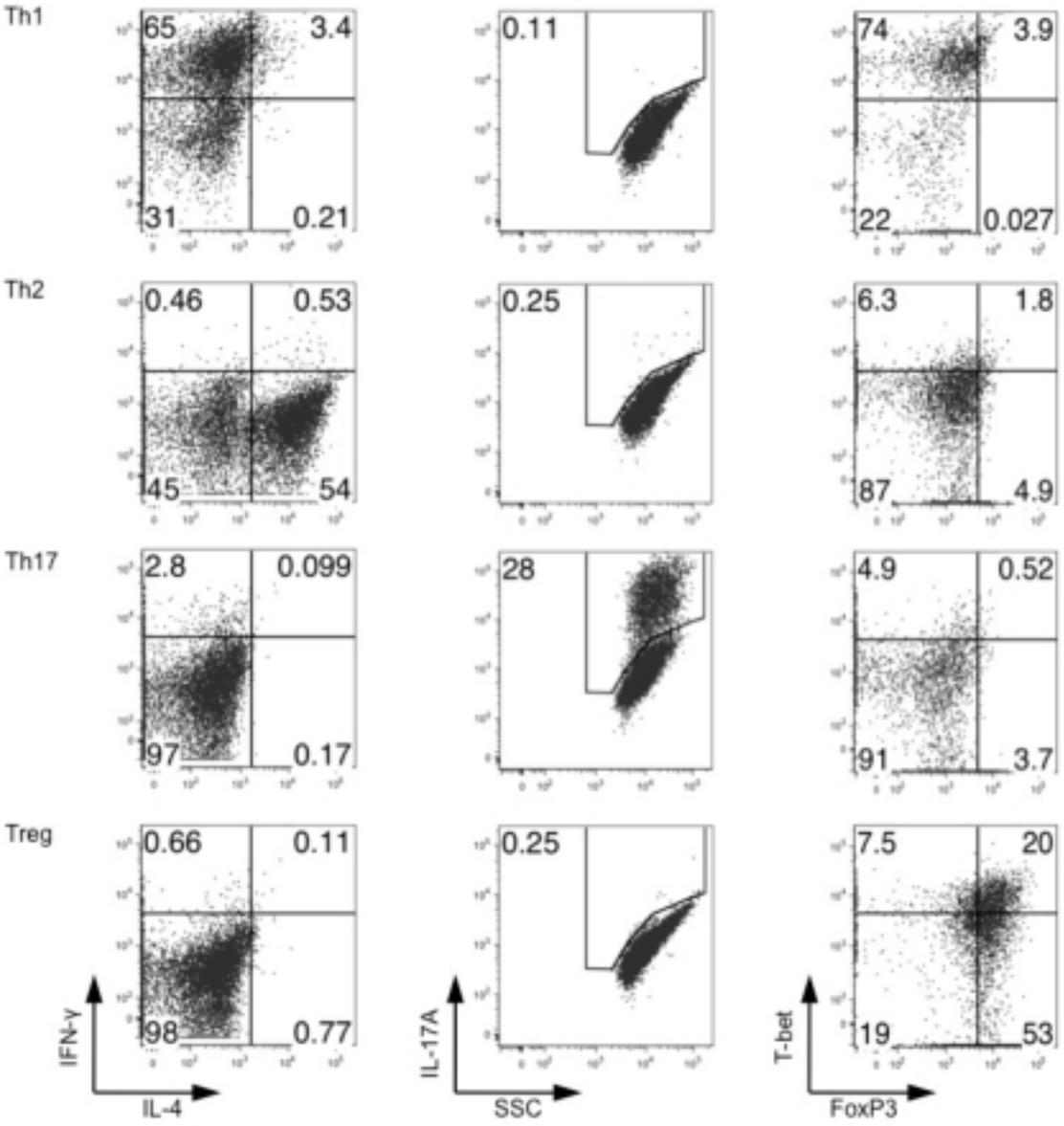

Figure 4.1 Flow cytometric validation of *in vitro* naive T helper cell subset polarisation. Representative flow cytometry plots for intracellular staining of the indicated cytokines and transcription factors.

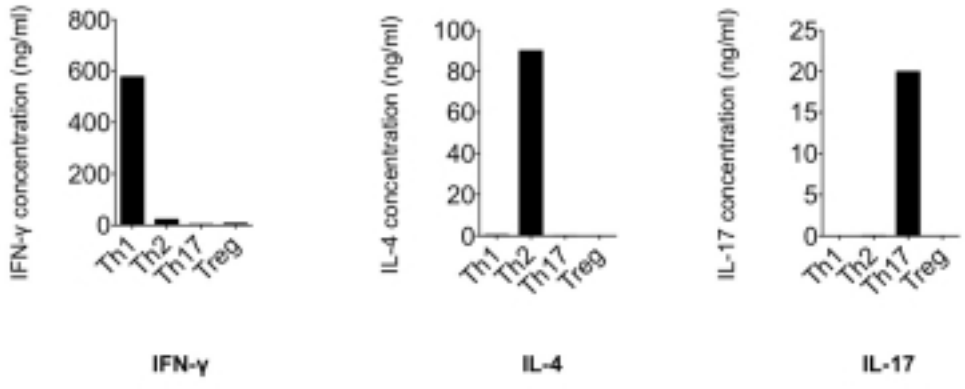

Figure 4.2 ELISA validation of *in vitro* naive T helper cell subset polarisation. Representative data from supernatant harvested following 24 hour reactivation with anti-CD3 and anti-CD28 in fresh medium at day 7 of culture. Mean of 2 replicates is shown.

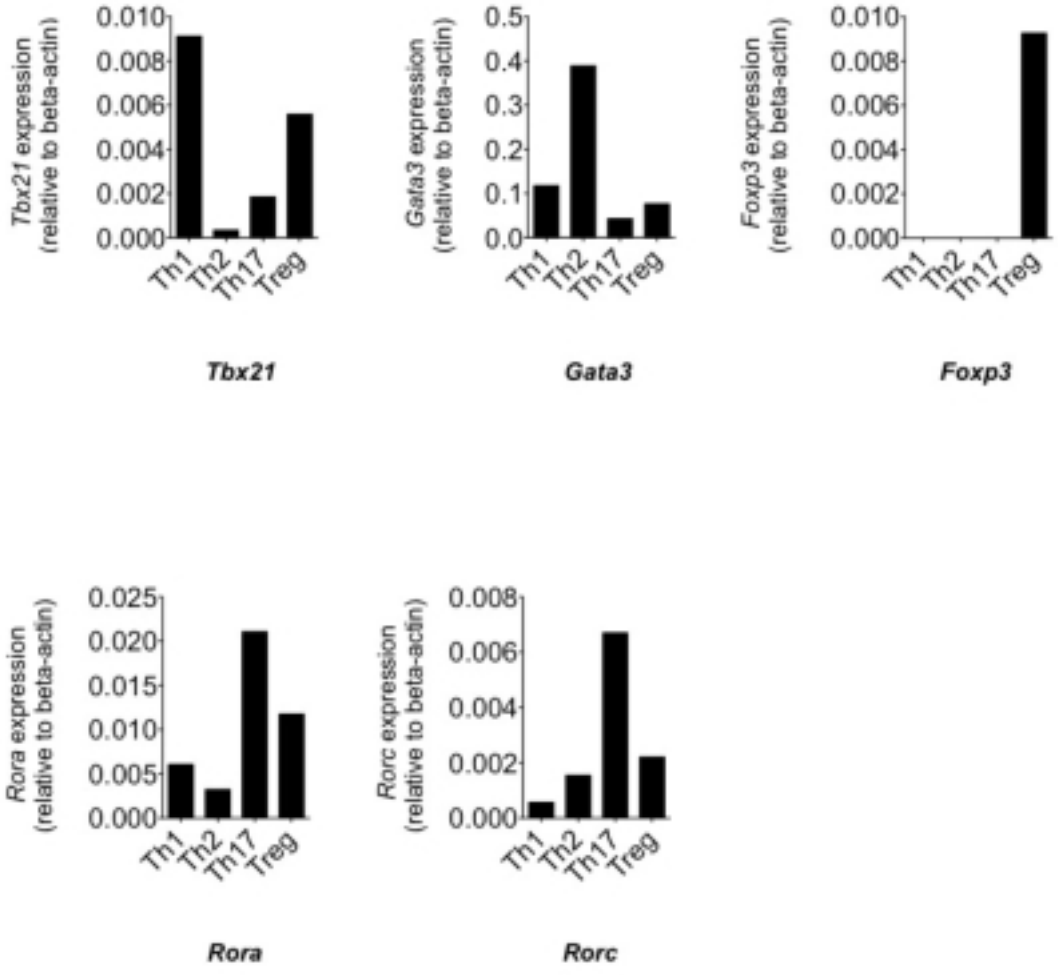

Figure 4.3 qRT-PCR validation of *in vitro* naive T helper cell subset polarisation. Representative data from RNA purified at day 7 of culture. Expression shown as $2^{-\Delta Ct}$ relative to beta-actin (*Actb*). Mean of 2 replicates is shown.

All samples were assessed by these methods to ensure appropriate polarisation prior to being subjected to microarray analysis. RNA was then extracted and assessed for purity and absence of any degradation by spectrophotometry and microchannel electrophoresis (Agilent BioAnalyzer) analysis.

4.3. miRNA expression profile of T helper cell subsets

Microarray profiling of miRNAs was performed in collaboration with Cepheid Inc. (Toulouse, France) who have developed custom miRNA microarrays, which are described briefly here. These arrays are spotted with probes for all known conserved miRNAs contained in miRBase release 11.0 (April 2008). In addition, more than 2000 putative novel miRNAs (at the time of miRBase release 11.0) were predicted *in silico* based on genome folding into the characteristic miRNA hairpin precursor structure. Probes specific for these putative miRNAs were also included in the microarray design. All probes were present in duplicate on each array slide. RNA was first subjected to size fractionation with RNAs of less than approximately 40nt in length retained for labelling and hybridization, in order to increase the specificity of the microarrays for the detection of mature miRNAs. Quality control, background correction and normalisation were all performed with a number of BioConductor packages as described in Appendix A.

For the purpose of detecting differential miRNA expression between T cell subsets, a primary round of microarrays was performed (hereafter termed "Round A"), consisting of 2 biological replicates of Th1, Th2, Th17, iTreg and 3 biological replicates of naïve T

cells. Manual inspection of these microarrays revealed minimal presence of bad spots and the representation of array layout shown in Figure 4.4 demonstrates that samples were evenly hybridized across the slide.

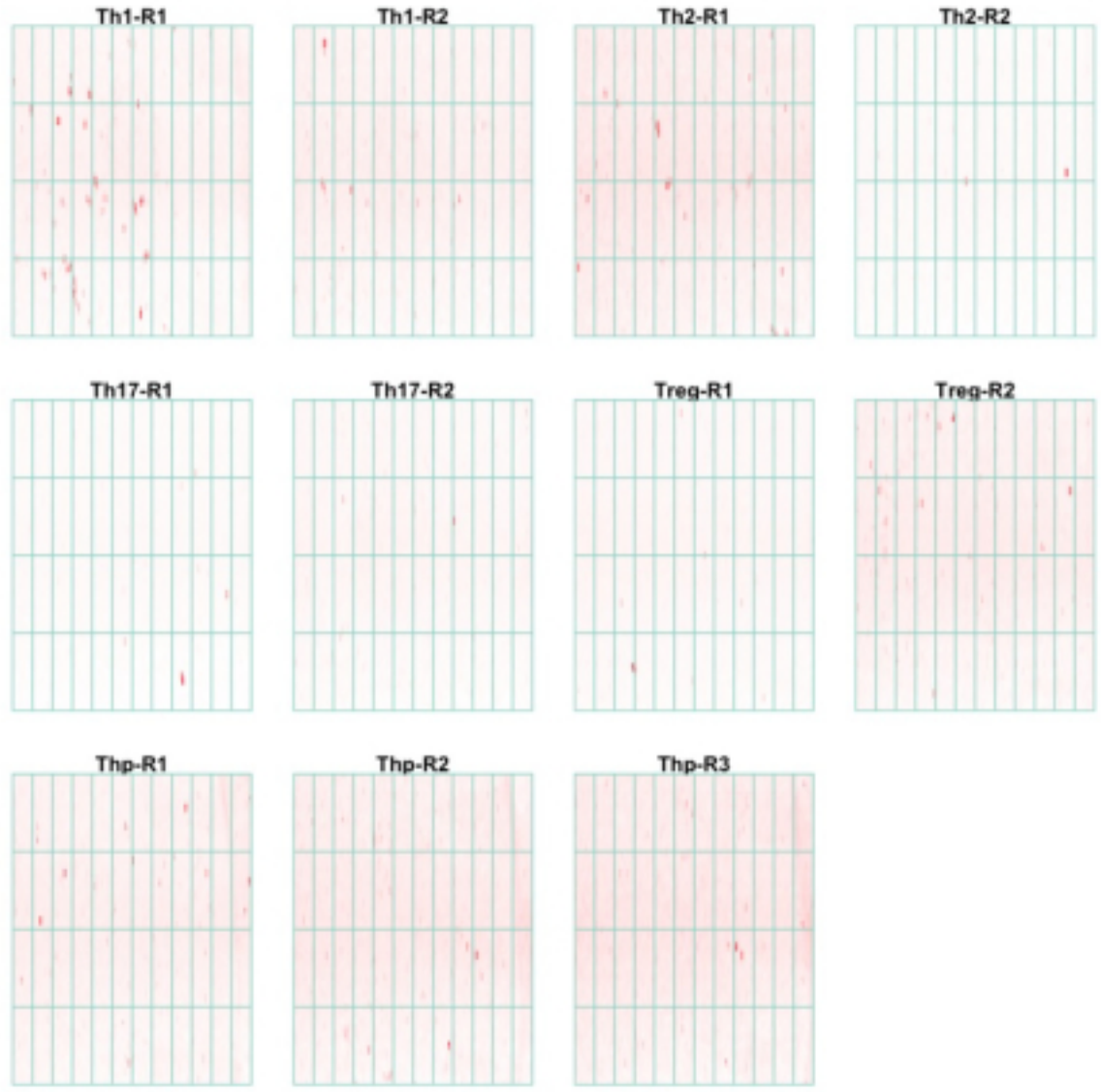

Figure 4.4 Intensity of background staining on each microarray slide. Graphical representation of background intensity with low intensity appearing white and high intensity red. 'R' suffix denotes biological replicate number. Lines represent block design on array (48 blocks, 360 spots per block).

Background correction is first performed by subtracting local background intensities from spot intensities. This can correct for any gradient effects that are observed in

background intensity on the microarray slide. A comparison of pre- and post-background correction miRNA expression intensities is shown in Figure 4.5.

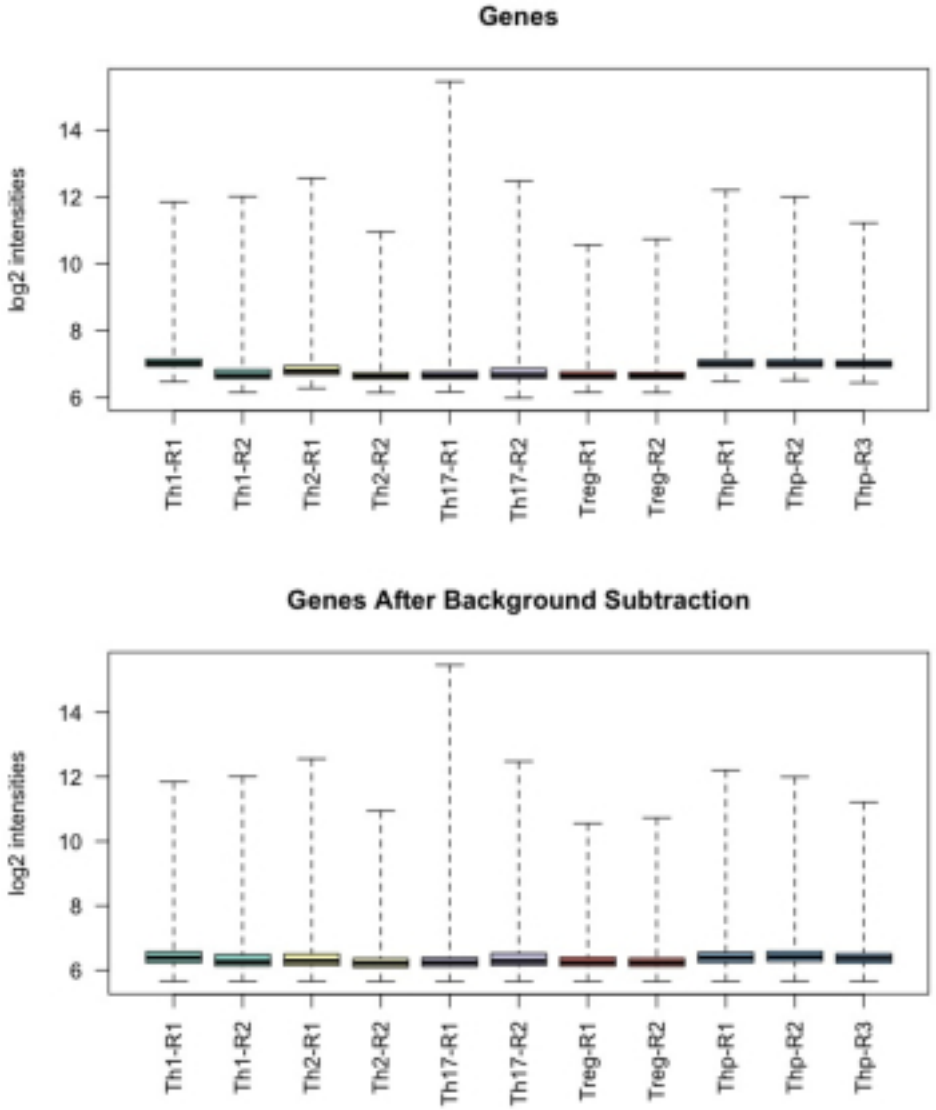

Figure 4.5 Boxplots demonstrating effect of background correction on intensity of miRNA probes. Y-axis scale is $\log_2$(intensity); whiskers denote maximum and minimum values.

Following background correction, normalisation is then performed to correct for any slide-to-slide variation in global intensity. Normalisation is performed using the variance stabilisation method described by Huber et al. (Huber et al., 2002). Boxplots of the pre- and post-normalisation miRNA expression data are shown in Figure 4.6.

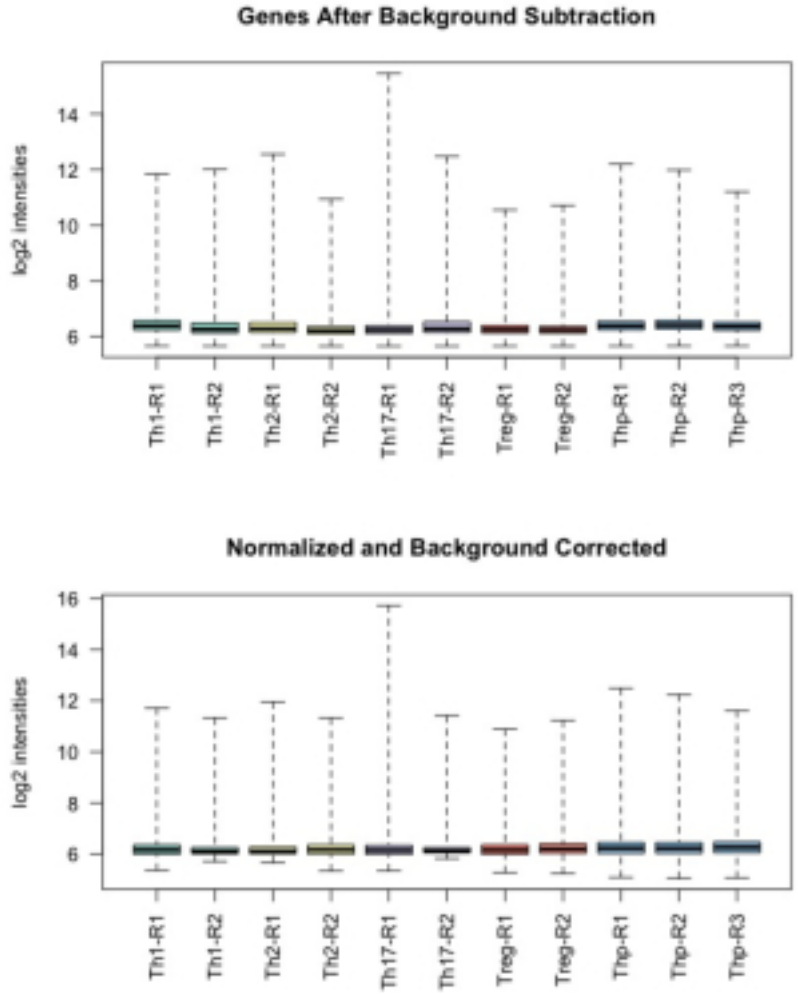

Figure 4.6 Comparison of pre- and post-normalisation gene expression boxplots. Y-axis scale is $\log_2$(intensity); whiskers denote maximum and minimum values.

In addition, the effect of normalization can be visualised by plotting probe intensity variance between microarrays against the ranked mean intensity, with well-normalised data tending towards an approximately flat line, as demonstrated in Figure 4.7.

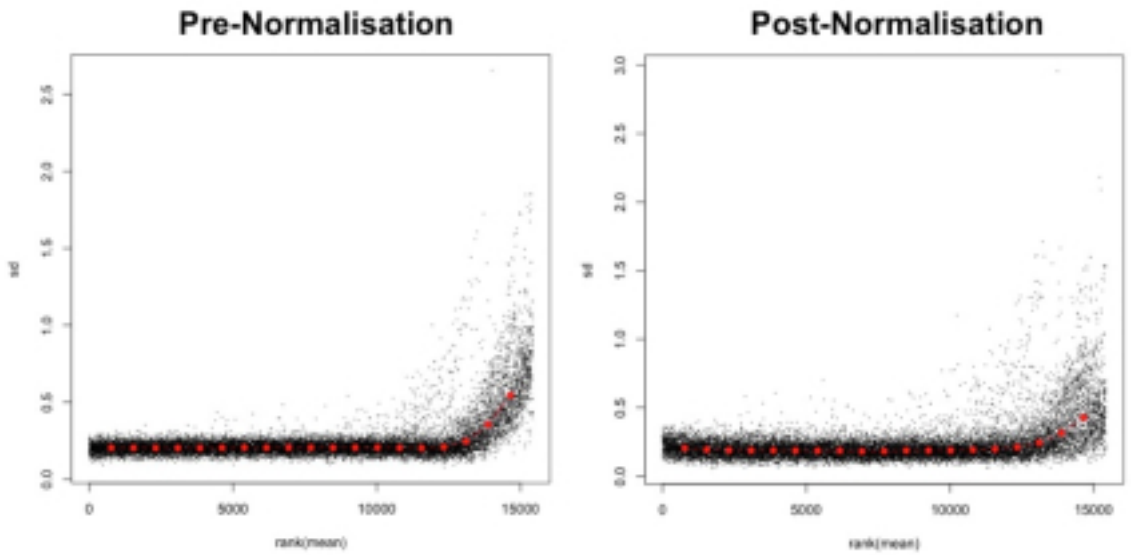

Figure 4.7 Plots of standard deviation vs. rank of mean, pre- and post-normalisation. Following normalisation, the fitted line (red dots) tends closer towards the horizontal, indicating the effect of normalisation.

Following background correction, normalization and averaging of intra-array technical replicate spot intensities, the correlation between biological replicate microarrays can be calculated as a measure of inter-array variation. Dot plots of the relationship between expression of each miRNA on biological replicate microarrays are shown in Figure 4.8, along with the calculated Pearson correlation coefficient.

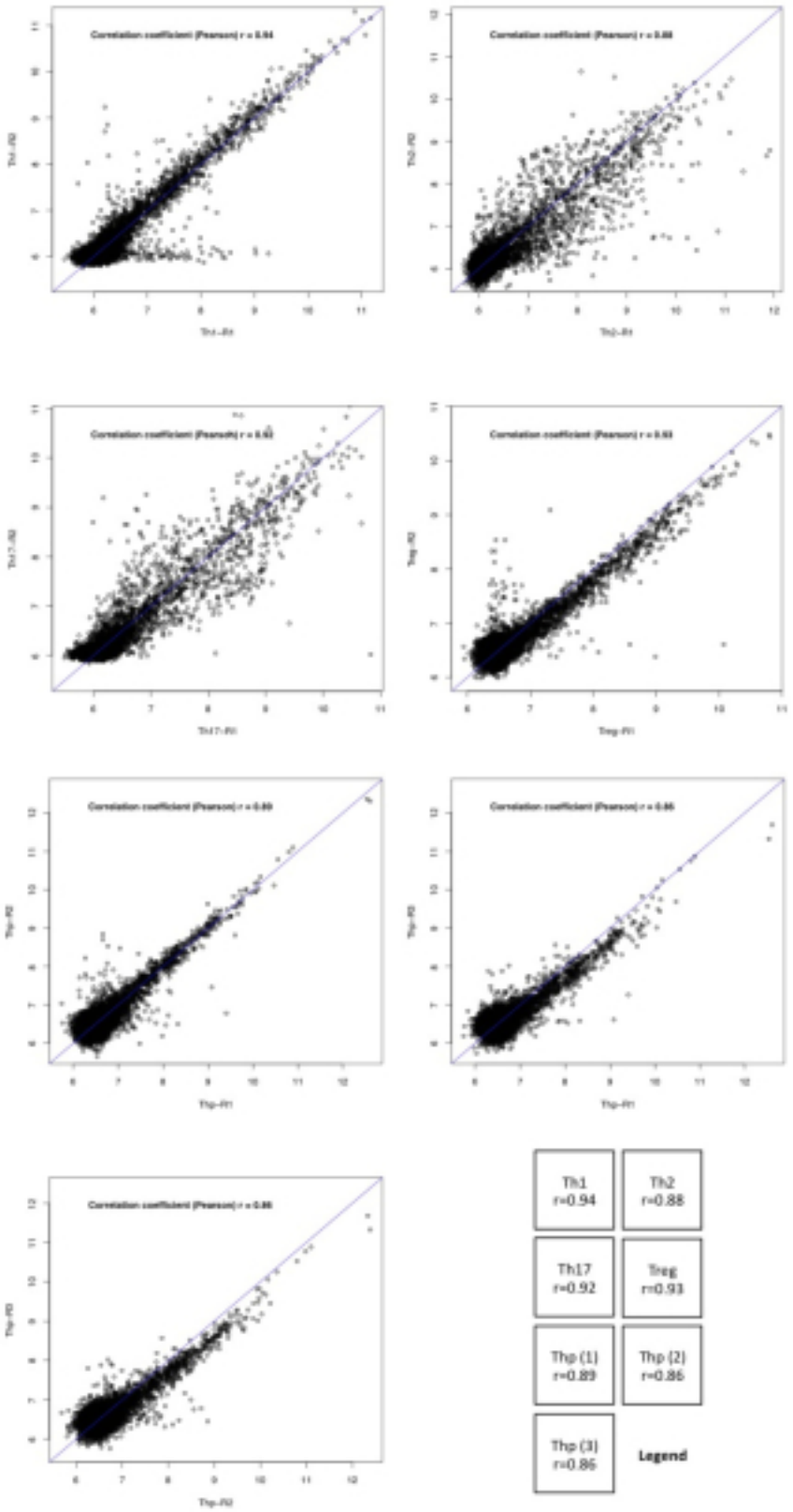

Figure 4.8 Correlation between biological replicate microarrays. Points indicate expression of miRNAs in each replicate, with one replicate per axis in the conditions indicated by the legend. Diagonal blue line in each plot is y=x. Expression is plotted on both axes as $\log_2$(normalised, background-corrected intensity). Pearson correlation coefficient is calculated and noted in legend.

Following pre-processing and quality control of these data, analysis was performed in order to determine whether patterns of miRNA expression could be detected between T cell subsets. Mean miRNA expression between biological replicate microarrays was first calculated. Only the expression of those validated miRNAs included in miRBase 11.0 is considered hereafter. Fold-change was calculated between individual subsets for all miRNAs, with the greatest difference in expression being observed for miR-150, which was downregulated approximately 32-fold in Th1 when compared with Thp. In order to focus on differentially expressed miRNAs, a fold-change cut-off of 2.0 between any two conditions was set, which identified 79 of 836 miRbase miRNAs as being differentially expressed. Analysis was then performed using the software package 'Mayday' (Battke et al., 2010), with the Self-Organising Map (SOM) algorithm used to perform clustering of genes with similar patterns of expression. All miRNAs were included in this analysis regardless of variance between biological replicates, in order to retain the maximum number of miRNAs for candidate identification. Figure 4.9 illustrates the results of this analysis.

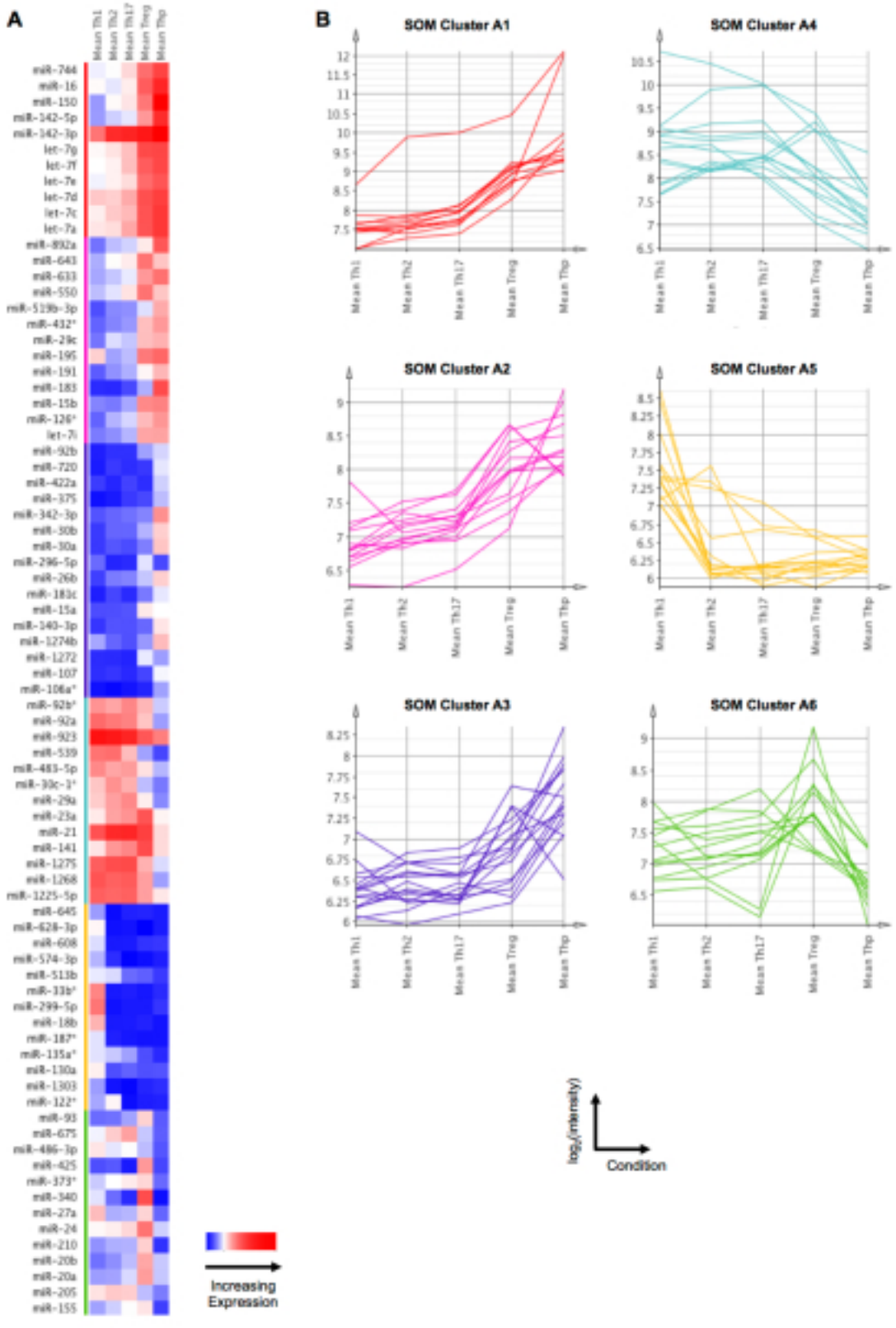

Figure 4.9 Differentially expressed miRNAs in T helper cell subsets. (A) Heatmap of miRNA expression in the indicated subsets, grouped according to Self-Organising Map (SOM) clustering. (B) Profile plot of miRNA expression in individual clusters. Each line represents an individual miRNA and line colours correspond with colours indicated to left of heatmap in (A).

Following this, quantitative RT-PCR was performed for the selected miRNAs miR-142-3p, miR-142-5p and miR-21, which demonstrated similar patterns of expression when compared with the microarray data (Figure 4.10).

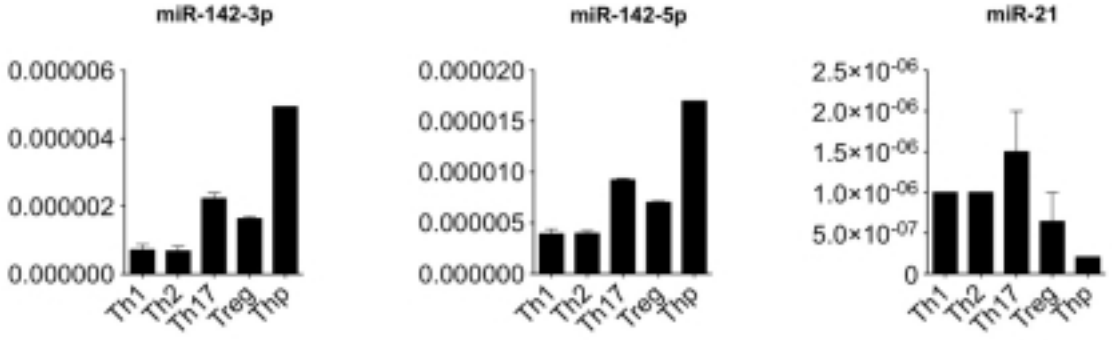

Figure 4.10 miRNA qRTPCR in T cell subsets. qRTPCR was performed on RNA samples obtained from the indicated subsets. Expression is shown as 2^{-Ct}; mean of two replicates shown ± SEM.

miRNAs from each cluster and a qualitative interpretation of the observed pattern of expression are listed in Table 4.1.

SOM Cluster	miRNAs	Description
SOM Cluster A1	miR-744, miR-16, miR-150, miR-142-5p, miR-142-3p, let-7g, let-7f, let-7e, let-7d, let-7c, let-7a	Higher expression in Thp and Treg when compared with effector subsets
SOM Cluster A2	miR-892a, miR-643, miR-633, miR-550, miR-519b-3p, miR-432*, miR-29c, miR-195, miR-191, miR-183, miR-15b, miR-126*, let-7i	Higher expression in Thp and Treg when compared with effector subsets
SOM Cluster A3	miR-92b, miR-720, miR-422a, miR-375, miR-342-3p, miR-30b, miR-30a, miR-296-5p, miR-26b, miR-181c, miR-15a, miR-140-3p, miR-1274b, miR-1272, miR-107, miR-106a*	Higher expression in Thp and Treg when compared with effector subsets; lower overall expression than Clusters A1 & A2
SOM Cluster A4	miR-92b*, miR-92a, miR-923, miR-539, miR-483-5p, miR-30c-1*, miR-29a, miR-23a, miR-21, miR-141, miR-1275, miR-1268, miR-1225-5p	Higher expression in effector and Treg subsets when compared with Thp
SOM Cluster A5	miR-645, miR-628-3p, miR-608, miR-574-3p, miR-513b, miR-33b*, miR-299-5p, miR-18b, miR-187*, miR-135a*, miR-130a, miR-1303, miR-122*	Higher expression in Th1 when compared with other subsets
SOM Cluster A6	miR-93, miR-675, miR-486-3p, miR-425, miR-373*, miR-340, miR-27a, miR-24, miR-210, miR-20b, miR-20a, miR-205, miR-155	Higher expression in Treg when compared with other subsets

Table 4.1 Self-Organising Map (SOM) clusters derived from differentially expressed miRNAs with a fold-change of >2.0 detected between at least 2 WT T cell subsets. A qualitative description of the observed expression pattern for each cluster is provided.

These data suggest that distinct patterns of miRNA expression exist, in particular when naïve T helper cells are compared with differentiated effector T cells. The analysis performed is deliberately permissive, in order to identify as many potential candidates as possible, however it does not represent a definitive description of those miRNAs that are differentially expressed, and further validation is required. Nonetheless, these data provide evidence that miRNA expression is dynamically regulated during the differentiation of T helper cells and suggest a number of candidates of interest for further study.

4.4. Validation of miRNA expression patterns and expression in the absence of T-bet

Having established patterns of miRNA expression in T helper cell subsets, I next investigated whether miRNA expression may be related to master-regulatory transcription factor activity. In order to do this, a further round of microarray profiling (hereafter termed "Round B") of T cell subsets derived from both WT and T-bet$^{-/-}$ mice was performed, including Thp, Th1, Th2, Th17 and iTreg. Two independent biological replicates were produced and analysed for each condition in both genotypes. This approach therefore allows for comparison of Round B WT expression data with the Round A WT microarrays that have been described above, in addition to generating novel data from Round B T-bet$^{-/-}$ T cells. As before, the efficiency of polarisation was determined by flow cytometry, ELISA and qRT-PCR, and is shown for T-bet$^{-/-}$ cells in Figure 4.11 - Figure 4.13 (WT data comparable to that shown in section 4.3).

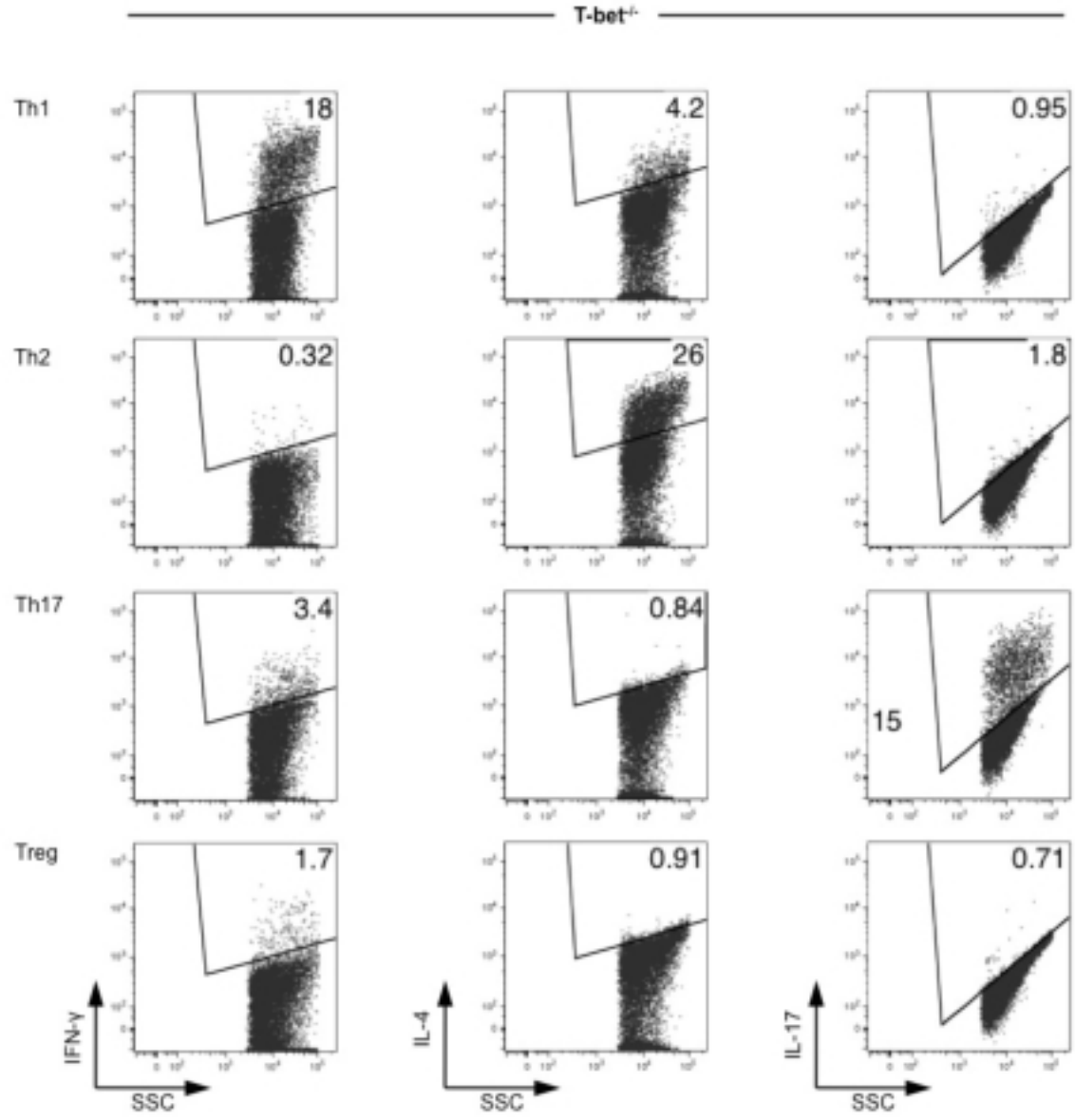

Figure 4.11 Cytokine expression by *in vitro* polarised T cell subsets derived from T-bet$^{-/-}$ naïve T cells. Representative flow cytometric plots are shown for the indicated cytokines plotted against side scatter (SSC); plots gated on live cells.

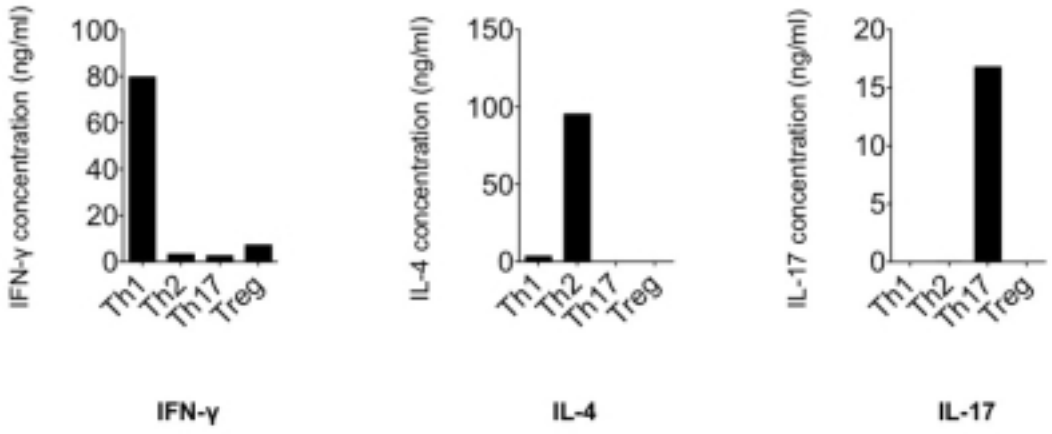

Figure 4.12 ELISA detection of secreted cytokines produced by T-bet$^{-/-}$ naïve CD4^{+} T cells polarised *in vitro* to the indicated conditions. Representative data from supernatant harvested following 24-hour reactivation with anti-CD3 and anti-CD28 in fresh medium at day 7 of culture. Mean of 2 replicates is shown.

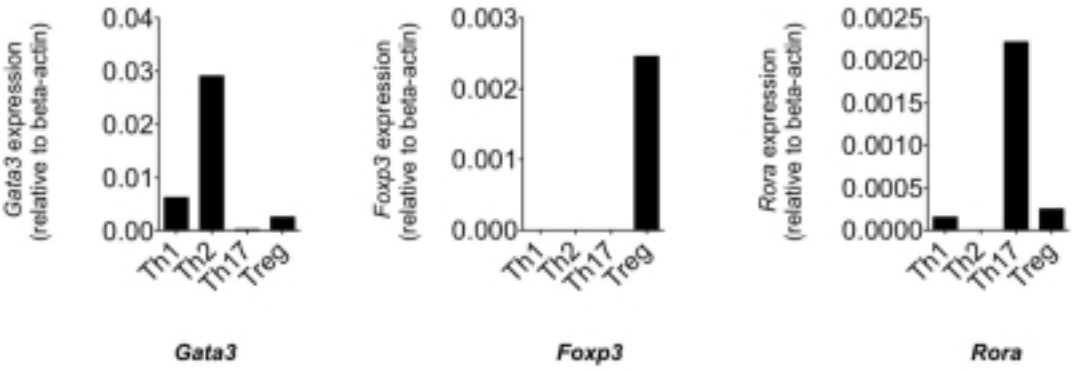

Note: *Tbx21* expression not detected after 40 PCR cycles in any condition (data not shown)

Figure 4.13 qRT-PCR validation of *in vitro* polarisation of T-bet$^{-/-}$ naïve T helper cells. Representative data from RNA purified at day 7 of culture. Expression shown as $2^{-\Delta Ct}$ relative to beta-actin (*Actb*). Mean of 2 replicates is shown.

Microarray analysis was again performed in collaboration with Cepheid Inc., using an updated version of their custom miRNA microarray platform, still containing all miRBase 11.0 miRNAs. Prior to data analysis, a series of quality control, background correction and normalisation steps were once again performed. Figure 4.14

demonstrates the background intensity across the microarrays and qualitative analysis suggests that significant variation in hybridization occurred with both WT Th17 biological replicates. Further analysis showed a significant difference in median intensity on these microarrays when compared with other samples and, as a result, Th17 samples were excluded from later analysis.

Figure 4.14 Intensity of background staining on each microarray slide. Graphical representation of background intensity with low intensity appearing white and high intensity red. 'R' suffix denotes biological replicate number. KO = T-bet$^{-/-}$. Lines represent block design on array (48 blocks, 360 spots per block).

The distribution of spot intensities before and after background correction and normalisation is demonstrated in Figure 4.15 and Figure 4.16.

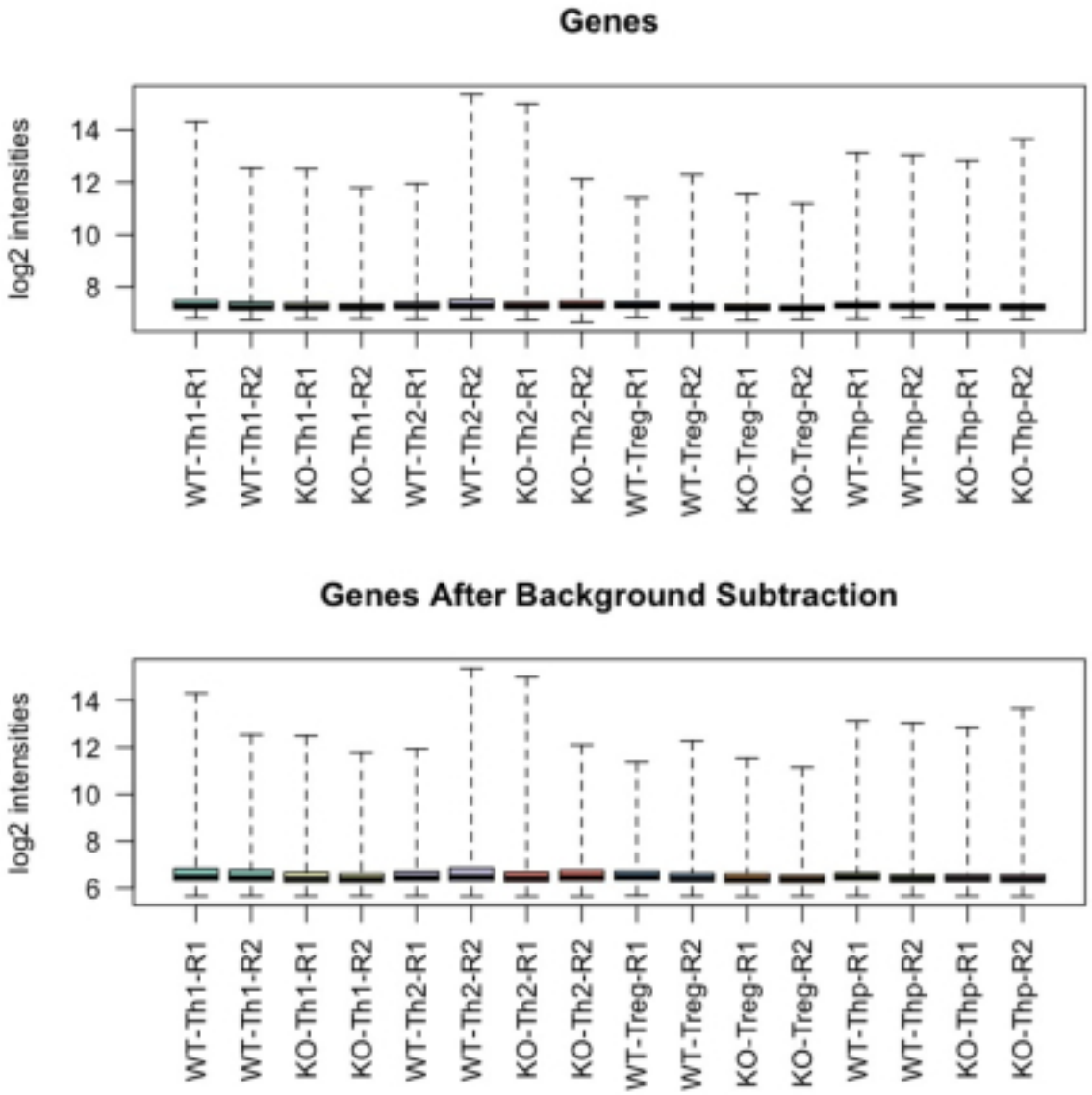

Figure 4.15 Boxplot demonstrating distribution of spot intensities before and after background subtraction. KO = T-bet$^{-/-}$. Y-axis scale is $\log_2$(intensity); whiskers denote maximum and minimum values.

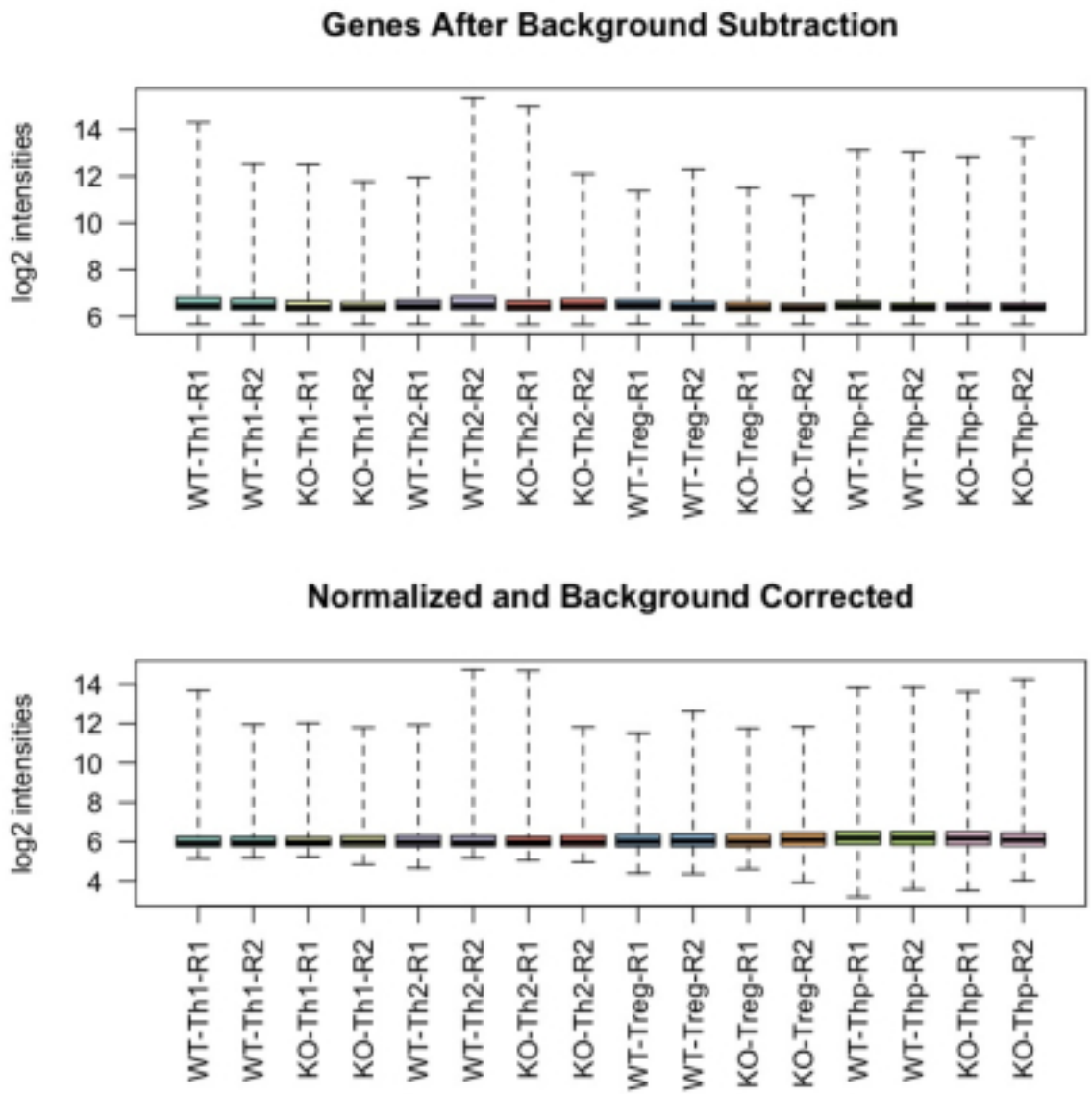

Figure 4.16 Boxplot demonstrating distribution of spot intensities before and after normalisation. KO = T-bet$^{-/-}$. Y-axis scale is $\log_2$(intensity); whiskers denote maximum and minimum values.

The effect of normalisation is again visualised by plotting the standard deviation against the rank of mean intensity as shown in Figure 4.17.

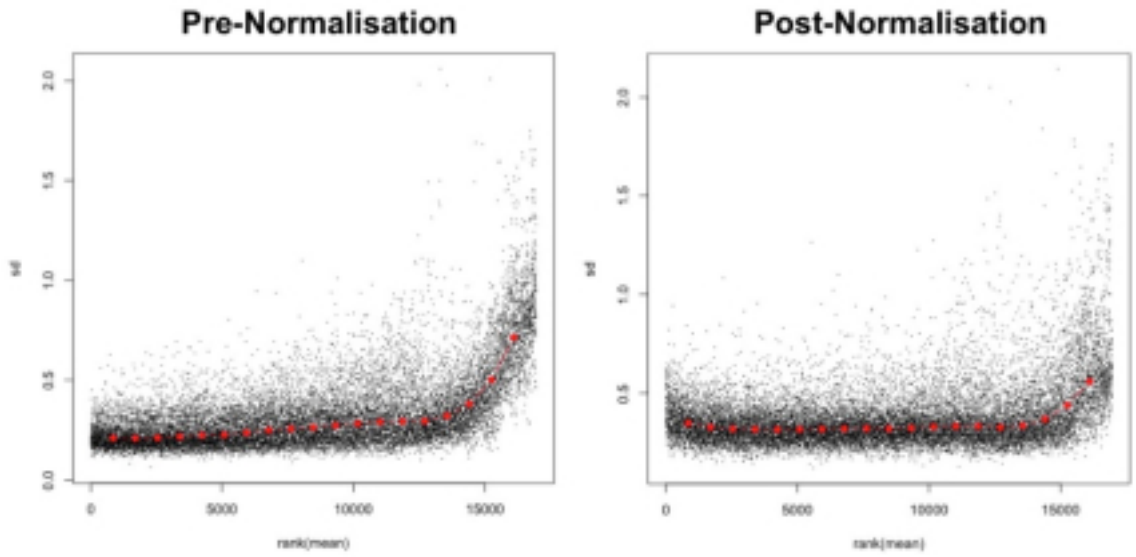

Figure 4.17 Plots of standard deviation vs. rank of mean, pre- and post-normalisation. Following normalisation, the fitted line (red dots) tends closer towards the horizontal, indicating the effect of normalisation.

The correlation in gene expression between the two independent biological replicates analysed for each T cell subset is shown in Figure 4.18.

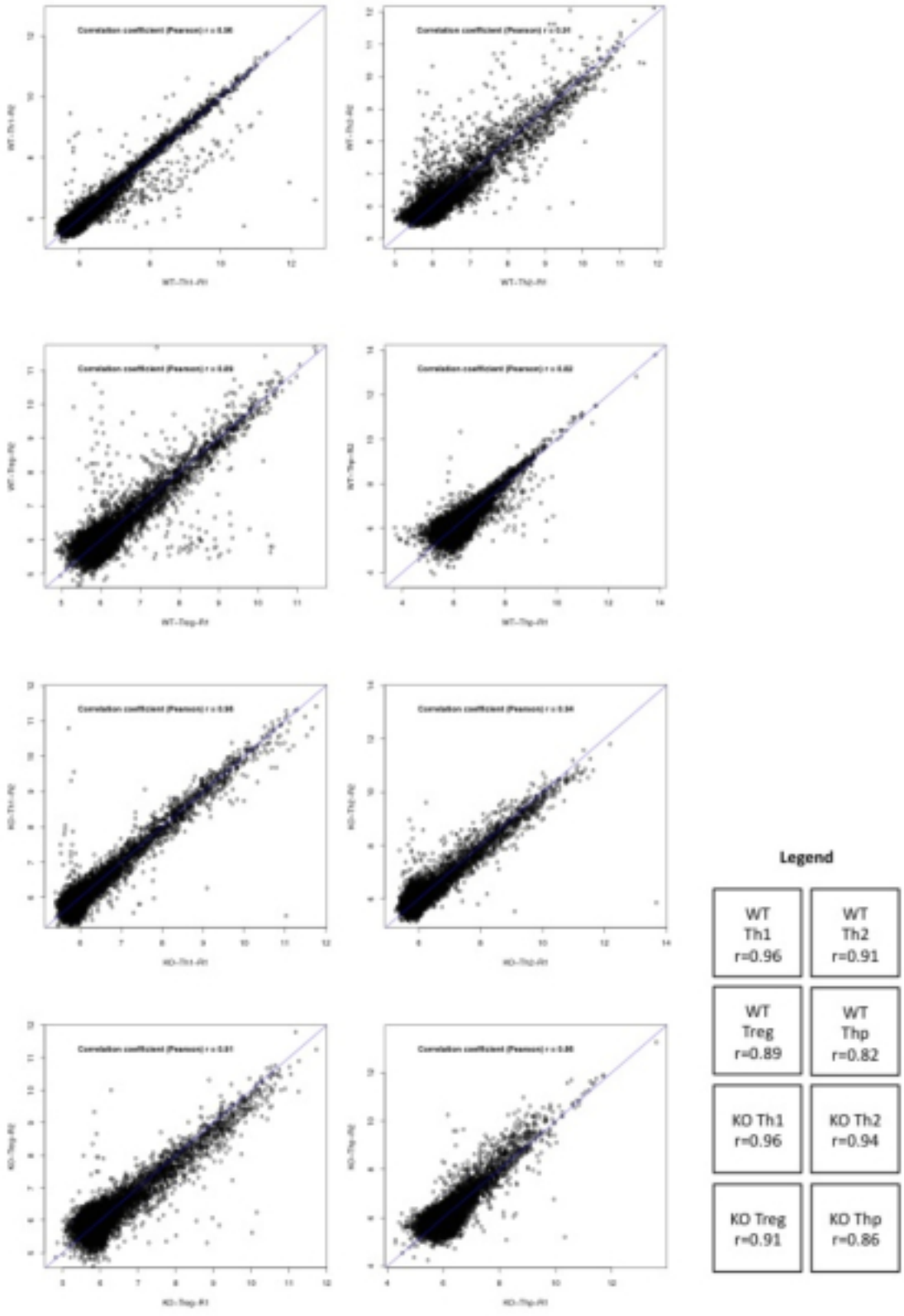

Figure 4.18 Correlation between biological replicate microarrays. Points indicate expression of miRNAs in each replicate, with one replicate per axis in the conditions indicated by the legend. Diagonal blue line in each plot is y=x. Expression is plotted on both axes as $\log_2$(normalised, background-corrected intensity). KO=T-bet$^{-/-}$. Pearson correlation coefficient is calculated and noted in legend.

Following these quality control analyses, this group of microarrays was subjected to the same initial analysis of differentially expressed genes as that described in section 4.3. WT samples were first analysed alone in order to allow comparison with results from Round A. With a fold-change cut-off of 2.0, a total of 116 miRNAs were identified as being differentially-expressed between WT T cell subsets in the Round B dataset. The results following SOM clustering are shown in the heatmap and multi-profile plots in Figure 4.19.

A

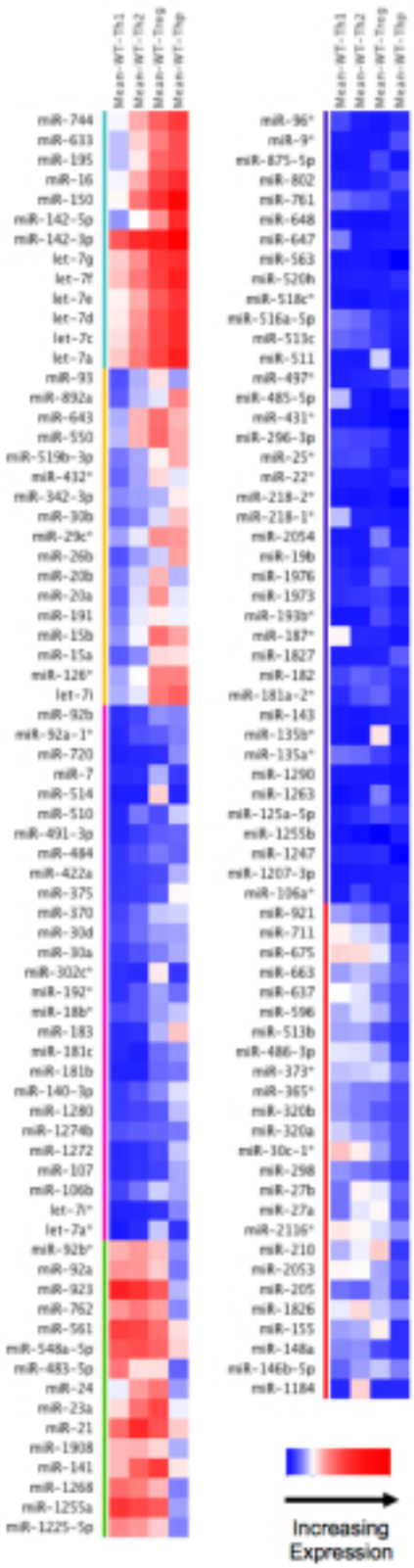
Mean-WT-Th1
Mean-WT-Th2
Mean-WT-Treg
Mean-WT-Thp
miR-744
miR-633
miR-195
miR-16
miR-150
miR-142-5p
miR-142-3p
let-7g
let-7f
let-7e
let-7d
let-7c
let-7a
miR-93
miR-892a
miR-643
miR-550
miR-519b-3p
miR-432*
miR-342-3p
miR-30b
miR-29c*
miR-26b
miR-20b
miR-20a
miR-191
miR-15b
miR-15a
miR-126*
let-7i
miR-92b
miR-92a-1*
miR-720
miR-7
miR-514
miR-510
miR-491-3p
miR-484
miR-422a
miR-375
miR-370
miR-30d
miR-30a
miR-302c*
miR-192*
miR-18b*
miR-183
miR-181c
miR-181b
miR-140-3p
miR-1280
miR-1274b
miR-1272
miR-107
miR-106b
let-7i*
let-7a*
miR-92b*
miR-92a
miR-923
miR-762
miR-561
miR-548a-5p
miR-483-5p
miR-24
miR-23a
miR-21
miR-1908
miR-141
miR-1268
miR-1255a
miR-1225-5p
Mean-WT-Th1
Mean-WT-Th2
Mean-WT-Treg
Mean-WT-Thp
miR-96*
miR-9*
miR-875-5p
miR-802
miR-761
miR-648
miR-647
miR-563
miR-520h
miR-518c*
miR-516a-5p
miR-513c
miR-511
miR-497*
miR-485-5p
miR-431*
miR-296-3p
miR-25*
miR-22*
miR-218-2*
miR-218-1*
miR-2054
miR-19b
miR-1976
miR-1973
miR-193b*
miR-187*
miR-1827
miR-182
miR-181a-2*
miR-143
miR-135b*
miR-135a*
miR-1290
miR-1263
miR-125a-5p
miR-1255b
miR-1247
miR-1207-3p
miR-106a*
miR-921
miR-711
miR-675
miR-663
miR-637
miR-596
miR-513b
miR-486-3p
miR-373*
miR-365*
miR-320b
miR-320a
miR-30c-1*
miR-298
miR-27b
miR-27a
miR-2116*
miR-210
miR-2053
miR-205
miR-1826
miR-155
miR-148a
miR-146b-5p
miR-1184
Increasing Expression

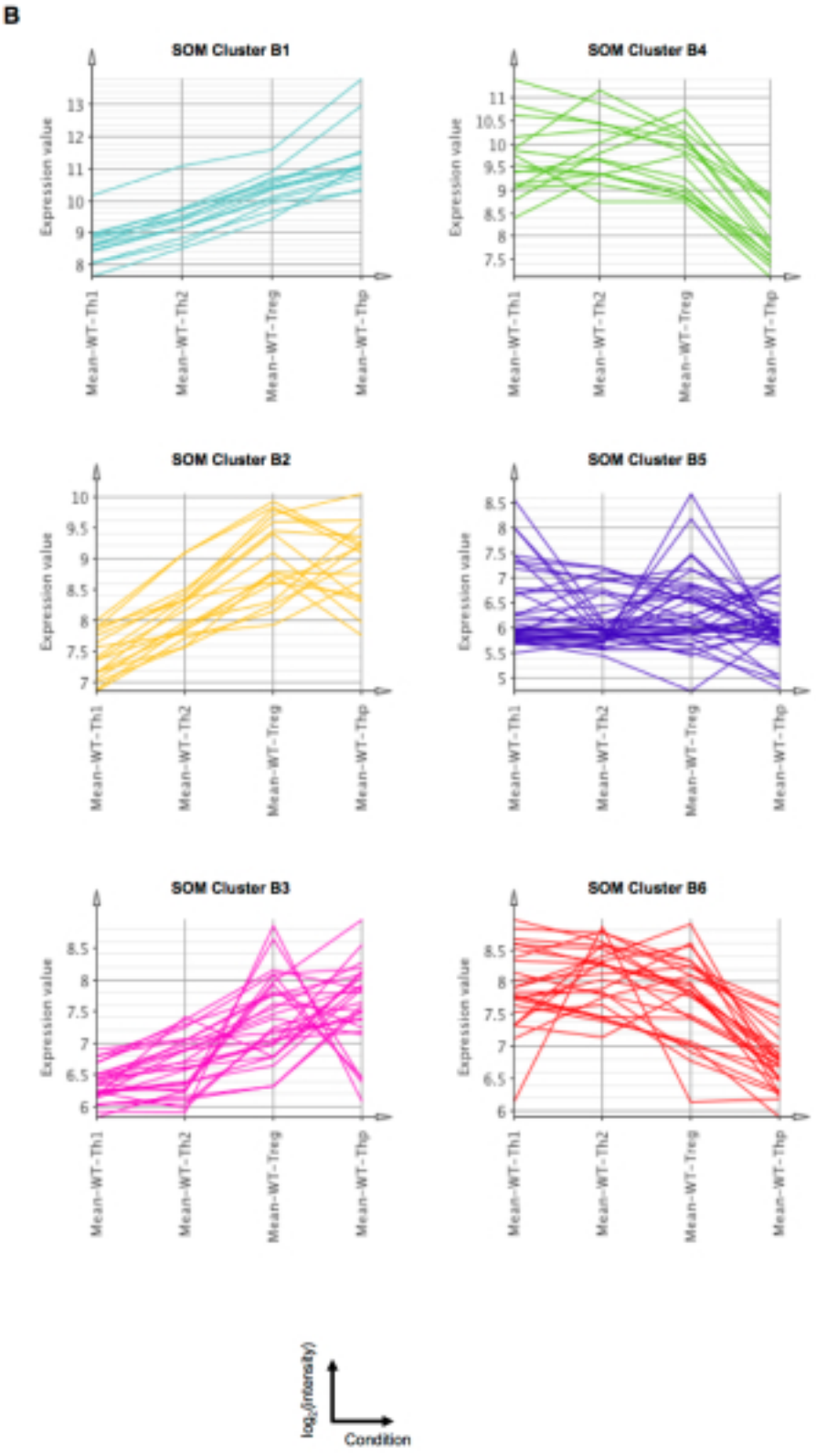

Figure 4.19 Differentially expressed genes in microarray Round B WT T cell subsets. (A) Heatmap of miRNA expression in the indicated subsets, grouped according to Self-Organising Map (SOM) clustering. (B) Profile plot of miRNA expression in individual clusters. Each line represents an individual miRNA and line colours correspond with colours indicated to left of heatmap in (A).

miRNAs from each cluster and a qualitative interpretation of the observed pattern of expression are listed in Table 4.2.

SOM Cluster	miRNAs	Description
SOM Cluster B1	miR-142-3p, miR-744, miR-150, miR-633, miR-142-5p, miR-16, let-7d, let-7c, let-7a, miR-195, let-7g, let-7f, let-7e	Higher expression in Thp and Treg when compared with effector subsets
SOM Cluster B2	miR-342-3p, miR-30b, miR-20b, miR-519b-3p, miR-20a, miR-93, miR-550, miR-26b, miR-432*, miR-15a, miR-15b, miR-643, miR-892a, miR-126*, miR-29c*, miR-191, let-7i	Higher expression in Thp and Treg when compared with effector subsets
SOM Cluster B3	miR-106b, miR-92b, miR-30a, let-7i*, miR-1280, miR-18b*, miR-514, miR-30d, miR-720, miR-1274b, miR-484, let-7a*, miR-92a-1*, miR-7, miR-302c*, miR-370, miR-375, miR-422a, miR-510, miR-192*, miR-140-3p, miR-181b, miR-181c, miR-1272, miR-491-3p, miR-183, miR-107	Higher expression in Thp and/or Treg when compared with effector subsets; lower overall expression than Clusters B1 & B2
SOM Cluster B4	miR-483-5p, miR-92a, miR-1908, miR-548a-5p, miR-21, miR-24, miR-923, miR-141, miR-1255a, miR-561, miR-92b*, miR-1225-5p, miR-762, miR-1268, miR-23a	Higher expression in effector and Treg subsets when compared with Thp
SOM Cluster B5	miR-187*, miR-19b, miR-1290, miR-875-5p, miR-802, miR-22*, miR-513c, miR-106a*, miR-516a-5p, miR-296-3p, miR-218-1*, miR-431*, miR-9*, miR-485-5p, miR-181a-2*, miR-518c*, miR-1255b, miR-218-2*, miR-143, miR-135a*, miR-1247, miR-563, miR-648, miR-647, miR-1976, miR-1973, miR-1207-3p, miR-520h, miR-1263, miR-2054, miR-511, miR-497*, miR-96*, miR-761, miR-125a-5p, miR-1827, miR-193b*, miR-25*, miR-135b*, miR-182	Mixed, no overall pattern
SOM Cluster B6	miR-1184, miR-486-3p, miR-30c-1*, miR-513b, miR-205, miR-148a, miR-711, miR-210, miR-155, miR-921, miR-298, miR-27a, miR-27b, miR-637, miR-373*, miR-365*, miR-596, miR-2053, miR-663, miR-1826, miR-2116*, miR-320b, miR-675, miR-320a, miR-146b-5p	Higher expression in effector and Treg subsets when compared with Thp

Table 4.2 Self-Organising Map (SOM) clusters derived from differentially expressed miRNAs with a fold-change of >2.0 detected between at least 2 WT T cell subsets. Data is from Round B WT microarrays (performed alongside T-bet$^{-/-}$ microarrays). A qualitative description of the observed expression pattern (if any) for each cluster is provided.

These clusters of differentially-expressed miRNAs can be compared with those generated from the first group of microarrays. The overlap in gene lists between closely-matched clusters is shown in Figure 4.20.

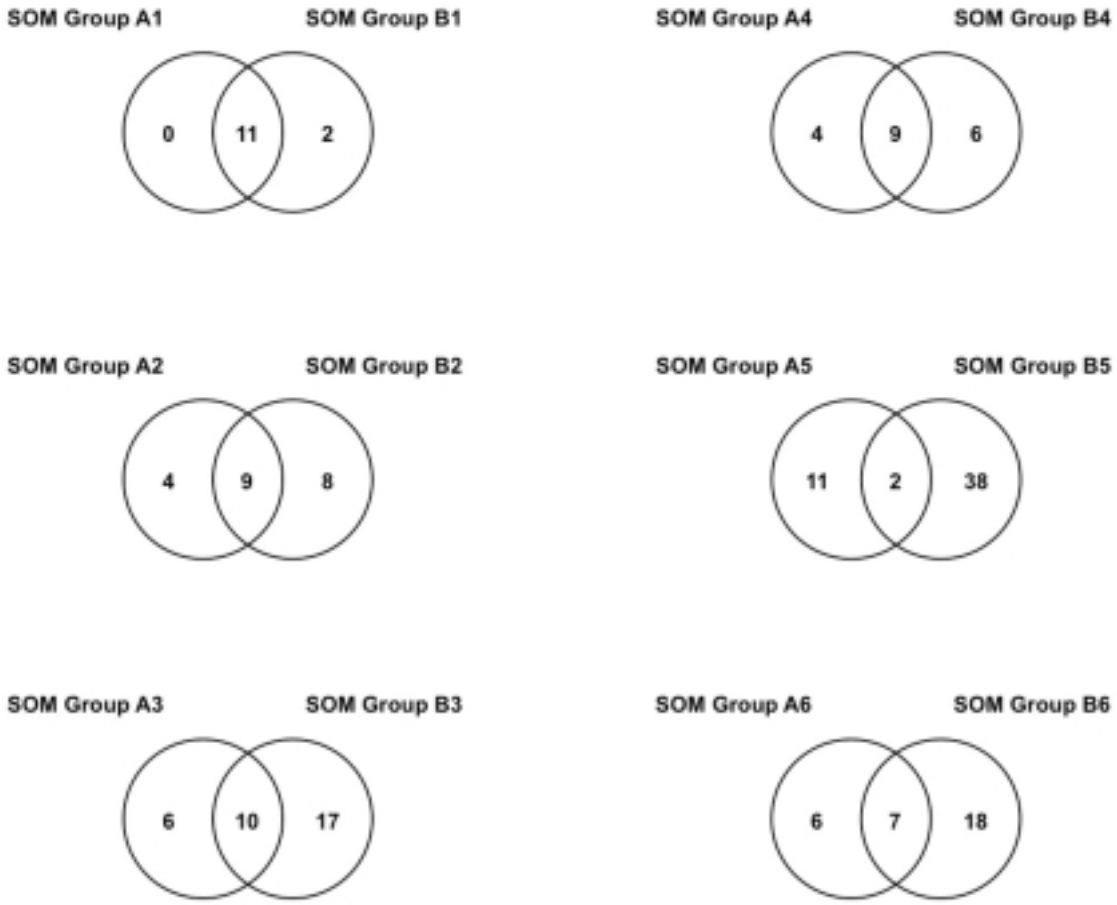

Figure 4.20 Overlap between data generated in Round A and B WT microarrays. Venn diagrams were constructed for the self-organising map (SOM) clusters indicated above.

The degree of agreement was observed to be greater in some clusters. For example, all of those miRNAs identified in group A1 were re-identified as clustering together in group B1; by contrast there was low overlap between clusters A5 and B5. For all 6 pairs of clusters, a mean of 62% of miRNAs were re-identified in the Round B series of microarrays as being both differentially-expressed and clustered together in the same group. In total, 59 of 79 (75%) differentially-expressed miRNAs identified in the Round

A microarray series were re-identified in Round B as being differentially-expressed with a fold-change of >2.0 between any two conditions.

These data suggest that there is consistency between these independent miRNA microarray experiments, and that a group of miRNAs are reproducibly differentially-expressed between T cell subsets. This set of miRNAs can be clustered into consensus SOM clusters, and this analysis is shown for side-by-side comparison of both rounds of microarrays in Figure 4.21.

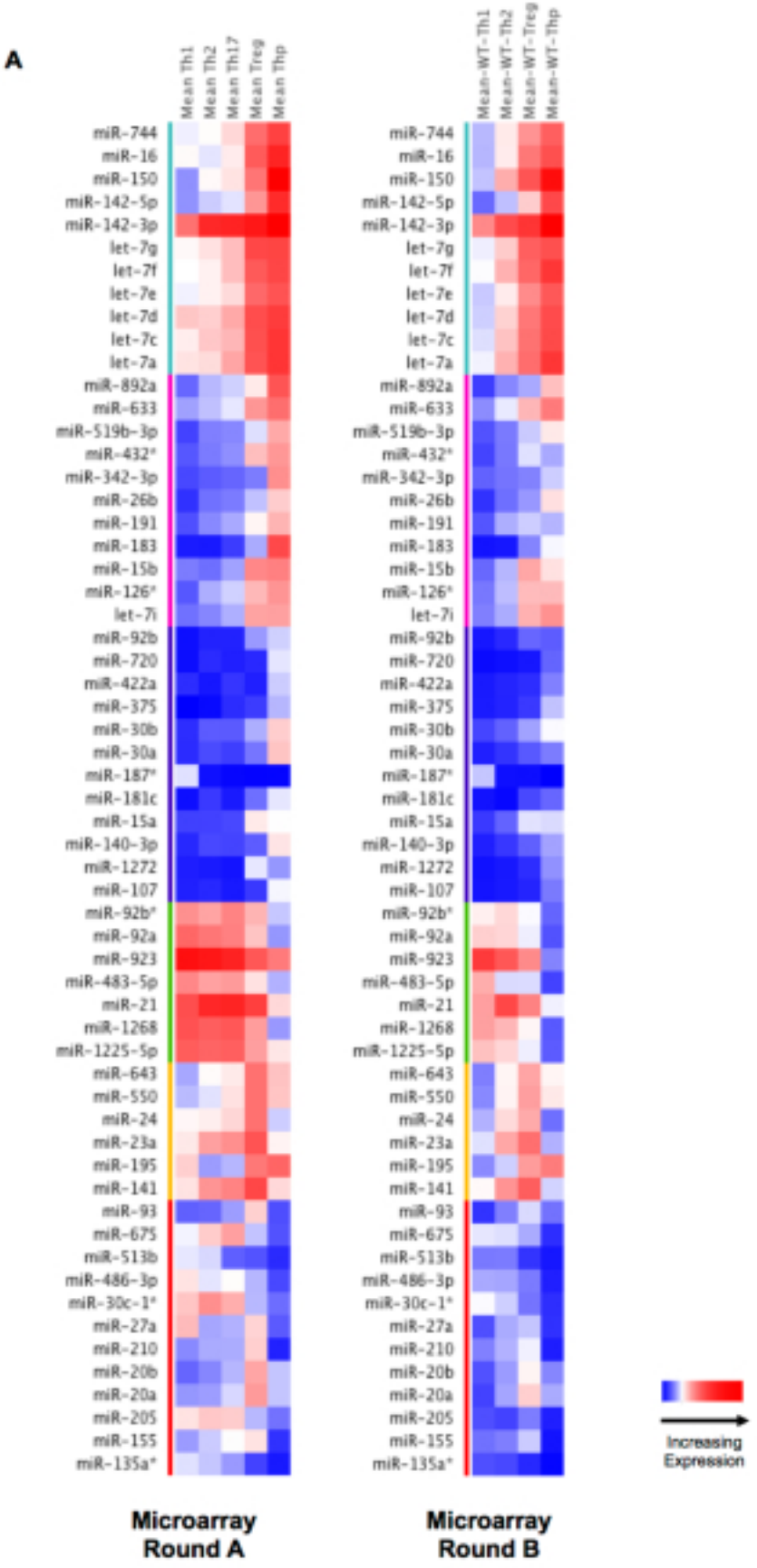
A
Mean Th1
Mean Th2
Mean Th17
Mean Treg
Mean Thp
Mean-WT-Th1
Mean-WT-Th2
Mean-WT-Treg
Mean-WT-Thp
miR-744
miR-16
miR-150
miR-142-5p
miR-142-3p
let-7g
let-7f
let-7e
let-7d
let-7c
let-7a
miR-892a
miR-633
miR-519b-3p
miR-432*
miR-342-3p
miR-26b
miR-191
miR-183
miR-15b
miR-126*
let-7i
miR-92b
miR-720
miR-422a
miR-375
miR-30b
miR-30a
miR-187*
miR-181c
miR-15a
miR-140-3p
miR-1272
miR-107
miR-92b*
miR-92a
miR-923
miR-483-5p
miR-21
miR-1268
miR-1225-5p
miR-643
miR-550
miR-24
miR-23a
miR-195
miR-141
miR-93
miR-675
miR-513b
miR-486-3p
miR-30c-1*
miR-27a
miR-210
miR-20b
miR-20a
miR-205
miR-155
miR-135a*
Increasing Expression
Microarray Round A
Microarray Round B

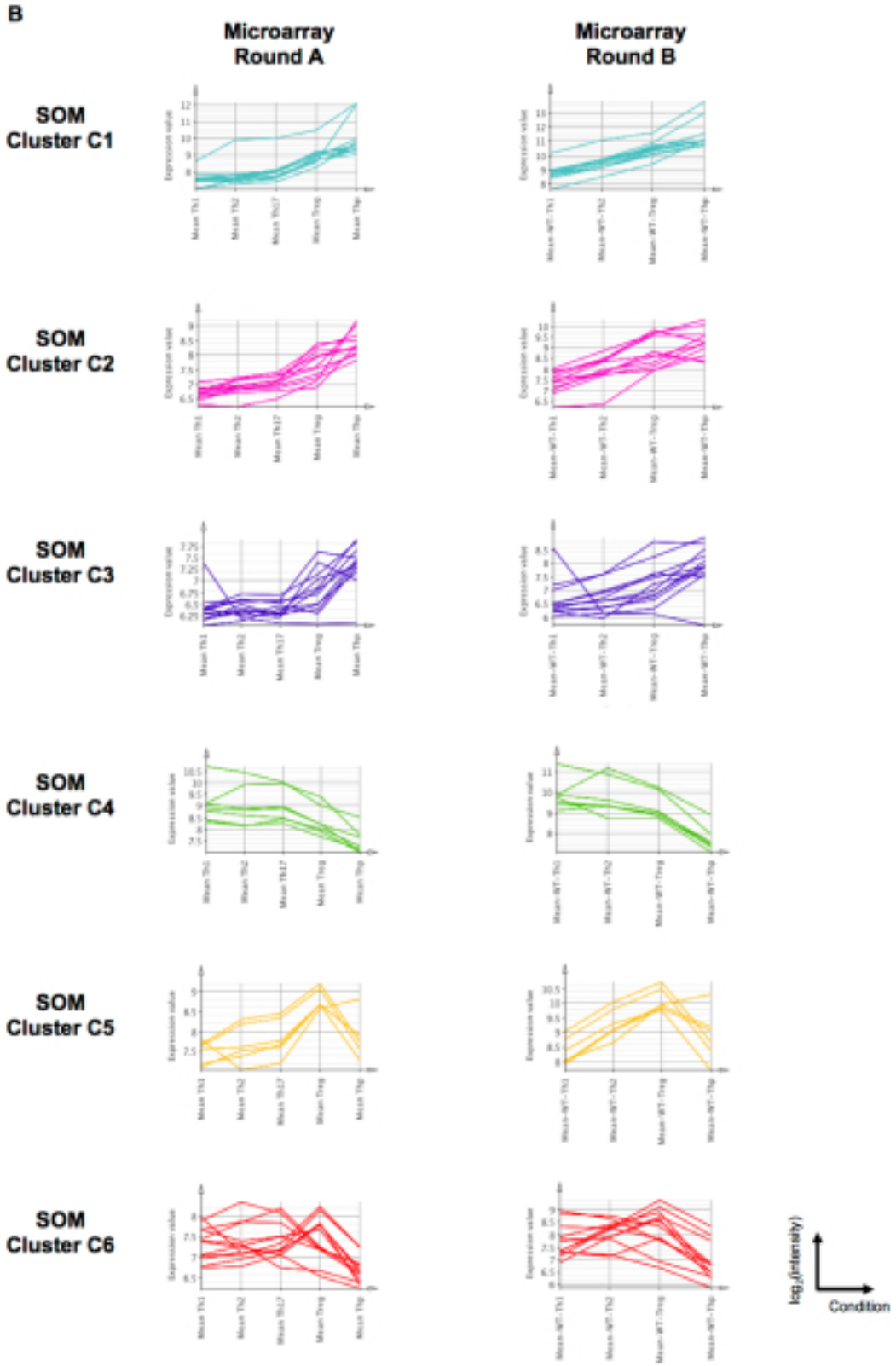

Figure 4.21 Side-by-side comparison of microarray Round A and B. Heatmaps in panel (A) and expression profile plots in panel (B) shown grouped according to consensus SOM clusters. In panel (B), each line represents an individual miRNA and line colours correspond with colours indicated to left of heatmap in panel (A).

The miRNAs that make up each individual cluster are shown in Table 4.3, along with a brief description of the observed expression pattern.

SOM Cluster	miRNAs	Description
SOM Cluster C1	miR-744, miR-16, miR-150, miR-142-5p, miR-142-3p, let-7g, let-7f, let-7e, let-7d, let-7c, let-7a	Higher expression in Thp and Treg when compared with effector subsets
SOM Cluster C2	miR-892a, miR-633, miR-519b-3p, miR-432*, miR-342-3p, miR-26b, miR-191, miR-183, miR-15b, miR-126*, let-7i	Higher expression in Thp and Treg when compared with effector subsets
SOM Cluster C3	miR-92b, miR-720, miR-422a, miR-375, miR-30b, miR-30a, miR-187*, miR-181c, miR-15a, miR-140-3p, miR-1272, miR-107	Higher expression in Thp and/or Treg when compared with effector subsets; lower overall expression than Clusters C1 & C2
SOM Cluster C4	miR-92b*, miR-92a, miR-923, miR-483-5p, miR-21, miR-1268, miR-1225-5p	Higher expression in effector and Treg subsets when compared with Thp
SOM Cluster C5	miR-643, miR-550, miR-24, miR-23a, miR-195, miR-141	Higher expression in Treg when compared with other subsets
SOM Cluster C6	miR-93, miR-675, miR-513b, miR-486-3p, miR-30c-1*, miR-27a, miR-210, miR-20b, miR-20a, miR-205, miR-155, miR-135a*	Higher expression in effector and/or Treg subsets when compared with Thp, lower overall expression than Cluster C4

Table 4.3 Consensus SOM clusters. Self-Organising Map (SOM) clusters derived from differentially expressed miRNAs with a fold-change of >2.0 detected between at least 2 WT T cell subsets in both Round A and B microarray series. A qualitative description of the observed expression pattern for each cluster is provided.

The microarray experiments comprising the Round A and B microarray series were performed consecutively and approximately one year apart, indicating that the patterns of differential expression demonstrated in the consensus clusters are reproducible within this laboratory and with this microarray technology. However it is advisable that the expression of individual candidate miRNAs of interest should be validated by an alternate method, such as qRT-PCR, as part of any further study into the function of that specific miRNA.

As described earlier, the WT microarrays in Round B were performed alongside corresponding T-bet$^{-/-}$ microarrays. In order to determine the effect of T-bet deletion on miRNA expression in these T cell subsets, fold change was calculated between WT and T-bet$^{-/-}$ samples, and results were analysed for differential miRNA expression. Unfortunately, this analysis did not reveal any consistently differentially-expressed miRNAs between those subsets that express T-bet, namely Th1 and iTreg (Figure 4.22).

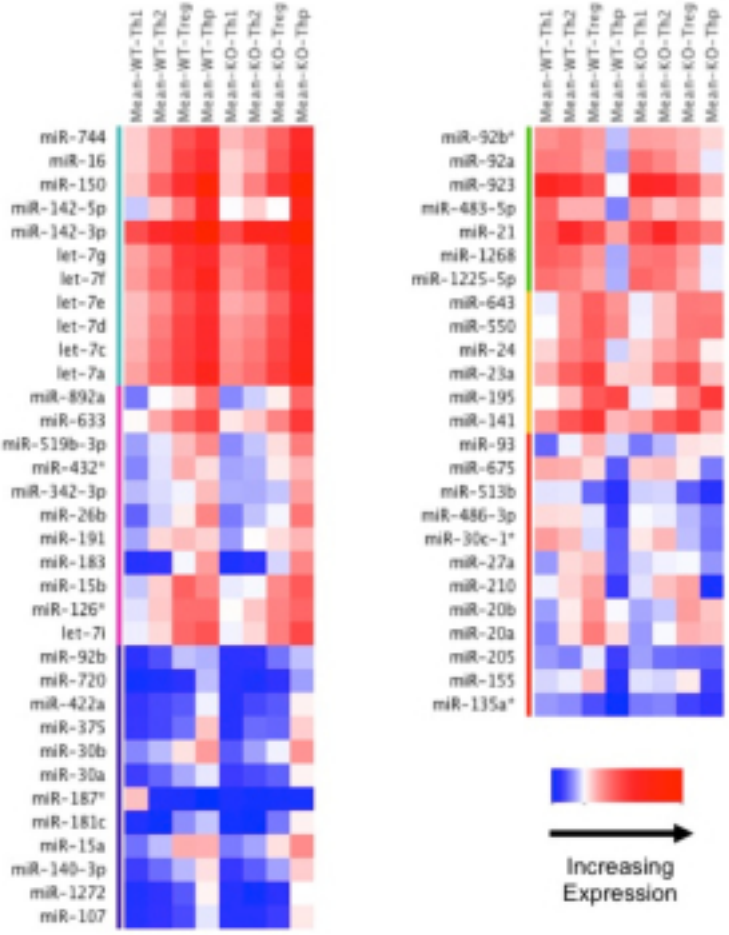

Figure 4.22 Expression of miRNAs in WT and T-bet$^{-/-}$ T helper cell subsets. Heatmap data shown is grouped according to the consensus SOM clusters detailed in Table 4.3. Mean of two biological replicates is shown. WT=wild-type, KO=T-bet$^{-/-}$.

However candidate gene analysis using qRT-PCR was also performed. Comparison of miR-142-3p and miR-142-5p expression between WT and T-bet$^{-/-}$ Th1 and iTreg cells

did demonstrate increased expression of these genes in T-bet$^{-/-}$ cells (Figure 4.23). These data likely reflect increased sensitivity of qRT-PCR for the detection of differential expression with smaller fold changes.

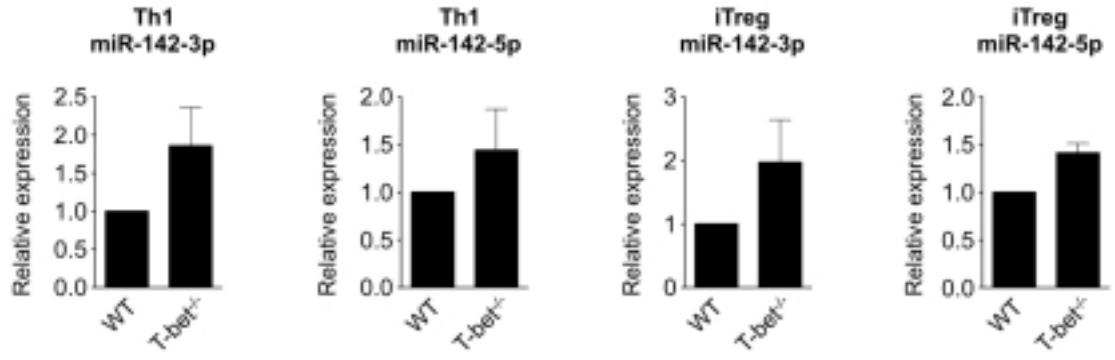

Figure 4.23 Expression of miR-142-3p and miR-142-5p in WT and T-bet$^{-/-}$ Th1 and iTreg cells, normalized to WT. Data expressed as $2^{-\Delta\Delta Ct}$ relative to WT, data normalised to U6 internal control; n=3 independent biological replicates, error bars=SEM.

Collectively, these data have demonstrated that distinct patterns of miRNA expression exist between T cell subsets, and that some of these patterns are highly reproducible, in particular those miRNAs whose expression is up- or down-regulated following activation and differentiation of naïve T cells into effector subsets. In addition, a potential candidate of interest, mir-142, has been identified as being differentially expressed between WT and T-bet-deficient cells.

4.5. Binding of T-bet, GATA-3 and FoxP3 at the mir-142 locus

Our laboratory has previously developed techniques for detecting transcription factor binding on a genome-wide scale in T cell subsets, and has recently published data describing the binding of T-bet and GATA-3 in human Th1 and Th2 cells as determined by Chromatin-immunoprecipitation coupled with genome-wide promoter microarray

analysis (ChIP-Chip) (Jenner et al., 2009). We have since repeated these experiments using next-generation sequencing technology (ChIP-seq) to identify the binding sites of T-bet and GATA-3 in human Th1 and Th2 cells (A. Hertweck, unpublished data), and T-bet and FoxP3 in mouse Th1 and Treg cells (Gokmen, 2011). These datasets can be analysed to determine whether transcription factor binding occurs at miRNA genomic loci. For example, in human Th1 and Th2 cells, ChIP-Chip (Jenner et al., 2009) (Figure 4.24) and ChIP-Seq (A. Hertweck, unpublished data) (Figure 4.25) experiments reveal binding of both T-bet and GATA-3 at the mir-142 genomic locus.

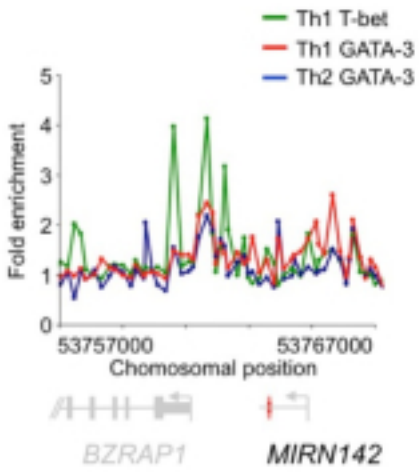

Figure 4.24 ChIP-Chip experiments show binding of T-bet and GATA-3 at the human mir-142 genomic locus. Immunoprecipitation was performed for T-bet in *in vitro*-polarised Th1 cells and GATA-3 in both Th1 and Th2 cells. Precipitated DNA was then hybridised to promoter microarray as described in (Jenner et al., 2009). Data courtesy of Dr. R. Jenner/Prof. G. Lord.

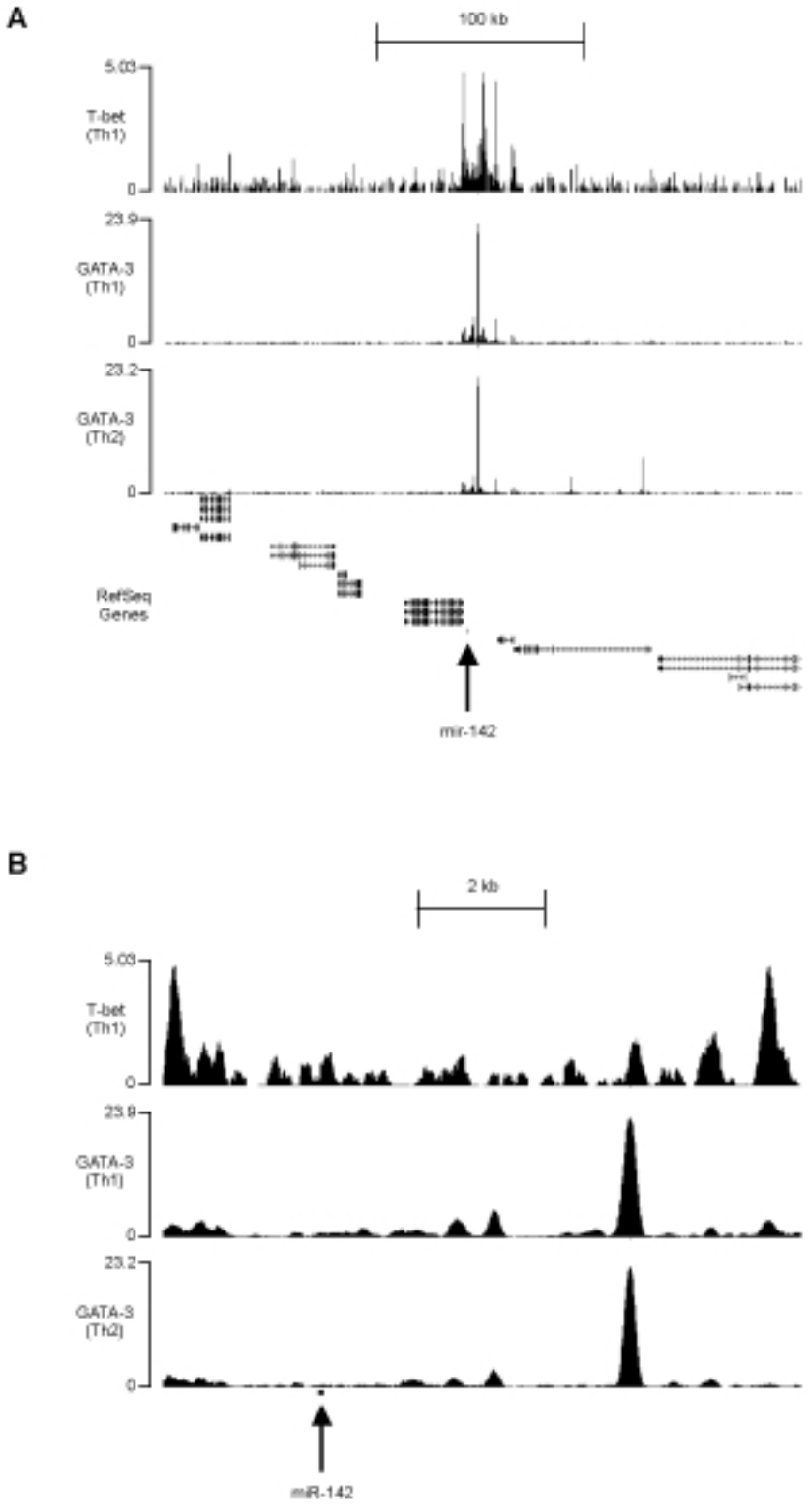

Figure 4.25 ChIP-seq experiments demonstrate binding of T-bet and GATA-3 at the mir-142 genomic locus in human Th1 and Th2 cells. (A) Approximately 300 kilobase view of mir-142 genomic locus. (B) Approximately 10 kilobase view of mir-142 genomic locus. Data expressed as sequencing reads per million background-subtracted total reads. Position of mir-142 indicated by arrow; neighbouring genes are shown in panel (A). Transcription factor of interest and cell type indicated to left of each row. Data courtesy of Dr. A. Hertweck/Prof. G. Lord.

In addition, murine experiments reveal binding of both T-bet and FoxP3 at the mir-142 genomic locus in *in vitro*-differentiated Th1 and Treg cells (Figure 4.26).

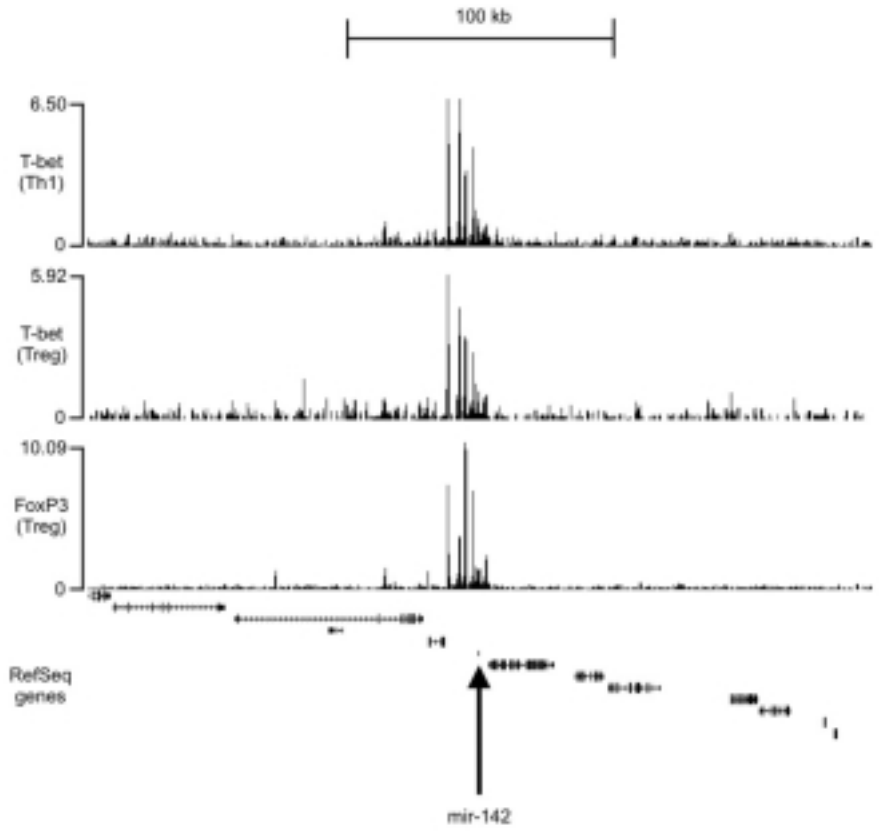

Figure 4.26 T-bet and FoxP3 bind to the mir-142 locus in murine Th1 and iTreg cells. ChIP-Seq was performed for T-bet and FoxP3 in murine *in vitro*-differentiated Th1 and iTreg cells. Approximately 300 kilobase genomic region shown; data expressed as sequencing reads per million background-subtracted total reads. Arrow indicates position of mir-142; transcription factor of interest & cell type indicated to left of row. Data courtesy of Dr R. Gökmen/Prof G. Lord.

Collectively, these data demonstrate that three master regulatory T cell transcription factors bind at the mir-142 locus, and that T-bet binding is present at the mir-142 locus in both human and mouse Th1 cells. These findings of transcription factor binding at the mir-142 locus do not in themselves suggest any specific regulation of mir-142 expression by these transcription factors. However they support the generation of the hypothesis that mir-142 is of importance in pathways that control T cell function and differentiation. This hypothesis is more generally reinforced by the findings that mir-

142 expression is dynamically regulated between naïve and activated cell types, and that T-bet deficiency can result in dysregulated expression of mir-142.

4.6. Discussion

A large number of miRNAs have been identified within the last decade, and it remains a major challenge to determine which miRNAs should be prioritised for functional investigation. A range of methods are of use in this endeavour, including expression profiling through techniques such as qRT-PCR, sequencing and microarray analysis. As it is clear that changes in miRNA expression correlate with functional activity, comparison of miRNA expression between differentiated cell types can be used to identify miRNAs that are of potential importance in specifying cell phenotype. In addition, analysis of processes such as transcription factor binding can identify features of miRNA transcription that may be functionally related to the phenotype. Many of these technologies operate at the genome-wide scale and therefore provide large datasets that can be subjected to further analysis. In this situation, genome-wide techniques are frequently employed as hypothesis-generating methods in order to identify candidate genes that may then be investigated functionally.

In this study, I have aimed to test the hypothesis that specific miRNAs are responsible for controlling fundamentally-important and interrelated T helper cell processes such as homeostasis, function and lineage commitment. The data presented in this chapter represent the first stage of this process, specifically the identification of a group of miRNAs that are differentially expressed between naïve and activated T helper cell types. In addition, experiments were performed to determine whether miRNAs are differentially expressed when the T helper cell transcription factor T-bet is absent.

Finally, transcription factor binding data are analysed to determine whether binding at a candidate miRNA locus is detected. Collectively these data have allowed for the identification of a specific candidate miRNA that is the subject of further functional investigation as part of this study, the results of which are detailed in the following chapters.

The microarray experiments that have been performed have identified a number of miRNAs as being differentially expressed between WT subsets, and demonstrate consistent patterns of clustering. The use of two independent microarray experiments, each with two biological replicates per condition, allows for reduction of the number of identified candidate miRNAs to a group of 59 that are found to be consistently differentially expressed. With regard to the primary aim of these experiments, microarray analysis has therefore successfully identified a number of potential candidates of interest. A secondary outcome of these experiments has been to describe patterns of miRNA expression that may be able to distinguish subsets from each other. However further work using an alternative technology such as qRT-PCR is recommended in order to validate the expression patterns of individual miRNAs, as a definitive description of miRNA expression patterns in T cell subsets is beyond the scope of this study.

Having identified a primary group of candidate miRNAs, I used a number of complementary approaches in order to further refine these data and thereby permit testing of the original hypothesis that specific miRNAs are critically important in fundamental T helper cell processes. An additional set of microarrays was performed in order to compare T-bet-deficient cells with WT cells, however these microarrays did not detect any consistent difference in miRNA expression between these genotypes. This

suggests that the differences in miRNA expression between differentiated cells from these two genotypes are too small to be detected with miRNA microarray technology. However, the use of qRT-PCR did show differential expression of miR-142-3p and miR-142-5p, indicating that the absence of T-bet can indeed have an effect on miRNA expression.

Analysis of ChIP datasets generated within our laboratory demonstrated that T-bet is found at the mir-142 genomic locus in both human and mouse Th1 cells, and also provided evidence that additional master regulatory transcription factors including GATA-3 and FoxP3 bind mir-142. These data are not intended to describe the way in which these transcription factors interact with mir-142 or whether they exert any control over mir-142 expression. However they do suggest that mir-142 is a part of multiple transcription factor-regulated networks that have been widely demonstrated to be of critical importance in T helper cell differentiation and function. Future work may employ promoter assays to determine the nature of any regulation of mir-142 expression by these transcription factors.

The datasets generated in this part of the study are intended to form the basis of further study. Indeed, the remainder of this thesis is concerned with the analysis of mir-142 function in T helper cells. However, a number of other differentially-expressed miRNAs were identified through analysis of these microarrays. In particular, the members of SOM cluster C1 are more highly expressed in Thp and iTreg when compared with effector populations. Some of these miRNAs, such as miR-744, are of unknown function in T helper cells, and potentially merit further investigation. In addition, many of the miRNAs that make up SOM cluster C5 were found to be specifically upregulated in iTreg cells, yet none of these has to date been ascribed to any particular function in

these cells. Any further characterisation of these miRNAs should begin with validation of differential expression through alternate means such as qRT-PCR or Northern Blot, and could include analysis of ChIP datasets to determine whether master regulatory transcription factors also bind to the genomic loci of these miRNAs.

This type of analysis could be extended into an additional potential opportunity for unbiased mining of these datasets based on an integrated bioinformatics approach. Following the generation of highly purified T cell subsets from which RNA was extracted for miRNA expression analysis, additional Affymetrix® microarrays were performed in parallel (see Appendix B). These allow analysis of protein-coding gene expression on the genome-wide scale, and so we have therefore generated miRNA expression data, mRNA expression data and transcription factor ChIP binding data from the same cell types. These large and complex datasets could potentially be integrated with miRNA target prediction, transcription factor binding and gene ontology databases in order to identify and describe some of the complex regulatory networks that govern T cell function (Figure 4.27). This would represent a challenging bioinformatics project that is not currently supported in its entirety by open source or freely accessible software, and would be likely to necessitate the production of custom software. As a result, this was not within the scope of this project at this time, but remains a potential additional outcome of the work.

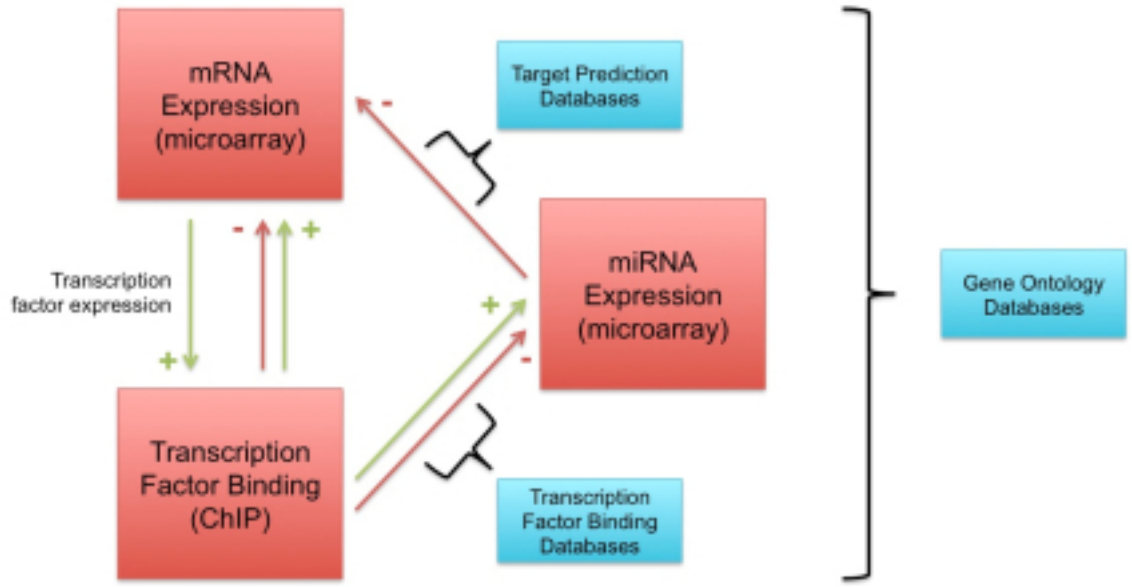

Figure 4.27 Schematic representation of bioinformatic integration of datasets. Datasets generated from analysis of primary T cells are shown in red boxes. Blue boxes indicate publicly available databases. Arrows indicated interactions between indicated components.

In summary, this first phase of the study has described differential miRNA expression in T cells and identified a candidate miRNA for further investigation of a possible role in T helper cell function. In addition, expression profiling of miRNAs in T helper cells has identified a number of other candidates of interest for future studies. These data may potentially allow for future integrated bioinformatics analysis in order to characterise the relationships and pathways the connect miRNAs with protein-coding and other genes in these cells, thereby improving our understanding of the way in which the function of these cells is regulated.

5. The role of mir-142 in T helper cell homeostasis

5.1. Introduction

These data have demonstrated that mir-142 expression is dynamically regulated in T cell subsets, and that T cell master regulatory transcription factors such as T-bet, GATA-3 and FoxP3 bind to the genomic locus of mir-142. It has also been previously demonstrated that *in vitro* mir-142 overexpression in haematopoietic precursors results in an increase both in the number of T cells, and in the ratio of T cells to B cells (Chen et al., 2004). The mechanism for this alteration in T cell numbers has not previously been addressed, but it indicates that mir-142 possesses regulatory function over the mechanisms that control lymphoid homeostasis. Coupled with the evidence that transcriptional control of mir-142 expression involves subset-specific transcription factors, this presented sufficient reason to systematically investigate the function of mir-142 in T cells and their subsets. I therefore sought to address the hypothesis that mir-142 plays a critical role in T cell homeostasis, differentiation and function.

5.2. mir-142-deficient mice have a specific defect in T cell homeostasis

In order to determine the nature of any functional role of mir-142 in T cells, we developed lines of both constitutive and conditional mir-142-deficient mice. Offspring of heterozygous constitutive knockout mice (mir-142$^{+/-}$) are born at the expected

Mendelian rate (Figure 5.1) and homozygous mir-142-deficient mice (mir-142$^{-/-}$) remain healthy beyond at least 18 months of age, with no sign of spontaneous disease. This suggests that mir-142 deficiency does not impair fetal development in general, and that there is no spontaneous development of life-threatening diseases such as autoimmunity, cancer or infection when mice are housed under the SPF conditions maintained in our breeding facility.

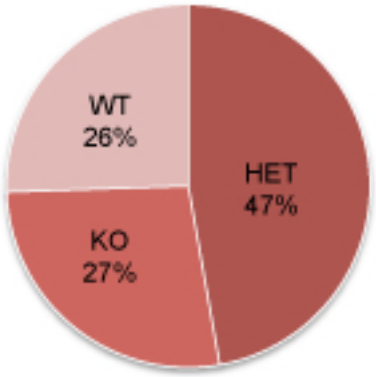

Figure 5.1 Genotype frequency for offspring of heterozygous mir-142$^{+/-}$ mice. WT=wild-type, mir-142$^{+/+}$; HET=mir-142$^{+/-}$; KO=mir-142$^{-/-}$. n=235.

In order to validate the gene knockout strategy, the expression of mir-142 in wild-type littermate (WT) and mir-142$^{-/-}$ mice was measured with both Northern blot and qRT-PCR. Expression of mir-142 is highest in the thymus and spleen (Chen et al., 2004). Northern blot analysis of total RNA isolated from spleen and thymus of WT and mir-142$^{-/-}$ mice showed that neither miR-142-3p nor miR-142-5p could be detected in mir-142$^{-/-}$ mice, despite being readily detectable in WT (Figure 5.2). Similarly, qRT-PCR was able to detect miR-142-3p and miR-142-5p expression in WT naïve T cells but not in mir-142$^{-/-}$ (Figure 5.2).

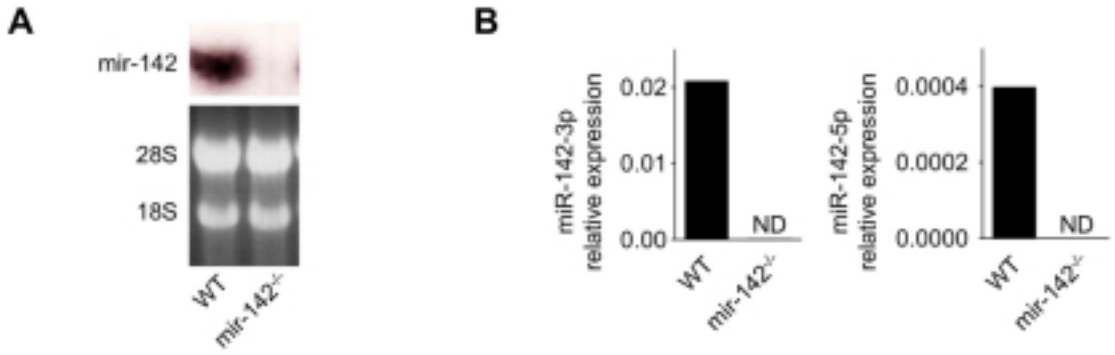

Figure 5.2 Expression of mir-142 in WT and mir-142$^{-/-}$ mice. (A) Northern blot performed on total RNA from WT and mir-142$^{-/-}$ pooled spleen and thymus, probed with miR-142-3p and miR-142-5p probes (Upper panel). Lower panel is ethidium bromide-stained RNA gel to demonstrate equal RNA loading. (B) qRT-PCR demonstrating expression of miR-142-3p (left panel) and miR-142-5p (right panel) in WT and mir-142$^{-/-}$ naïve T cells. ND=not detected above threshold after 35 cycles of PCR. Data representative of 2 independent experiments.

These data confirmed that mir-142$^{-/-}$ mice do not express mir-142, and so initial phenotyping of the mice was carried out in order to identify any obvious defects arising as a result of this deficiency. Flow cytometric analysis was first performed, which revealed a marked reduction in CD3^{+} T cell numbers in the periphery of mir-142$^{-/-}$ mice when compared with WT (Figure 5.3).

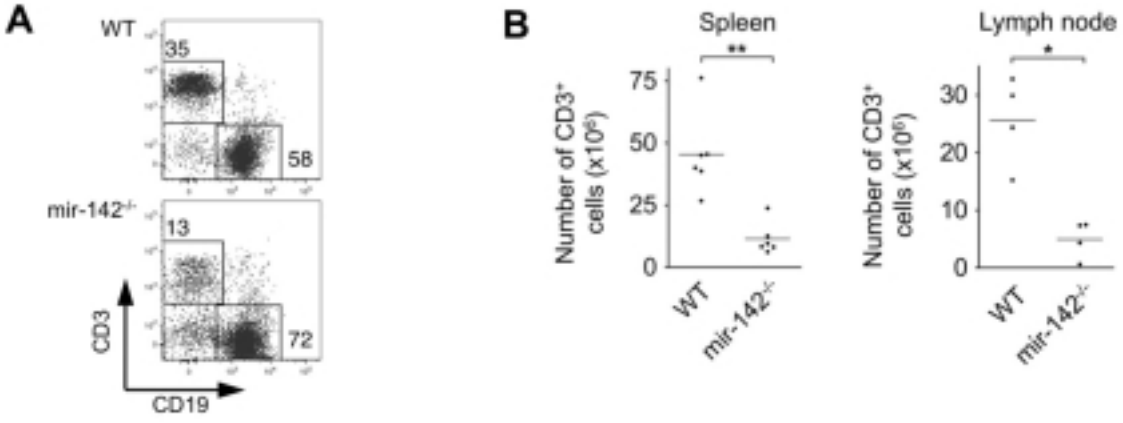

Figure 5.3 mir-142$^{-/-}$ mice exhibit a deficiency in peripheral T cell numbers. (A) Flow cytometric analysis of spleen isolated from WT and mir-142$^{-/-}$ mice. Plot shown is gated on live lymphocytes. Data representative of 6 independent experiments. (B) Absolute number of CD3$^+$ T cells in spleen and pooled peripheral lymph nodes (axillary, cervical, inguinal) isolated from WT and mir-142$^{-/-}$ mice. n=6 and 4 independent experiments for spleen and lymph node respectively. *P<0.05, **P<0.01 (unpaired Student's t-test)

In addition, a number of other immune cell lineages were assessed by flow cytometry, however no defect was observed in the number of CD19$^+$ B cells, CD11c$^+$ MHC Class II$^+$ dendritic cells or NKp46$^+$ cells (Figure 5.4).

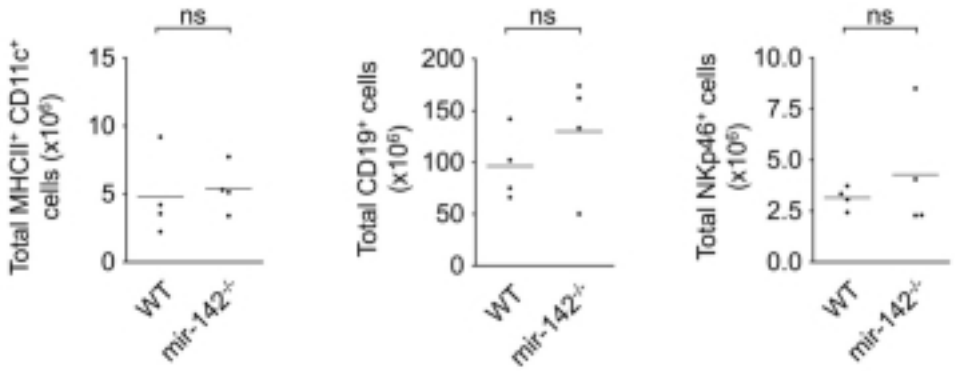

Figure 5.4 No deficiency is observed in other major immune lineages. Total cell counts for MHC class II$^+$ CD11c$^+$ dendritic cells, CD19$^+$ B cells and NKp46$^+$ cells isolated from spleen of WT and mir-142$^{-/-}$ mice. n=4 independent experiments. ns=not significant (unpaired Student's t-test).

This T cell-specific deficiency is somewhat surprising, given that mir-142 is known to be widely expressed in the immune system (Landgraf et al., 2007). Further analysis was

therefore performed in order to compare T cell phenotype between mir-142$^{-/-}$ and WT littermate mice. Staining for the lineage markers CD4 and CD8 revealed that there is no difference in the ratio between CD4^{+} and CD8^{+} cells in mir-142$^{-/-}$ mice when compared with WT, indicating that both lineages are equally deficient in mir-142$^{-/-}$ mice (Figure 5.5).

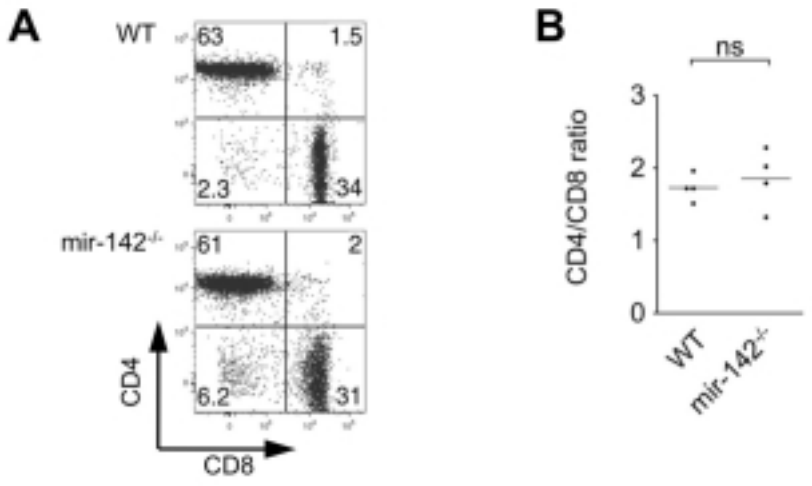

Figure 5.5 CD4^{+} and CD8^{+} T cell lineages are affected equally. (A) Representative flow cytometric staining of splenic CD3^{+} T cells. (B) Ratio between CD4^{+} and CD8^{+} T cells isolated from WT and mir-142$^{-/-}$ mice. n=4 independent experiments.

Next, the ratio of naïve and memory CD4^{+} T cells was assessed. Naïve cells were defined for this purpose as CD4^{+} CD62L^{high} CD44^{low} and memory as CD4^{+} CD62L^{low} CD44^{high}. A small but significant difference in the percentage of naïve and memory cells was observed, with a reduction in the proportion of naïve cells (Figure 5.6).

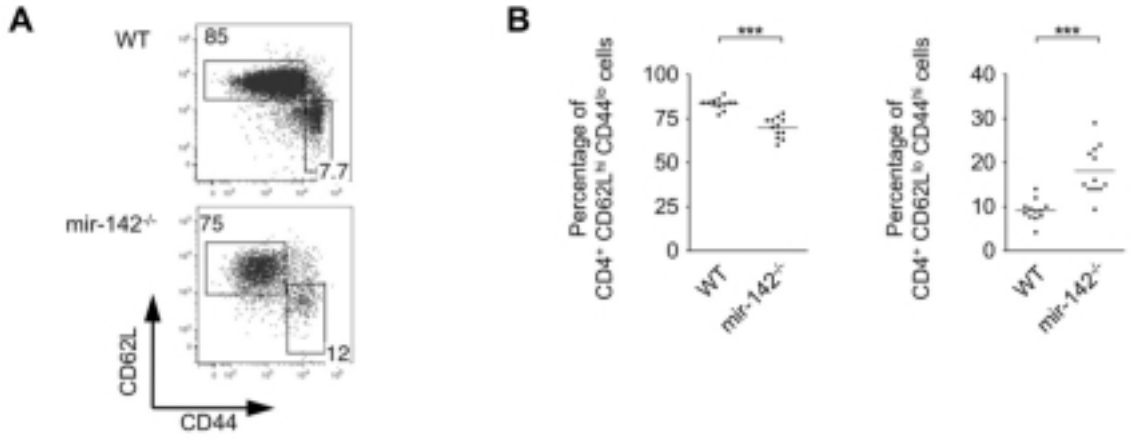

Figure 5.6 Reduction in proportion of naive T helper cells in mir-142$^{-/-}$ mice. (A) Representative staining of CD62L and CD44 on CD4$^+$ T cells. (B) Percentage of naïve (CD62L^{high} CD44^{low}) and memory (CD62L^{low} CD44^{high}) CD4$^+$ T cells. n=12 independent experiments; ***p<0.001 (unpaired Student's t-test).

However, there was no difference in the percentage of naïve T cells expressing the surface marker CD25 (Figure 5.7).

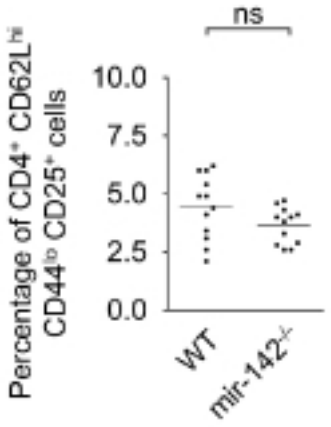

Figure 5.7 Percentage of CD25$^+$ naive T cells in WT and mir-142$^{-/-}$ mice. n=12 independent experiments, ns = not significant (unpaired Student's t-test).

In order to assess whether the deficiency in T cells was associated with architectural abnormalities in lymphoid tissue, immunohistochemistry was performed. The paucity of

T cells was clearly demonstrated in splenic sections, however structural abnormalities were not seen and follicle formation was evident (Figure 5.8).

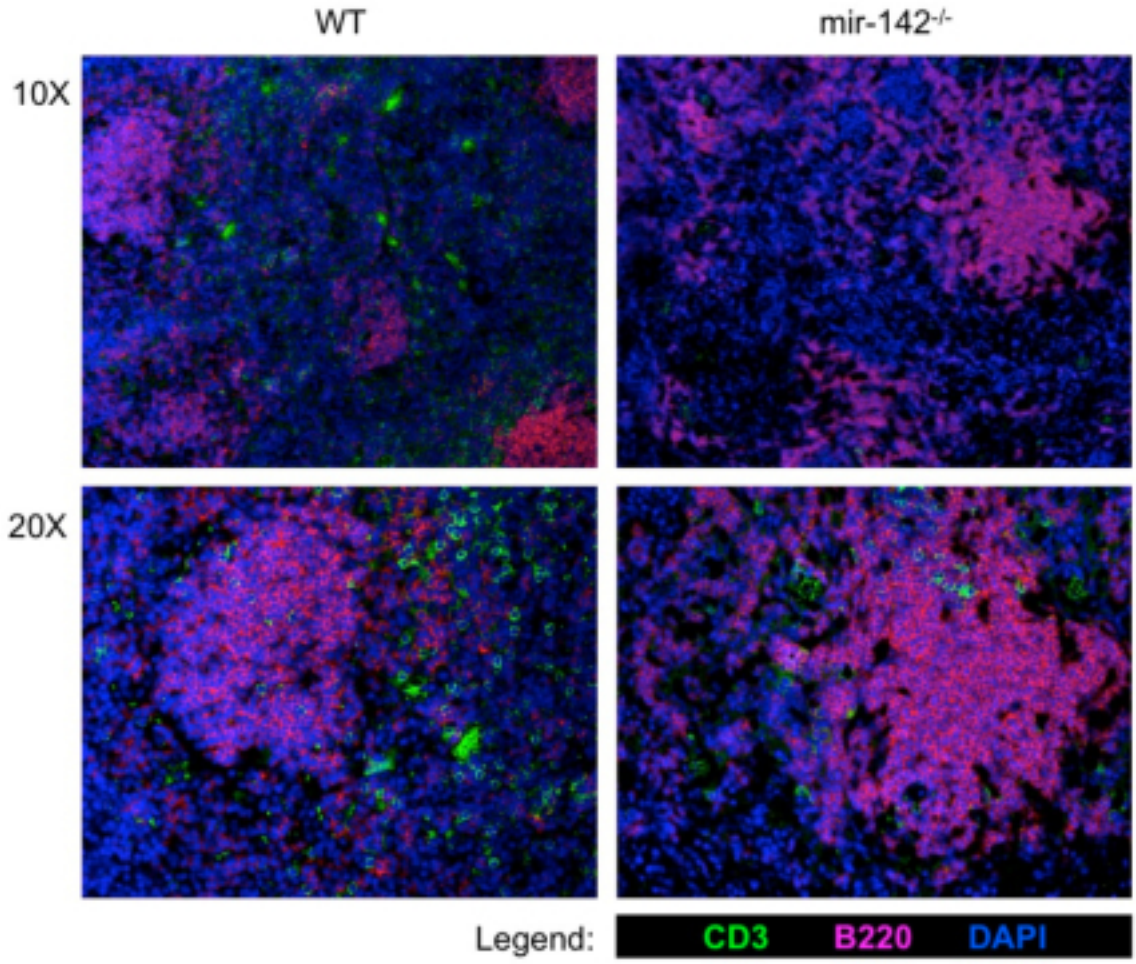

Figure 5.8 Immunohistochemical analysis of WT and mir-142$^{-/-}$ spleen demonstrates paucity of T cells, but evidence of follicle formation. Staining performed by Dr. E. Marks, magnification as indicated.

These data collectively identify a specific, prominent defect in T cell numbers that affects both CD4^{+} and CD8^{+} lineages equally. This initial screening analysis did not detect obvious abnormalities in non-T cell lineages, and so the T cell defect was selected for further investigation. However it is possible that subtle differences in other cell types exist and as such it is important to determine whether the T cell defect arises

as a direct and intrinsic result of mir-142 deficiency in T cells or if it is due to defects in other cell types.

5.3. The defect is T cell-intrinsic and post-developmental

In order to determine whether the defect was intrinsic to the lymphoid system or if it was due to loss in non-lymphoid lineages, I generated bone marrow chimeric mice. This was achieved by reconstitution of sublethally-irradiated RAG-1$^{-/-}$ mice with cells derived from bone marrow of either mir-142$^{-/-}$ or WT mice. At four weeks following transfer, CD3^{+} T cell numbers were profoundly reduced in recipients of mir-142$^{-/-}$ cells, despite CD19^{+} B cells having reconstituted equally in both (Figure 5.9).

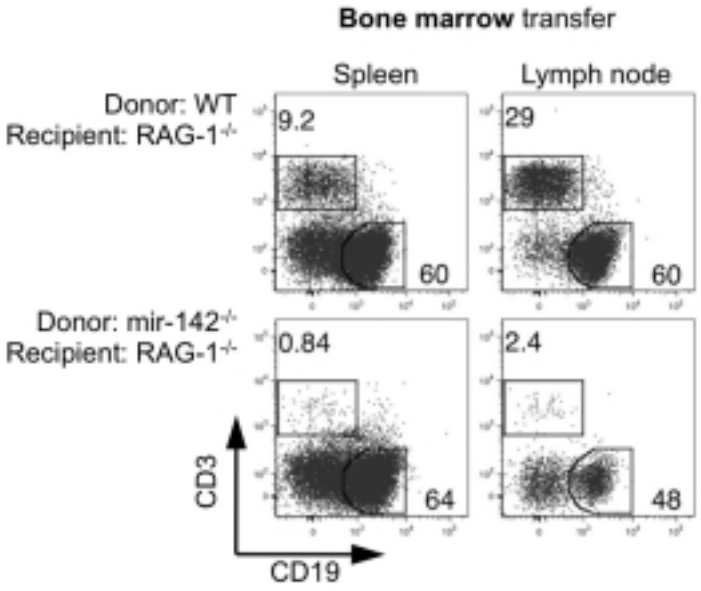

Figure 5.9 mir-142-deficient bone marrow is insufficient for the reconstitution of T cells in sublethally-irradiated lymphopenic RAG-1$^{-/-}$ mice, despite appropriate reconstitution of CD19^{+} B cells. Flow cytometric analysis of spleen and pooled peripheral lymph nodes at four weeks post-transfer. Representative plot of 2 independent experiments with a total of 4 mice per group.

These experiments established that mir-142 deficiency in the lymphoid compartment was sufficient to cause the T cell-deficient phenotype. In order to further define the lineage in which mir-142 deficiency results in reduced T cell numbers, conditional mir-142$^{fl/fl}$ mice were crossed with CD4-Cre mice, so as to specifically delete mir-142 in CD4-expressing cells. These mice reproduced the defect observed in constitutively mir-142-deficient mice, with a reduction in T cells seen in mir-142$^{fl/fl}$ CD4-Cre^{+} mice when compared with mir-142$^{fl/fl}$ CD4-Cre^{-} littermate mice (Figure 5.10).

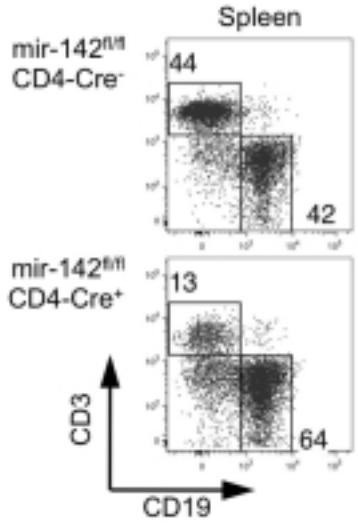

Figure 5.10 Conditional deletion of mir-142 in T cells reproduces the T cell defect that is seen in constitutively mir-142-deficient mice. Flow cytometric analysis of spleen from littermate mice with genotype as indicated. Plots representative of 3 independent experiments.

These data indicated that the defect is T cell-intrinsic, as non-T cell lineages in these CD4-Cre^{+} mice have not undergone deletion of mir-142. In order to determine the effect of mir-142 loss specifically in mature CD4^{+} T helper cells, a series of T cell transfer experiments were performed, in which naïve T cells (defined as CD4^{+} CD62L^{high} CD44^{low} CD25^{-}) were isolated by flow cytometric sorting and transferred intraperitoneally into lymphopenic RAG-1$^{-/-}$ mice. Under these conditions, WT T cells

proliferated and were readily detectable at four weeks, however T cells from mir-142$^{-/-}$ littermate mice were almost completely absent (Figure 5.11).

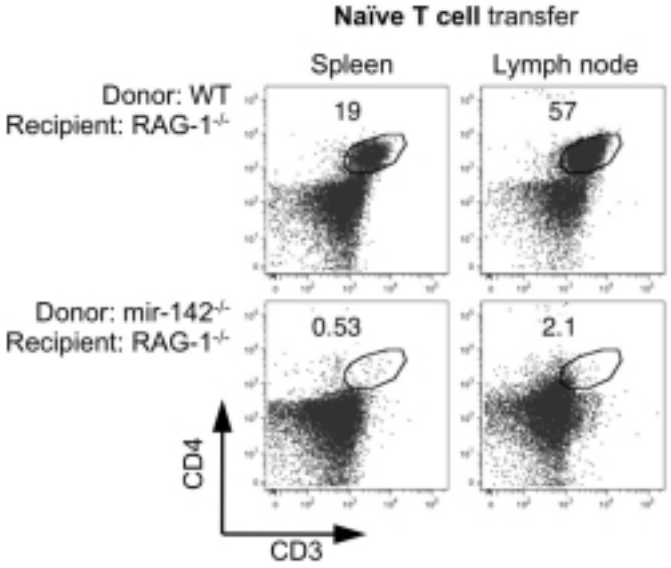

Figure 5.11 mir-142$^{-/-}$ naïve T cells do not proliferate *in vivo* when transferred into a lymphopenic host. 0.5x10^6 naïve T cells were injected intraperitoneally into RAG1$^{-/-}$ mice. At four weeks following transfer, mice were culled and flow cytometry performed. Spleen and mesenteric lymph nodes (mLN) were analysed for the presence of T cells. Plots representative of 2 independent experiments with 4 mice per group

These data demonstrate an intrinsic defect in the homeostasis of mir-142-deficient CD4$^+$ T helper cells. As there was effectively no expansion in T cell numbers following transfer, there existed the possibility that mature mir-142$^{-/-}$ CD4$^+$ T cells were incapable of proliferating. In order to determine whether this was the case, naïve T cells from WT and mir-142$^{-/-}$ mice were isolated and stimulated *in vitro* with plate bound anti-CD3 and anti-CD28 antibodies under non-polarising conditions. Proliferation was assessed by cell division analysis with the cell-labelling dye CFSE, and the rate of apoptosis was also assessed by staining for Annexin V and propidium iodide inclusion. Both cell division and apoptosis were measured daily for 5 days in order to provide a timecourse analysis. These experiments demonstrated that mir-142$^{-/-}$ naïve T cells are capable of

proliferating normally in response to TCR stimulus, and have similar rates of apoptosis when compared with WT cells (Figure 5.12).

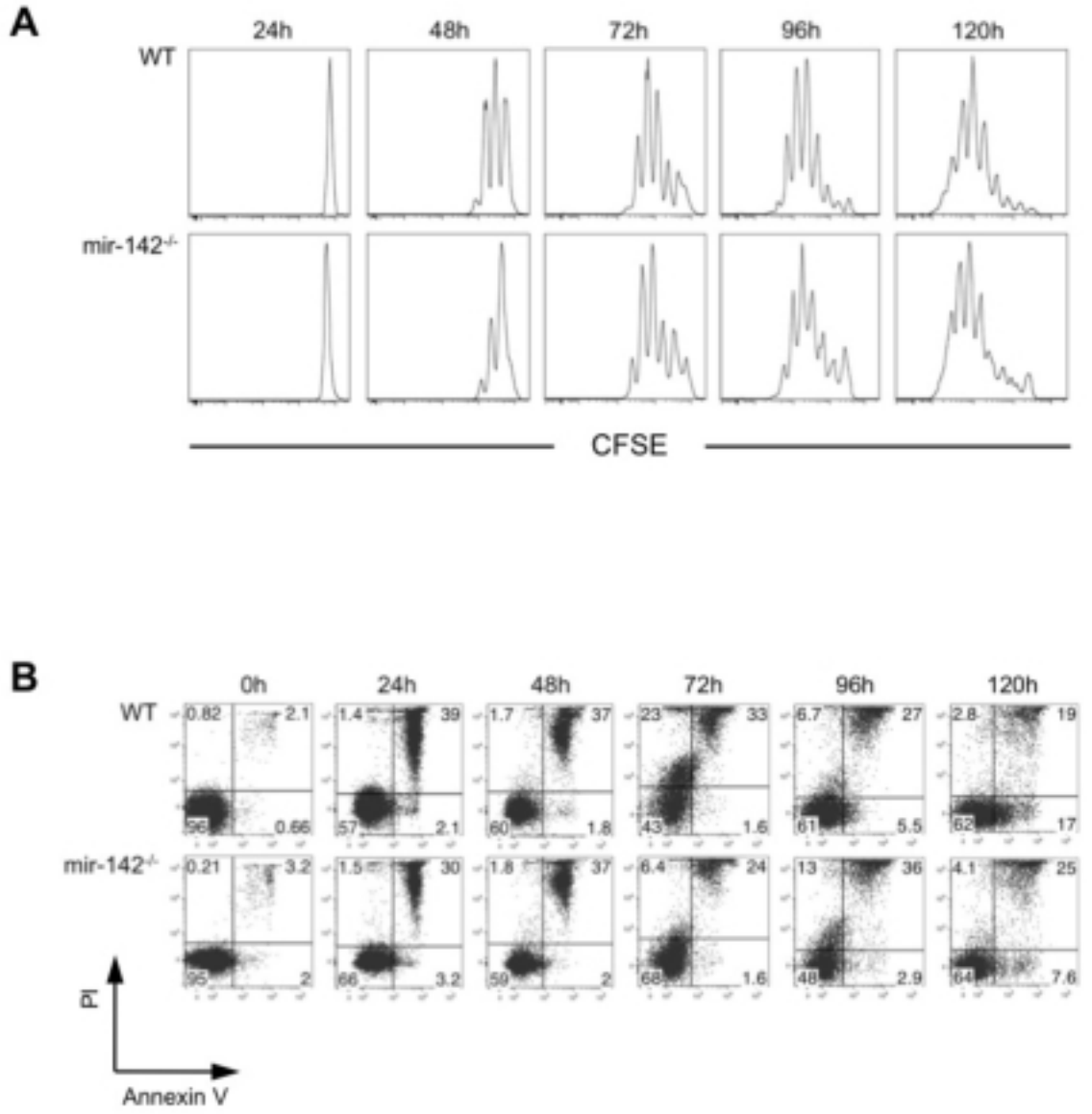

Figure 5.12 mir-142$^{-/-}$ naive CD4$^+$ T cells proliferate normally in response to TCR stimulation. (A) Naïve CD4$^+$ T cells were isolated from mir-142$^{-/-}$ and WT littermate mice, labelled with CFSE and then stimulated *in vitro* with anti-CD3 and anti-CD28 antibodies in non-polarising conditions. Proliferation was assessed by flow cytometry at the indicated timepoints. (B) Apoptosis rates were also measured in these cells at the indicated time points. PI=propidium iodide. Both (A) and (B) representative of 2 independent experiments.

This stimulation was also carried out with a titration of the strength of TCR stimulus, by varying both the concentration of anti-CD3 and anti-CD28. This demonstrated similar responses to stimulation for both WT and mir-142$^{-/-}$ cells (Figure 5.13).

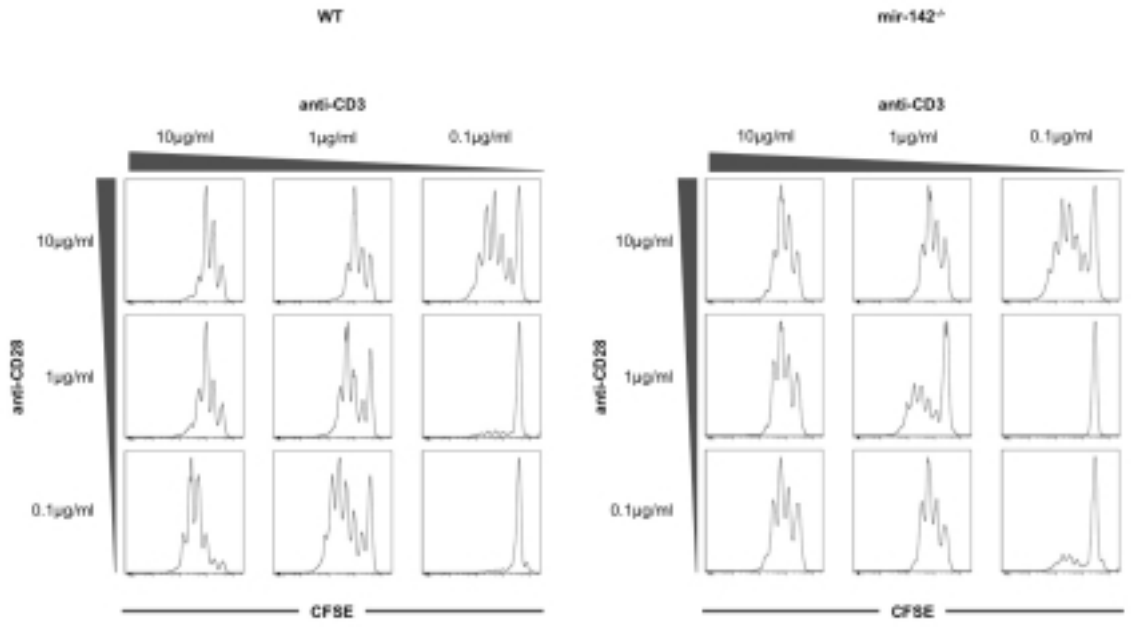

Figure 5.13 mir-142$^{-/-}$ T cells respond to TCR activation and co-stimulation in a dose-dependent manner. WT (left) and mir-142$^{-/-}$ (right) naïve CD4^{+} T cells were isolated and labelled with CFSE. Cells were stimulated with plate-bound anti-CD3 and anti-CD28 at the indicated concentrations for 4 days.

In addition, cells were co-cultured with irradiated splenocytes in order to provide co-stimulation, in the presence of varying concentrations of soluble anti-CD3. Again, T cell proliferation was seen to be similar between WT and mir-142$^{-/-}$ cells (Figure 5.14).

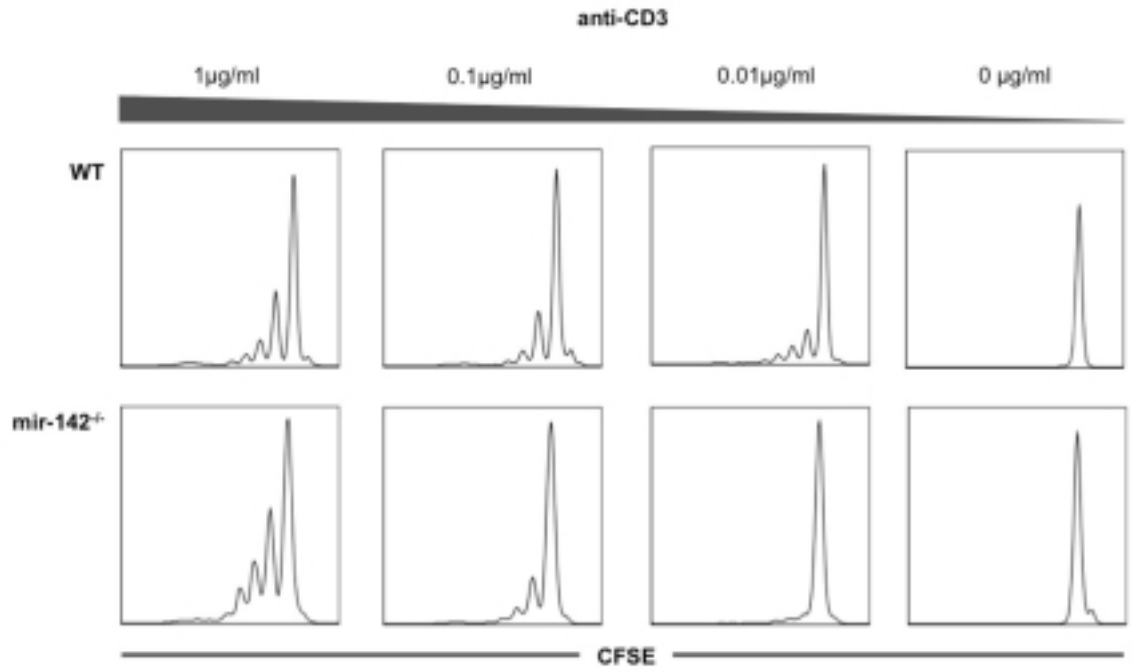

Figure 5.14 mir-142$^{-/-}$ T cells respond to TCR ligation in the presence of cell-mediated co-stimulation. Naïve CD4^{+} T cells were isolated from WT and mir-142$^{-/-}$ mice and labelled with CFSE. Cells were then stimulated *in vitro* for 4 days with soluble anti-CD3 antibodies in the presence of irradiated splenocytes, at a co-culture ratio of 1:1.

Clearly these cells are capable of proliferating *in vitro* when stimulated through the TCR. In order to determine whether this activation was sufficient to overcome the *in vivo* defect in T cell expansion, *in vitro*-activated cells from WT and mir-142$^{-/-}$ mice were transferred into RAG-1$^{-/-}$ mice. Again, WT cells proliferated *in vivo* and were readily detectable by flow cytometry, whereas mir-142$^{-/-}$ cells were markedly absent (Figure 5.15). These data showed that mir-142$^{-/-}$ T cells exhibit an intrinsic proliferation defect *in vivo*, even after *in vitro* stimulation.

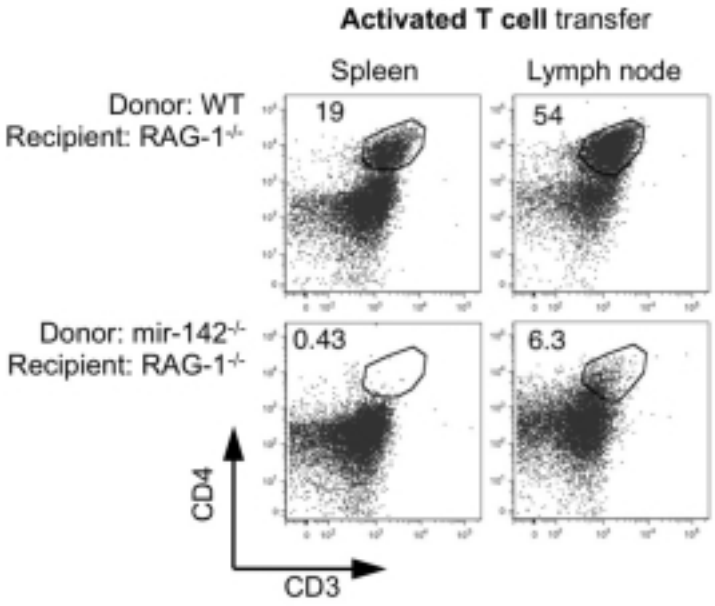

Figure 5.15 Activated mir-142$^{-/-}$ CD4^{+} T cells do not proliferate *in vivo*. Naïve CD4^{+} T cells were isolated from mir-142$^{-/-}$ and WT littermate mice and then activated for 7 days *in vitro* with plate-bound anti-CD3 and anti-CD28. 1x10^{6} cells were then injected intraperitoneally into RAG-1$^{-/-}$ mice. After a further 3 weeks, mice were culled and spleen and mLN were subjected to flow cytometric analysis. Data representative of 2 independent experiments with a total of 4 mice per group.

mir-142 is expressed at multiple stages of T cell development, with greatest expression occurring in naïve T cells and in the thymus (Chen et al., 2004). The observed defective T cell homeostasis in mir-142$^{-/-}$ mice could potentially be due to mir-142 deficiency at an earlier stage of T cell development. In order to address this, experiments were performed in which mir-142 was deleted *in vitro* at 24 hours after stimulation, by transduction of mir-142$^{fl/fl}$ naïve T cells with either Cre-expressing retrovirus or control retrovirus. These cells were then cultured *in vitro* for a total of 7 days, and subsequently transferred into RAG-1$^{-/-}$ mice. In this way, T cells were allowed to develop and undergo initial activation normally (i.e. before mir-142 deficiency was induced), allowing any potential developmental effects of mir-142 deficiency to be negated. *In vitro* cell survival was unimpaired in both WT and mir-142$^{fl/fl}$ cells transduced with Cre-

expressing retrovirus, indicating that Cre expression did not directly affect cell survival (data not shown). However, flow cytometric analysis of spleen and mLN following transfer again demonstrated that mir-142 deficient cells did not proliferate *in vivo*, despite originating from the same pool of cells that were transduced with control retrovirus, and which did proliferate *in vivo* (Figure 5.16). WT cells transduced with Cre-expressing retrovirus showed similar survival to control-transduced cells (data not shown).

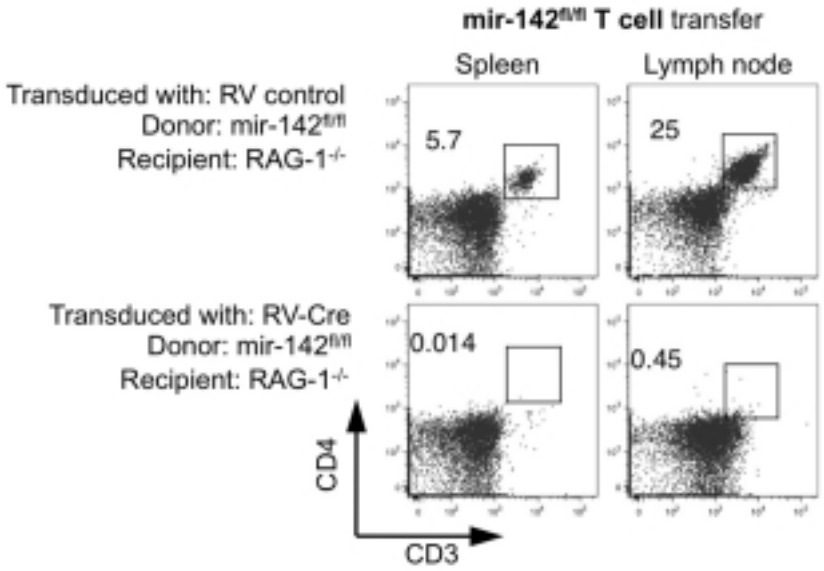

Figure 5.16 mir-142 is required during *in vivo* expansion of CD4$^+$ T cells. Naïve CD4$^+$ T cells were isolated from WT and mir-142$^{-/-}$ mice, activated *in vitro* with plate bound anti-CD3 and anti-CD28 antibodies in non-polarising conditions, and transduced at 24 hours with either RV-Cre or control retrovirus. At day 7, GFP$^+$ cells were cell-sorted and 1x10^6 cells were transferred intraperitoneally into RAG-1$^{-/-}$ mice. After 3 weeks, mice were culled and spleen and mLN were analysed by flow cytometry. Representative of 2 independent experiments with 4 mice per group.

Collectively, these data demonstrate that mir-142 is critically important for normal homeostasis of mature T cells, and that this is a T cell-intrinsic requirement. However, it is important to investigate the mechanism that is responsible for this deficiency. In order to determine the fate of transferred cells, a short-term T cell transfer model was developed in which naïve CD4$^+$ T cells were fluorescently labelled, injected

intraperitoneally into RAG-1$^{-/-}$ mice, and then harvested at 5 days following transfer. This allowed for early analysis of cell fate at a timepoint when WT cells have begun to divide, and when mir-142$^{-/-}$ T cells are still recoverable in sufficient numbers to permit analysis. These experiments demonstrated that mir-142$^{-/-}$ cells recovered from the peritoneal cavity had completely failed to divide within the first 5 days, compared with WT cells that showed significant proliferation (Figure 5.17). Spleen, mLN, pLN, thymus, liver and lung were analysed from both WT and mir-142$^{-/-}$ mice but T cells were not found in either case (data not shown).

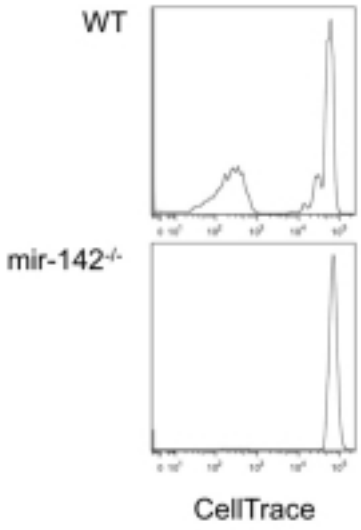

Figure 5.17 mir-142$^{-/-}$ naive CD4$^+$ T cells fail to divide at 5 days following transfer. 2.5x10^6 naïve CD4$^+$ T cells were labelled with the fluorescent dye CellTrace and injected intraperitoneally into RAG-1$^{-/-}$ mice. At 5 days following transfer, mice were culled and peritoneal lavage was performed. Cells were analysed by flow cytometry. Data representative of 3 independent experiments.

Recovered cells were also assessed for rates of apoptosis. Very few (<5%) cells recovered from the peritoneum stained positive (indicating cell death) with cell viability dyes, likely as a result of rapid clearance of dead cells by peritoneal macrophages (Savill et al., 1993). However the proportion of early apoptotic cells could be assessed with the use of Fitc-conjugated VAD-FMK, a fluorescent cell-permeable caspase

inhibitor which binds to activated caspase in apoptotic cells. This demonstrated that there were higher rates of apoptosis in recovered mir-142$^{-/-}$ T cells when compared with WT (Figure 5.18).

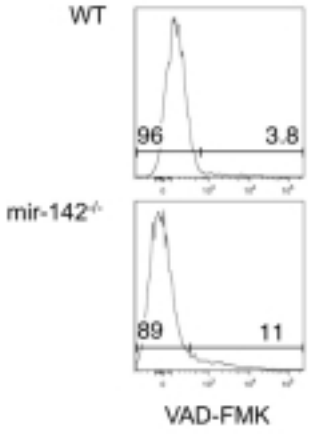

Figure 5.18 mir-142$^{-/-}$ T cells have higher rates of apoptosis following transfer. Cells were prepared and harvested as in Figure 5.17. Cells were stained with anti-CD3, anti-CD4 and VAD-FMK-Fitc, and analysed by flow cytometry. Plots shown are gated on CD3$^+$ CD4$^+$ T cells. Data representative of 2 independent experiments.

The result of the defect in proliferation and increased apoptosis is that by 5 days there is a large difference in the total number of T cells recovered from recipients of WT and mir-142$^{-/-}$ cells, with very few cells recovered from the latter (Figure 5.19).

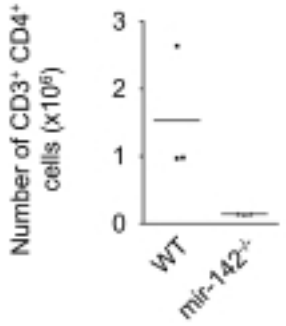

Figure 5.19 Fewer T cells are recovered at 5 days from mice receiving mir-142$^{-/-}$ cells. Cells were prepared and harvested as in Figure 5.17. Cells were recovered from the peritoneum, counted and stained with anti-CD3 and anti-CD4 antibodies. n=2 independent experiments with 3 mice per group in total.

One potential mechanism for this phenotype could be either lack of or presence of an autocrine stimulus that respectively promotes or inhibits T cell expansion. In order to address this, an *in vivo* short-term co-transfer was performed in which naïve T cells from WT and mir-142$^{-/-}$ mice were isolated and labelled with different fluorescent cell-labelling dyes, permitting identification of the individual populations at day 5. This allowed it to be determined whether the defect in mir-142$^{-/-}$ cell survival was reversed if these cells were co-transferred with WT cells, or conversely whether the survival of WT cells was impaired by the co-transfer of mir-142$^{-/-}$ cells. Alternatively, no difference in mir-142$^{-/-}$ cell survival would be expected if the defect was wholly cell-intrinsic. The result demonstrated that in this situation WT cells proliferate whereas mir-142$^{-/-}$ cells do not, and consequently the percentage of cells recovered that are WT is much greater than for those that are mir-142$^{-/-}$, despite equal numbers being transferred initially (Figure 5.20).

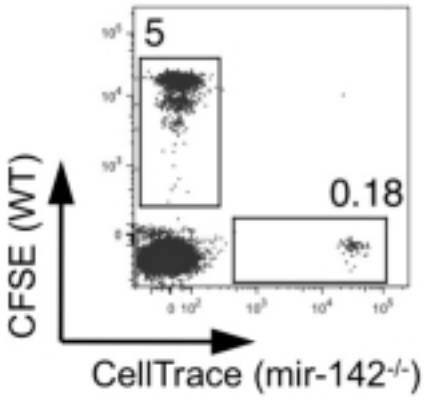

Figure 5.20 Co-transfer of equal numbers of WT and mir-142$^{-/-}$ cells does not affect the defect. Naïve CD4^{+} T cells were isolated from WT and mir-142$^{-/-}$ mice, and labelled with CFSE and CellTrace, respectively. 2.5x10^{6} cells of each type were then injected intraperitoneally into RAG-1$^{-/-}$ mice. Cells were then harvested at day 5 following transfer.

These data demonstrated that the mechanism is cell-intrinsic, and results in increased apoptosis and a failure of proliferation. The ultimate consequence of this is reflected in

the outcome of long-term T cell transfers into lymphopenic mice. When WT cells are transferred, a characteristic T cell-mediated colitis develops (Powrie et al., 1994) which causes weight loss and diarrhoea, and ultimately results in death of the animal, although the experiment is stopped by protocol when animal weight has decreased to 80% of initial weight. Following transfer of mir-142$^{-/-}$ cells, no such colitis developed. Mice remained healthy and did not lose weight, and colon weights of dissected mice were normal compared with the increase in weight of WT recipient colons (Figure 5.21). Histology revealed the characteristic features of colitis in WT recipients, whereas colonic mucosa appeared normal in recipients of mir-142$^{-/-}$ cells (Figure 5.22).

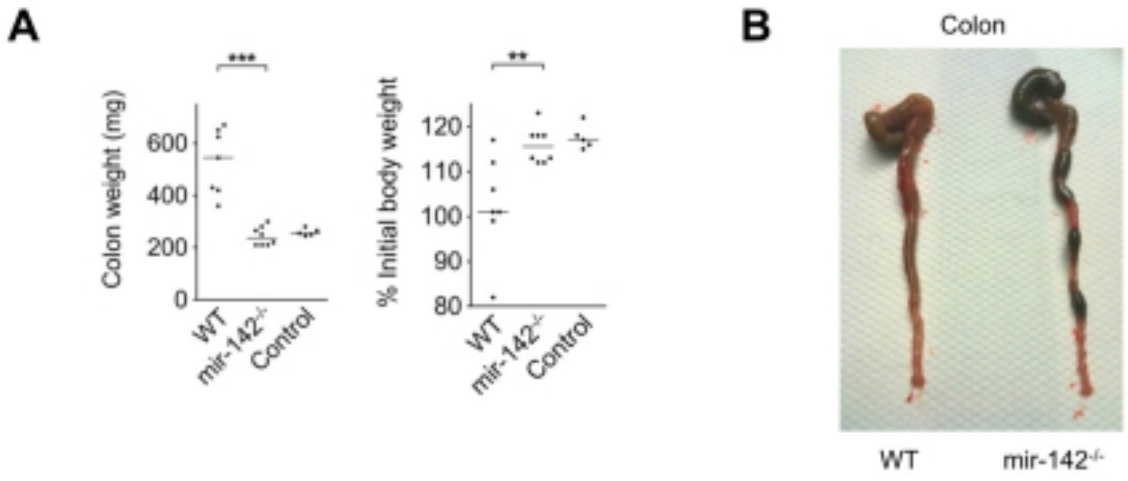

Figure 5.21 mir-142$^{-/-}$ T cells do not cause colitis when transferred into lymphopenic hosts. Naïve CD4^{+} T cells were isolated from WT and mir-142$^{-/-}$ mice, and 0.5x10^{6} were transferred intraperitoneally into RAG-1$^{-/-}$ recipients. At four weeks following transfer, mice were dissected and weighed. (A) Colon weight (left) and change in body weight (right) for recipients of WT cells, mir-142$^{-/-}$ cells or PBS (Control). Data represents 3 independent experiments. ***p<0.001 (Mann Whitney U test). (B) Representative photograph of colon from recipient of WT or mir-142$^{-/-}$ T cells, demonstrating shortening of colon and wall thickening.

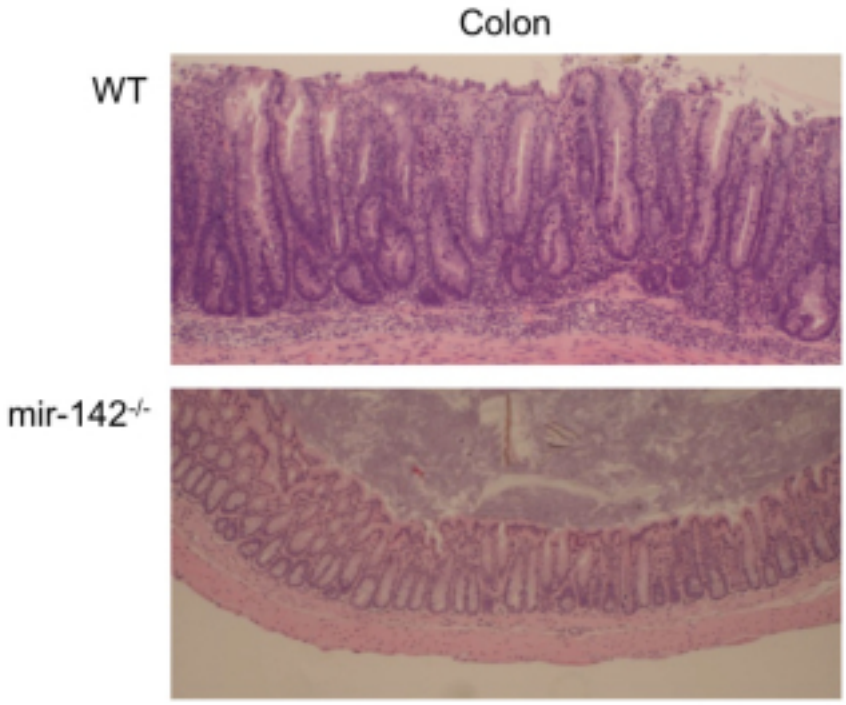

Figure 5.22 Recipients of mir-142$^{-/-}$ do not show histological evidence of colitis. Representative photograph of Haematoxylin and Eosin stained transverse section through proximal colon. Both panels shown at same magnification.

Collectively these data have demonstrated a T cell intrinsic defect in mir-142$^{-/-}$ CD4^{+} T cell homeostasis that results in impaired proliferation *in vivo* and increased apoptosis, with the consequence that mir-142$^{-/-}$ naïve T cells are unable to cause colitis. This reflects the critical importance of mir-142 in the normal function of T cells, and suggests that mir-142 directly controls the expression of genes and pathways that regulate T cell homeostasis.

5.4. mir-142 controls retinoic acid signalling in T cells

The principal function of miRNAs is to suppress the translation of multiple target mRNAs into protein. As discussed in section 1.1.3, recent evidence suggests that the majority of miRNA targets undergo target degradation as the mechanism of post-

transcriptional regulation in mammalian cells (Guo et al., 2010). It is therefore possible to employ genome-wide microarray profiling of mRNA expression in order to detect miRNA targets. In this case, comparison between WT and mir-142$^{-/-}$ naïve CD4^{+} T cells was performed, because the homeostatic abnormality is readily observed in naïve T cells without additional experimental intervention. Two biological replicate samples of naïve CD4^{+} T cells were cell-sorted, and RNA was then isolated from these. Microarray analysis was then performed on these samples. Following data acquisition and normalisation, these data were then analysed in order to determine which predicted target mRNAs should be selected as candidates and subjected to further analysis. The schema for this process is illustrated in Figure 5.23. Briefly, fold change was calculated between mean gene expression values in mir-142$^{-/-}$ and WT cells. Predicted targets for both miR-142-3p and miR-142-5p were obtained from the databases TargetScan Mouse (Release 5.1), PITA (version 6.0, TOP targets list), PicTar (mouse predictions), and miRanda (August 2010 Release, mirSVR score=Good). These target predictions were then compared, and only targets that were predicted by all four databases were selected for further inclusion in the candidate gene analysis.

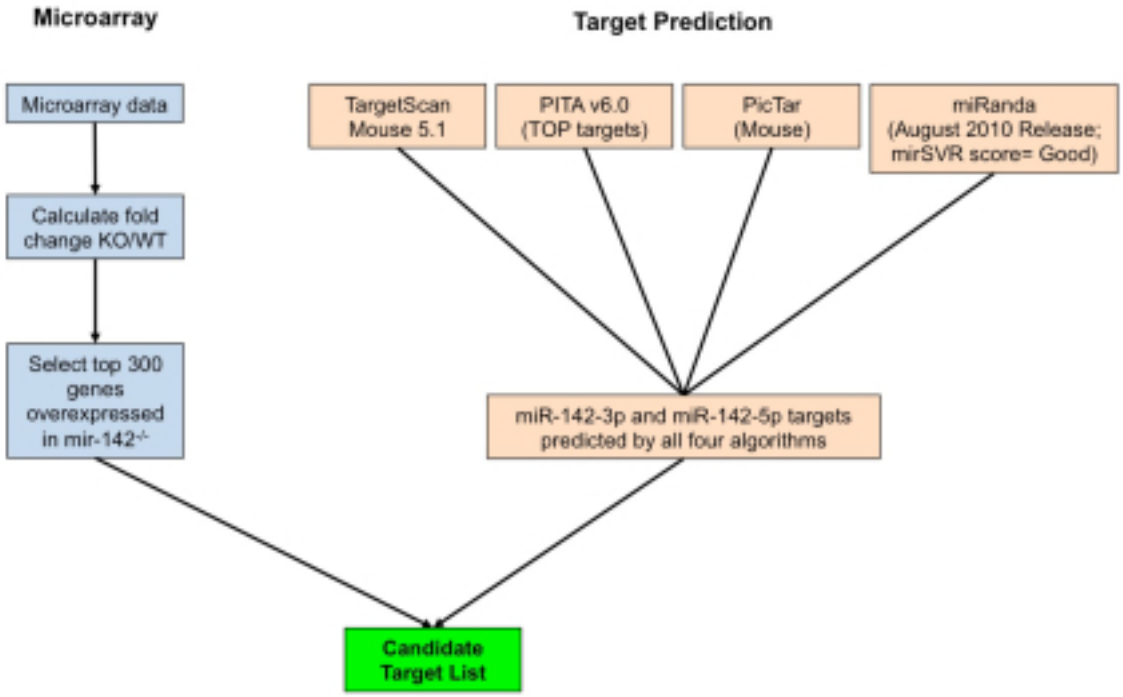

Figure 5.23 Analysis method for identification of miR-142-3p and miR-142-5p target genes.

When the top 300 differentially expressed genes were analysed with this method, a total of five candidate genes were identified, as demonstrated in the Venn diagram shown in Figure 5.24.

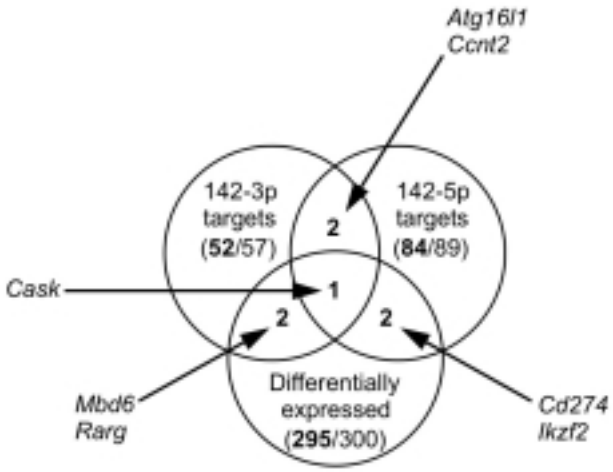

Figure 5.24 Differentially expressed candidate genes in mir-142$^{-/-}$ naive CD4^{+} T cells. Gene lists derived following method detailed in Figure 5.23.

Following the identification of these genes, a literature search was conducted to identify those known to have a potential role in the regulation of T cell homeostasis, and both *Rarg* and *Ikzf2* were identified as possible candidates. *Ikzf2* encodes the gene Helios, which is known to play a role in T cell development (Zhang et al., 2007). However, the 3'UTR of *Ikzf2* failed to show repression in luciferase assay following expression of mir-142 (data not shown), and so it was not considered further for candidate gene analysis. Retinoic acid receptor γ (RARγ, *Rarg*) is known to be expressed in T cells, and signalling through this receptor has previously been shown to induce thymic apoptosis *in vivo*, whilst *in vitro* studies have shown that RARγ signalling can inhibit T cell proliferation and induce apoptosis (Szondy et al., 1997; Tóth et al., 2001; Ludányi et al., 2005). miR-142-3p is predicted to target *Rarg* through a highly-conserved 8mer sequence in the 3'UTR (Figure 5.25). The 3'UTR of *Rarg* was therefore cloned into the PsiCHECK-2 luciferase reporter vector in order to determine whether targeting occurs, and a mutant form was also constructed in which the seed sequence match was disrupted (Figure 5.25).

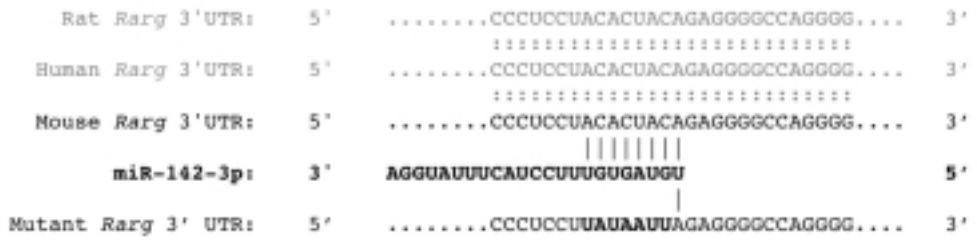

Figure 5.25 miR-142-3p is predicted to target a highly-conserved 8mer sequence in the *Rarg* 3'UTR. Shown is local conservation (100%) between the rat, human and mouse isoforms of *Rarg*. Vertical bars demonstrate canonical Watson-Crick matches between miRNA seed region and target sequence. Lower sequence indicates mutated Rarg 3'UTR generated for validation in luciferase assay.

Luciferase assay was performed in which either control or mir-142 vector was expressed in the presence of either wild-type or mutant *Rarg* luciferase vector. This demonstrated that *Rarg* is a target of miR-142-3p, and that mutation of the target site prevents this, confirming the identity and location of the target site (Figure 5.26).

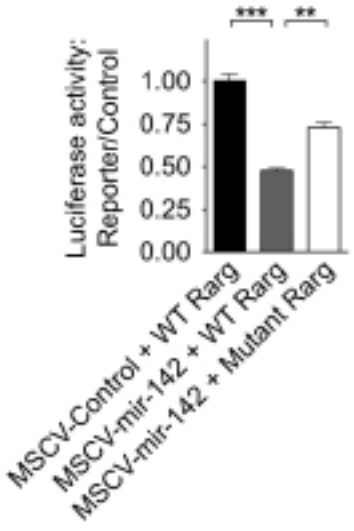

Figure 5.26 *Rarg* is validated as a target of miR-142-3p by luciferase assay. Vectors were prepared as described and transfected into target cells in the indicated combinations. n=3 per condition, ***P<0.001, **P<0.01 (Mann Whitney U-test).

The RAR family comprises three members, α, β and γ, of which only RARα and γ are expressed in naïve $CD4^+$ T cells (Ohoka et al., 2011). Analysis of microarrays revealed that RARα expression is unchanged in the absence of mir-142, whereas RARγ expression is highly upregulated in mir-$142^{-/-}$ naïve T cells (Figure 5.27).

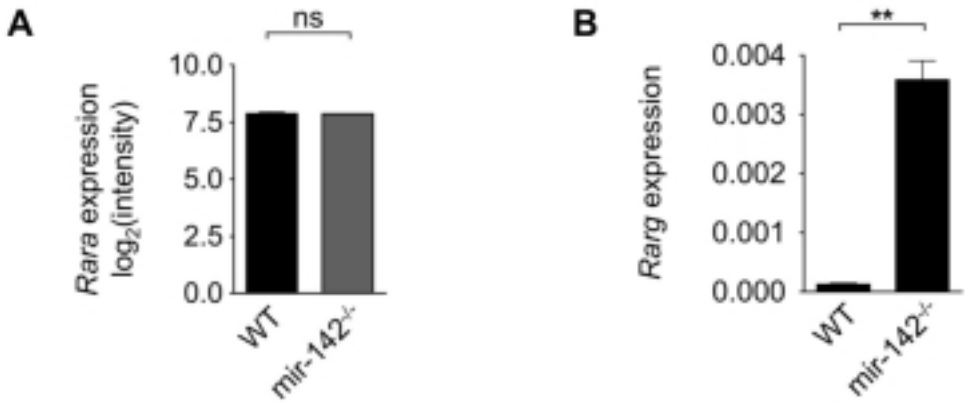

Figure 5.27 Expression of RARα and RARγ mRNA in mir-142$^{-/-}$ naive CD4^{+} T cells. (A) Expression of retinoic acid receptor α mRNA, as measured by microarray expression profiling, is unchanged between WT and mir-142$^{-/-}$ cells. (B) RARγ expression is massively increased in mir-142$^{-/-}$ cells as measured by qRT-PCR. **P<0.01 (Mann Whitney U-test). Mean of two biological replicates is shown as $2^{-\Delta Ct}$ relative to beta-actin expression; error bars denote standard deviation.

In order to determine whether there was constitutive activation of RARγ signalling *in vivo*, the microarray data from WT and mir-142$^{-/-}$ naïve CD4^{+} T cells was compared with published datasets that have identified targets of RARγ (Su and Gudas, 2008). This demonstrated dysregulated expression of a number of RARγ targets consistent with constitutive upregulation of RARγ signalling (Figure 5.28). In particular, Hoxa5 is a RAR-regulated transcription factor that is known to possess significant pro-apoptotic function (Chen et al., 2007; Su and Gudas, 2008).

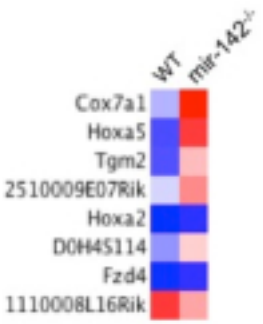

Figure 5.28 Dysregulated expression of RARγ target genes in mir-142$^{-/-}$ naive CD4^{+} T cells. Genes with a fold change of >1.5 consistent with previously published data were included. RARγ targets identified from (Su and Gudas, 2008) Appendix B (RA-responsive genes with at least a twofold change in expression in F9 Wt cells relative to F9 RARγ$^{-/-}$ cells after RA treatment for 24 h). Mean expression levels are shown from microarray data.

In order to assess the effect of *in vitro* culture on RARγ expression, a timecourse experiment was performed in which WT and mir-142$^{-/-}$ naïve CD4^{+} T cells were stimulated *in vitro* for 5 days. RARγ expression was assessed at multiple timepoints, and was found to be rapidly extinguished following *in vitro* culture (Figure 5.29).

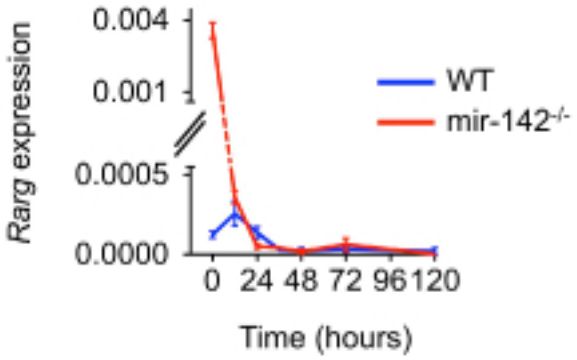

Figure 5.29 RARγ expression is rapidly extinguished following *in vitro* culture. WT and mir-142$^{-/-}$ naïve CD4^{+} T cells were activated *in vitro* in non-polarising conditions, and sampled at the indicated timepoints. qRT-PCR was performed for *Rarg*. Mean of two biological replicates is shown as $2^{-\Delta Ct}$ relative to beta-actin expression; error bars denote standard deviation.

As a consequence of this, *in vitro* experiments which examined the effects of RARγ agonists and antagonists were uninformative (data not shown). Nonetheless it was

important to determine whether retinoic acid signalling through RARγ affects T cell survival. In order to do this, RARγ was cloned into a retroviral vector and overexpressed in WT cells *in vitro*, in the presence of varying concentrations of retinoic acid (Figure 5.30). This demonstrated that retroviral expression of RARγ alone in WT Thp did not result in any increase in cell death *in vitro*. However, supplementation with retinoic acid in the context of forced RARγ expression resulted in dose-dependent apoptosis, confirming that RARγ regulates naïve T cell survival in a retinoic acid-dependent manner. Taken together, these data show that RARγ is a direct target of mir-142 *in vitro* and *in vivo* and that derepression of this gene contributes to the observed homeostatic defect in mir-142$^{-/-}$ mice.

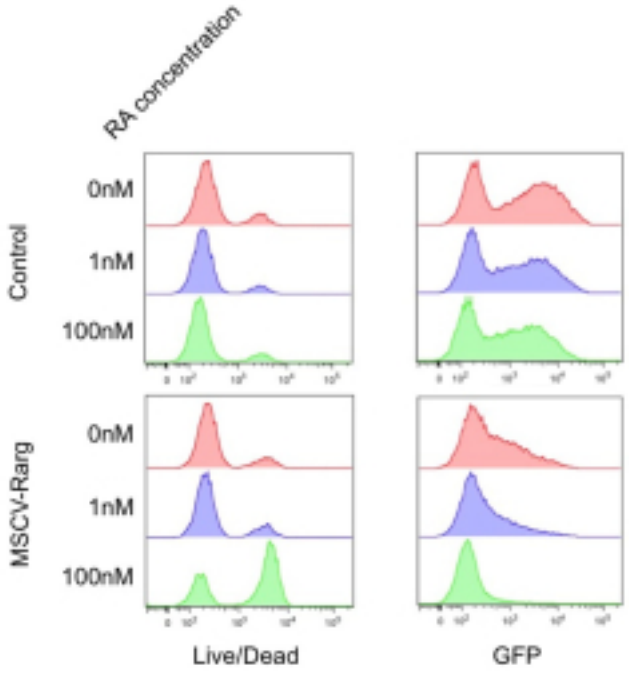

Figure 5.30 Retinoic acid signalling via RARγ increases apoptosis in naive CD4$^+$ T cells. WT cells were isolated, activated *in vitro* with anti-CD3 and CD28 in non-polarising conditions and then transduced at 24 hours with either control or RARγ-expressing retrovirus. After a further 12 hours cells were divided and cultured in the presence of varying concentration of retinoic acid (as indicated). At day 7, cells were harvested and stained with cell viability dye. Shown are histograms gated on GFP$^+$ cells (left panel) and live cells (right panel). Retroviral transduction performed by A. Hertweck. GFP=green fluorescent protein. RA= retinoic acid. Control=MSCV empty expression vector.

In summary, mir-142 deficiency results in markedly dysregulated homeostasis of $CD4^+$ T cells *in vivo* and is intrinsically required for their survival. Collectively, the data presented above demonstrate that RARγ is a direct target of mir-142, that RARγ expression and signalling is increased in mir-$142^{-/-}$ $CD4^+$ T cells, and that retinoic acid signalling via this receptor results in impaired T cell survival. Together, these data suggest that RARγ is a functional target of mir-142 that is likely to contribute to the T cell homeostatic defect that is observed in mir-$142^{-/-}$.

5.5. Discussion

These data allow for a number of general and specific observations to be made regarding both miRNA biology and the function of mir-142. To date, only a limited number of examples of miRNA knockout mice with immune system phenotypes have been reported in the literature. With regard to T cell-intrinsic abnormalities, miR-155 and miR-146a-deficient mice have been described, as discussed in section 1.4. Interestingly, in both of these cases transcription factors were likewise identified as principal targets of the miRNAs in question. With the addition of the data presented in this section, it is becoming increasingly apparent that multiple specific miRNAs play critical roles in the control of T cell function, and that by modulating transcription factor expression they are able to regulate the entire transcriptional programme within the cell. It is also clear that deficiency of just one miRNA can be sufficient to seriously impair the ability of individual cell lineages to function normally, as is the case for mir-142.

Despite the wide expression of mir-142 in the haematopoietic system, it was striking to observe that the main defect in these mice appears to be restricted to the T cell compartment. In addition, the mechanism that results in this phenotype is intrinsic to T

cells and independent of mir-142 deficiency in other cell types. These results do not preclude a role for mir-142 in non-T cell lineages but if there are any other abnormalities, they appear to be much more subtle. However, there was good *a priori* reason to suspect a role for mir-142 in T cell function, given that mir-142 is differentially expressed between naïve and effector T cells, and that a number of well-characterised, T cell-specific master regulatory transcription factors were found to bind at the mir-142 genomic locus. This suggests that analysis of binding by tissue-specific transcription factors could potentially be used more generally to identify key candidate miRNAs for functional analysis. In addition, it provides further evidence of the enormous complexity of gene regulatory networks, and suggests that integrating these pathways into models of cellular homeostasis will become increasingly difficult in the future.

With regard to the observed phenotype, it is clear that mir-142 is of critical importance in the maintenance of normal T cell homeostasis, and that mir-142 deficiency negatively impacts on T cell survival. Interestingly, a very similar defect in T cell homeostasis was reported in mice which lack the miRNA processing enzyme Dicer in T cells (Muljo et al., 2005). These mice are characterised by a significantly reduced number of mature T cells, and increased rates of apoptosis are detected in these cells. It is important to note that these animals are deficient in almost all mature miRNAs, yet many features of their phenotype are reproduced simply by deletion of one miRNA: mir-142. This suggests that mir-142 deficiency is an important contributor to the T cell phenotype observed in these Dicer-deficient mice, and provides further evidence that mir-142 plays a non-redundant, central role in the regulation of T cell function.

The finding that mir-142-deficient T helper cells are incapable of causing colitis in the T cell transfer model is also of potential clinical significance. Human inflammatory bowel disease (IBD) encompasses a group of debilitating, chronic conditions with a complex and poorly-understood aetiology. The pathogenesis of the major forms of the disease, Crohn's disease and Ulcerative Colitis (UC), is believed to be largely T cell-dependent (Khor et al., 2011), and this is reflected in the frequency with which mutations in T cell-related genes are identified in genome-wide association studies of IBD. The T cell transfer model of colitis allows for controlled, experimental manipulation of T cell biology *in vivo*, in the context of T cell-mediated pathology. If these interventions are found to modify the disease course, it may be possible both to gain insight into the disease mechanism and potentially to provide information that may be of some translatable benefit for sufferers of chronic immune-mediated disease. The fact that mir-142 is critically important for T cells to become pathogenic in this model suggests that targeting of mir-142 should be investigated as a potential therapeutic intervention in the management of T cell-mediated disease. It would be unwise at this stage to attempt to extrapolate any potential results from such a highly controlled and abnormal *in vivo* environment as that employed in this model, but the T cell-specificity of the homeostatic defect in mir-142$^{-/-}$ mice supports the notion that targeting of mir-142 could be employed to selectively modulate T cell function.

Clearly, more work is needed to characterise the biology of mir-142 before experiments can even be designed to test the effect of such interventions. In particular, it will be important to determine the range and identity of target genes that are affected by changes in mir-142 expression in these cells. miRNAs, by their nature, target multiple genes and whilst this study has successfully identified a relevant target of mir-142, it is

likely that derepression of multiple targets contributes to the observed phenotype in these mice. These may potentially be identified by relaxation of the criteria by which the microarray data were analysed to include more differentially expressed genes, or by reducing the stringency with which target prediction databases were selected. Alternatively, a number of techniques have recently been described that approach the problem of target identification in different ways. For example, proteomic data may be compared between cells with differing expression of a specific miRNA (Selbach et al., 2008). In addition, parallel sequencing of target mRNAs undergoing miRNA-mediated suppression can be achieved by immunoprecipitation of argonaute proteins, and could be compared between cells in which a specific miRNA was either present or absent (Chi et al., 2009). This study has demonstrated some of the challenges in identifying valid miRNA targets based on *in silico* prediction. However, the mir-142$^{-/-}$ mice may, in future, allow for the generation of experimental evidence that could be used to refine and validate prediction algorithms, by employing some of these novel techniques.

The identification of RARγ as a target of miR-142-3p is particularly interesting, as it is increasingly evident that RA signalling plays a central role in a range of T cell processes, both in development and function. RA is a metabolite of Vitamin A, an essential nutrient that plays a role in a broad range of biological processes. It is of particular importance in the normal function of the immune system, and Vitamin A supplementation significantly improves rates of childhood mortality in malnourished populations (Sommer et al., 1986). Vitamin A or its precursors are absorbed in the gut and transported to the liver, where it may be stored in the form of retinyl esters. These are then hydrolysed to retinol which is taken up by cells and further hydrolysed to retinal. Retinal is then converted to one of the isoforms of RA by retinal

dehydrogenases (RALDH). RA isoforms include all-trans retinoic acid (ATRA), which is generally the most abundant form of RA (Kane et al., 2008), and 9-cis-retinoic acid. RA functions through binding to a number of nuclear receptors, including RARs, retinoid X receptors (RXRs), and PPARβδ (Keller et al., 1993). Whilst RA is naturally present in serum (Kane et al., 2008), a major provider of RA to T cells is a gastrointestinal tract-resident subset of DCs (Iwata et al., 2004). RA can induce the expression of the integrin heterodimer $\alpha_4\beta_7$ and CCR9 on T cells, which both promote homing to the gut (Iwata et al., 2004). RA has also been shown to be capable of inducing the differentiation of iTreg, in combination with other cytokines such as TGF-β and IL-2 (Mucida et al., 2007; Schambach et al., 2007; Xiao et al., 2008b), through a mechanism that is dependent on RARα expression (Hill et al., 2008). Th17 differentiation also appears to be enhanced by RA in some settings, as low dose RA supplementation was found to promote the development of Th17 cells *in vitro* (Uematsu et al., 2008). However, other reports have described inhibition of Th17 differentiation in favour of iTreg polarisation (Mucida et al., 2007), so the precise role for RA in Th17 development remains to be determined. 9-cis-retinoic acid has also been shown to promote the development of Th2 cells (Stephensen et al., 2002). In more general terms, RA has also been found to promote T cell proliferation when supplemented *in vitro* (Ertesvag et al., 2002). Intriguingly, it has recently been shown that retinoic acid signalling through RARα promotes pro-inflammatory $CD4^+$ T cell responses and is required for normal T cell proliferation *in vivo* (Hall et al., 2011). The finding that RARα expression is unchanged in mir-$142^{-/-}$ T helper cells, whereas RARγ is greatly increased, suggests that the relative expression levels of these receptors may be of importance in tuning T cell proliferation and survival, and that mir-142 is a key checkpoint in this mechanism. It has previously been demonstrated that constitutively

RARγ-deficient mice are non-viable and exhibit defective growth (Lohnes et al., 1993). A report in 2007 described mice in which RARγ was conditionally deleted in all haematopoietic cells (Dzhagalov et al., 2007). This study focused primarily on $CD8^+$ T cells and macrophages, which were found to have impaired cytokine production, but T cell development and proliferation was found to be unimpaired in these mice (Dzhagalov et al., 2007). However it is known that there is a complex system of functional redundancy amongst retinoic acid receptors that is dependent on the cell type, which could potentially obscure attempts to dissect the role of RARγ in RARγ-deficient cells (Taneja et al., 1996). As a consequence, the loss of RARγ expression cannot necessarily be expected to affect T cell homeostasis in a complementary manner to the overexpression of RARγ as described in this section.

In summary, the study of mir-142-deficient mice has provided further insight into fundamental T cell biology and the role of miRNAs. In addition, a functional role for RARγ has been identified in $CD4^+$ T cell homeostasis. These mouse lines will provide a platform for experiments that aim to improve understanding of the mechanisms that govern miRNA target selection and regulation. In addition, the biological pathways that have been uncovered represent opportunities to further study the way in which T cell homeostasis is regulated, and in future this knowledge may potentially be exploited for the benefit of patients with immune-mediated disease.

6. The role of mir-142 in T helper cell lineage commitment

6.1. Introduction

T helper cell lineage commitment is directed by the expression of subset-specifying master regulatory transcription factors. These function to promote the expression of cytokines and receptors that define and reinforce the phenotype of the cell. However, as described in section 1.2, lineage stability is increasingly being recognised to be variable under certain circumstances, and the mechanisms that control the plasticity of subsets are unclear. We have observed that mir-142 expression is dynamically regulated in T helper cells, and that several master regulatory transcription factors bind at the mir-142 locus. In light of these findings, I proceeded to address the hypothesis that mir-142 plays a role in the differentiation and lineage stability of T helper cell subsets, in addition to its function in the regulation of T cell homeostasis that has been described in the previous chapter. I therefore analysed the differentiation of mir-142-deficient T cells in order to determine whether mir-142 is required for the regulation of this process.

6.2. mir-142-deficient T helper cells default to a Th1 phenotype upon activation

Activation of WT naïve T helper cells through T cell receptor stimulation results in proliferation and expansion of cell numbers. This may be achieved *in vitro* through the use of anti-CD3 and anti-CD28 antibodies. In the absence of any skewing cytokines that are known to promote differentiation to a particular T cell subset, this does not typically

result in significant production of subset-specific cytokine by these cells. As expected, this phenotype was observed for Thp isolated from WT littermate mice, however I found that mir-142$^{-/-}$ Thp defaulted to significant hyperproduction of the hallmark Th1 cytokine IFN-γ upon activation under these neutral conditions (Figure 6.1 and Figure 6.2).

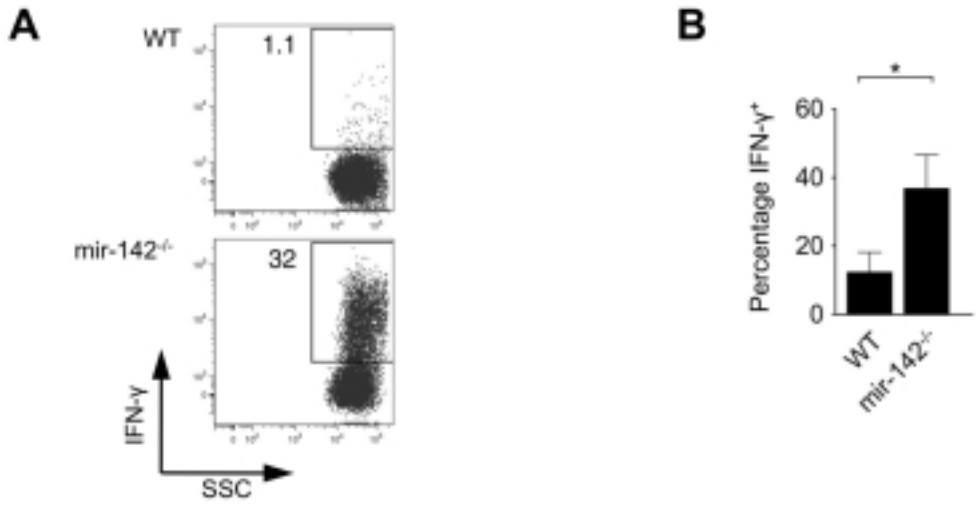

Figure 6.1 mir-142$^{-/-}$ naïve T helper cells default to production of IFN-γ upon activation in non-polarising conditions. Flow cytometric analysis of intracellular cytokine expression demonstrates increased IFN-γ staining. (A) Representative dot plot gated on live CD4^{+} cells following 1 week of *in vitro* culture. (B) Comparison of percentage of cells staining positive for IFN-γ following 1 week of *in vitro* culture. (n=6 independent experiments; *p<0.05, Wilcoxon signed ranks test).

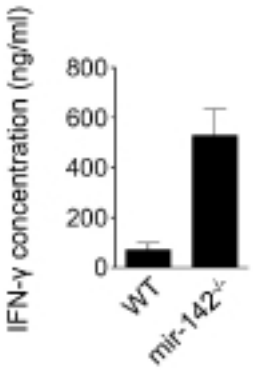

Figure 6.2 Concentration of IFN-γ secreted into culture supernatant by activated mir-142$^{-/-}$ T helper cells is elevated compared with WT. ELISA was performed for IFN-γ on supernatant harvested from non-polarising *in vitro* cultures of WT and mir-142$^{-/-}$ cells. n=2 independent experiments.

This discrepancy could potentially result from factors causing polarisation of cells during *in vivo* development, and basal expression of Th1 cytokines could contribute to enhanced Th1 differentiation during initial *in vitro* culture. However further timecourse analysis revealed that naïve T cells do not express or produce IFN-γ prior to stimulation, but rather that IFN-γ overexpression begins soon after the initiation of activation and continues throughout the duration of culture (Figure 6.3 and Figure 6.4).

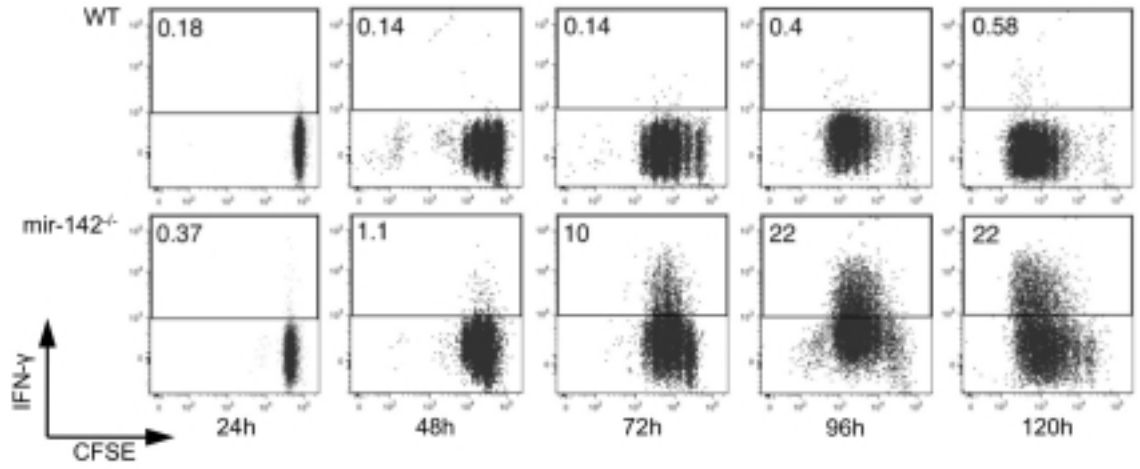

Figure 6.3 Timecourse of IFN-γ expression demonstrates progressive acquisition of the IFN-γ hyperproduction phenotype. Naïve T cells were labelled with CFSE and activated in non-polarising conditions. Cells were subjected to intracellular cytokine staining at the indicated timepoints. Data representative of 3 independent experiments.

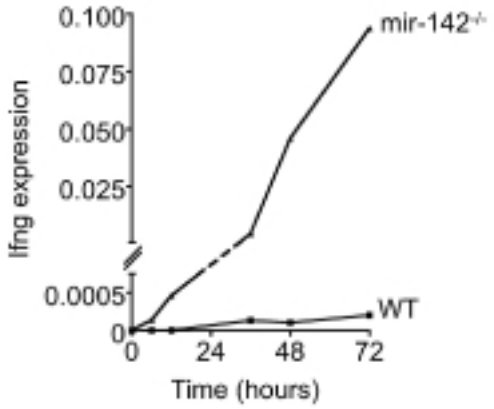

Figure 6.4 Timecourse of IFN-γ expression as determined by qRT-PCR demonstrates progressive overexpression in mir-142$^{-/-}$ T helper cells. Naïve T cells were cultured in non-polarising conditions, harvested at the indicated timepoints and subjected to qRT-PCR analysis. Data representative of 2 independent experiments. The mean of two replicates is shown as $2^{-\delta Ct}$ relative to beta-actin expression.

These data demonstrate that mir-142-deficient cells only undergo polarisation towards the Th1 phenotype following activation, and indicate that naïve cells do not express or secrete IFN-γ directly *ex vivo*. In order to determine whether this propensity for differentiation results from a cell-intrinsic deficiency of mir-142, I again employed the mir-142 conditional knockout mouse. This allows for the deletion of mir-142 at defined stages of T cell development through crossing with deleter mice or the use of Cre-expressing retroviruses. Crossing with the CD4-Cre deleter mouse enables deletion of mir-142 at the double positive (DP) stage of T cell thymic development, allowing for T cell-intrinsic effects of mir-142 deletion to be determined. Once again, Thp isolated from these mice defaulted to IFN-γ overexpression following *in vitro* stimulation, reflecting the abnormality seen in constitutive mir-142$^{-/-}$ cells (Figure 6.5).

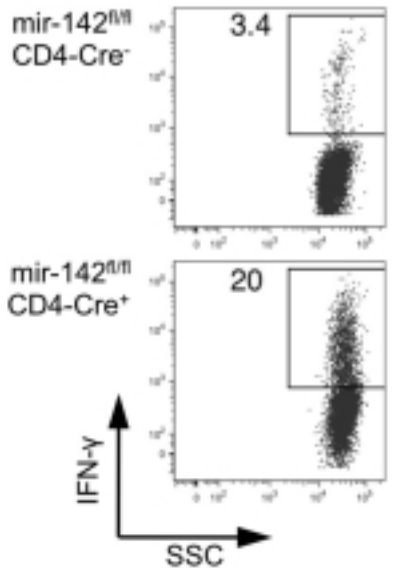

Figure 6.5 Conditional deletion of mir-142 in T cells reproduces the phenotype observed in globally deficient mice. Naïve T helper cells were isolated from littermate mir-142$^{fl/fl}$ mice that were either positive or negative for the CD4-Cre transgene. Cells were cultured for 1 week *in vitro* under non-polarising conditions. Results representative of 2 independent experiments.

These data demonstrate that abnormal production of IFN-γ occurs as a result of T cell–intrinsic deficiency of mir-142. In order to further isolate the stage of the T cell lifecycle at which mir-142 is critically important for the regulation of T cell differentiation, I used retrovirus-mediated expression of the Cre transgene at 24 hours following *in vitro* stimulation of naïve T cells, in order to selectively delete mir-142 after the initiation of activation. Again, marked overexpression of IFN-γ was observed at 7 days following activation when compared with control-transduced cells (Figure 6.6).

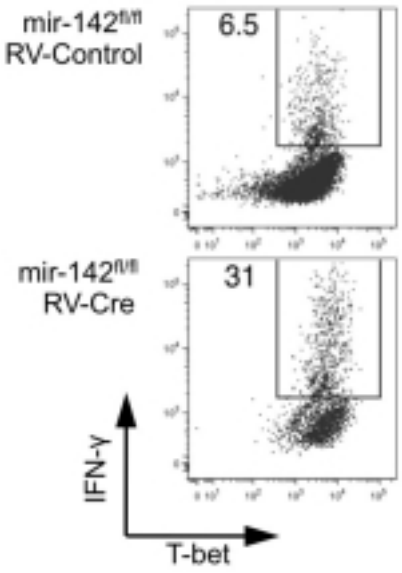

Figure 6.6 Retrovirus-mediated deletion of mir-142 after the initiation of TCR stimulation reproduces the phenotype of IFN-γ overexpression observed in constitutively mir-142-deficient T cells. mir-142$^{fl/fl}$ Thp were isolated and then transduced with RV-Cre or control retrovirus 24 hours after the start of cell culture in non-polarising conditions. Cells were then harvested and analysed by intracellular staining at day 7. Plots gated on live GFP^{+} cells. Data representative of 3 independent experiments.

Collectively, these data confirmed that the defect was due to cell-intrinsic loss of mir-142 and that these effects were due to mir-142 deficiency during the time of cell activation, rather than during prior development. In order to demonstrate that the loss of mir-142 expression was the primary factor responsible for this phenotype, I proceeded to use retroviral overexpression of mir-142 in activated, constitutively mir-142-deficient Thp, in order to restore mir-142 expression. These experiments showed that the excess production of IFN-γ was markedly reduced by the reconstitution of mir-142 expression, confirming that mir-142 directly regulates the process of T cell subset differentiation (Figure 6.7).

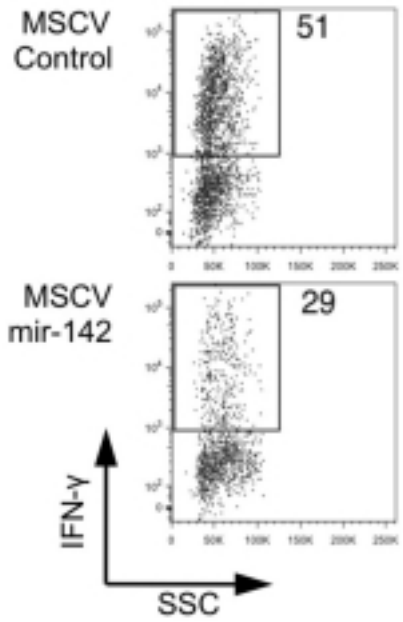

Figure 6.7 Reconstitution of mir-142 expression limits default overexpression of IFN-γ in mir-142-deficient T helper cells. Naïve T helper cells from mir-142$^{-/-}$ mice were isolated, cultured in non-polarising conditions and then transduced at 24 hours with either control or mir-142-overexpressing retrovirus. Plots gated on live GFP^{+} cells. At day 7, cells were harvested and analysed by intracellular cytokine staining. Data representative of 3 independent experiments.

Thus it has been demonstrated that mir-142 is critically important for normal T cell subset differentiation occurring after activation, and that this specific defect is reversed when mir-142-deficient T cells are re-complemented with mir-142.

6.3. mir-142-deficient T helper cells are capable of differentiation to multiple subsets, but lineage stability is impaired in the absence of mir-142

The data presented thus far demonstrate that mir-142-deficient T helper cells default to the production of IFN-γ when cultured in non-polarising conditions and that this is a cell-intrinsic, post-developmental phenomenon. This raises the possibility that mir-142-deficient Thp are incapable of differentiation to non-Th1 subsets on account of default

Th1 polarisation. In order to address this, I performed subset differentiation experiments in which cells were cultured under conditions that promote differentiation towards individual subsets. Interestingly, I found that mir-142-deficient cells were able to differentiate to effector subset lineages, when cultured in the presence of appropriate skewing cytokines (Figure 6.8 and Figure 6.9).

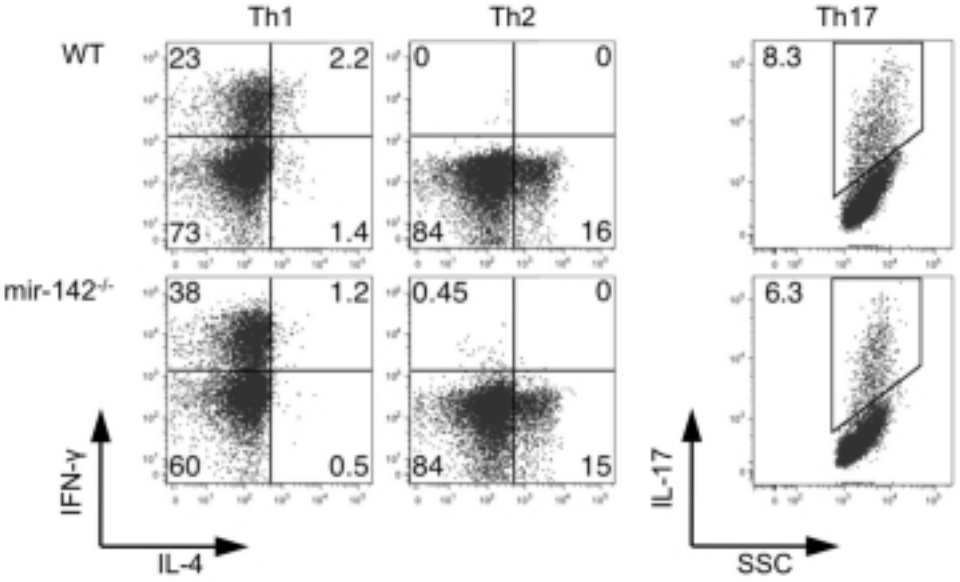

Figure 6.8 Differentiation of mir-142-deficient cells to effector T cell subsets. Cells were cultured under the appropriate skewing conditions for 7 days and then harvested for intracellular cytokine analysis. Flow cytometric plots gated on live cells; data representative of 3 independent experiments.

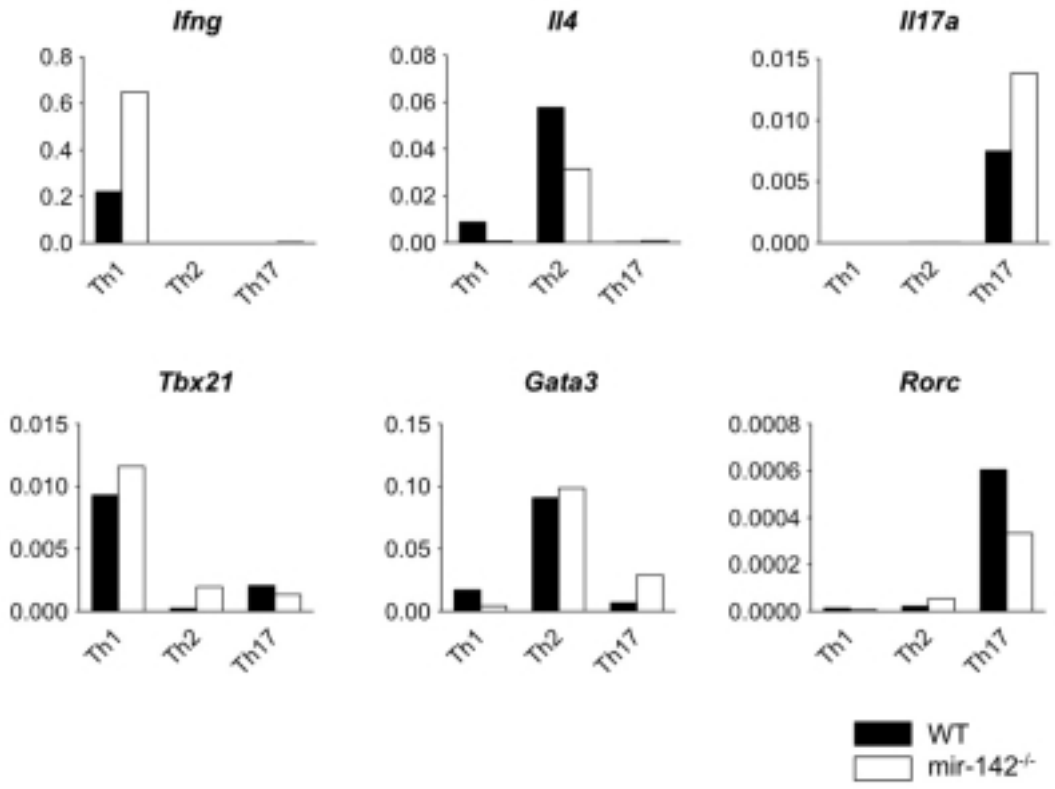

Figure 6.9 mir-142$^{-/-}$ T helper cells are capable of undergoing subset differentiation. Thp were isolated and cultured for 7 days in appropriate skewing conditions. RNA was harvested and analysed by qRT-PCR for the indicated genes. Data shown as $2^{-\Delta Ct}$; mean of 2 replicates is shown.

This differentiation was characterised by high expression of the appropriate lineage-defining cytokines and transcription factors, and low or absent expression of those genes expressed by opposing lineages, although the relative level of gene expression between genotypes was found to be variable (data not shown). In order to determine whether lineage stability was affected in the absence of mir-142, crossover experiments were performed in which cells were initially cultured for 3 days in either Th1- or Th2-promoting conditions, and were then washed and re-cultured under conditions promoting differentiation to the opposing subset. These experiments showed that lineage stability was impaired in the absence of mir-142, with mir-142$^{-/-}$ cells that were initially cultured under Th2 conditions being observed to express elevated levels of

IFN-γ when switched to Th1 conditions, unlike WT cells which did not (Figure 6.10 and Figure 6.11).

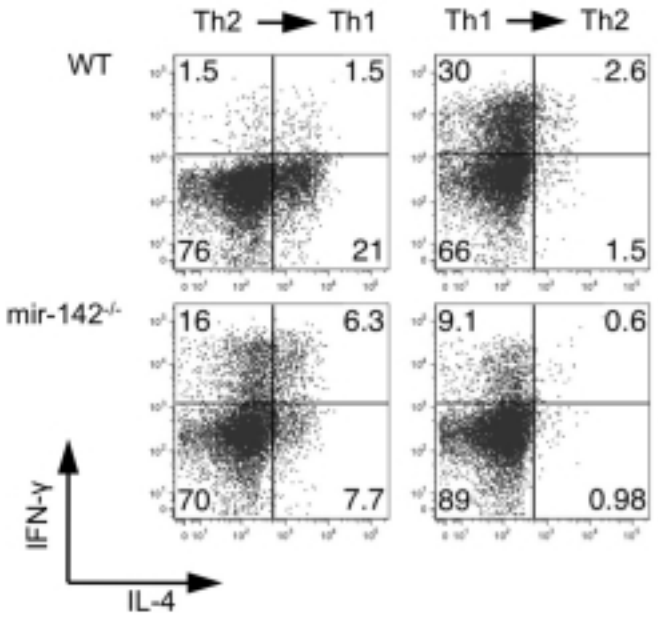

Figure 6.10 Lineage stability is impaired in differentiated mir-142-deficient T helper cells. Cells were cultured in either Th1 or Th2 conditions and then switched at day 3 to the opposing culture condition (as indicated above plots). After a total of 7 days, cells were harvested and analysed by flow cytometry. IFN-γ expression was increased in mir-142$^{-/-}$ cells switched from Th2 to Th1 conditions when compared with WT. Data representative of 3 independent experiments.

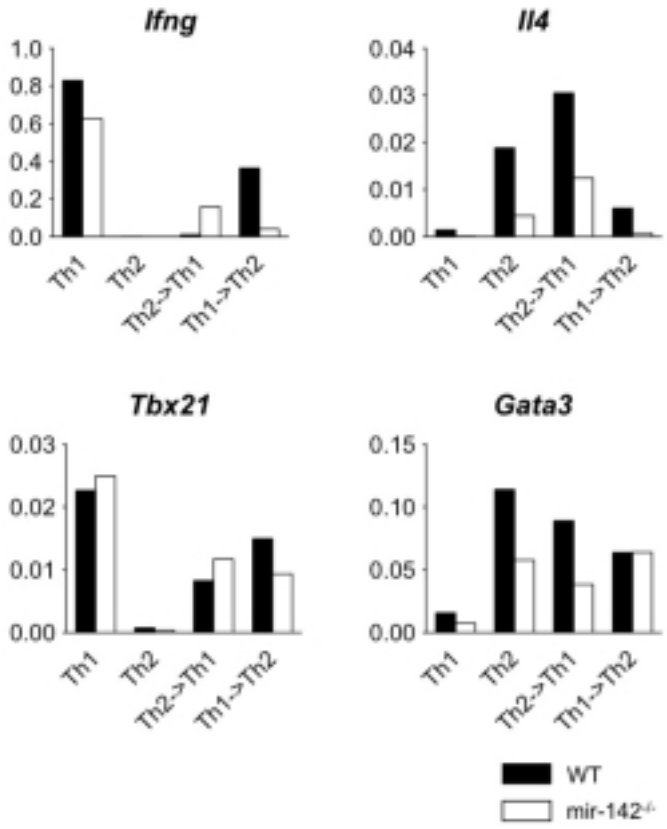

Figure 6.11 qRT-PCR demonstrating effect on cytokine expression of crossover experiment. Cells were cultured as described in Figure 6.10. RNA was harvested at day 7 and subjected to qRT-PCR analysis. Data shown as $2^{-\Delta Ct}$ relative to beta actin; mean of 2 replicates shown.

Collectively, these data suggest that mir-142-deficient cells default to production of IFN-γ under permissive conditions (i.e. Th0), and that the stability of non-Th1 lineages is adversely affected in the absence of mir-142. These conclusions are supported by *in vivo* data from T cell transfer experiments. When WT Thp were transferred into lymphocyte-deficient mice (as described in section 5.2), cells proliferated and characteristically produced both IL-17 and IFN-γ, ultimately causing a lethal T cell-mediated colitis. Upon flow cytometric analysis of the small number of mir-142$^{-/-}$ T cells that are identifiable at 4 weeks after transfer into RAG-deficient mice, these cells had, by contrast, defaulted to the sole production of IFN-γ with expression of IL-17 being largely absent (Figure 6.12).

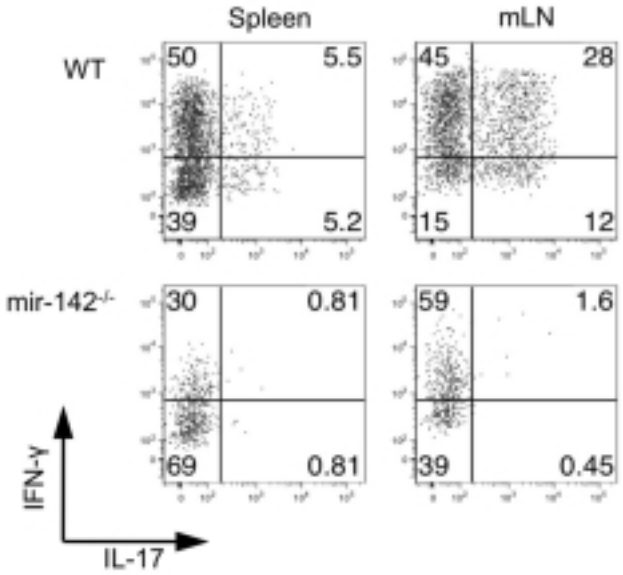

Figure 6.12 Analysis of *in vivo*-transferred mir-142$^{-/-}$ Thp reveals default production of IFN-γ and absence of IL-17. Naïve T cells were transferred into RAG1$^{-/-}$ mice and harvested after 4 weeks. Cells were subjected to intracellular cytokine staining. Plots gated on live CD3^{+} CD4^{+} lymphocytes; data representative of 2 independent experiments.

These data demonstrate that mir-142 deficiency does not prevent differentiation to alternative phenotypes, but that in the absence of skewing factors that promote the differentiation of non-Th1 subsets, mir-142$^{-/-}$ Thp tend to default to the Th1 phenotype. In addition, mir-142$^{-/-}$ Th2 cells were found to be more readily subvertible to the Th1 phenotype in the absence of mir-142, however additional data will be required to determine whether any more general effects on the stability of other T cell subsets exist.

6.4. mir-142 regulates T cell differentiation through targeting of T-bet

Having demonstrated that mir-142-deficient T cells exhibit abnormal differentiation and lineage stability, I next attempted to identify any targets of mir-142 that were responsible for promoting default differentiation to the Th1 phenotype. In order to do

this, a further set of microarrays was performed allowing for protein-coding gene expression to be profiled in mir-142-deficient cells. These were performed on cells that had been activated for 36 hours in non-polarising conditions. At this timepoint, protein synthesis of IFN-γ has not yet increased in mir-142$^{-/-}$ cells (see Figure 6.3), and so any differences in gene expression observed at this stage would not be secondary to the effects of increased IFN-γ receptor binding. Following quality control and data normalisation, initial analysis of Th1-related transcription factors, cytokines and surface markers demonstrated widespread upregulation of many of these genes in mir-142$^{-/-}$ T cells analysed at 36 hours (Figure 6.13).

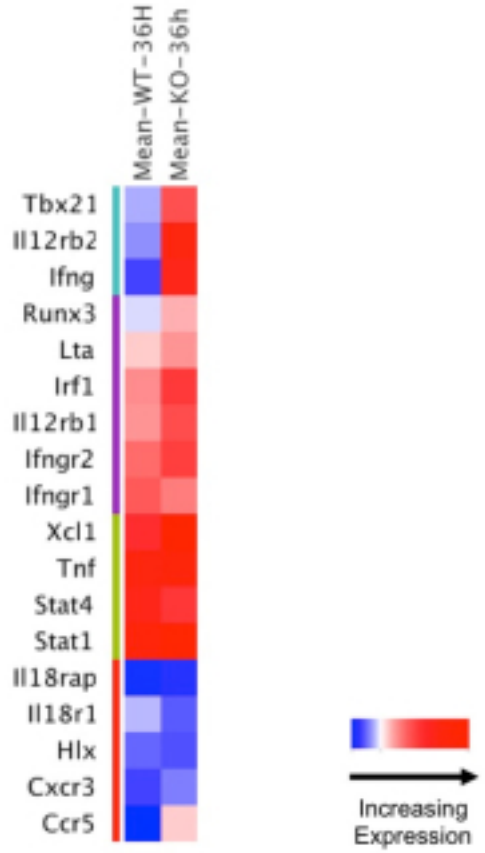

Figure 6.13 Increased expression of Th1-associated genes at 36 hours following stimulation of mir-142$^{-/-}$ Thp. Naïve Thp were stimulated *in vitro* for 36 hours, at which point RNA was extracted and microarray analysis performed. Selected genes have been associated with increased expression in Th1 cells, and are clustered by Self-organising map method into 4 clusters (indicated by coloured bar to left of heatmap). Mean of two biological replicates shown; WT = wild-type, KO = mir-142$^{-/-}$.

Analysis of miRNA target prediction databases did not identify any predicted target genes that were associated with Th1 development, however candidate gene analysis identified *Tbx21* (which encodes T-bet) as the most highly upregulated Th1 transcription factor, being approximately 8-fold higher expressed in mir-142$^{-/-}$ cells at 36 hours when compared with WT. Timecourse analysis using qRT-PCR demonstrated that Tbx21 expression is upregulated earlier following stimulation in mir-142$^{-/-}$ cells when compared with WT (Figure 6.14).

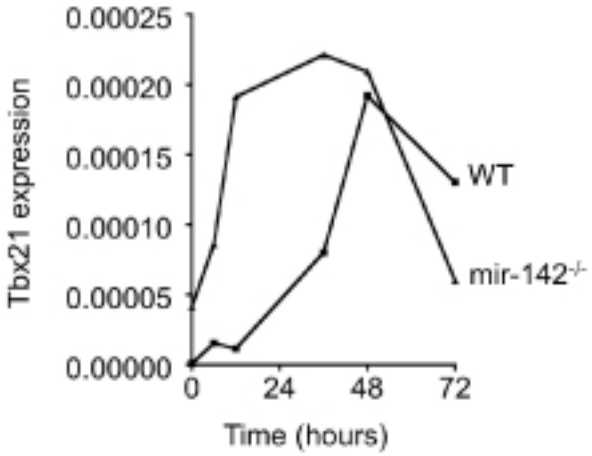

Figure 6.14 Timecourse qRT-PCR analysis of *Tbx21* expression in WT and mir-142$^{-/-}$ cells. Thp were isolated and activated *in vitro* in non-polarising conditions. Cells were sampled and RNA was extracted at multiple timepoints. qRT-PCR was performed for *Tbx21*. Mean of 2 replicates shown; data shown as $2^{-\Delta Ct}$ relative to beta actin.

Given this derepression of T-bet mRNA expression in stimulated mir-142$^{-/-}$ cells, I therefore considered whether T-bet could itself be a target of mir-142. The target analysis software packages StaRmiR and RNAhybrid (Kertesz et al., 2007; Rehmsmeier et al., 2004) were employed in order to detect potential binding sites, and both identified multiple partial sites for miR-142-3p in the T-bet 3'UTR (Figure 6.15 and Figure 6.16).

miR-142_3p

```
1) mfe: -22.6 kcal/mol

position  242
target 5' U         AAC     AUGG   C  G 3'
          UCCAUGGAG   GGAGA    ACU CA
          AGGUAUUUC   CCUUU    UGA GU
miRNA  3'           AU      G      U    5'



2) mfe: -22.1 kcal/mol

position  101
target 5'    U              GG   A 3'
             UGGAG AGGAAGCG  GCA
             AUUUC UCCUUUGU  UGU
miRNA  3' AGGU     A        GA     5'



3) mfe: -21.3 kcal/mol

position  602
target 5' U   UCG           G     U 3'
          UCU   GGAG GGGGGA GCUAU
          AGG   UUUC UCCUUU UGAUG
miRNA  3'     UA     A      G     U 5'



4) mfe: -20.5 kcal/mol

position  147
target 5' U   UGGCCCACA         G   G 3'
          UCC         AGGAAAUAC ACA
          AGG         UCCUUUGUG UGU
miRNA  3'     UAUUUCA           A     5'



5) mfe: -20.3 kcal/mol

position  319
target 5' G  G GGUGG     CC            U 3'
          UC G     GGAGU  AGGAGA GCUGC
          AG U     UUUCA  UCCUUU UGAUG
miRNA  3'    G A                G     U 5'
```

Figure 6.15 Predicted target sites of miR-142-3p in the T-bet 3'UTR identified by the prediction software RNAhybrid. Top 5 predicted sites are shown.

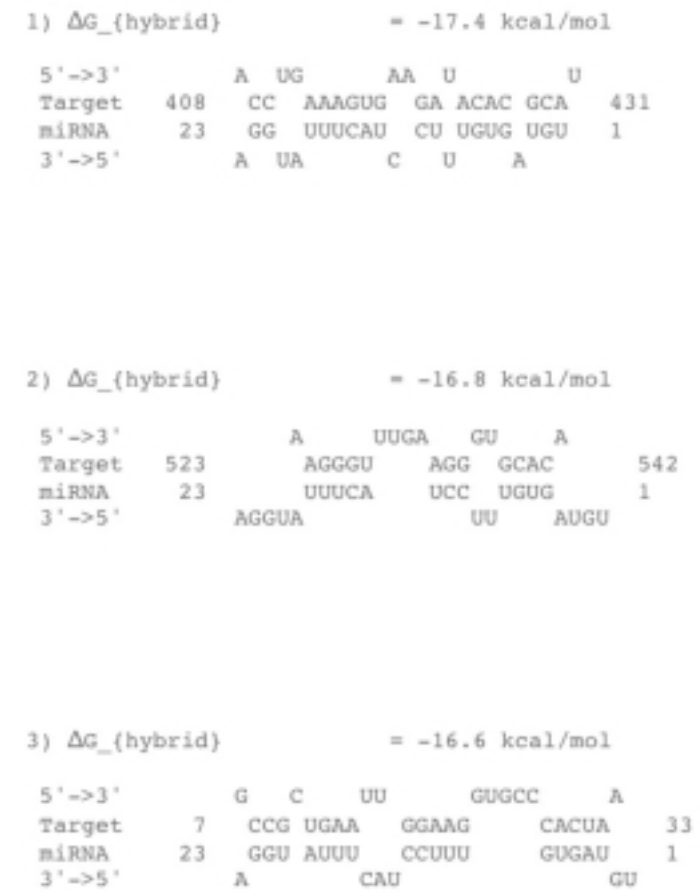

Figure 6.16 Predicted target sites of miR-142-3p identified in the T-bet 3'UTR by the target prediction software StaRmiR. Standard algorithm settings were used as follows: Model to use: Structure Model (Worm); Report target hits from: 3'UTR only; ΔG_{hybrid} threshold: -15kcal/mol; $\Delta G_{initiation}$: 4.09 kcal/mol; Folding temperature: 37°C; Ionic conditions: 1M NaCl, no divalent ions. 3 sites were predicted and all are shown here.

The multiple predicted sites for mir-142 targeting of T-bet that were identified by these algorithms suggested that T-bet should be analysed further as a potential target of mir-142. Luciferase assay was therefore performed in order to determine whether mir-142 could suppress expression via the 3'UTR. Due to the large number of target sites predicted by these algorithms (which made target site mutagenesis unfeasible), I

compared the effects of mir-142 on luciferase activity with a non-targeting miRNA mir-181a. Results showed that mir-142 expression vector suppressed luciferase activity when compared with empty vector and the non-targeting control mir-181a vector, suggesting that mir-142 does regulate T-bet expression via its 3'UTR (Figure 6.17).

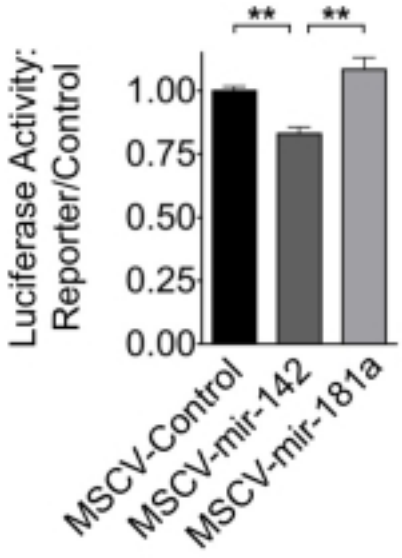

Figure 6.17 Targeting of the T-bet 3'UTR by mir-142. The T-bet 3'UTR was cloned into the PsiCHECK-2 luciferase vector. Expression vectors were co-transfected with luciferase reporter into target cells as indicated. n=3 per condition, **P<0.01 (Mann Whitney U-test).

I then sought to determine whether the mechanism of default Th1 lineage commitment in mir-142$^{-/-}$ T cells was dependent on T-bet. Unfortunately, the proximity of mir-142 to T-bet on the same chromosome made a double gene knockout strategy unfeasible (Figure 6.18).

Figure 6.18 Schematic demonstrating proximity of mir-142 and T-bet on mouse chromosome 11, which precludes a double gene knockout study.

I therefore employed a dominant negative (DN) approach in order to directly suppress the function of T-bet, as described previously (Mullen et al., 2002). In this model, the DNA-binding domain of T-bet is fused with the repression domain of *Drosophila* engrailed, thereby suppressing T-bet transcription factor activity. mir-142$^{-/-}$ Thp were cultured in non-polarising conditions and transduced with either control retrovirus or the DN-T-bet construct. Flow cytometry performed at day 7 demonstrated reversal of the default IFN-γ hyperproduction observed in mir-142$^{-/-}$ cells (Figure 6.19).

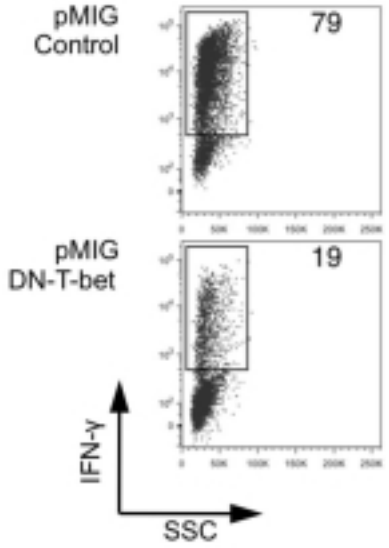

Figure 6.19 Dominant negative suppression of T-bet activity reverses the default phenotype observed in mir-142$^{-/-}$ cells cultured *in vitro*. Thp were isolated and cultured in non-polarising conditions, and transduced with the indicated retroviral construct at 24 hours. Cultures were then continued for a total of 7 days. Cells were harvested and analysed by flow cytometry. Plots are gated on live GFP^{+} cells, data representative of 2 independent experiments.

In summary, these data demonstrate that mir-142 is a critical regulator of T helper cell subset differentiation, and that absence of mir-142 results in default Th1 phenotype acquisition. In addition, T-bet is identified as a target of mir-142 and suppression of T-bet function reverses the phenotype observed in mir-142$^{-/-}$ cells, suggesting that mir-142

may prevent default Th1 differentiation by suppression of early T-bet activity following naïve T helper cell activation.

6.5. Discussion

These data collectively demonstrate the critical importance of mir-142 for the normal function of T helper cells. In addition to the homeostatic defect described in chapter 5, mir-142-deficient T cells undergo abnormal differentiation upon activation, producing large amounts of IFN-γ and upregulating the expression of a number of Th1-related genes. In a similar manner to the homeostatic defect, these abnormalities of subset differentiation occur because mir-142 targets a key T cell transcription factor, again highlighting that miRNAs sit at the heart of the regulatory networks that govern T cell function.

In general terms, these data further reinforce the view that individual miRNAs can possess multiple regulatory roles that are essential for the maintenance of cellular function. These findings are not unexpected given that miRNAs are known to be capable of targeting multiple genes. In addition, evolutionary conservation of miRNAs is high, suggesting that their ability to regulate vital cellular processes is indispensible for normal cell activity. However, while a large number of miRNAs are expressed in T cells, it appears that in this case there is no redundancy in mir-142 function, with the loss of this single miRNA being sufficient to significantly disrupt T cell function. This is particularly interesting because Dicer knockout mice, which are deficient in all mature miRNAs, also exhibit default production of IFN-γ in a similar manner to mir-142$^{-/-}$ mice (Muljo et al., 2005). In addition, the lineage stability of Dicer-deficient T cells was shown to be defective. Thus mir-142$^{-/-}$ mice have reproduced three of the T

cell phenotypes that have been described in Dicer-deficient mice, suggesting that mir-142 deficiency may be a major contributor to the homeostatic and functional abnormalities seen in these animals. Again, this highlights the critical importance of this single miRNA to T cell function, and provides a useful model platform for the further study of T cell development and functional biology in general, given that these phenotypic effects can be induced experimentally in a controlled manner through the use of mir-142 conditional knockout mice.

The starting points for this study were the observations that mir-142 expression is dynamically regulated in T cells, and that multiple master regulatory transcription factors bind to mir-142. The finding that mir-142 directly targets T-bet demonstrates that mir-142 is a part of the regulatory network that controls T cell differentiation. In addition, the fact that mir-142 is bound by T-bet in both human and mouse Th1 cells indicates that mir-142 and T-bet exist as part of a regulatory loop that tunes T cell differentiation. These data are currently insufficient to describe the way in which T-bet might regulate mir-142 expression, and future work will aim to investigate this intriguing relationship. However, these findings show mir-142 to be centrally involved in the networks that control T cell subset differentiation.

The data presented in this chapter and chapter 5 demonstrate that mir-142 is capable of targeting multiple transcription factors in T cells, thereby controlling the development and function of these cells. However it should be noted that miRNAs are likely to target many genes in order to function, and further work is necessary to determine the additional targets of mir-142 in these cells. I investigated whether mir-142 targeting of *Rarg* could potentially be contributory to the observed abnormalities in T cell differentiation, however the use of a number of RARγ agonists and antagonists in WT

and mir-142$^{-/-}$ cells did not specifically affect T cell subset differentiation, and RARγ overexpression did not either (data not shown). It remains possible that an undetermined common target exists that contributes to both the homeostatic and differentiation defects, and future study of candidate targets will attempt to determine whether this is the case; however no such unifying target was identified during the course of this work. As described in section 5.5, a number of new technologies have recently been developed that will potentially be of benefit in attempts to identify additional mir-142 targets. Indeed it seems probable that mir-142 functions through the regulation of multiple pathways and targets, and it will continue to be a major challenge to integrate these findings in order to improve our understanding of T cell biology.

In addition, some more specific conclusions can be drawn from the data presented in this chapter. The effects of mir-142 deficiency on subset differentiation and lineage stability are of potential interest in the study of disease and disease models, with certain pathological processes being linked with individual T cell subsets, as described in section 1.2.1. The fact that mir-142 could potentially control the lineage stability and phenotype of the cell in the setting of both desired and undesired immune responses raises the possibility that our understanding of mir-142-regulated pathways might be exploited in order to both track disease activity and modulate the cellular phenotype so as to improve the clinical outcome. This could potentially be explored in experimental settings such as experimental autoimmune diseases, infections with specific pathogens, and allotransplantation models, possibly employing miRNA antagomir technology to inhibit mir-142 function where appropriate. In addition, the study of mir-142 expression in human T cell-mediated diseases may be performed in order to determine its utility as a potential biomarker of disease.

In summary, these data provide further evidence of a central role for mir-142 in the regulation of T helper cell function. Through the use of both conditional and constitutive mir-142-deficient mice, I have been able to isolate a post-developmental function for mir-142 in maintaining lineage stability and regulating Th1 differentiation, through targeting of T-bet. Future work is necessary to identify additional target genes that may contribute to this phenotype, and the way in which transcriptional regulation of mir-142 by master regulatory transcription factors controls its function in this context. In addition, studies of the contribution of mir-142 to established T helper cell-mediated disease models could potentially provide further insight into the biology of T helper cell differentiation.

7. Discussion

The data presented in this thesis were generated from experiments designed to determine whether specific miRNAs possess critical roles in the function and differentiation of T helper cells. Through the use of multiple complementary methods, a candidate miRNA, mir-142, was identified and selected for further study, which revealed that mir-142 is critically important for the processes of normal T cell homeostasis and differentiation. In addition, functional targets of mir-142 were identified that are responsible for the phenotype observed in mir-142$^{-/-}$ mice. Whilst a number of specific conclusions have been discussed in the preceding chapters, some more general outcomes of this work are described below, in addition to potential future avenues of exploration such as dataset integration and the discovery of additional miRNA targets.

7.1. miRNA expression profiling and candidate selection

The initial approach that was employed to identify candidate miRNAs was to use microarray profiling of miRNA expression in order to detect differential expression of miRNAs between T cell subsets, and then to compare these data with additional, complementary datasets, such as transcription factor ChIP-seq. These methods were able to identify a set of miRNAs that are differentially expressed between subsets, and this was found to be reproducible. Since completing these experiments, newer technologies have emerged, including massively parallel miRNA-sequencing. Similar experiments could be performed using these new technologies, in order to further validate the datasets and to potentially identify novel miRNAs that were not included in the microarray platform. The gene clusters that have been described could also be

further investigated and refined through these means. In addition, such technologies may provide enhanced sensitivity and specificity, allowing for smaller differences between subsets or genotypes to be discovered.

Having identified a group of miRNAs of interest, there are a number of potential applications for these data. Firstly, as described in section 4.6, it may be possible to bioinformatically integrate the miRNA expression data with multiple additional datasets, such as mRNA expression and ChIP-seq, in order to begin to describe a functional atlas of the regulatory networks within T cells. The benefits of this might include identification of novel biological molecules of importance in these processes, and the ability to discover critical pathways that could potentially be targeted in order to modulate T cell function. The scope of this kind of project would likely be determined by the number of datasets, the degree of complexity of included data, and the available computing power. In addition, it would require development of novel software methods, although some aspects have already been described, for example miRNA-mRNA expression integration (Huang et al., 2011).

In the more immediate term, these data can be analysed in order to select further miRNAs for functional analysis, by using the same approach that identified mir-142. A number of miRNAs displayed large changes in expression when cells were activated, and these are potential candidates of interest for future studies. miRNAs that are found to be bound by master regulatory transcription factors might also be prioritised for investigation. In addition, those miRNAs whose expression is found to change on activation might be selected for analysis as possible biomarkers of T cell-mediated immune responses, such as in infection and allograft rejection.

More generally, these data reflect that significant changes in the expression of multiple miRNAs occur in T helper cells when they are activated and undergo differentiation. These findings are in keeping with those of a number of other haematopoietic cell types (Monticelli et al., 2005; Landgraf et al., 2007). Collectively these studies reinforce the concept that changes in miRNA expression are functionally related to the regulation of the cellular phenotype, and show that miRNA expression profiling can be a useful tool for candidate identification.

7.2. Relative importance of mir-142 in T helper cells

The findings that both T cell homeostasis and differentiation are disrupted in the absence of mir-142 highlight the importance of this miRNA for normal T cell function. Moreover, the significance of this gene is further reinforced when considered in relation to the reports of T cell-specific conditional Dicer- and Drosha-deficient mice, which exhibit considerable phenotypic overlap with mir-142$^{-/-}$ mice. These mice are globally deficient in all miRNAs, yet have a similar reduction in the peripheral T cell population, and these T cells also undergo preferential differentiation towards a Th1-like phenotype (Cobb et al., 2005; Muljo et al., 2005; Chong et al., 2008). The finding that mir-142 deficiency resembles global miRNA deficiency is particularly intriguing and could potentially be explored further by reconstitution of Dicer- and Drosha-deficient T cells by transfection with synthetic mature miR-142-3p, miR-142-5p or both.

To date, there are only a limited number of miRNA knockout mice that have been reported in the literature, of which few are described as possessing T cells with abnormal function. Of those that have, both miR-146a and miR-29 deficient mice displayed enhanced IFN-γ responses but no T cell homeostatic defects (Lu et al., 2010;

Ma et al., 2011a). Conversely, miR-155 deficient mice showed default adoption of a Th2-like phenotype, and again exhibited no defect in T cell numbers (Rodriguez et al., 2007). Thus there appears to be some overlap and cross-regulation between miRNAs in the control of subset differentiation, but no other specific miRNAs with such profound effects on T cell homeostasis have yet been identified. As more individual miRNA knockout mice are developed, analysed and reported it will be interesting to see how any T cell phenotypes compare with those of other miRNA-deficient mice, and also with the abnormalities observed in Dicer- and Drosha-deficient T cells.

Given that a clear defect in T cell homeostasis was readily observed in mir-142$^{-/-}$ mice, I elected to focus on this abnormality in the first instance. However, mir-142 is expressed in other immune cell types, including B cells, NK cells and dendritic cells. Preliminary phenotyping has not detected quantitative defects in any of these compartments, however work is ongoing to determine whether mir-142 possesses a functional role in these cells. In addition, the role of mir-142 in T cells continues to be studied. Our group has performed initial phenotyping of thymus from mir-142-deficient mice, which has not revealed any specific abnormalities in thymic T cell maturation (data not shown). However mir-142 expression appears to be dynamically regulated between stages of this process, suggesting a potential function for mir-142 in T cell development. It is possible that redundancy between miRNAs may obscure efforts to identify any function of mir-142 in thymocytes and thus a number of experimental tools including conditional knockouts and TCR-transgenic mice are being employed in order to study this. In addition, phenotypic analysis of mir-142$^{-/-}$ mice reveals a defect in the number of naturally occurring Treg, and impaired *in vitro* differentiation of iTreg (data not shown).

The mechanisms that are responsible for these defects are currently the subject of a major ongoing research programme in our laboratory.

Clearly the biology of mir-142 is complicated due to its expression in multiple immune cell types. However, with the use of techniques such as bone marrow transfer, conditional *in vivo* deletion and retroviral *in vitro* deletion I have been able to progressively isolate the stage of T cell development at which its cell-intrinsic expression is critically important, showing that the phenotype is reproduced even when mir-142 is deleted in mature T cells. These approaches will continue to be indispensible in the future study of this gene, particularly given the major defects in mir-142$^{-/-}$ T helper cell function described in this study.

7.3. Insights into miRNA biology

The data presented in this thesis have been generated in the context of existing knowledge and understanding of miRNA biology. In order to identify targets of mir-142, a number of current target prediction databases were searched and specific algorithms were also used to determine potential targets. Whilst I have identified at least two targets of mir-142, it is highly likely that multiple other targets exist that are specifically involved in the function of this miRNA. The gold standard of target validation remains the luciferase assay, but this is a slow and labour-intensive method that is only suited to the validation of a limited number of candidate targets. As I have done, it is possible to select targets based on changes in expression seen with genome-wide expression profiling, and evidence suggests that approximately 80% of miRNA targets will exhibit changes in mRNA abundance (Guo et al., 2010). However this will always risk missing the minority of targets that undergo translational repression, and necessarily entails

making an effectively arbitrary decision of fold-change cut-off. Proteomic techniques that are able to quantify changes in protein expression of miRNA targets have also been used in order to detect a broader range of target genes (Baek et al., 2008; Selbach et al., 2008; Jovanovic et al., 2010). However these typically require specific *in vitro* conditions and large quantities of cellular material that may make their use less feasible for the study of primary cells such as T cells.

It would be most desirable to specifically capture miRNA-target complexes and then profile the genes that are undergoing regulation by a specific miRNA. Some experimental methods have recently been described that use this approach, and it will be interesting to employ them in the study of mir-142. To date, however, none of them allow this procedure to be performed in the undisturbed natural cellular environment of the miRNA; for example the TAP-Tar technique requires transfection of streptavidin-labelled synthetic miRNA and pulldown of Flag-tagged transgenic Argonaute protein (Nonne et al., 2010). This could potentially disturb the normal processes by which the miRNA-RISC complex mediates suppression. An alternative approach might be to compare mir-142$^{-/-}$ cells with WT, and profile all those mRNAs that are being repressed within the RISC through Argonaute immunoprecipitation. However the deletion of mir-142 within these cells results in a multitude of downstream changes in gene expression, and many of these will not be due to loss of direct targeting by mir-142, instead being secondary to changes in expression of other genes such as transcription factors. These changes will likely be reflected in the profile of genes found within the RISC, and this could therefore cloud attempts to identify mir-142 targets.

In the absence of an ideal miRNA precipitation technology, which would leave cells undisturbed and specifically identify targets of individual miRNAs, the best approach

currently appears to be to employ multiple complementary methods such as those mentioned above and target prediction algorithms, and to then consider the results together. A possible benefit of such a systematic study would be to analyse identified targets in order to improve target prediction algorithms, potentially refining our understanding of the motifs, structures and sequences that define a target site. Indeed, the conditional mir-142-deficient mouse may be of use in this aim, as miRNA knockdown studies have previously been used to analyse and improve target prediction methods (Betel et al., 2010).

7.4. Additional future applications of this work

The data presented in this thesis focus on the basic biology of miRNAs, and include the first description of mir-142$^{-/-}$ mice. As discussed above, there remain many further experiments that can be performed to complement this work and advance our understanding of these molecules. At this stage, a number of potential future applications for this work can be envisaged, and some of these have already been discussed above.

In addition to these, it is also worth highlighting that there is the potential to exploit understanding of miRNA biology in order to manipulate cell function for therapeutic gain. Chemically-modified RNA molecules that antagonise miRNA function have recently been described, incorporating perfectly complementary sites for a specific miRNA. When these are introduced into a cell, they act as a 'sponge' that can reduce the availability of that miRNA and thereby inhibit its function. Systemic administration of these antagonists has recently been reported in non-human primates, with silencing of miR-122 in liver resulting in significant reduction in total plasma cholesterol without

evidence of toxicity at the doses reported (Elmén et al., 2008). Clearly, much remains to be evaluated regarding the biology of mir-142, but it might be possible in the first instance to experimentally test suppression of mir-142 in the setting of T cell-mediated colitis, given that I have shown mir-142-deficient T cells to be unable to induce colitis. However it is important to remember that our understanding of mir-142 biology is currently limited, meaning that these experiments may need to be reconsidered as new data become available.

7.5. Conclusions

In summary, this thesis has examined the role of miRNAs in T helper cells and has identified mir-142 as being critically important for T helper cell function. The miRNA expression profiling that has been performed may potentially yield additional candidates for future study, and the mechanisms of mir-142 function will continue to be examined. In addition, this work has confirmed the importance of individual miRNAs in fundamental processes such as cellular homeostasis and differentiation, and may be of relevance to future attempts to modulate the immune system through miRNA targeting.

8. References

Acosta-Rodriguez, E.V., Napolitani, G., Lanzavecchia, A., and Sallusto, F. (2007). Interleukins 1β and 6 but not transforming growth factor-β are essential for the differentiation of interleukin 17–producing human T helper cells. Nat Immunol *8*, 942–949.

Afkarian, M., Sedy, J.R., Yang, J., Jacobson, N.G., Cereb, N., Yang, S.Y., Murphy, T.L., and Murphy, K.M. (2002). T-bet is a STAT1-induced regulator of IL-12R expression in naïve CD4+ T cells. Nat Immunol *3*, 549–557.

Aggarwal, S., Ghilardi, N., Xie, M.-H., de Sauvage, F.J., and Gurney, A.L. (2003). Interleukin-23 promotes a distinct CD4 T cell activation state characterized by the production of interleukin-17. J Biol Chem *278*, 1910–1914.

Ambros, V., Bartel, B., Bartel, D.P., Burge, C.B., Carrington, J.C., Chen, X., Dreyfuss, G., Eddy, S.R., Griffiths-Jones, S., Marshall, M., et al. (2003). A uniform system for microRNA annotation. Rna *9*, 277–279.

Amsen, D., Antov, A., Jankovic, D., Sher, A., Radtke, F., Souabni, A., Busslinger, M., McCright, B., Gridley, T., and Flavell, R.A. (2007). Direct regulation of Gata3 expression determines the T helper differentiation potential of Notch. Immunity *27*, 89–99.

Ando, D.G., Clayton, J., Kono, D., Urban, J.L., and Sercarz, E.E. (1989). Encephalitogenic T cells in the B10.PL model of experimental allergic encephalomyelitis (EAE) are of the Th-1 lymphokine subtype. Cell. Immunol. *124*, 132–143.

Annunziato, F., Cosmi, L., Santarlasci, V., Maggi, L., Liotta, F., Mazzinghi, B., Parente, E., Filì, L., Ferri, S., Frosali, F., et al. (2007). Phenotypic and functional features of human Th17 cells. J Exp Med *204*, 1849–1861.

Arasu, P., Wightman, B., and Ruvkun, G. (1991). Temporal regulation of lin-14 by the antagonistic action of two other heterochronic genes, lin-4 and lin-28. Genes Dev *5*, 1825–1833.

Awasthi, A., and Kuchroo, V.K. (2009). Immunology. The yin and yang of follicular helper T cells. Science *325*, 953–955.

Awasthi, A., Carrier, Y., Peron, J.P.S., Bettelli, E., Kamanaka, M., Flavell, R.A., Kuchroo, V.K., Oukka, M., and Weiner, H.L. (2007). A dominant function for interleukin 27 in generating interleukin 10-producing anti-inflammatory T cells. Nat Immunol *8*, 1380–1389.

Baek, D., Villén, J., Shin, C., Camargo, F.D., Gygi, S.P., and Bartel, D.P. (2008). The impact of microRNAs on protein output. Nature *455*, 64–71.

Bai, A., Hu, H., Yeung, M., and Chen, J. (2007). Kruppel-like factor 2 controls T cell trafficking by activating L-selectin (CD62L) and sphingosine-1-phosphate receptor 1

transcription. J Immunol *178*, 7632–7639.

Banerjee, A., Schambach, F., Dejong, C., Hammond, S., and Reiner, S. (2009). Micro-RNA-155 Inhibits IFN-gamma Signaling in CD4(+) T cells. Eur J Immunol.

Bartel, D.P. (2009). MicroRNAs: target recognition and regulatory functions. Cell *136*, 215–233.

Battke, F., Symons, S., and Nieselt, K. (2010). Mayday--integrative analytics for expression data. BMC Bioinformatics *11*, 121.

Bayer, A.L., Yu, A., Adeegbe, D., and Malek, T.R. (2005). Essential role for interleukin-2 for CD4(+)CD25(+) T regulatory cell development during the neonatal period. J Exp Med *201*, 769–777.

Becher, B., Durell, B.G., and Noelle, R.J. (2002). Experimental autoimmune encephalitis and inflammation in the absence of interleukin-12. Journal of Clinical Investigation *110*, 493–497.

Behm-Ansmant, I., Rehwinkel, J., Doerks, T., Stark, A., Bork, P., and Izaurralde, E. (2006). mRNA degradation by miRNAs and GW182 requires both CCR4:NOT deadenylase and DCP1:DCP2 decapping complexes. Genes Dev *20*, 1885–1898.

Bellavia, D., Campese, A.F., Vacca, A., Gulino, A., and Screpanti, I. (2003). Notch3, another Notch in T cell development. Semin. Immunol. *15*, 107–112.

Bending, D., La Peña, De, H., Veldhoen, M., Phillips, J.M., Uyttenhove, C., Stockinger, B., and Cooke, A. (2009). Highly purified Th17 cells from BDC2.5NOD mice convert into Th1-like cells in NOD/SCID recipient mice. J. Clin. Invest. *119*, 565–572.

Bennett, C.L., Christie, J., Ramsdell, F., Brunkow, M.E., Ferguson, P.J., Whitesell, L., Kelly, T.E., Saulsbury, F.T., Chance, P.F., and Ochs, H.D. (2001). The immune dysregulation, polyendocrinopathy, enteropathy, X-linked syndrome (IPEX) is caused by mutations of FOXP3. Nat Genet *27*, 20–21.

Benson, M.J., Pino-Lagos, K., Rosemblatt, M., and Noelle, R.J. (2007). All-trans retinoic acid mediates enhanced T reg cell growth, differentiation, and gut homing in the face of high levels of co-stimulation. J Exp Med *204*, 1765–1774.

Berezikov, E., Chung, W.-J., Willis, J., Cuppen, E., and Lai, E.C. (2007). Mammalian mirtron genes. Mol Cell *28*, 328–336.

Beriou, G., Bradshaw, E.M., Lozano, E., Costantino, C.M., Hastings, W.D., Orban, T., Elyaman, W., Khoury, S.J., Kuchroo, V.K., Baecher-Allan, C., et al. (2010). TGF-beta induces IL-9 production from human Th17 cells. The Journal of Immunology *185*, 46–54.

Bernstein, E., Caudy, A.A., Hammond, S.M., and Hannon, G.J. (2001). Role for a bidentate ribonuclease in the initiation step of RNA interference. Nature *409*, 363–366.

Bernstein, E., Kim, S.Y., Carmell, M.A., Murchison, E.P., Alcorn, H., Li, M.Z., Mills,

A.A., Elledge, S.J., Anderson, K.V., and Hannon, G.J. (2003). Dicer is essential for mouse development. Nat Genet *35*, 215–217.

Betel, D., Koppal, A., Agius, P., Sander, C., and Leslie, C. (2010). Comprehensive modeling of microRNA targets predicts functional non-conserved and non-canonical sites. Genome Biol *11*, R90.

Bettelli, E., Carrier, Y., Gao, W., Korn, T., Strom, T.B., Oukka, M., Weiner, H.L., and Kuchroo, V.K. (2006). Reciprocal developmental pathways for the generation of pathogenic effector TH17 and regulatory T cells. Nature *441*, 235–238.

Bhattacharyya, S.N., Habermacher, R., Martine, U., Closs, E.I., and Filipowicz, W. (2006). Relief of microRNA-mediated translational repression in human cells subjected to stress. Cell *125*, 1111–1124.

Blom, L., Poulsen, B.C., Jensen, B.M., Hansen, A., and Poulsen, L.K. (2011). IL-33 induces IL-9 production in human CD4+ T cells and basophils. PLoS ONE *6*, e21695.

Bohnsack, M.T., Czaplinski, K., and Gorlich, D. (2004). Exportin 5 is a RanGTP-dependent dsRNA-binding protein that mediates nuclear export of pre-miRNAs. Rna *10*, 185–191.

Bonecchi, R., Bianchi, G., Bordignon, P.P., D'Ambrosio, D., Lang, R., Borsatti, A., Sozzani, S., Allavena, P., Gray, P.A., Mantovani, A., et al. (1998). Differential expression of chemokine receptors and chemotactic responsiveness of type 1 T helper cells (Th1s) and Th2s. J Exp Med *187*, 129–134.

Bopp, T., Becker, C., Klein, M., Klein-Hessling, S., Palmetshofer, A., Serfling, E., Heib, V., Becker, M., Kubach, J., Schmitt, S., et al. (2007). Cyclic adenosine monophosphate is a key component of regulatory T cell-mediated suppression. J Exp Med *204*, 1303–1310.

Borchert, G.M., Lanier, W., and Davidson, B.L. (2006). RNA polymerase III transcribes human microRNAs. Nat Struct Mol Biol *13*, 1097–1101.

Borsellino, G., Kleinewietfeld, M., Di Mitri, D., Sternjak, A., Diamantini, A., Giometto, R., Höpner, S., Centonze, D., Bernardi, G., Dell'Acqua, M.L., et al. (2007). Expression of ectonucleotidase CD39 by Foxp3+ Treg cells: hydrolysis of extracellular ATP and immune suppression. Blood *110*, 1225–1232.

Breitfeld, D., Ohl, L., Kremmer, E., Ellwart, J., Sallusto, F., Lipp, M., and Förster, R. (2000). Follicular B helper T cells express CXC chemokine receptor 5, localize to B cell follicles, and support immunoglobulin production. J Exp Med *192*, 1545–1552.

Brennecke, J., Stark, A., Russell, R.B., and Cohen, S.M. (2005). Principles of microRNA-target recognition. Plos Biol *3*, e85.

Brunkow, M.E., Jeffery, E.W., Hjerrild, K.A., Paeper, B., Clark, L.B., Yasayko, S.A., Wilkinson, J.E., Galas, D., Ziegler, S.F., and Ramsdell, F. (2001). Disruption of a new forkhead/winged-helix protein, scurfin, results in the fatal lymphoproliferative disorder of the scurfy mouse. Nat Genet *27*, 68–73.

Brüstle, A., Heink, S., Huber, M., Rosenplänter, C., Stadelmann, C., Yu, P., Arpaia, E., Mak, T.W., Kamradt, T., and Lohoff, M. (2007). The development of inflammatory T(H)-17 cells requires interferon-regulatory factor 4. Nat Immunol *8*, 958–966.

Byrne, J.A., Stankovic, A.K., and Cooper, M.D. (1994). A novel subpopulation of primed T cells in the human fetus. J Immunol *152*, 3098–3106.

Cai, X., Hagedorn, C.H., and Cullen, B.R. (2004). Human microRNAs are processed from capped, polyadenylated transcripts that can also function as mRNAs. Rna *10*, 1957–1966.

Campbell, I.L., Kay, T.W., Oxbrow, L., and Harrison, L.C. (1991). Essential role for interferon-gamma and interleukin-6 in autoimmune insulin-dependent diabetes in NOD/Wehi mice. Journal of Clinical Investigation *87*, 739–742.

Cao, X., Cai, S.F., Fehniger, T.A., Song, J., Collins, L.I., Piwnica-Worms, D.R., and Ley, T.J. (2007). Granzyme B and perforin are important for regulatory T cell-mediated suppression of tumor clearance. Immunity *27*, 635–646.

Chang, H.-C., Sehra, S., Goswami, R., Yao, W., Yu, Q., Stritesky, G.L., Jabeen, R., McKinley, C., Ahyi, A.-N., Han, L., et al. (2010). The transcription factor PU.1 is required for the development of IL-9-producing T cells and allergic inflammation. Nat Immunol *11*, 527–534.

Chatila, T.A., Blaeser, F., Ho, N., Lederman, H.M., Voulgaropoulos, C., Helms, C., and Bowcock, A.M. (2000). JM2, encoding a fork head-related protein, is mutated in X-linked autoimmunity-allergic disregulation syndrome. Journal of Clinical Investigation *106*, R75–81.

Chen, C.-Z., Li, L., Lodish, H.F., and Bartel, D.P. (2004). MicroRNAs modulate hematopoietic lineage differentiation. Science *303*, 83–86.

Chen, G., Hardy, K., Bunting, K., Daley, S., Ma, L., and Shannon, M.F. (2010). Regulation of the IL-21 gene by the NF-kappaB transcription factor c-Rel. The Journal of Immunology *185*, 2350–2359.

Chen, H., Zhang, H., Lee, J., Liang, X., Wu, X., Zhu, T., Lo, P.-K., Zhang, X., and Sukumar, S. (2007). HOXA5 acts directly downstream of retinoic acid receptor beta and contributes to retinoic acid-induced apoptosis and growth inhibition. Cancer Res. *67*, 8007–8013.

Chen, W., Jin, W., Hardegen, N., Lei, K.-J., Li, L., Marinos, N., McGrady, G., and Wahl, S.M. (2003). Conversion of peripheral CD4+CD25- naive T cells to CD4+CD25+ regulatory T cells by TGF-beta induction of transcription factor Foxp3. J Exp Med *198*, 1875–1886.

Chen, X., Das, R., Komorowski, R., Beres, A., Hessner, M.J., Mihara, M., and Drobyski, W.R. (2009). Blockade of interleukin-6 signaling augments regulatory T-cell reconstitution and attenuates the severity of graft-versus-host disease. Blood *114*, 891–900.

Chendrimada, T.P., Gregory, R.I., Kumaraswamy, E., Norman, J., Cooch, N., Nishikura, K., and Shiekhattar, R. (2005). TRBP recruits the Dicer complex to Ago2 for microRNA processing and gene silencing. Nature *436*, 740–744.

Cherwinski, H.M., Schumacher, J.H., Brown, K.D., and Mosmann, T.R. (1987). Two types of mouse helper T cell clone. III. Further differences in lymphokine synthesis between Th1 and Th2 clones revealed by RNA hybridization, functionally monospecific bioassays, and monoclonal antibodies. J Exp Med *166*, 1229–1244.

Chi, S., Zang, J., Mele, A., and Darnell, R. (2009). Argonaute HITS-CLIP decodes microRNA-mRNA interaction maps. Nature.

Chong, M.M.W., Rasmussen, J.P., Rudensky, A.Y., Rundensky, A.Y., and Littman, D.R. (2008). The RNAseIII enzyme Drosha is critical in T cells for preventing lethal inflammatory disease. J Exp Med *205*, 2005–2017.

Cobb, B.S., Hertweck, A., Smith, J., O'Connor, E., Graf, D., Cook, T., Smale, S.T., Sakaguchi, S., Livesey, F.J., Fisher, A.G., et al. (2006). A role for Dicer in immune regulation. J Exp Med *203*, 2519–2527.

Cobb, B.S., Nesterova, T.B., Thompson, E., Hertweck, A., O'Connor, E., Godwin, J., Wilson, C.B., Brockdorff, N., Fisher, A.G., Smale, S.T., et al. (2005). T cell lineage choice and differentiation in the absence of the RNase III enzyme Dicer. J Exp Med *201*, 1367–1373.

Collison, L.W., Workman, C.J., Kuo, T.T., Boyd, K., Wang, Y., Vignali, K.M., Cross, R., Sehy, D., Blumberg, R.S., and Vignali, D.A.A. (2007). The inhibitory cytokine IL-35 contributes to regulatory T-cell function. Nature *450*, 566–569.

Constant, S., Pfeiffer, C., Woodard, A., Pasqualini, T., and Bottomly, K. (1995). Extent of T cell receptor ligation can determine the functional differentiation of naive CD4+ T cells. J Exp Med *182*, 1591–1596.

Cote-Sierra, J., Foucras, G., Guo, L., Chiodetti, L., Young, H.A., Hu-Li, J., Zhu, J., and Paul, W.E. (2004). Interleukin 2 plays a central role in Th2 differentiation. Proc Natl Acad Sci USA *101*, 3880–3885.

Crotty, S. (2011). Follicular helper CD4 T cells (TFH). Annu Rev Immunol *29*, 621–663.

Crotty, S., Johnston, R.J., and Schoenberger, S.P. (2010). Effectors and memories: Bcl-6 and Blimp-1 in T and B lymphocyte differentiation. Nat Immunol *11*, 114–120.

Cua, D.J., Sherlock, J., Chen, Y., Murphy, C.A., Joyce, B., Seymour, B., Lucian, L., To, W., Kwan, S., Churakova, T., et al. (2003). Interleukin-23 rather than interleukin-12 is the critical cytokine for autoimmune inflammation of the brain. Nature *421*, 744–748.

Curotto de Lafaille, M.A., Lino, A.C., Kutchukhidze, N., and Lafaille, J.J. (2004). CD25- T cells generate CD25+Foxp3+ regulatory T cells by peripheral expansion. J Immunol *173*, 7259–7268.

Curtale, G., Citarella, F., Carissimi, C., Goldoni, M., Carucci, N., Fulci, V., Franceschini, D., Meloni, F., Barnaba, V., and Macino, G. (2010). An emerging player in the adaptive immune response: microRNA-146a is a modulator of IL-2 expression and activation-induced cell death in T lymphocytes. Blood *115*, 265–273.

D'Ambrosio, D., Iellem, A., Bonecchi, R., Mazzeo, D., Sozzani, S., Mantovani, A., and Sinigaglia, F. (1998). Selective up-regulation of chemokine receptors CCR4 and CCR8 upon activation of polarized human type 2 Th cells. J Immunol *161*, 5111–5115.

Dardalhon, V., Awasthi, A., Kwon, H., Galileos, G., Gao, W., Sobel, R.A., Mitsdoerffer, M., Strom, T.B., Elyaman, W., Ho, I.-C., et al. (2008). IL-4 inhibits TGF-beta-induced Foxp3+ T cells and, together with TGF-beta, generates IL-9+ IL-10+ Foxp3(-) effector T cells. Nat Immunol *9*, 1347–1355.

Deaglio, S., Dwyer, K.M., Gao, W., Friedman, D., Usheva, A., Erat, A., Chen, J.-F., Enjyoji, K., Linden, J., Oukka, M., et al. (2007). Adenosine generation catalyzed by CD39 and CD73 expressed on regulatory T cells mediates immune suppression. J Exp Med *204*, 1257–1265.

Debray-Sachs, M., Carnaud, C., Boitard, C., Cohen, H., Gresser, I., Bedossa, P., and Bach, J.F. (1991). Prevention of diabetes in NOD mice treated with antibody to murine IFN gamma. J Autoimmun *4*, 237–248.

del Peso, L., González, V.M., Hernández, R., Barr, F.G., and Núñez, G. (1999). Regulation of the forkhead transcription factor FKHR, but not the PAX3-FKHR fusion protein, by the serine/threonine kinase Akt. Oncogene *18*, 7328–7333.

Diederichs, S. (2007). Dual Role for Argonautes in MicroRNA Processing and Posttranscriptional Regulation of MicroRNA Expression. Cell *131*, 1097–1108.

Djuretic, I.M., Levanon, D., Negreanu, V., Groner, Y., Rao, A., and Ansel, K.M. (2007). Transcription factors T-bet and Runx3 cooperate to activate Ifng and silence Il4 in T helper type 1 cells. Nat Immunol *8*, 145–153.

Doench, J.G., and Sharp, P.A. (2004). Specificity of microRNA target selection in translational repression. Genes Dev *18*, 504–511.

Dominitzki, S., Fantini, M.C., Neufert, C., Nikolaev, A., Galle, P.R., Scheller, J., Monteleone, G., Rose-John, S., Neurath, M.F., and Becker, C. (2007). Cutting edge: trans-signaling via the soluble IL-6R abrogates the induction of FoxP3 in naive CD4+CD25 T cells. J Immunol *179*, 2041–2045.

Du, C., Liu, C., Kang, J., Zhao, G., Ye, Z., Huang, S., Li, Z., Wu, Z., and Pei, G. (2009). MicroRNA miR-326 regulates TH-17 differentiation and is associated with the pathogenesis of multiple sclerosis. Nat Immunol 1–9.

Duhen, T., Geiger, R., Jarrossay, D., Lanzavecchia, A., and Sallusto, F. (2009). Production of interleukin 22 but not interleukin 17 by a subset of human skin-homing memory T cells. Nat Immunol *10*, 857–863.

Durant, L., Watford, W.T., Ramos, H.L., Laurence, A., Vahedi, G., Wei, L., Takahashi,

H., Sun, H.-W., Kanno, Y., Powrie, F., et al. (2010). Diverse targets of the transcription factor STAT3 contribute to T cell pathogenicity and homeostasis. Immunity *32*, 605–615.

Dzhagalov, I., Chambon, P., and He, Y.-W. (2007). Regulation of CD8+ T lymphocyte effector function and macrophage inflammatory cytokine production by retinoic acid receptor gamma. J Immunol *178*, 2113–2121.

Easow, G., Teleman, A.A., and Cohen, S.M. (2007). Isolation of microRNA targets by miRNP immunopurification. Rna *13*, 1198–1204.

Ebert, P., Jiang, S., Xie, J., Li, Q., and Davis, M. (2009). An endogenous positively selecting peptide enhances mature T cell responses and becomes an autoantigen in the absence of microRNA miR-181a. Nat Immunol.

Eck, S.C., Zhu, P., Pepper, M., Bensinger, S.J., Freedman, B.D., and Laufer, T.M. (2006). Developmental alterations in thymocyte sensitivity are actively regulated by MHC class II expression in the thymic medulla. J Immunol *176*, 2229–2237.

Elmén, J., Lindow, M., Schütz, S., Lawrence, M., Petri, A., Obad, S., Lindholm, M., Hedtjärn, M., Hansen, H.F., Berger, U., et al. (2008). LNA-mediated microRNA silencing in non-human primates. Nature *452*, 896–899.

Else, K.J., Hültner, L., and Grencis, R.K. (1992). Cellular immune responses to the murine nematode parasite Trichuris muris. II. Differential induction of TH-cell subsets in resistant versus susceptible mice. Immunology *75*, 232–237.

Enright, A.J., John, B., Gaul, U., Tuschl, T., Sander, C., and Marks, D.S. (2003). MicroRNA targets in Drosophila. Genome Biol *5*, R1.

Ertesvag, A., Engedal, N., Naderi, S., and Blomhoff, H.K. (2002). Retinoic acid stimulates the cell cycle machinery in normal T cells: involvement of retinoic acid receptor-mediated IL-2 secretion. J Immunol *169*, 5555–5563.

Esser, C., Rannug, A., and Stockinger, B. (2009). The aryl hydrocarbon receptor in immunity. Trends in Immunology *30*, 447–454.

Eulalio, A., Huntzinger, E., and Izaurralde, E. (2008). GW182 interaction with Argonaute is essential for miRNA-mediated translational repression and mRNA decay. Nat Struct Mol Biol *15*, 346–353.

Eulalio, A., Huntzinger, E., Nishihara, T., Rehwinkel, J., Fauser, M., and Izaurralde, E. (2009). Deadenylation is a widespread effect of miRNA regulation. Rna *15*, 21–32.

Fallarino, F., Grohmann, U., Hwang, K.W., Orabona, C., Vacca, C., Bianchi, R., Belladonna, M.L., Fioretti, M.C., Alegre, M.-L., and Puccetti, P. (2003). Modulation of tryptophan catabolism by regulatory T cells. Nat Immunol *4*, 1206–1212.

Fang, T.C., Yashiro-Ohtani, Y., Del Bianco, C., Knoblock, D.M., Blacklow, S.C., and Pear, W.S. (2007). Notch directly regulates Gata3 expression during T helper 2 cell differentiation. Immunity *27*, 100–110.

Farh, K.K.-H., Grimson, A., Jan, C., Lewis, B.P., Johnston, W.K., Lim, L.P., Burge, C.B., and Bartel, D.P. (2005). The widespread impact of mammalian MicroRNAs on mRNA repression and evolution. Science *310*, 1817–1821.

Faulkner, H., Humphreys, N., Renauld, J.C., Van Snick, J., and Grencis, R. (1997). Interleukin-9 is involved in host protective immunity to intestinal nematode infection. Eur J Immunol *27*, 2536–2540.

Fazilleau, N., Mark, L., McHeyzer-Williams, L.J., and McHeyzer-Williams, M.G. (2009). Follicular helper T cells: lineage and location. Immunity *30*, 324–335.

Fire, A., Xu, S., Montgomery, M.K., Kostas, S.A., Driver, S.E., and Mello, C.C. (1998). Potent and specific genetic interference by double-stranded RNA in Caenorhabditis elegans. Nature *391*, 806–811.

Fitzgerald, D.C., Zhang, G.-X., El-Behi, M., Fonseca-Kelly, Z., Li, H., Yu, S., Saris, C.J.M., Gran, B., Ciric, B., and Rostami, A. (2007). Suppression of autoimmune inflammation of the central nervous system by interleukin 10 secreted by interleukin 27-stimulated T cells. Nat Immunol *8*, 1372–1379.

Fontenot, J.D., Gavin, M.A., and Rudensky, A.Y. (2003). Foxp3 programs the development and function of CD4+CD25+ regulatory T cells. Nat Immunol *4*, 330–336.

Fontenot, J.D., Rasmussen, J.P., Gavin, M.A., and Rudensky, A.Y. (2005). A function for interleukin 2 in Foxp3-expressing regulatory T cells. Nat Immunol *6*, 1142–1151.

Forbes, E.E., Groschwitz, K., Abonia, J.P., Brandt, E.B., Cohen, E., Blanchard, C., Ahrens, R., Seidu, L., McKenzie, A., Strait, R., et al. (2008). IL-9- and mast cell-mediated intestinal permeability predisposes to oral antigen hypersensitivity. Journal of Experimental Medicine *205*, 897–913.

Forman, J.J., Legesse-Miller, A., and Coller, H.A. (2008). A search for conserved sequences in coding regions reveals that the let-7 microRNA targets Dicer within its coding sequence. Proc Natl Acad Sci USA *105*, 14879–14884.

Friedman, R.C., Farh, K.K.-H., Burge, C.B., and Bartel, D.P. (2009). Most mammalian mRNAs are conserved targets of microRNAs. Genome Res. *19*, 92–105.

Fukuda, T., Yamagata, K., Fujiyama, S., Matsumoto, T., Koshida, I., Yoshimura, K., Mihara, M., Naitou, M., Endoh, H., Nakamura, T., et al. (2007). DEAD-box RNA helicase subunits of the Drosha complex are required for processing of rRNA and a subset of microRNAs. Nat Cell Biol *9*, 604–611.

Gagnon, J., Chen, X.L., Forand-Boulerice, M., Leblanc, C., Raman, C., Ramanathan, S., and Ilangumaran, S. (2010). Increased antigen responsiveness of naive CD8 T cells exposed to IL-7 and IL-21 is associated with decreased CD5 expression. Immunology and Cell Biology *88*, 451–460.

Gaidatzis, D., van Nimwegen, E., Hausser, J., and Zavolan, M. (2007). Inference of miRNA targets using evolutionary conservation and pathway analysis. BMC Bioinformatics *8*, 69.

Gatfield, D., Le Martelot, G., Vejnar, C.E., Gerlach, D., Schaad, O., Fleury-Olela, F., Ruskeepää, A.-L., Oresic, M., Esau, C.C., Zdobnov, E.M., et al. (2009). Integration of microRNA miR-122 in hepatic circadian gene expression. Genes Dev *23*, 1313–1326.

Georgopoulos, K., Moore, D.D., and Derfler, B. (1992). Ikaros, an early lymphoid-specific transcription factor and a putative mediator for T cell commitment. Science *258*, 808–812.

Gessner, A., Blum, H., and Röllinghoff, M. (1993). Differential regulation of IL-9-expression after infection with Leishmania major in susceptible and resistant mice. Immunobiology *189*, 419–435.

Ghisi, M., Corradin, A., Basso, K., Frasson, C., Serafin, V., Mukherjee, S., Mussolin, L., Ruggero, K., Bonanno, L., Guffanti, A., et al. (2011). Modulation of microRNA expression in human T-cell development: targeting of NOTCH3 by miR-150. Blood *117*, 7053–7062.

Ghoreschi, K., Laurence, A., Yang, X.-P., Tato, C.M., Mcgeachy, M.J., Konkel, J.E., Ramos, H.L., Wei, L., Davidson, T.S., Bouladoux, N., et al. (2010). Generation of pathogenic T(H)17 cells in the absence of TGF-β signalling. Nature *467*, 967–971.

Giraldez, A.J., Mishima, Y., Rihel, J., Grocock, R.J., van Dongen, S., Inoue, K., Enright, A.J., and Schier, A.F. (2006). Zebrafish MiR-430 promotes deadenylation and clearance of maternal mRNAs. Science *312*, 75–79.

Gokmen, R. (2011). The role of the transcription factor T-bet in the differentiation and function of T helper subsets. King's College London.

Gondek, D.C., Lu, L.-F., Quezada, S.A., Sakaguchi, S., and Noelle, R.J. (2005). Cutting edge: contact-mediated suppression by CD4+CD25+ regulatory cells involves a granzyme B-dependent, perforin-independent mechanism. J Immunol *174*, 1783–1786.

Gran, B., Zhang, G.-X., Yu, S., Li, J., Chen, X.-H., Ventura, E.S., Kamoun, M., and Rostami, A. (2002). IL-12p35-deficient mice are susceptible to experimental autoimmune encephalomyelitis: evidence for redundancy in the IL-12 system in the induction of central nervous system autoimmune demyelination. J Immunol *169*, 7104–7110.

Gregory, R.I., Yan, K.-P., Amuthan, G., Chendrimada, T., Doratotaj, B., Cooch, N., and Shiekhattar, R. (2004). The Microprocessor complex mediates the genesis of microRNAs. Nature *432*, 235–240.

Grenningloh, R., Kang, B.Y., and Ho, I.-C. (2005). Ets-1, a functional cofactor of T-bet, is essential for Th1 inflammatory responses. J Exp Med *201*, 615–626.

Griffiths-Jones, S. (2004). The microRNA Registry. Nucleic Acids Res. *32*, D109–11.

Griffiths-Jones, S., Bateman, A., Marshall, M., Khanna, A., and Eddy, S.R. (2003). Rfam: an RNA family database. Nucleic Acids Res. *31*, 439–441.

Griffiths-Jones, S., Grocock, R.J., van Dongen, S., Bateman, A., and Enright, A.J.

(2006). miRBase: microRNA sequences, targets and gene nomenclature. Nucleic Acids Res. *34*, D140–4.

Grimson, A., Farh, K.K.-H., Johnston, W.K., Garrett-Engele, P., Lim, L.P., and Bartel, D.P. (2007). MicroRNA targeting specificity in mammals: determinants beyond seed pairing. Mol Cell *27*, 91–105.

Grishok, A., Pasquinelli, A.E., Conte, D., Li, N., Parrish, S., Ha, I., Baillie, D.L., Fire, A., Ruvkun, G., and Mello, C.C. (2001). Genes and mechanisms related to RNA interference regulate expression of the small temporal RNAs that control C. elegans developmental timing. Cell *106*, 23–34.

Grossman, Z., and Singer, A. (1996). Tuning of activation thresholds explains flexibility in the selection and development of T cells in the thymus. Proc Natl Acad Sci USA *93*, 14747–14752.

Grün, D., Wang, Y.-L., Langenberger, D., Gunsalus, K.C., and Rajewsky, N. (2005). microRNA target predictions across seven Drosophila species and comparison to mammalian targets. PLoS Comp Biol *1*, e13.

Gu, S., Jin, L., Zhang, F., Sarnow, P., and Kay, M.A. (2009). Biological basis for restriction of microRNA targets to the 3' untranslated region in mammalian mRNAs. Nat Struct Mol Biol *16*, 144–150.

Guo, H., Ingolia, N.T., Weissman, J.S., and Bartel, D.P. (2010). Mammalian microRNAs predominantly act to decrease target mRNA levels. Nature *466*, 835–840.

Hall, J.A., Cannons, J.L., Grainger, J.R., Santos, Dos, L.M., Hand, T.W., Naik, S., Wohlfert, E.A., Chou, D.B., Oldenhove, G., Robinson, M., et al. (2011). Essential role for retinoic acid in the promotion of CD4(+) T cell effector responses via retinoic acid receptor alpha. Immunity *34*, 435–447.

Hamilton, A.J., and Baulcombe, D.C. (1999). A species of small antisense RNA in posttranscriptional gene silencing in plants. Science *286*, 950–952.

Hammell, M., Long, D., Zhang, L., Lee, A., Carmack, C.S., Han, M., Ding, Y., and Ambros, V. (2008). mirWIP: microRNA target prediction based on microRNA-containing ribonucleoprotein-enriched transcripts. Nat Meth *5*, 813–819.

Han, J., Pedersen, J.S., Kwon, S.C., Belair, C.D., Kim, Y.-K., Yeom, K.-H., Yang, W.-Y., Haussler, D., Blelloch, R., and Kim, V.N. (2009). Posttranscriptional crossregulation between Drosha and DGCR8. Cell *136*, 75–84.

Harrington, L.E., Hatton, R.D., Mangan, P.R., Turner, H., Murphy, T.L., Murphy, K.M., and Weaver, C.T. (2005). Interleukin 17-producing CD4+ effector T cells develop via a lineage distinct from the T helper type 1 and 2 lineages. Nat Immunol *6*, 1123–1132.

Hataye, J., Moon, J.J., Khoruts, A., Reilly, C., and Jenkins, M.K. (2006). Naive and memory CD4+ T cell survival controlled by clonal abundance. Science *312*, 114–116.

Hayashi, N., Yoshimoto, T., Izuhara, K., Matsui, K., Tanaka, T., and Nakanishi, K.

(2007). T helper 1 cells stimulated with ovalbumin and IL-18 induce airway hyperresponsiveness and lung fibrosis by IFN-gamma and IL-13 production. Proc Natl Acad Sci USA *104*, 14765–14770.

He, L., Thomson, J.M., Hemann, M.T., Hernando-Monge, E., Mu, D., Goodson, S., Powers, S., Cordon-Cardo, C., Lowe, S.W., Hannon, G.J., et al. (2005). A microRNA polycistron as a potential human oncogene. Nature *435*, 828–833.

Hegazy, A.N., Peine, M., Helmstetter, C., Panse, I., FrOhlich, A., Bergthaler, A., Flatz, L., Pinschewer, D.D., Radbruch, A., and LOhning, M. (2010). Interferons direct Th2 cell reprogramming to generate a stable GATA-3(+)T-bet(+) cell subset with combined Th2 and Th1 cell functions. Immunity *32*, 116–128.

Heinzel, F.P., Sadick, M.D., Holaday, B.J., Coffman, R.L., and Locksley, R.M. (1989). Reciprocal expression of interferon gamma or interleukin 4 during the resolution or progression of murine leishmaniasis. Evidence for expansion of distinct helper T cell subsets. J Exp Med *169*, 59–72.

Hendrickson, D.G., Hogan, D.J., McCullough, H.L., Myers, J.W., Herschlag, D., Ferrell, J.E., and Brown, P.O. (2009). Concordant regulation of translation and mRNA abundance for hundreds of targets of a human microRNA. Plos Biol *7*, e1000238.

Hill, J.A., Hall, J.A., Sun, C.-M., Cai, Q., Ghyselinck, N., Chambon, P., Belkaid, Y., Mathis, D., and Benoist, C. (2008). Retinoic acid enhances Foxp3 induction indirectly by relieving inhibition from CD4+CD44hi Cells. Immunity *29*, 758–770.

Ho, I.-C., Tai, T.-S., and Pai, S.-Y. (2009). GATA3 and the T-cell lineage: essential functions before and after T-helper-2-cell differentiation. Nat Rev Immunol *9*, 125–135.

Ho, I.C., Hodge, M.R., Rooney, J.W., and Glimcher, L.H. (1996). The proto-oncogene c-maf is responsible for tissue-specific expression of interleukin-4. Cell *85*, 973–983.

Hori, S., Nomura, T., and Sakaguchi, S. (2003). Control of regulatory T cell development by the transcription factor Foxp3. Science *299*, 1057–1061.

Hosken, N.A., Shibuya, K., Heath, A.W., Murphy, K.M., and O'Garra, A. (1995). The effect of antigen dose on CD4+ T helper cell phenotype development in a T cell receptor-alpha beta-transgenic model. J Exp Med *182*, 1579–1584.

Hou, J., Wang, P., Lin, L., Liu, X., Ma, F., An, H., Wang, Z., and Cao, X. (2009). MicroRNA-146a feedback inhibits RIG-I-dependent Type I IFN production in macrophages by targeting TRAF6, IRAK1, and IRAK2. The Journal of Immunology *183*, 2150–2158.

Hsieh, C.S., Macatonia, S.E., Tripp, C.S., Wolf, S.F., O'Garra, A., and Murphy, K.M. (1993). Development of TH1 CD4+ T cells through IL-12 produced by Listeria-induced macrophages. Science *260*, 547–549.

Huang, B., Zhao, J., Lei, Z., Shen, S., Li, D., Shen, G.-X., Zhang, G.-M., and Feng, Z.-H. (2009). miR-142-3p restricts cAMP production in CD4+CD25- T cells and CD4+CD25+ TREG cells by targeting AC9 mRNA. EMBO Reports *10*, 180–185.

Huang, F., Kitaura, Y., Jang, I., Naramura, M., Kole, H.H., Liu, L., Qin, H., Schlissel, M.S., and Gu, H. (2006). Establishment of the major compatibility complex-dependent development of CD4+ and CD8+ T cells by the Cbl family proteins. Immunity *25*, 571–581.

Huang, G.T., Athanassiou, C., and Benos, P.V. (2011). mirConnX: condition-specific mRNA-microRNA network integrator. Nucleic Acids Res. *39*, W416–23.

Huang, T., Wei, B., Velazquez, P., Borneman, J., and Braun, J. (2005). Commensal microbiota alter the abundance and TCR responsiveness of splenic naïve CD4+ T lymphocytes. Clin Immunol *117*, 221–230.

Huber, M., Steinwald, V., Guralnik, A., Brustle, A., Kleemann, P., Rosenplanter, C., Decker, T., and Lohoff, M. (2007). IL-27 inhibits the development of regulatory T cells via STAT3. International Immunology *20*, 223–234.

Huber, W., Heydebreck, von, A., Sültmann, H., Poustka, A., and Vingron, M. (2002). Variance stabilization applied to microarray data calibration and to the quantification of differential expression. Bioinformatics *18 Suppl 1*, S96–104.

Huntzinger, E., and Izaurralde, E. (2011). Gene silencing by microRNAs: contributions of translational repression and mRNA decay. Nat Rev Genet *12*, 99–110.

Hutvágner, G., and Zamore, P.D. (2002). A microRNA in a multiple-turnover RNAi enzyme complex. Science *297*, 2056–2060.

Hutvágner, G., McLachlan, J., Pasquinelli, A.E., Bálint, E., Tuschl, T., and Zamore, P.D. (2001). A cellular function for the RNA-interference enzyme Dicer in the maturation of the let-7 small temporal RNA. Science *293*, 834–838.

Hwang, E.S., Szabo, S.J., Schwartzberg, P.L., and Glimcher, L.H. (2005). T helper cell fate specified by kinase-mediated interaction of T-bet with GATA-3. Science *307*, 430–433.

Hwang, H.-W., Wentzel, E.A., and Mendell, J.T. (2007). A hexanucleotide element directs microRNA nuclear import. Science *315*, 97–100.

Irizarry, R.A., Hobbs, B., Collin, F., Beazer-Barclay, Y.D., Antonellis, K.J., Scherf, U., and Speed, T.P. (2003). Exploration, normalization, and summaries of high density oligonucleotide array probe level data. Biostatistics *4*, 249–264.

Ivanov, I., Mckenzie, B., Zhou, L., Tadokoro, C., Lepelley, A., Lafaille, J., Cua, D., and Littman, D. (2006). The Orphan Nuclear Receptor RORγt Directs the Differentiation Program of Proinflammatory IL-17+ T Helper Cells. Cell *126*, 1121–1133.

Iwata, M., Hirakiyama, A., Eshima, Y., Kagechika, H., Kato, C., and Song, S.-Y. (2004). Retinoic acid imprints gut-homing specificity on T cells. Immunity *21*, 527–538.

Jackson, J.G., Kreisberg, J.I., Koterba, A.P., Yee, D., and Brattain, M.G. (2000). Phosphorylation and nuclear exclusion of the forkhead transcription factor FKHR after epidermal growth factor treatment in human breast cancer cells. Oncogene *19*, 4574–

4581.

Jenner, R.G., Townsend, M.J., Jackson, I., Sun, K., Bouwman, R.D., Young, R.A., Glimcher, L.H., and Lord, G.M. (2009). The transcription factors T-bet and GATA-3 control alternative pathways of T-cell differentiation through a shared set of target genes. Proc Natl Acad Sci USA *106*, 17876–17881.

Jindra, P.T., Bagley, J., Godwin, J.G., and Iacomini, J. (2010). Costimulation-dependent expression of microRNA-214 increases the ability of T cells to proliferate by targeting Pten. The Journal of Immunology *185*, 990–997.

John, B., Enright, A.J., Aravin, A., Tuschl, T., Sander, C., and Marks, D.S. (2004). Human MicroRNA targets. Plos Biol *2*, e363.

Johnston, R.J., Poholek, A.C., DiToro, D., Yusuf, I., Eto, D., Barnett, B., Dent, A.L., Craft, J., and Crotty, S. (2009). Bcl6 and Blimp-1 are reciprocal and antagonistic regulators of T follicular helper cell differentiation. Science *325*, 1006–1010.

Jones, M.R., Quinton, L.J., Blahna, M.T., Neilson, J.R., Fu, S., Ivanov, A.R., Wolf, D.A., and Mizgerd, J.P. (2009). Zcchc11-dependent uridylation of microRNA directs cytokine expression. Nature *11*, 1157–1163.

Jopling, C.L., Yi, M., Lancaster, A.M., Lemon, S.M., and Sarnow, P. (2005). Modulation of hepatitis C virus RNA abundance by a liver-specific MicroRNA. Science *309*, 1577–1581.

Jovanovic, M., Reiter, L., Picotti, P., Lange, V., Bogan, E., Hurschler, B.A., Blenkiron, C., Lehrbach, N.J., Ding, X.C., Weiss, M., et al. (2010). A quantitative targeted proteomics approach to validate predicted microRNA targets in C. elegans. Nat Meth *7*, 837–842.

Kane, M.A., Folias, A.E., Wang, C., and Napoli, J.L. (2008). Quantitative profiling of endogenous retinoic acid in vivo and in vitro by tandem mass spectrometry. Anal. Chem. *80*, 1702–1708.

Kano, S.-I., Sato, K., Morishita, Y., Vollstedt, S., Kim, S., Bishop, K., Honda, K., Kubo, M., and Taniguchi, T. (2008). The contribution of transcription factor IRF1 to the interferon-γ–interleukin 12 signaling axis and TH1 versus TH-17 differentiation of CD4+ T cells. Nat Immunol *9*, 34–41.

Kaplan, M.H., Schindler, U., Smiley, S.T., and Grusby, M.J. (1996a). Stat6 is required for mediating responses to IL-4 and for development of Th2 cells. Immunity *4*, 313–319.

Kaplan, M.H., Sun, Y.L., Hoey, T., and Grusby, M.J. (1996b). Impaired IL-12 responses and enhanced development of Th2 cells in Stat4-deficient mice. Nature *382*, 174–177.

Katoh, T., Sakaguchi, Y., Miyauchi, K., Suzuki, T., Kashiwabara, S.-I., Baba, T., and Suzuki, T. (2009). Selective stabilization of mammalian microRNAs by 3' adenylation mediated by the cytoplasmic poly(A) polymerase GLD-2. Genes Dev *23*, 433–438.

Kawahara, Y., Zinshteyn, B., Chendrimada, T.P., Shiekhattar, R., and Nishikura, K. (2007a). RNA editing of the microRNA-151 precursor blocks cleavage by the Dicer-TRBP complex. EMBO Reports *8*, 763–769.

Kawahara, Y., Zinshteyn, B., Sethupathy, P., Iizasa, H., Hatzigeorgiou, A.G., and Nishikura, K. (2007b). Redirection of silencing targets by adenosine-to-inosine editing of miRNAs. Science *315*, 1137–1140.

Keller, H., Dreyer, C., Medin, J., Mahfoudi, A., Ozato, K., and Wahli, W. (1993). Fatty acids and retinoids control lipid metabolism through activation of peroxisome proliferator-activated receptor-retinoid X receptor heterodimers. Proc Natl Acad Sci USA *90*, 2160–2164.

Kennedy, M.K., Glaccum, M., Brown, S.N., Butz, E.A., Viney, J.L., Embers, M., Matsuki, N., Charrier, K., Sedger, L., Willis, C.R., et al. (2000). Reversible defects in natural killer and memory CD8 T cell lineages in interleukin 15-deficient mice. J Exp Med *191*, 771–780.

Kerdiles, Y.M., Beisner, D.R., Tinoco, R., Dejean, A.S., Castrillon, D.H., DePinho, R.A., and Hedrick, S.M. (2009). Foxo1 links homing and survival of naive T cells by regulating L-selectin, CCR7 and interleukin 7 receptor. Nat Immunol *10*, 176–184.

Kertesz, M., Iovino, N., Unnerstall, U., Gaul, U., and Segal, E. (2007). The role of site accessibility in microRNA target recognition. Nat Genet *39*, 1278–1284.

Ketting, R.F., Fischer, S.E., Bernstein, E., Sijen, T., Hannon, G.J., and Plasterk, R.H. (2001). Dicer functions in RNA interference and in synthesis of small RNA involved in developmental timing in C. elegans. Genes Dev *15*, 2654–2659.

Khattri, R., Cox, T., Yasayko, S.-A., and Ramsdell, F. (2003). An essential role for Scurfin in CD4+CD25+ T regulatory cells. Nat Immunol *4*, 337–342.

Khor, B., Gardet, A., and Xavier, R.J. (2011). Genetics and pathogenesis of inflammatory bowel disease. Nature *474*, 307–317.

Kim, C.H., Rott, L.S., Clark-Lewis, I., Campbell, D.J., Wu, L., and Butcher, E.C. (2001). Subspecialization of CXCR5+ T cells: B helper activity is focused in a germinal center-localized subset of CXCR5+ T cells. J Exp Med *193*, 1373–1381.

Kim, V.N., Han, J., and Siomi, M.C. (2009). Biogenesis of small RNAs in animals. Nat Rev Mol Cell Biol *10*, 126–139.

Kloosterman, W.P., Wienholds, E., Ketting, R.F., and Plasterk, R.H.A. (2004). Substrate requirements for let-7 function in the developing zebrafish embryo. Nucleic Acids Res. *32*, 6284–6291.

Knoechel, B., Lohr, J., Kahn, E., Bluestone, J.A., and Abbas, A.K. (2005). Sequential development of interleukin 2-dependent effector and regulatory T cells in response to endogenous systemic antigen. J Exp Med *202*, 1375–1386.

Kobie, J.J., Shah, P.R., Yang, L., Rebhahn, J.A., Fowell, D.J., and Mosmann, T.R.

(2006). T regulatory and primed uncommitted CD4 T cells express CD73, which suppresses effector CD4 T cells by converting 5'-adenosine monophosphate to adenosine. J Immunol *177*, 6780–6786.

Koch, M., Tucker-Heard, G., Perdue, N., Killebrew, J., Urdahl, K., and Campbell, D. (2009). The transcription factor T-bet controls regulatory T cell homeostasis and function during type 1 inflammation. Nat Immunol.

Kohlhaas, S., Garden, O.A., Scudamore, C., Turner, M., Okkenhaug, K., and Vigorito, E. (2009). Cutting edge: the Foxp3 target miR-155 contributes to the development of regulatory T cells. The Journal of Immunology *182*, 2578–2582.

Kondrack, R.M., Harbertson, J., Tan, J.T., McBreen, M.E., Surh, C.D., and Bradley, L.M. (2003). Interleukin 7 regulates the survival and generation of memory CD4 cells. J Exp Med *198*, 1797–1806.

Kopf, M., Le Gros, G., Bachmann, M., Lamers, M.C., Bluethmann, H., and Köhler, G. (1993). Disruption of the murine IL-4 gene blocks Th2 cytokine responses. Nature *362*, 245–248.

Korn, T., Bettelli, E., Gao, W., Awasthi, A., Jäger, A., Strom, T.B., Oukka, M., and Kuchroo, V.K. (2007). IL-21 initiates an alternative pathway to induce proinflammatory T(H)17 cells. Nature *448*, 484–487.

Kozomara, A., and Griffiths-Jones, S. (2011). miRBase: integrating microRNA annotation and deep-sequencing data. Nucleic Acids Res. *39*, D152–7.

Krek, A., Grün, D., Poy, M.N., Wolf, R., Rosenberg, L., Epstein, E.J., MacMenamin, P., da Piedade, I., Gunsalus, K.C., Stoffel, M., et al. (2005). Combinatorial microRNA target predictions. Nat Genet *37*, 495–500.

Krol, J., Busskamp, V., Markiewicz, I., Stadler, M.B., Ribi, S., Richter, J., Duebel, J., Bicker, S., Fehling, H.J., SchUbeler, D., et al. (2010a). Characterizing light-regulated retinal microRNAs reveals rapid turnover as a common property of neuronal microRNAs. Cell *141*, 618–631.

Krol, J., Loedige, I., and Filipowicz, W. (2010b). The widespread regulation of microRNA biogenesis, function and decay. Nat Rev Genet *11*, 597–610.

Kurata, H., Lee, H.J., O'Garra, A., and Arai, N. (1999). Ectopic expression of activated Stat6 induces the expression of Th2-specific cytokines and transcription factors in developing Th1 cells. Immunity *11*, 677–688.

Lagos-Quintana, M., Rauhut, R., Lendeckel, W., and Tuschl, T. (2001). Identification of novel genes coding for small expressed RNAs. Science *294*, 853–858.

Lagos-Quintana, M., Rauhut, R., Yalcin, A., Meyer, J., Lendeckel, W., and Tuschl, T. (2002). Identification of tissue-specific microRNAs from mouse. Curr Biol *12*, 735–739.

Lai, E.C. (2002). Micro RNAs are complementary to 3' UTR sequence motifs that mediate negative post-transcriptional regulation. Nat Genet *30*, 363–364.

Lall, S., Grün, D., Krek, A., Chen, K., Wang, Y.-L., Dewey, C.N., Sood, P., Colombo, T., Bray, N., MacMenamin, P., et al. (2006). A genome-wide map of conserved microRNA targets in C. elegans. Curr Biol *16*, 460–471.

Landgraf, P., Rusu, M., Sheridan, R., Sewer, A., Iovino, N., Aravin, A., Pfeffer, S., Rice, A., Kamphorst, A.O., Landthaler, M., et al. (2007). A mammalian microRNA expression atlas based on small RNA library sequencing. Cell *129*, 1401–1414.

Langrish, C.L., Chen, Y., Blumenschein, W.M., Mattson, J., Basham, B., Sedgwick, J.D., Mcclanahan, T., Kastelein, R.A., and Cua, D.J. (2005). IL-23 drives a pathogenic T cell population that induces autoimmune inflammation. J Exp Med *201*, 233–240.

Lau, N.C., Lim, L.P., Weinstein, E.G., and Bartel, D.P. (2001). An abundant class of tiny RNAs with probable regulatory roles in Caenorhabditis elegans. Science *294*, 858–862.

Laurence, A., Tato, C.M., Davidson, T.S., Kanno, Y., Chen, Z., Yao, Z., Blank, R.B., Meylan, F., Siegel, R., Hennighausen, L., et al. (2007). Interleukin-2 signaling via STAT5 constrains T helper 17 cell generation. Immunity *26*, 371–381.

Lazarevic, V., Chen, X., Shim, J.-H., Hwang, E.S., Jang, E., Bolm, A.N., Oukka, M., Kuchroo, V.K., and Glimcher, L.H. (2011). T-bet represses T(H)17 differentiation by preventing Runx1-mediated activation of the gene encoding RORγt. Nat Immunol *12*, 96–104.

Le Gros, G., Ben-Sasson, S.Z., Seder, R., Finkelman, F.D., and Paul, W.E. (1990). Generation of interleukin 4 (IL-4)-producing cells in vivo and in vitro: IL-2 and IL-4 are required for in vitro generation of IL-4-producing cells. J Exp Med *172*, 921–929.

Lee, I., Ajay, S.S., Yook, J.I., Kim, H.S., Hong, S.H., Kim, N.H., Dhanasekaran, S.M., Chinnaiyan, A.M., and Athey, B.D. (2009a). New class of microRNA targets containing simultaneous 5"-UTR and 3-"UTR interaction sites. Genome Res. *19*, 1175–1183.

Lee, R., Feinbaum, R., and Ambros, V. (2004a). A short history of a short RNA. Cell *116*, S89–92, 1 p following S96.

Lee, R.C., and Ambros, V. (2001). An extensive class of small RNAs in Caenorhabditis elegans. Science *294*, 862–864.

Lee, R.C., Feinbaum, R.L., and Ambros, V. (1993). The C. elegans heterochronic gene lin-4 encodes small RNAs with antisense complementarity to lin-14. Cell *75*, 843–854.

Lee, Y., Ahn, C., Han, J., Choi, H., Kim, J., Yim, J., Lee, J., Provost, P., Rådmark, O., Kim, S., et al. (2003). The nuclear RNase III Drosha initiates microRNA processing. Nature *425*, 415–419.

Lee, Y., Jeon, K., Lee, J.-T., Kim, S., and Kim, V.N. (2002). MicroRNA maturation: stepwise processing and subcellular localization. Embo J *21*, 4663–4670.

Lee, Y., Kim, M., Han, J., Yeom, K.-H., Lee, S., Baek, S.H., and Kim, V.N. (2004b). MicroRNA genes are transcribed by RNA polymerase II. Embo J *23*, 4051–4060.

Lee, Y.K., Turner, H., Maynard, C.L., Oliver, J.R., Chen, D., Elson, C.O., and Weaver, C.T. (2009b). Late developmental plasticity in the T helper 17 lineage. Immunity *30*, 92–107.

Lewis, B.P., Burge, C.B., and Bartel, D.P. (2005). Conserved seed pairing, often flanked by adenosines, indicates that thousands of human genes are microRNA targets. Cell *120*, 15–20.

Lewis, B.P., Shih, I.-H., Jones-Rhoades, M.W., Bartel, D.P., and Burge, C.B. (2003). Prediction of mammalian microRNA targets. Cell *115*, 787–798.

Li, Q.-J., Chau, J., Ebert, P.J.R., Sylvester, G., Min, H., Liu, G., Braich, R., Manoharan, M., Soutschek, J., Skare, P., et al. (2007). miR-181a is an intrinsic modulator of T cell sensitivity and selection. Cell *129*, 147–161.

Li, X., and Carthew, R.W. (2005). A microRNA mediates EGF receptor signaling and promotes photoreceptor differentiation in the Drosophila eye. Cell *123*, 1267–1277.

Li, Z., Wu, F., Brant, S.R., and Kwon, J.H. (2011). IL-23 receptor regulation by Let-7f in human CD4+ memory T cells. The Journal of Immunology *186*, 6182–6190.

Lighvani, A.A., Frucht, D.M., Jankovic, D., Yamane, H., Aliberti, J., Hissong, B.D., Nguyen, B.V., Gadina, M., Sher, A., Paul, W.E., et al. (2001). T-bet is rapidly induced by interferon-gamma in lymphoid and myeloid cells. Proc Natl Acad Sci USA *98*, 15137–15142.

Lim, L.P., Lau, N.C., Garrett-Engele, P., Grimson, A., Schelter, J.M., Castle, J., Bartel, D.P., Linsley, P.S., and Johnson, J.M. (2005). Microarray analysis shows that some microRNAs downregulate large numbers of target mRNAs. Nature *433*, 769–773.

Lin, L., Hron, J.D., and Peng, S.L. (2004a). Regulation of NF-kappaB, Th activation, and autoinflammation by the forkhead transcription factor Foxo3a. Immunity *21*, 203–213.

Lin, L., Spoor, M.S., Gerth, A.J., Brody, S.L., and Peng, S.L. (2004b). Modulation of Th1 activation and inflammation by the NF-kappaB repressor Foxj1. Science *303*, 1017–1020.

Liu, J., Carmell, M.A., Rivas, F.V., Marsden, C.G., Thomson, J.M., Song, J.-J., Hammond, S.M., Joshua-Tor, L., and Hannon, G.J. (2004). Argonaute2 is the catalytic engine of mammalian RNAi. Science *305*, 1437–1441.

Liu, Z., Li, Z., Mao, K., Zou, J., Wang, Y., Tao, Z., Lin, G., Tian, L., Ji, Y., Wu, X., et al. (2009). Dec2 promotes Th2 cell differentiation by enhancing IL-2R signaling. The Journal of Immunology *183*, 6320–6329.

Loetscher, P., Uguccioni, M., Bordoli, L., Baggiolini, M., Moser, B., Chizzolini, C., and Dayer, J.M. (1998). CCR5 is characteristic of Th1 lymphocytes. Nature *391*, 344–345.

Lohnes, D., Kastner, P., Dierich, A., Mark, M., LeMeur, M., and Chambon, P. (1993). Function of retinoic acid receptor gamma in the mouse. Cell *73*, 643–658.

Lohoff, M., Mittrücker, H.-W., Prechtl, S., Bischof, S., Sommer, F., Kock, S., Ferrick, D.A., Duncan, G.S., Gessner, A., and Mak, T.W. (2002). Dysregulated T helper cell differentiation in the absence of interferon regulatory factor 4. Proc Natl Acad Sci USA *99*, 11808–11812.

Long, D., Lee, R., Williams, P., Chan, C.Y., Ambros, V., and Ding, Y. (2007). Potent effect of target structure on microRNA function. Nat Struct Mol Biol *14*, 287–294.

Lu, L.-F., Boldin, M.P., Chaudhry, A., Lin, L.-L., Taganov, K.D., Hanada, T., Yoshimura, A., Baltimore, D., and Rudensky, A.Y. (2010). Function of miR-146a in controlling Treg cell-mediated regulation of Th1 responses. Cell *142*, 914–929.

Lu, L.-F., Thai, T.-H., Calado, D.P., Chaudhry, A., Kubo, M., Tanaka, K., Loeb, G.B., Lee, H., Yoshimura, A., Rajewsky, K., et al. (2009). Foxp3-dependent microRNA155 confers competitive fitness to regulatory T cells by targeting SOCS1 protein. Immunity *30*, 80–91.

Ludányi, K., Nagy, Z.S., Alexa, M., Reichert, U., Michel, S., Fésüs, L., and Szondy, Z. (2005). Ligation of RARgamma inhibits proliferation of phytohaemagglutinin-stimulated T-cells via down-regulating JAK3 protein levels. Immunol Lett *98*, 103–113.

Lund, E., Güttinger, S., Calado, A., Dahlberg, J.E., and Kutay, U. (2004). Nuclear export of microRNA precursors. Science *303*, 95–98.

Lytle, J.R., Yario, T.A., and Steitz, J.A. (2007). Target mRNAs are repressed as efficiently by microRNA-binding sites in the 5“ UTR as in the 3” UTR. Proc Natl Acad Sci USA *104*, 9667–9672.

Ma, F., Xu, S., Liu, X., Zhang, Q., Xu, X., Liu, M., Hua, M., Li, N., Yao, H., and Cao, X. (2011a). The microRNA miR-29 controls innate and adaptive immune responses to intracellular bacterial infection by targeting interferon-γ. Nat Immunol *12*, 861–869.

Ma, J., Wang, R., Fang, X., Ding, Y., and Sun, Z. (2011b). Critical Role of TCF-1 in Repression of the IL-17 Gene. PLoS ONE *6*, e24768 EP –.

Maggi, E., Biswas, P., Del Prete, G., Parronchi, P., Macchia, D., Simonelli, C., Emmi, L., De Carli, M., Tiri, A., and Ricci, M. (1991). Accumulation of Th-2-like helper T cells in the conjunctiva of patients with vernal conjunctivitis. J Immunol *146*, 1169–1174.

Malhotra, N., Robertson, E., and Kang, J. (2010). SMAD2 is essential for TGF beta-mediated Th17 cell generation. Journal of Biological Chemistry *285*, 29044–29048.

Mangan, P.R., Harrington, L.E., O'Quinn, D.B., Helms, W.S., Bullard, D.C., Elson, C.O., Hatton, R.D., Wahl, S.M., Schoeb, T.R., and Weaver, C.T. (2006). Transforming growth factor-beta induces development of the T(H)17 lineage. Nature *441*, 231–234.

Mantel, P.-Y., Kuipers, H., Boyman, O., Rhyner, C., Ouaked, N., Rückert, B., Karagiannidis, C., Lambrecht, B.N., Hendriks, R.W., Crameri, R., et al. (2007). GATA3-driven Th2 responses inhibit TGF-beta1-induced FOXP3 expression and the formation of regulatory T cells. Plos Biol *5*, e329.

Marson, A., Kretschmer, K., Frampton, G.M., Jacobsen, E.S., Polansky, J.K., MacIsaac, K.D., Levine, S.S., Fraenkel, E., Boehmer, von, H., and Young, R.A. (2007). Foxp3 occupancy and regulation of key target genes during T-cell stimulation. Nature *445*, 931–935.

Martinez, G.J., Zhang, Z., Reynolds, J.M., Tanaka, S., Chung, Y., Liu, T., Robertson, E., Lin, X., Feng, X.-H., and Dong, C. (2010). Smad2 positively regulates the generation of Th17 cells. Journal of Biological Chemistry *285*, 29039–29043.

Martin-Fontecha, A., Thomsen, L.L., Brett, S., Gerard, C., Lipp, M., Lanzavecchia, A., and Sallusto, F. (2004). Induced recruitment of NK cells to lymph nodes provides IFN-gamma for T(H)1 priming. Nat Immunol *5*, 1260–1265.

Mathur, A.N., Chang, H.-C., Zisoulis, D.G., Stritesky, G.L., Yu, Q., O'Malley, J.T., Kapur, R., Levy, D.E., Kansas, G.S., and Kaplan, M.H. (2007). Stat3 and Stat4 direct development of IL-17-secreting Th cells. J Immunol *178*, 4901–4907.

Mattes, J., Collison, A., Plank, M., Phipps, S., and Foster, P. (2009). Antagonism of microRNA-126 suppresses the effector function of TH2 cells and the development of allergic airways disease. Proc Natl Acad Sci USA.

McHugh, R.S., Whitters, M.J., Piccirillo, C.A., Young, D.A., Shevach, E.M., Collins, M., and Byrne, M.C. (2002). CD4(+)CD25(+) immunoregulatory T cells: gene expression analysis reveals a functional role for the glucocorticoid-induced TNF receptor. Immunity *16*, 311–323.

Miranda, K.C., Huynh, T., Tay, Y., Ang, Y.-S., Tam, W.-L., Thomson, A.M., Lim, B., and Rigoutsos, I. (2006). A pattern-based method for the identification of MicroRNA binding sites and their corresponding heteroduplexes. Cell *126*, 1203–1217.

Monticelli, S., Ansel, K.M., Xiao, C., Socci, N.D., Krichevsky, A.M., Thai, T.-H., Rajewsky, N., Marks, D.S., Sander, C., Rajewsky, K., et al. (2005). Monticell MicroRNA profiling of the murine hematopoietic system Genome Biol 2005. Genome Biol *6*, R71.

Mosmann, T.R., Cherwinski, H., Bond, M.W., Giedlin, M.A., and Coffman, R.L. (1986). Two types of murine helper T cell clone. I. Definition according to profiles of lymphokine activities and secreted proteins. J Immunol *136*, 2348–2357.

Mucida, D., Kutchukhidze, N., Erazo, A., Russo, M., Lafaille, J.J., and Curotto de Lafaille, M.A. (2005). Oral tolerance in the absence of naturally occurring Tregs. Journal of Clinical Investigation *115*, 1923–1933.

Mucida, D., Park, Y., Kim, G., Turovskaya, O., Scott, I., Kronenberg, M., and Cheroutre, H. (2007). Reciprocal TH17 and regulatory T cell differentiation mediated by retinoic acid. Science *317*, 256–260.

Muljo, S.A., Ansel, K.M., Kanellopoulou, C., Livingston, D.M., Rao, A., and Rajewsky, K. (2005). Aberrant T cell differentiation in the absence of Dicer. J Exp Med *202*, 261–269.

Mullen, A.C., High, F.A., Hutchins, A.S., Lee, H.W., Villarino, A.V., Livingston, D.M., Kung, A.L., Cereb, N., Yao, T.P., Yang, S.Y., et al. (2001). Role of T-bet in commitment of TH1 cells before IL-12-dependent selection. Science *292*, 1907–1910.

Mullen, A.C., Hutchins, A.S., High, F.A., Lee, H.W., Sykes, K.J., Chodosh, L.A., and Reiner, S.L. (2002). Hlx is induced by and genetically interacts with T-bet to promote heritable TH1 gene induction. Nat Immunol *3*, 652–658.

Murphy, C.A., Langrish, C.L., Chen, Y., Blumenschein, W., Mcclanahan, T., Kastelein, R.A., Sedgwick, J.D., and Cua, D.J. (2003). Divergent pro- and antiinflammatory roles for IL-23 and IL-12 in joint autoimmune inflammation. J Exp Med *198*, 1951–1957.

Murugaiyan, G., Beynon, V., Mittal, A., Joller, N., and Weiner, H.L. (2011). Silencing MicroRNA-155 Ameliorates Experimental Autoimmune Encephalomyelitis. The Journal of Immunology *187*, 2213–2221.

Nagata, K., Tanaka, K., Ogawa, K., Kemmotsu, K., Imai, T., Yoshie, O., Abe, H., Tada, K., Nakamura, M., Sugamura, K., et al. (1999). Selective expression of a novel surface molecule by human Th2 cells in vivo. J Immunol *162*, 1278–1286.

Neufert, C., Becker, C., Wirtz, S., Fantini, M.C., Weigmann, B., Galle, P.R., and Neurath, M.F. (2007). IL-27 controls the development of inducible regulatory T cells and Th17 cellsvia differential effects on STAT1. Eur J Immunol *37*, 1809–1816.

Nielsen, C.B., Shomron, N., Sandberg, R., Hornstein, E., Kitzman, J., and Burge, C.B. (2007). Determinants of targeting by endogenous and exogenous microRNAs and siRNAs. Rna *13*, 1894–1910.

Nograles, K.E., Zaba, L.C., Shemer, A., Fuentes-Duculan, J., Cardinale, I., Kikuchi, T., Ramon, M., Bergman, R., Krueger, J.G., and Guttman-Yassky, E. (2009). IL-22-producing "T22" T cells account for upregulated IL-22 in atopic dermatitis despite reduced IL-17-producing TH17 T cells. J. Allergy Clin. Immunol. *123*, 1244–52.e2.

Nonne, N., Ameyar-Zazoua, M., Souidi, M., and Harel-Bellan, A. (2010). Tandem affinity purification of miRNA target mRNAs (TAP-Tar). Nucleic Acids Res. *38*, e20.

Nurieva, R., Yang, X.O., Martinez, G., Zhang, Y., Panopoulos, A.D., Ma, L., Schluns, K., Tian, Q., Watowich, S.S., Jetten, A.M., et al. (2007). Essential autocrine regulation by IL-21 in the generation of inflammatory T cells. Nature *448*, 480–483.

Nurieva, R.I., Chung, Y., Hwang, D., Yang, X.O., Kang, H.S., Ma, L., Wang, Y.-H., Watowich, S.S., Jetten, A.M., Tian, Q., et al. (2008). Generation of T follicular helper cells is mediated by interleukin-21 but independent of T helper 1, 2, or 17 cell lineages. Immunity *29*, 138–149.

Nurieva, R.I., Chung, Y., Martinez, G.J., Yang, X.O., Tanaka, S., Matskevitch, T.D., Wang, Y.-H., and Dong, C. (2009). Bcl6 mediates the development of T follicular helper cells. Science *325*, 1001–1005.

O'Connell, R.M., Kahn, D., Gibson, W.S.J., Round, J.L., Scholz, R.L., Chaudhuri, A.A., Kahn, M.E., Rao, D.S., and Baltimore, D. (2010). MicroRNA-155 promotes

autoimmune inflammation by enhancing inflammatory T cell development. Immunity *33*, 607–619.

Ohoka, Y., Yokota, A., Takeuchi, H., Maeda, N., and Iwata, M. (2011). Retinoic acid-induced CCR9 expression requires transient TCR stimulation and cooperativity between NFATc2 and the retinoic acid receptor/retinoid X receptor complex. The Journal of Immunology *186*, 733–744.

Okamoto, K., Iwai, Y., Oh-hora, M., Yamamoto, M., Morio, T., Aoki, K., Ohya, K., Jetten, A.M., Akira, S., Muta, T., et al. (2010). IkappaBzeta regulates T(H)17 development by cooperating with ROR nuclear receptors. Nature *464*, 1381–1385.

Okamura, K., Hagen, J.W., Duan, H., Tyler, D.M., and Lai, E.C. (2007). The mirtron pathway generates microRNA-class regulatory RNAs in Drosophila. Cell *130*, 89–100.

Oppmann, B., Lesley, R., Blom, B., Timans, J.C., Xu, Y., Hunte, B., Vega, F., Yu, N., Wang, J., Singh, K., et al. (2000). Novel p19 protein engages IL-12p40 to form a cytokine, IL-23, with biological activities similar as well as distinct from IL-12. Immunity *13*, 715–725.

Ouyang, W., Beckett, O., Ma, Q., Paik, J.-H., DePinho, R.A., and Li, M.O. (2010). Foxo proteins cooperatively control the differentiation of Foxp3+ regulatory T cells. Nat Immunol *11*, 618–627.

Ouyang, W., Löhning, M., Gao, Z., Assenmacher, M., Ranganath, S., Radbruch, A., and Murphy, K.M. (2000). Stat6-independent GATA-3 autoactivation directs IL-4-independent Th2 development and commitment. Immunity *12*, 27–37.

Pan, F., Yu, H., Dang, E.V., Barbi, J., Pan, X., Grosso, J.F., Jinasena, D., Sharma, S.M., McCadden, E.M., Getnet, D., et al. (2009). Eos mediates Foxp3-dependent gene silencing in CD4+ regulatory T cells. Science *325*, 1142–1146.

Pandiyan, P., Zheng, L., Ishihara, S., Reed, J., and Lenardo, M.J. (2007). CD4+CD25+Foxp3+ regulatory T cells induce cytokine deprivation-mediated apoptosis of effector CD4+ T cells. Nat Immunol *8*, 1353–1362.

Park, H., Li, Z., Yang, X.O., Chang, S.H., Nurieva, R., Wang, Y.-H., Wang, Y., Hood, L., Zhu, Z., Tian, Q., et al. (2005). A distinct lineage of CD4 T cells regulates tissue inflammation by producing interleukin 17. Nat Immunol *6*, 1133–1141.

Park, J.-H., Adoro, S., Lucas, P.J., Sarafova, S.D., Alag, A.S., Doan, L.L., Erman, B., Liu, X., Ellmeier, W., Bosselut, R., et al. (2007). "Coreceptor tuning": cytokine signals transcriptionally tailor CD8 coreceptor expression to the self-specificity of the TCR. Nat Immunol *8*, 1049–1059.

Park, J.-H., Yu, Q., Erman, B., Appelbaum, J.S., Montoya-Durango, D., Grimes, H.L., and Singer, A. (2004). Suppression of IL7Ralpha transcription by IL-7 and other prosurvival cytokines: a novel mechanism for maximizing IL-7-dependent T cell survival. Immunity *21*, 289–302.

Paroo, Z., Ye, X., Chen, S., and Liu, Q. (2009). Phosphorylation of the human

microRNA-generating complex mediates MAPK/Erk signaling. Cell *139*, 112–122.

Parronchi, P., Macchia, D., Piccinni, M.P., Biswas, P., Simonelli, C., Maggi, E., Ricci, M., Ansari, A.A., and Romagnani, S. (1991). Allergen- and bacterial antigen-specific T-cell clones established from atopic donors show a different profile of cytokine production. Proc Natl Acad Sci USA *88*, 4538–4542.

Pasare, C., and Medzhitov, R. (2003). Toll pathway-dependent blockade of CD4+CD25+ T cell-mediated suppression by dendritic cells. Science *299*, 1033–1036.

Pasquinelli, A.E., Reinhart, B.J., Slack, F., Martindale, M.Q., Kuroda, M.I., Maller, B., Hayward, D.C., Ball, E.E., Degnan, B., Müller, P., et al. (2000). Conservation of the sequence and temporal expression of let-7 heterochronic regulatory RNA. Nature *408*, 86–89.

Passerini, L., Allan, S.E., Battaglia, M., Di Nunzio, S., Alstad, A.N., Levings, M.K., Roncarolo, M.G., and Bacchetta, R. (2008). STAT5-signaling cytokines regulate the expression of FOXP3 in CD4+CD25+ regulatory T cells and CD4+CD25- effector T cells. International Immunology *20*, 421–431.

Perez-Villar, J.J., Whitney, G.S., Bowen, M.A., Hewgill, D.H., Aruffo, A.A., and Kanner, S.B. (1999). CD5 negatively regulates the T-cell antigen receptor signal transduction pathway: involvement of SH2-containing phosphotyrosine phosphatase SHP-1. Mol. Cell. Biol. *19*, 2903–2912.

Polic, B., Kunkel, D., Scheffold, A., and Rajewsky, K. (2001). How alpha beta T cells deal with induced TCR alpha ablation. Proc Natl Acad Sci USA *98*, 8744–8749.

Powrie, F., Leach, M.W., Mauze, S., Menon, S., Caddle, L.B., and Coffman, R.L. (1994). Inhibition of Th1 responses prevents inflammatory bowel disease in scid mice reconstituted with CD45RBhi CD4+ T cells. Immunity *1*, 553–562.

Presky, D.H., Yang, H., Minetti, L.J., Chua, A.O., Nabavi, N., Wu, C.Y., Gately, M.K., and Gubler, U. (1996). A functional interleukin 12 receptor complex is composed of two beta-type cytokine receptor subunits. Proc Natl Acad Sci USA *93*, 14002–14007.

Quirion, M.R., Gregory, G.D., Umetsu, S.E., Winandy, S., and Brown, M.A. (2009). Cutting edge: Ikaros is a regulator of Th2 cell differentiation. The Journal of Immunology *182*, 741–745.

Rapoport, M.J., Jaramillo, A., Zipris, D., Lazarus, A.H., Serreze, D.V., Leiter, E.H., Cyopick, P., Danska, J.S., and Delovitch, T.L. (1993). Interleukin 4 reverses T cell proliferative unresponsiveness and prevents the onset of diabetes in nonobese diabetic mice. J Exp Med *178*, 87–99.

Rathmell, J.C., Farkash, E.A., Gao, W., and Thompson, C.B. (2001). IL-7 enhances the survival and maintains the size of naive T cells. J Immunol *167*, 6869–6876.

Read, S., Malmström, V., and Powrie, F. (2000). Cytotoxic T lymphocyte-associated antigen 4 plays an essential role in the function of CD25(+)CD4(+) regulatory cells that control intestinal inflammation. J Exp Med *192*, 295–302.

Rehmsmeier, M., Steffen, P., Hochsmann, M., and Giegerich, R. (2004). Fast and effective prediction of microRNA/target duplexes. Rna *10*, 1507–1517.

Reinhart, B.J., Slack, F.J., Basson, M., Pasquinelli, A.E., Bettinger, J.C., Rougvie, A.E., Horvitz, H.R., and Ruvkun, G. (2000). The 21-nucleotide let-7 RNA regulates developmental timing in Caenorhabditis elegans. Nature *403*, 901–906.

Ritchie, W., Rajasekhar, M., Flamant, S., and Rasko, J.E.J. (2009). Conserved expression patterns predict microRNA targets. PLoS Comp Biol *5*, e1000513.

Robins, H., Li, Y., and Padgett, R.W. (2005). Incorporating structure to predict microRNA targets. Proc Natl Acad Sci USA *102*, 4006–4009.

Robinson, D.S., Hamid, Q., Ying, S., Tsicopoulos, A., Barkans, J., Bentley, A.M., Corrigan, C., Durham, S.R., and Kay, A.B. (1992). Predominant TH2-like bronchoalveolar T-lymphocyte population in atopic asthma. N Engl J Med *326*, 298–304.

Rochman, Y., Spolski, R., and Leonard, W.J. (2009). New insights into the regulation of T cells by gamma(c) family cytokines. Nat Rev Immunol *9*, 480–490.

Rodriguez, A., Vigorito, E., Clare, S., Warren, M.V., Couttet, P., Soond, D.R., van Dongen, S., Grocock, R.J., Das, P.P., Miska, E.A., et al. (2007). Requirement of bic/microRNA-155 for normal immune function. Science *316*, 608–611.

Rogge, L., Barberis-Maino, L., Biffi, M., Passini, N., Presky, D.H., Gubler, U., and Sinigaglia, F. (1997). Selective expression of an interleukin-12 receptor component by human T helper 1 cells. J Exp Med *185*, 825–831.

Rossi, R.L., Rossetti, G., Wenandy, L., Curti, S., Ripamonti, A., Bonnal, R.J.P., Birolo, R.S., Moro, M., Crosti, M.C., Gruarin, P., et al. (2011). Distinct microRNA signatures in human lymphocyte subsets and enforcement of the naive state in CD4+ T cells by the microRNA miR-125b. Nat Immunol *12*, 796–803.

Rotteveel, F.T., Kuenen, B., Kokkelink, I., Meager, A., and Lucas, C.J. (1990). Relative increase of inflammatory CD4+ T cells in the cerebrospinal fluid of multiple sclerosis patients and control individuals. Clin Exp Immunol *79*, 15–20.

Ruby, J.G., Jan, C.H., and Bartel, D.P. (2007). Intronic microRNA precursors that bypass Drosha processing. Nature *448*, 83–86.

Sadlack, B., Merz, H., Schorle, H., Schimpl, A., Feller, A.C., and Horak, I. (1993). Ulcerative colitis-like disease in mice with a disrupted interleukin-2 gene. Cell *75*, 253–261.

Saetrom, P., Heale, B.S.E., Snøve, O., Aagaard, L., Alluin, J., and Rossi, J.J. (2007). Distance constraints between microRNA target sites dictate efficacy and cooperativity. Nucleic Acids Res. *35*, 2333–2342.

Sakaguchi, S., Sakaguchi, N., Asano, M., Itoh, M., and Toda, M. (1995). Immunologic self-tolerance maintained by activated T cells expressing IL-2 receptor alpha-chains

(CD25). Breakdown of a single mechanism of self-tolerance causes various autoimmune diseases. J Immunol *155*, 1151–1164.

Sakaguchi, S., Wing, K., and Miyara, M. (2007). Regulatory T cells - a brief history and perspective. Eur J Immunol *37 Suppl 1*, S116–23.

Salgame, P., Abrams, J.S., Clayberger, C., Goldstein, H., Convit, J., Modlin, R.L., and Bloom, B.R. (1991). Differing lymphokine profiles of functional subsets of human CD4 and CD8 T cell clones. Science *254*, 279–282.

Sallusto, F., Lenig, D., Mackay, C.R., and Lanzavecchia, A. (1998). Flexible programs of chemokine receptor expression on human polarized T helper 1 and 2 lymphocytes. J Exp Med *187*, 875–883.

Sandberg, R., Neilson, J.R., Sarma, A., Sharp, P.A., and Burge, C.B. (2008). Proliferating cells express mRNAs with shortened 3' untranslated regions and fewer microRNA target sites. Science *320*, 1643–1647.

Savill, J., Fadok, V., Henson, P., and Haslett, C. (1993). Phagocyte recognition of cells undergoing apoptosis. Immunol. Today *14*, 131–136.

Schaerli, P., Willimann, K., Lang, A.B., Lipp, M., Loetscher, P., and Moser, B. (2000). CXC chemokine receptor 5 expression defines follicular homing T cells with B cell helper function. J Exp Med *192*, 1553–1562.

Schambach, F., Schupp, M., Lazar, M.A., and Reiner, S.L. (2007). Activation of retinoic acid receptor-alpha favours regulatory T cell induction at the expense of IL-17-secreting T helper cell differentiation. Eur J Immunol *37*, 2396–2399.

Schluns, K.S., Kieper, W.C., Jameson, S.C., and Lefrançois, L. (2000). Interleukin-7 mediates the homeostasis of naïve and memory CD8 T cells in vivo. Nat Immunol *1*, 426–432.

Schmidt-Weber, C.B., Akdis, M., and Akdis, C.A. (2007). TH17 cells in the big picture of immunology. J. Allergy Clin. Immunol. *120*, 247–254.

Schmitt, E., Germann, T., Goedert, S., Hoehn, P., Huels, C., Koelsch, S., Kühn, R., Müller, W., Palm, N., and Rüde, E. (1994). IL-9 production of naive CD4+ T cells depends on IL-2, is synergistically enhanced by a combination of TGF-beta and IL-4, and is inhibited by IFN-gamma. J Immunol *153*, 3989–3996.

Schraml, B.U., Hildner, K., Ise, W., Lee, W.-L., Smith, W.A.-E., Solomon, B., Sahota, G., Sim, J., Mukasa, R., Cemerski, S., et al. (2009). The AP-1 transcription factor Batf controls T(H)17 differentiation. Nature *460*, 405–409.

Schulz, E.G., Mariani, L., Radbruch, A., and Höfer, T. (2009). Sequential polarization and imprinting of type 1 T helper lymphocytes by interferon-gamma and interleukin-12. Immunity *30*, 673–683.

Schwamborn, J.C., Berezikov, E., and Knoblich, J.A. (2009). The TRIM-NHL protein TRIM32 activates microRNAs and prevents self-renewal in mouse neural progenitors.

Cell *136*, 913–925.

Scott, P., Natovitz, P., Coffman, R.L., Pearce, E., and Sher, A. (1988). Immunoregulation of cutaneous leishmaniasis. T cell lines that transfer protective immunity or exacerbation belong to different T helper subsets and respond to distinct parasite antigens. J Exp Med *168*, 1675–1684.

Seddon, B., and Zamoyska, R. (2002). TCR signals mediated by Src family kinases are essential for the survival of naive T cells. J Immunol *169*, 2997–3005.

Segal, B.M., Dwyer, B.K., and Shevach, E.M. (1998). An interleukin (IL)-10/IL-12 immunoregulatory circuit controls susceptibility to autoimmune disease. J Exp Med *187*, 537–546.

Seitz, H., Tushir, J.S., and Zamore, P.D. (2011). A 5'-uridine amplifies miRNA/miRNA* asymmetry in Drosophila by promoting RNA-induced silencing complex formation. Silence *2*, 4.

Selbach, M., Schwanhäusser, B., Thierfelder, N., Fang, Z., Khanin, R., and Rajewsky, N. (2008). Widespread changes in protein synthesis induced by microRNAs. Nature.

Selmaj, K., Raine, C.S., Cannella, B., and Brosnan, C.F. (1991). Identification of lymphotoxin and tumor necrosis factor in multiple sclerosis lesions. Journal of Clinical Investigation *87*, 949–954.

Shimizu, J., Yamazaki, S., Takahashi, T., Ishida, Y., and Sakaguchi, S. (2002). Stimulation of CD25(+)CD4(+) regulatory T cells through GITR breaks immunological self-tolerance. Nat Immunol *3*, 135–142.

Shimoda, K., van Deursen, J., Sangster, M.Y., Sarawar, S.R., Carson, R.T., Tripp, R.A., Chu, C., Quelle, F.W., Nosaka, T., Vignali, D.A., et al. (1996). Lack of IL-4-induced Th2 response and IgE class switching in mice with disrupted Stat6 gene. Nature *380*, 630–633.

Sokol, C.L., Barton, G.M., Farr, A.G., and Medzhitov, R. (2008). A mechanism for the initiation of allergen-induced T helper type 2 responses. Nat Immunol *9*, 310–318.

Sommer, A., Tarwotjo, I., Djunaedi, E., West, K.P., Loeden, A.A., Tilden, R., and Mele, L. (1986). Impact of vitamin A supplementation on childhood mortality. A randomised controlled community trial. Lancet *1*, 1169–1173.

Stark, A., Brennecke, J., Russell, R.B., and Cohen, S.M. (2003). Identification of Drosophila MicroRNA targets. Plos Biol *1*, E60.

Steiner, D.F., Thomas, M.F., Hu, J.K., Yang, Z., Babiarz, J.E., Allen, C.D.C., Matloubian, M., Blelloch, R., and Ansel, K.M. (2011). MicroRNA-29 Regulates T-Box Transcription Factors and Interferon-γ Production in Helper T Cells. Immunity *35*, 169–181.

Stephen, T.L., Tikhonova, A., Riberdy, J.M., and Laufer, T.M. (2009). The activation threshold of CD4+ T cells is defined by TCR/peptide-MHC class II interactions in the

thymic medulla. The Journal of Immunology *183*, 5554–5562.

Stephensen, C.B., Rasooly, R., Jiang, X., Ceddia, M.A., Weaver, C.T., Chandraratna, R.A.S., and Bucy, R.P. (2002). Vitamin A enhances in vitro Th2 development via retinoid X receptor pathway. J Immunol *168*, 4495–4503.

Stittrich, A.-B., Haftmann, C., Sgouroudis, E., Kühl, A.A., Hegazy, A.N., Panse, I., Riedel, R., Flossdorf, M., Dong, J., Fuhrmann, F., et al. (2010). The microRNA miR-182 is induced by IL-2 and promotes clonal expansion of activated helper T lymphocytes. Nat Immunol *11*, 1057–1062.

Stumhofer, J.S., Silver, J.S., Laurence, A., Porrett, P.M., Harris, T.H., Turka, L.A., Ernst, M., Saris, C.J.M., O'Shea, J.J., and Hunter, C.A. (2007). Interleukins 27 and 6 induce STAT3-mediated T cell production of interleukin 10. Nat Immunol *8*, 1363–1371.

Su, D., and Gudas, L.J. (2008). Gene expression profiling elucidates a specific role for RARgamma in the retinoic acid-induced differentiation of F9 teratocarcinoma stem cells. Biochem. Pharmacol. *75*, 1129–1160.

Surh, C.D., and Sprent, J. (2008). Homeostasis of naive and memory T cells. Immunity *29*, 848–862.

Suto, A., Kashiwakuma, D., Kagami, S.-I., Hirose, K., Watanabe, N., Yokote, K., Saito, Y., Nakayama, T., Grusby, M.J., Iwamoto, I., et al. (2008). Development and characterization of IL-21-producing CD4+ T cells. Journal of Experimental Medicine *205*, 1369–1379.

Sutton, C., Brereton, C., Keogh, B., Mills, K.H.G., and Lavelle, E.C. (2006). A crucial role for interleukin (IL)-1 in the induction of IL-17-producing T cells that mediate autoimmune encephalomyelitis. J Exp Med *203*, 1685–1691.

Swain, S.L., Weinberg, A.D., English, M., and Huston, G. (1990). IL-4 directs the development of Th2-like helper effectors. J Immunol *145*, 3796–3806.

Szabo, S.J., Dighe, A.S., Gubler, U., and Murphy, K.M. (1997). Regulation of the interleukin (IL)-12R beta 2 subunit expression in developing T helper 1 (Th1) and Th2 cells. J Exp Med *185*, 817–824.

Szabo, S.J., Kim, S.T., Costa, G.L., Zhang, X., Fathman, C.G., and Glimcher, L.H. (2000). A novel transcription factor, T-bet, directs Th1 lineage commitment. Cell *100*, 655–669.

Szabolcs, P., Park, K.-D., Reese, M., Marti, L., Broadwater, G., and Kurtzberg, J. (2003). Coexistent naïve phenotype and higher cycling rate of cord blood T cells as compared to adult peripheral blood. Exp. Hematol. *31*, 708–714.

Szondy, Z., Reichert, U., Bernardon, J.M., Michel, S., Tóth, R., Ancian, P., Ajzner, E., and Fesus, L. (1997). Induction of apoptosis by retinoids and retinoic acid receptor gamma-selective compounds in mouse thymocytes through a novel apoptosis pathway. Mol Pharmacol *51*, 972–982.

Taganov, K.D., Boldin, M.P., Chang, K.-J., and Baltimore, D. (2006). NF-kappaB-dependent induction of microRNA miR-146, an inhibitor targeted to signaling proteins of innate immune responses. Proc Natl Acad Sci USA *103*, 12481–12486.

Tagawa, H., and Seto, M. (2005). A microRNA cluster as a target of genomic amplification in malignant lymphoma. Leukemia *19*, 2013–2016.

Takada, K., and Jameson, S.C. (2009). Naive T cell homeostasis: from awareness of space to a sense of place. Nat Rev Immunol *9*, 823–832.

Takahashi, T., Tagami, T., Yamazaki, S., Uede, T., Shimizu, J., Sakaguchi, N., Mak, T.W., and Sakaguchi, S. (2000). Immunologic self-tolerance maintained by CD25(+)CD4(+) regulatory T cells constitutively expressing cytotoxic T lymphocyte-associated antigen 4. J Exp Med *192*, 303–310.

Takaki, H., Ichiyama, K., Koga, K., Chinen, T., Takaesu, G., Sugiyama, Y., Kato, S., Yoshimura, A., and Kobayashi, T. (2008). STAT6 Inhibits TGF-beta1-mediated Foxp3 induction through direct binding to the Foxp3 promoter, which is reverted by retinoic acid receptor. J Biol Chem *283*, 14955–14962.

Takeda, K., Tanaka, T., Shi, W., Matsumoto, M., Minami, M., Kashiwamura, S., Nakanishi, K., Yoshida, N., Kishimoto, T., and Akira, S. (1996a). Essential role of Stat6 in IL-4 signalling. Nature *380*, 627–630.

Takeda, S., Rodewald, H.R., Arakawa, H., Bluethmann, H., and Shimizu, T. (1996b). MHC class II molecules are not required for survival of newly generated CD4+ T cells, but affect their long-term life span. Immunity *5*, 217–228.

Takimoto, T., Wakabayashi, Y., Sekiya, T., Inoue, N., Morita, R., Ichiyama, K., Takahashi, R., Asakawa, M., Muto, G., Mori, T., et al. (2010). Smad2 and Smad3 are redundantly essential for the TGF-beta-mediated regulation of regulatory T plasticity and Th1 development. The Journal of Immunology *185*, 842–855.

Tan, J.T., Dudl, E., LeRoy, E., Murray, R., Sprent, J., Weinberg, K.I., and Surh, C.D. (2001). IL-7 is critical for homeostatic proliferation and survival of naive T cells. Proc Natl Acad Sci USA *98*, 8732–8737.

Tanaka, S., Tsukada, J., Suzuki, W., Hayashi, K., Tanigaki, K., Tsuji, M., Inoue, H., Honjo, T., and Kubo, M. (2006). The interleukin-4 enhancer CNS-2 is regulated by Notch signals and controls initial expression in NKT cells and memory-type CD4 T cells. Immunity *24*, 689–701.

Taneja, R., Roy, B., Plassat, J.L., Zusi, C.F., Ostrowski, J., Reczek, P.R., and Chambon, P. (1996). Cell-type and promoter-context dependent retinoic acid receptor (RAR) redundancies for RAR beta 2 and Hoxa-1 activation in F9 and P19 cells can be artefactually generated by gene knockouts. Proc Natl Acad Sci USA *93*, 6197–6202.

Tao, X., Grant, C., Constant, S., and Bottomly, K. (1997). Induction of IL-4-producing CD4+ T cells by antigenic peptides altered for TCR binding. J Immunol *158*, 4237–4244.

Thierfelder, W.E., van Deursen, J.M., Yamamoto, K., Tripp, R.A., Sarawar, S.R., Carson, R.T., Sangster, M.Y., Vignali, D.A., Doherty, P.C., Grosveld, G.C., et al. (1996). Requirement for Stat4 in interleukin-12-mediated responses of natural killer and T cells. Nature *382*, 171–174.

Tone, Y., Furuuchi, K., Kojima, Y., Tykocinski, M.L., Greene, M.I., and Tone, M. (2008). Smad3 and NFAT cooperate to induce Foxp3 expression through its enhancer. Nat Immunol *9*, 194–202.

Tóth, R., Szegezdi, E., Reichert, U., Bernardon, J.M., Michel, S., Ancian, P., Kis-Tóth, K., Macsári, Z., Fésüs, L., and Szondy, Z. (2001). Activation-induced apoptosis and cell surface expression of Fas (CD95) ligand are reciprocally regulated by retinoic acid receptor alpha and gamma and involve nur77 in T cells. Eur J Immunol *31*, 1382–1391.

Trifari, S., Kaplan, C.D., Tran, E.H., Crellin, N.K., and Spits, H. (2009). Identification of a human helper T cell population that has abundant production of interleukin 22 and is distinct from T(H)-17, T(H)1 and T(H)2 cells. Nat Immunol *10*, 864–871.

Uematsu, S., Fujimoto, K., Jang, M.H., Yang, B.-G., Jung, Y.-J., Nishiyama, M., Sato, S., Tsujimura, T., Yamamoto, M., Yokota, Y., et al. (2008). Regulation of humoral and cellular gut immunity by lamina propria dendritic cells expressing Toll-like receptor 5. Nat Immunol *9*, 769–776.

Urban, J.F., Katona, I.M., Paul, W.E., and Finkelman, F.D. (1991). Interleukin 4 is important in protective immunity to a gastrointestinal nematode infection in mice. Proc Natl Acad Sci USA *88*, 5513–5517.

van Rooij, E., Sutherland, L.B., Qi, X., Richardson, J.A., Hill, J., and Olson, E.N. (2007). Control of stress-dependent cardiac growth and gene expression by a microRNA. Science *316*, 575–579.

Veldhoen, M., Hirota, K., Westendorf, A.M., Buer, J., Dumoutier, L., Renauld, J.-C., and Stockinger, B. (2008a). The aryl hydrocarbon receptor links TH17-cell-mediated autoimmunity to environmental toxins. Nature *453*, 106–109.

Veldhoen, M., Hocking, R.J., Atkins, C.J., Locksley, R.M., and Stockinger, B. (2006). TGFbeta in the context of an inflammatory cytokine milieu supports de novo differentiation of IL-17-producing T cells. Immunity *24*, 179–189.

Veldhoen, M., Uyttenhove, C., van Snick, J., Helmby, H., Westendorf, A., Buer, J., Martin, B., Wilhelm, C., and Stockinger, B. (2008b). Transforming growth factor-beta "reprograms" the differentiation of T helper 2 cells and promotes an interleukin 9-producing subset. Nat Immunol *9*, 1341–1346.

Ventura, A., Young, A.G., Winslow, M.M., Lintault, L., Meissner, A., Erkeland, S.J., Newman, J., Bronson, R.T., Crowley, D., Stone, J.R., et al. (2008). Targeted deletion reveals essential and overlapping functions of the miR-17 through 92 family of miRNA clusters. Cell *132*, 875–886.

Vivien, L., Benoist, C., and Mathis, D. (2001). T lymphocytes need IL-7 but not IL-4 or IL-6 to survive in vivo. International Immunology *13*, 763–768.

Wang, Y., Medvid, R., Melton, C., Jaenisch, R., and Blelloch, R. (2007). DGCR8 is essential for microRNA biogenesis and silencing of embryonic stem cell self-renewal. Nat Genet *39*, 380–385.

Wei, G., Wei, L., Zhu, J., Zang, C., Hu-Li, J., Yao, Z., Cui, K., Kanno, Y., Roh, T.-Y., Watford, W.T., et al. (2009). Global mapping of H3K4me3 and H3K27me3 reveals specificity and plasticity in lineage fate determination of differentiating CD4+ T cells. Immunity *30*, 155–167.

Wei, L., Laurence, A., Elias, K.M., and O'Shea, J.J. (2007). IL-21 is produced by Th17 cells and drives IL-17 production in a STAT3-dependent manner. J Biol Chem *282*, 34605–34610.

Wierenga, E.A., Snoek, M., de Groot, C., Chrétien, I., Bos, J.D., Jansen, H.M., and Kapsenberg, M.L. (1990). Evidence for compartmentalization of functional subsets of CD2+ T lymphocytes in atopic patients. J Immunol *144*, 4651–4656.

Wightman, B., Burglin, T.R., Gatto, J., Arasu, P., and Ruvkun, G. (1991). Negative regulatory sequences in the lin-14 3'-untranslated region are necessary to generate a temporal switch during Caenorhabditis elegans development. Genes Dev *5*, 1813–1824.

Wightman, B., Ha, I., and Ruvkun, G. (1993). Posttranscriptional regulation of the heterochronic gene lin-14 by lin-4 mediates temporal pattern formation in C. elegans. Cell *75*, 855–862.

Willenborg, D.O., Fordham, S., Bernard, C.C., Cowden, W.B., and Ramshaw, I.A. (1996). IFN-gamma plays a critical down-regulatory role in the induction and effector phase of myelin oligodendrocyte glycoprotein-induced autoimmune encephalomyelitis. J Immunol *157*, 3223–3227.

Wilson, N.J., Boniface, K., Chan, J.R., Mckenzie, B.S., Blumenschein, W.M., Mattson, J.D., Basham, B., Smith, K., Chen, T., Morel, F., et al. (2007). Development, cytokine profile and function of human interleukin 17–producing helper T cells. Nat Immunol *8*, 950–957.

Wofford, J.A., Wieman, H.L., Jacobs, S.R., Zhao, Y., and Rathmell, J.C. (2008). IL-7 promotes Glut1 trafficking and glucose uptake via STAT5-mediated activation of Akt to support T-cell survival. Blood *111*, 2101–2111.

Wu, H., Ye, C., Ramirez, D., and Manjunath, N. (2009). Alternative processing of primary microRNA transcripts by Drosha generates 5' end variation of mature microRNA. PLoS ONE *4*, e7566.

Wu, L., Fan, J., and Belasco, J.G. (2006). MicroRNAs direct rapid deadenylation of mRNA. Proc Natl Acad Sci USA *103*, 4034–4039.

Xiao, C., Srinivasan, L., Calado, D.P., Patterson, H.C., Zhang, B., Wang, J., Henderson, J.M., Kutok, J.L., and Rajewsky, K. (2008a). Lymphoproliferative disease and autoimmunity in mice with increased miR-17-92 expression in lymphocytes. Nat Immunol *9*, 405–414.

Xiao, S., Jin, H., Korn, T., Liu, S.M., Oukka, M., Lim, B., and Kuchroo, V.K. (2008b). Retinoic acid increases Foxp3+ regulatory T cells and inhibits development of Th17 cells by enhancing TGF-beta-driven Smad3 signaling and inhibiting IL-6 and IL-23 receptor expression. The Journal of Immunology *181*, 2277–2284.

Xu, L., Kitani, A., Fuss, I., and Strober, W. (2007). Cutting edge: regulatory T cells induce CD4+CD25-Foxp3- T cells or are self-induced to become Th17 cells in the absence of exogenous TGF-beta. J Immunol *178*, 6725–6729.

Yamamura, M., Uyemura, K., Deans, R.J., Weinberg, K., Rea, T.H., Bloom, B.R., and Modlin, R.L. (1991). Defining protective responses to pathogens: cytokine profiles in leprosy lesions. Science *254*, 277–279.

Yamane, H., Zhu, J., and Paul, W.E. (2005). Independent roles for IL-2 and GATA-3 in stimulating naive CD4+ T cells to generate a Th2-inducing cytokine environment. J Exp Med *202*, 793–804.

Yang, J.-S., Phillips, M.D., Betel, D., Mu, P., Ventura, A., Siepel, A.C., Chen, K.C., and Lai, E.C. (2011). Widespread regulatory activity of vertebrate microRNA* species. Rna *17*, 312–326.

Yang, W., Chendrimada, T.P., Wang, Q., Higuchi, M., Seeburg, P.H., Shiekhattar, R., and Nishikura, K. (2006). Modulation of microRNA processing and expression through RNA editing by ADAR deaminases. Nat Struct Mol Biol *13*, 13–21.

Yang, X.O., Angkasekwinai, P., Zhu, J., Peng, J., Liu, Z., Nurieva, R., Liu, X., Chung, Y., Chang, S.H., Sun, B., et al. (2009). Requirement for the basic helix-loop-helix transcription factor Dec2 in initial TH2 lineage commitment. Nat Immunol *10*, 1260–1266.

Yang, X.O., Nurieva, R., Martinez, G.J., Kang, H.S., Chung, Y., Pappu, B.P., Shah, B., Chang, S.H., Schluns, K.S., Watowich, S.S., et al. (2008a). Molecular antagonism and plasticity of regulatory and inflammatory T cell programs. Immunity *29*, 44–56.

Yang, X.O., Panopoulos, A.D., Nurieva, R., Chang, S.H., Wang, D., Watowich, S.S., and Dong, C. (2007a). STAT3 regulates cytokine-mediated generation of inflammatory helper T cells. J Biol Chem *282*, 9358–9363.

Yang, X.O., Pappu, B.P., Nurieva, R., Akimzhanov, A., Kang, H.S., Chung, Y., Ma, L., Shah, B., Panopoulos, A.D., Schluns, K.S., et al. (2008b). T helper 17 lineage differentiation is programmed by orphan nuclear receptors ROR alpha and ROR gamma. Immunity *28*, 29–39.

Yang, Y., Ochando, J.C., Bromberg, J.S., and Ding, Y. (2007b). Identification of a distant T-bet enhancer responsive to IL-12/Stat4 and IFNgamma/Stat1 signals. Blood *110*, 2494–2500.

Yao, Z., Fanslow, W.C., Seldin, M.F., Rousseau, A.M., Painter, S.L., Comeau, M.R., Cohen, J.I., and Spriggs, M.K. (1995). Herpesvirus Saimiri encodes a new cytokine, IL-17, which binds to a novel cytokine receptor. Immunity *3*, 811–821.

Yao, Z., Kanno, Y., Kerenyi, M., Stephens, G., Durant, L., Watford, W.T., Laurence, A., Robinson, G.W., Shevach, E.M., Moriggl, R., et al. (2007). Nonredundant roles for Stat5a/b in directly regulating Foxp3. Blood *109*, 4368–4375.

Yi, R., Doehle, B.P., Qin, Y., Macara, I.G., and Cullen, B.R. (2005). Overexpression of exportin 5 enhances RNA interference mediated by short hairpin RNAs and microRNAs. Rna *11*, 220–226.

Yu, D., Rao, S., Tsai, L.M., Lee, S.K., He, Y., Sutcliffe, E.L., Srivastava, M., Linterman, M., Zheng, L., Simpson, N., et al. (2009a). The transcriptional repressor Bcl-6 directs T follicular helper cell lineage commitment. Immunity *31*, 457–468.

Yu, Q., Sharma, A., Oh, S.Y., Moon, H.-G., Hossain, M.Z., Salay, T.M., Leeds, K.E., Du, H., Wu, B., Waterman, M.L., et al. (2009b). T cell factor 1 initiates the T helper type 2 fate by inducing the transcription factor GATA-3 and repressing interferon-gamma. Nat Immunol *10*, 992–999.

Yücel, R., Karsunky, H., Klein-Hitpass, L., and Möröy, T. (2003). The transcriptional repressor Gfi1 affects development of early, uncommitted c-Kit+ T cell progenitors and CD4/CD8 lineage decision in the thymus. J Exp Med *197*, 831–844.

Zaretsky, A.G., Taylor, J.J., King, I.L., Marshall, F.A., Mohrs, M., and Pearce, E.J. (2009). T follicular helper cells differentiate from Th2 cells in response to helminth antigens. Journal of Experimental Medicine *206*, 991–999.

Zhang, D.H., Cohn, L., Ray, P., Bottomly, K., and Ray, A. (1997). Transcription factor GATA-3 is differentially expressed in murine Th1 and Th2 cells and controls Th2-specific expression of the interleukin-5 gene. J Biol Chem *272*, 21597–21603.

Zhang, F., Meng, G., and Strober, W. (2008). Interactions among the transcription factors Runx1, RORgammat and Foxp3 regulate the differentiation of interleukin 17-producing T cells. Nat Immunol *9*, 1297–1306.

Zhang, Z., Swindle, C.S., Bates, J.T., Ko, R., Cotta, C.V., and Klug, C.A. (2007). Expression of a non-DNA-binding isoform of Helios induces T-cell lymphoma in mice. Blood *109*, 2190–2197.

Zhao, D.-M., Thornton, A.M., DiPaolo, R.J., and Shevach, E.M. (2006). Activated CD4+CD25+ T cells selectively kill B lymphocytes. Blood *107*, 3925–3932.

Zheng, S.G., Gray, J.D., Ohtsuka, K., Yamagiwa, S., and Horwitz, D.A. (2002). Generation ex vivo of TGF-beta-producing regulatory T cells from CD4+CD25- precursors. J Immunol *169*, 4183–4189.

Zheng, S.G., Wang, J., Wang, P., Gray, J.D., and Horwitz, D.A. (2007a). IL-2 is essential for TGF-beta to convert naive CD4+CD25- cells to CD25+Foxp3+ regulatory T cells and for expansion of these cells. J Immunol *178*, 2018–2027.

Zheng, W., and Flavell, R.A. (1997). The transcription factor GATA-3 is necessary and sufficient for Th2 cytokine gene expression in CD4 T cells. Cell *89*, 587–596.

Zheng, Y., Josefowicz, S.Z., Kas, A., Chu, T.-T., Gavin, M.A., and Rudensky, A.Y. (2007b). Genome-wide analysis of Foxp3 target genes in developing and mature regulatory T cells. Nature *445*, 936–940.

Zhou, L., Ivanov, I.I., Spolski, R., Min, R., Shenderov, K., Egawa, T., Levy, D.E., Leonard, W.J., and Littman, D.R. (2007). IL-6 programs T(H)-17 cell differentiation by promoting sequential engagement of the IL-21 and IL-23 pathways. Nat Immunol *8*, 967–974.

Zhu, J., and Paul, W.E. (2010). Peripheral CD4+ T-cell differentiation regulated by networks of cytokines and transcription factors. Immunol Rev *238*, 247–262.

Zhu, J., Cote-Sierra, J., Guo, L., and Paul, W.E. (2003). Stat5 activation plays a critical role in Th2 differentiation. Immunity *19*, 739–748.

Zhu, J., Guo, L., Min, B., Watson, C.J., Hu-Li, J., Young, H.A., Tsichlis, P.N., and Paul, W.E. (2002). Growth factor independent-1 induced by IL-4 regulates Th2 cell proliferation. Immunity *16*, 733–744.

Ørom, U.A., Nielsen, F.C., and Lund, A.H. (2008). MicroRNA-10a binds the 5'UTR of ribosomal protein mRNAs and enhances their translation. Mol Cell *30*, 460–471.

9. Appendices

9.1. Appendix A – Code used for the analysis of microarray data

9.1.1. miRNA microarrays

```
library(limma)
library(vsn)
library(Biobase)
library(RColorBrewer)
library(gplots)

> sessionInfo()
R version 2.12.1 (2010-12-16)
Platform: x86_64-apple-darwin9.8.0/x86_64 (64-bit)

locale:
[1] en_GB.UTF-8/en_GB.UTF-8/C/C/en_GB.UTF-8/en_GB.UTF-8

attached base packages:
[1] grid      stats     graphics  grDevices utils     datasets
methods   base

other attached packages:
 [1] gplots_2.10.1      KernSmooth_2.23-4  caTools_1.12
bitops_1.0-4.1     gdata_2.8.0
 [6] gtools_2.6.2       RColorBrewer_1.0-2 vsn_3.18.0
Biobase_2.10.0     limma_3.6.9

loaded via a namespace (and not attached):
[1] affy_1.28.0           affyio_1.18.0         lattice_0.19-17
preprocessCore_1.12.0
>

# Created a tab-delim text file with description of the arrays

targets<-readTargets("targets.txt")

# This defines the column name of the mean Cy5 foreground intensities

Cy5 <- "F635 Mean"

# This defines the column name of the mean Cy5 background intensities

Cy5b <- "B635 Mean"

# Read in GPR files, as a 2 colour array but set both colours the same,
and filter bad spots

RG <- read.maimages(targets$FileName,
      source="genepix",
      columns=list(R=Cy5,G=Cy5,Rb=Cy5b,Gb=Cy5b),
```

```
      annotation = c("Block", "Column", "Row","Flags", "ID", "Name",
"Status"),
      wt.fun=wtflags(weight=0,cutoff=-50)
      )

# Read the .gal file (description of the chip)

RG$genes<-readGAL("cepheid_G4_170310_v1.gal")

# Read in the spot types description (for controls, missing, genes
etc.)

spottypes<-readSpotTypes("spottypes.txt")

# remove the extraneous red channel values
RG$G <- NULL
RG$Gb <- NULL

# Then pull out all the spot type flags that have been assigned in any
arrays
RG$printer <- getLayout(RG$genes)
RG$genes$Status<-controlStatus(spottypes,RG)

row.names(RG$targets) <- targets$KARepName

# Then find all unique spot type identifiers
status <-unique(RG$genes$Status)

#Spatial heterogeneity on individual arrays can be highlighted by
examining imageplots of the background intensities. If the plots
suggest that some arrays are of lesser quality than others, it may be
useful to estimate array quality weights to be used in the linear
model analysis.
imageplot(log2(RG$Rb[,2]), RG$printer, low="white", high="red")

# Can define a function to do this for all chips on one page

chipplots<- function(RG) {
par(col=colors()[8], mfrow=c(5,4))
numcols = length(colnames(RG))
for (i in 1:numcols) {
plotname<-row.names(RG$targets[i,])
imageplot(log2(RG$Rb[,i]), RG$printer, low="white",
high="red",legend=F,main=c(row.names(RG$targets))[i])
}
}

chipplots(RG)



# Then want to get rid of everything except "gene" and "control" for
the purpose of normalisation
# In R, weights are assigned as 0 if unreliable and therefore should
be ignored or 1 if of normal quality
# Make a new data frame that has this updated weight info in it

w<-modifyWeights(RG$weights,RG$genes$Status,
values=c("qc","empty","removed","negctrl","not_spotted" ),multipliers=
0)
```

```
# Set up a colour palette

cols <- brewer.pal(10, "Set3")

# Make the colour palette so that duplicate samples show up in the
same colour
cols <- rep(cols,each=2)

# Can do box plots of Foreground and Background intensities, useful
for QC

par(mfrow=c(2,1),col=cols, mar=c(6,4,4,2))
boxplot(data.frame(log2(RG$Rb)),main="Background",col=cols,las=2,names
=row.names(RG$targets))
boxplot(data.frame(log2(RG$R)),main="Foreground",col=cols,las=2,names=
row.names(RG$targets))



# Can do box plots of Positive Controls, Negative Controls,
Specificity Controls and all genes (pre-BG correction)

par(mfrow=c(4,1),col=cols, mar=c(6,4,4,2))
boxplot(log2(RG$R[RG$genes$Status=="control",]),range=0,ylab="log2
intensities", main="Positive
Controls",col=cols,names=row.names(RG$targets),las=2)
boxplot(log2(RG$R[RG$genes$Status=="negctrl",]),range=0,ylab="log2
intensities", main="Negative
Controls",col=cols,names=row.names(RG$targets),las=2)
boxplot(log2(RG$R[RG$genes$Status=="qc",]),range=0,ylab="log2
intensities", main="Specificity
Controls",col=cols,names=row.names(RG$targets),las=2)
boxplot(log2(RG$R[RG$genes$Status=="gene",]),range=0,ylab="log2
intensities", main="Genes",col=cols,names=row.names(RG$targets),las=2)


# Then want to background correct

RGcorrected<-backgroundCorrect(RG$R,method="normexp", offset=50)

# Make a duplicate "RGList" class object that contains the BG
corrected values

RGcorrect <- RG
RGcorrect$R<-RGcorrected



# Can do box plots for both pre and post-background correction

cols <- brewer.pal(10, "Set3")
cols <- rep(cols,each=2)

par(mfrow=c(2,1),col="black")
boxplot(log2(RG$R[RG$genes$Status=="gene",]),range=0,ylab="log2
intensities", main="Genes",col=cols,names=row.names(RG$targets),las=2)
```

```
boxplot(log2(RGcorrect$R[RGcorrect$genes$Status=="gene",]),range=0,yla
b="log2 intensities", main="Genes After Background
Subtraction",col=cols,names=row.names(RG$targets),las=2)

# Create an array to identify just the gene (i.e. exclude the
controls)

idx = (RG$genes$Status == "gene")

# Retrieve just the genes (i.e. remove the controls)

RG.final <- RG[idx, ]
RGcorrect.final <- RGcorrect[idx, ]

# Change the column names to the ones I want

colnames(RG.final$R) <- targets$KARepName
colnames(RGcorrect.final$R) <- targets$KARepName

# Do the VSN normalisation.

mat.vsn <- vsnMatrix(RG.final$R)
matcorrect.vsn <- vsnMatrix(RGcorrect.final$R)

# Can look at the SDplot for this

meanSdPlot(mat.vsn)
meanSdPlot(matcorrect.vsn)

# Can compare with the SDplot for pre-normalisation (note requires log
data)

meanSdPlot(log(RGcorrect.final$R,2))

# view a boxplot of the normalized data
par(mfrow=c(3,1),col="black", mar=c(6,4,4,2))
boxplot(log2(RG$R[RG$genes$Status=="gene",]),range=0,ylab="log2
intensities", main="Genes",col=cols,names=row.names(RG$targets),las=2)
boxplot(log2(RGcorrect$R[RGcorrect$genes$Status=="gene",]),range=0,yla
b="log2 intensities", main="Genes After Background
Subtraction",col=cols,names=row.names(RG$targets),las=2)
boxplot(as.data.frame(mat.vsn@hx),range=0,ylab="log2 intensities",
main="Normalized",col=cols,names=row.names(RG$targets),las=2)


# Can view a box plot of normalised data both with and without BG
correction

par(mfrow=c(2,1),col="black", mar=c(6,4,4,2))
boxplot(as.data.frame(mat.vsn@hx),range=0,ylab="log2 intensities",
main="Normalized only",col=cols,names=row.names(RG$targets),las=2)
boxplot(as.data.frame(matcorrect.vsn@hx),range=0,ylab="log2
intensities", main="Normalized and Background
Corrected",col=cols,names=row.names(RG$targets),las=2)


# Can view a box plot of pre- vs post-normalisation

par(mfrow=c(2,1),col="black", mar=c(6,4,4,2))
```

```
boxplot(log2(RGcorrect$R[RGcorrect$genes$Status=="gene",]),range=0,yla
b="log2 intensities", main="Genes After Background
Subtraction",col=cols,names=row.names(RG$targets),las=2)
boxplot(as.data.frame(matcorrect.vsn@hx),range=0,ylab="log2
intensities", main="Normalized and Background
Corrected",col=cols,names=row.names(RG$targets),las=2)

#Assign mirbase names to M5 genes. Candidates do not have a mirname.
It could be that some candidates do have a mirbase name now but i
would need to recheck all oligos. Let me know if you want to update
that as well.
#That should include mirnames when available
oligo2mir =
read.table(file="OLIGOS_MIR_CORRESPONDANCE.txt",sep="\t",header=T,as.i
s=F)
df2 = data.frame(RG.final$gene$Name)
names(df2) = "oligo"
dat = merge(df2,oligo2mir,by="oligo",sort=F,all.y=F)

rownames(mat.vsn@hx) <- dat$mir
rownames(matcorrect.vsn@hx) <- dat$mir

# Want to unwrap the row names correctly as well

namesMatrix <- unwrapdups(rownames(mat.vsn@hx), ndups=2, spacing=1)
namesMatrixcorrect <- unwrapdups(rownames(matcorrect.vsn@hx), ndups=2,
spacing=1)


# Then do the unwrapping of the array data
matrix <- unwrapdups(mat.vsn, ndups=2, spacing=1)
matrixcorrect <- unwrapdups(matcorrect.vsn, ndups=2, spacing=1)

# Then rename the rows and columns to miRNAs and arrays respectively
rownames(matrix) <- namesMatrix[,1]
rownames(matrixcorrect) <- namesMatrixcorrect[,1]
colnames(matrix) <- duplicateCols(mat.vsn@hx)
colnames(matrixcorrect) <- duplicateCols(matcorrect.vsn@hx)

# Need to unlog data before taking the mean
unlogmatrix<-2^matrix
unlogmatrixcorrect<-2^matrixcorrect


# Then want to take the mean of the technical replicates

meanmatrix<-
t(aggregate(t(unlogmatrix),list(colnames(unlogmatrix)),mean))
meanmatrixcorrect<-
t(aggregate(t(unlogmatrixcorrect),list(colnames(unlogmatrixcorrect)),m
ean))

# Best to tidy up this as it has put the colnames in row 1 and all the
values are character vectors rather than numeric
# Write the names to the column name slot
colnames(meanmatrix)<-meanmatrix[1,]
colnames(meanmatrixcorrect)<-meanmatrixcorrect[1,]

# Remove the first row
meanmatrix<-meanmatrix[-1,]
```

```
meanmatrixcorrect<-meanmatrixcorrect[-1,]

# Convert the whole thing from character matrix to numeric
class(meanmatrix)<-"numeric"
class(meanmatrixcorrect)<-"numeric"

# Then relog the whole thing
meanmatrix<-log(meanmatrix, base=2)
meanmatrixcorrect<-log(meanmatrixcorrect, base=2)

# Then can save this

write.table(meanmatrix, file="KA-Entire-miRarraySetB-NoBGcorrect-
V4.csv")
write.table(meanmatrixcorrect, file="KA-Entire-miRarraySetB-
YesBGcorrect-V4.csv")

# Dot plot correlations - to do it for all arrays in a matrix

par(col="black")
point.panel <- function(x, y, pch, cex.point=1.5){
points(x, y, pch=pch, cex=cex.point, col="black")
abline(a=0,b=1, col="blue")
# lines(lowess(y~x), col = "white")

}

panel.cor.pearson <- function(x, y, digits=2, prefix="r=",
cex.cor=2, ...){
usr <- par("usr"); on.exit(par(usr))
par(usr = c(0, 1, 0, 1))
r <- (cor(x, y, method="pearson", use="pairwise.complete.obs"))
txt <- format(c(r, 0.123456789), digits=digits)[1]
t.value <- cor.test(x, y, method="pearson")$statistic
text(0.5, 0.5, txt, cex =2, font=2)
}

pairs(meanmatrix[,c(1:2)], lower.panel=panel.cor.pearson,

upper.panel=point.panel, cex=1.2, pch="." )

pairs(meanmatrixcorrect[,c(1:10)], lower.panel=panel.cor.pearson,

upper.panel=point.panel, cex=1.2, pch="." )

# Dot plot correlations - to do it for a pair of arrays at a time

pairplotKA<-function(plotmatrix,col1,col2,digits=2){
par(mfrow=c(1,1), mar=c(6,4,4,2))
plot(plotmatrix[,col1],plotmatrix[,col1], type="n",
xlab=colnames(plotmatrix)[col1], ylab=colnames(plotmatrix)[col2])
points(plotmatrix[,col1], plotmatrix[,col2], pch="°", cex=1.5,
col="black")
abline(a=0, b=1, col="blue")
usr <- par("usr"); on.exit(par(usr))

par(usr = c(0, 1, 0, 1))
r <- (cor(plotmatrix[,col1], plotmatrix[,col2], method="pearson",
use="pairwise.complete.obs"))
```

```
txt <- paste("Correlation coefficient (Pearson) r = ",format(c(r,
0.123456789), digits=digits)[1],sep="")
text(0.1, 0.9, txt, cex =1, font=2, pos=4)
}

# PDFs are huge when saved from Quartz viewer so do it manually
pdf(file="ArraySetA-Th1-PearsonDotPlot.pdf")
pairplotKA(meanmatrix, 1, 2)
dev.off()

# A function to do it automatically but only works if there are always
EXACTLY 2 replicates per condition (otherwise gets out of order)
genpairwiseplots<-function(plotfrommatrix){
filenamesubs<-c(colnames(plotfrommatrix))
for (i in (1:10)) {
filename=paste("ArraySetA-",filenamesubs[i*2],"-
PearsonDotPlot.pdf",sep="")
pdf(file=filename)
pairplotKA(plotfrommatrix,(i*2)-1,(i*2))
dev.off()
}
}
genpairwiseplots(meanmatrix)

genpairwiseplots<-function(plotfrommatrix){
filenamesubs<-c(colnames(plotfrommatrix))
for (i in (1:10)) {
filename=paste("ArraySetA-",filenamesubs[i*2],"-YesBGcorrect-
PearsonDotPlot.pdf",sep="")
pdf(file=filename)
pairplotKA(plotfrommatrix,(i*2)-1,(i*2))
dev.off()
}
}
genpairwiseplots(meanmatrixcorrect)
```

9.1.2. Affymetrix microarrays

```
library(oligo)
library(pd.mogene.1.0.st.v1)
library(annaffy)
library(mogene10sttranscriptcluster.db)

> sessionInfo()
R version 2.12.1 (2010-12-16)
Platform: x86_64-apple-darwin9.8.0/x86_64 (64-bit)

locale:
[1] en_GB.UTF-8/en_GB.UTF-8/C/C/en_GB.UTF-8/en_GB.UTF-8

attached base packages:
[1] stats     graphics  grDevices utils     datasets  methods   base

other attached packages:
 [1] mogene10sttranscriptcluster.db_6.0.1 org.Mm.eg.db_2.4.6
 [3] annaffy_1.22.0                       KEGG.db_2.4.5
 [5] GO.db_2.4.5                          AnnotationDbi_1.12.0
```

```
 [7] pd.mogene.1.0.st.v1_3.0.2            RSQLite_0.9-4
 [9] DBI_0.2-5                            oligo_1.14.0
[11] oligoClasses_1.12.2                  Biobase_2.10.0

loaded via a namespace (and not attached):
[1] affxparser_1.22.1     affyio_1.18.0         Biostrings_2.18.4
IRanges_1.8.9
[5] preprocessCore_1.12.0 splines_2.12.1


# Read in and normalise the Affymetrix microarray data:

KAgeneFS<-read.celfiles(list.celfiles())
KAgeneCore <- rma(KAgeneFS, target="core")

# Can add some phenotyping data for the dot plots later on (note in
this case the order of the pData must match the order of data
(expression) columns

pd = read.AnnotatedDataFrame("KApData.txt", header = TRUE, row.names =
1)
pData(KAgeneCore)<-phenoData(pd)

# Can do the "ArrayQualityMetrics" analysis

arrayQualityMetrics(expressionset = KAgeneCore, outdir =
"ArrayQualityMetricsQC1", force = FALSE,  do.logtransform = FALSE)


# Annotate the array data and save it

KAprobeids<-featureNames(KAgeneCore)
KAanncols<-aaf.handler()[c(1:3,6)]
KAannTable<-aafTableAnn(KAprobeids, "mogene10sttranscriptcluster.db",
KAanncols)
KAexprTable<-aafTableInt(KAgeneCore, probeids=KAprobeids)
KAmergeTable<-merge(KAannTable, KAexprTable)

saveText(KAmergeTable, "KA-EntireArray.txt")
```

9.2. Appendix B – WT and T-bet$^{-/-}$ Affymetrix microarrays

9.2.1. Transcription factor expression in T helper cell subsets

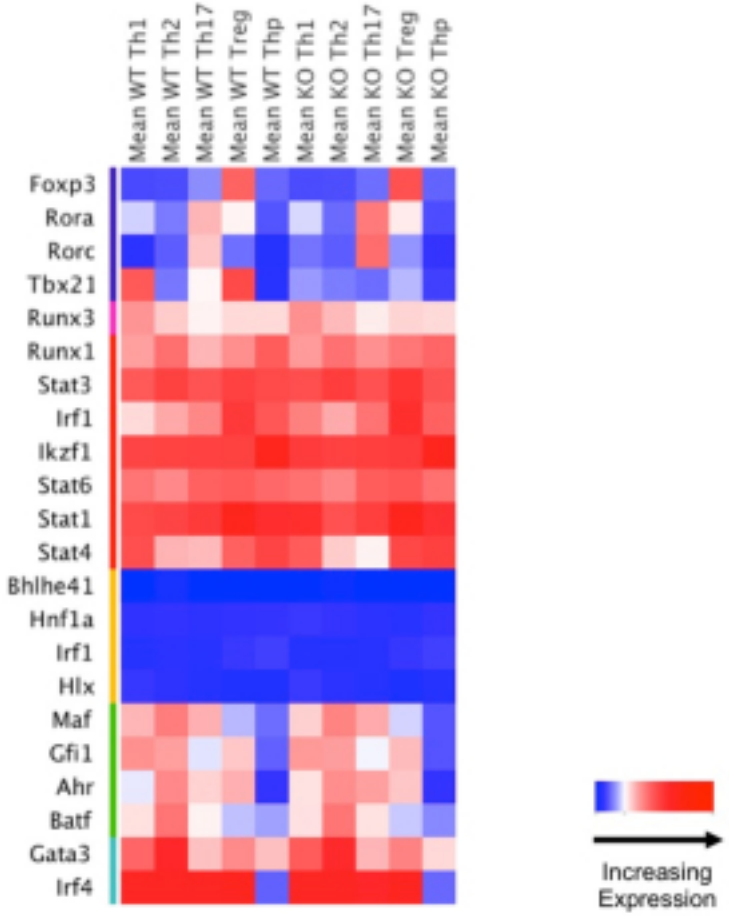

Heatmap showing expression of selected T cell-specific transcription factors (as identified in Chapter 1.2.2). Mean expression is shown for 2 biological replicates.

9.2.2. Cytokine expression in T helper cell subsets

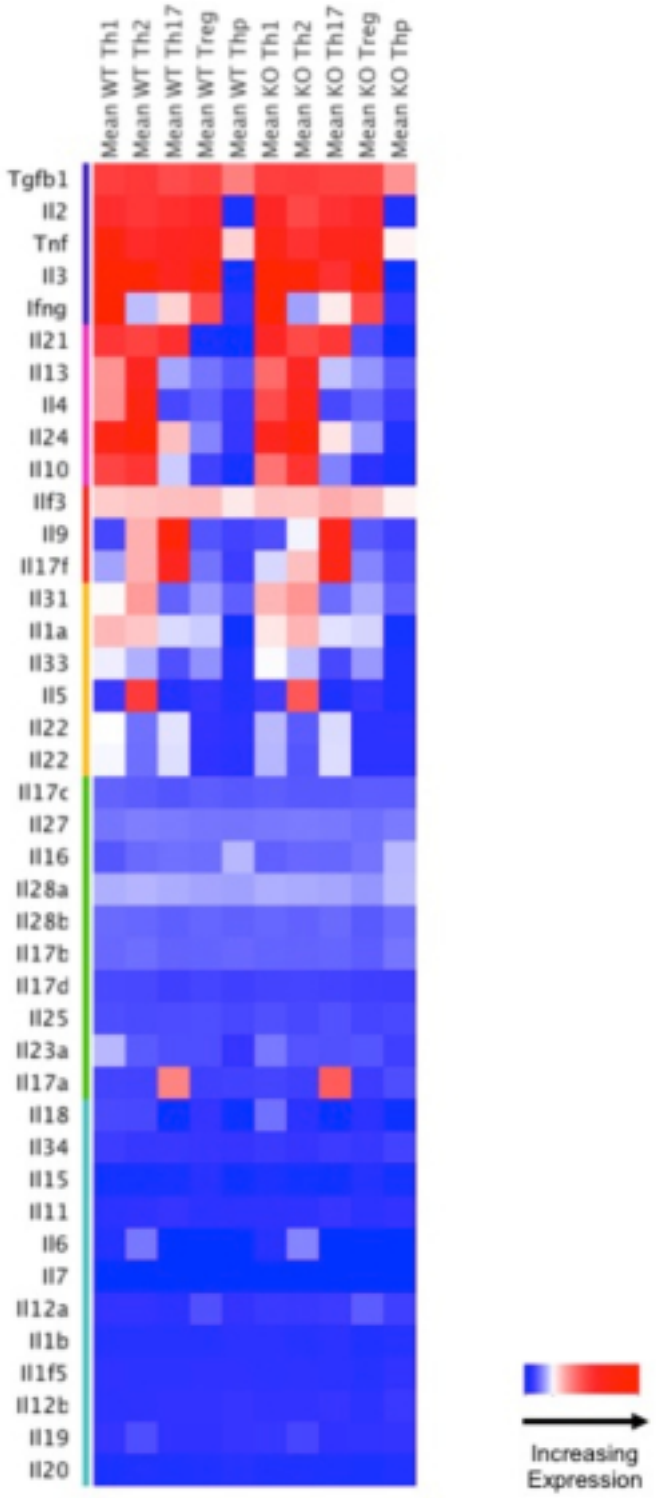

Heatmap showing expression of selected T cell-related cytokines (as identified in Chapter 1.2.2). Mean expression is shown for 2 biological replicates.

9.2.3. Chemokine and receptor expression in T helper cell subsets

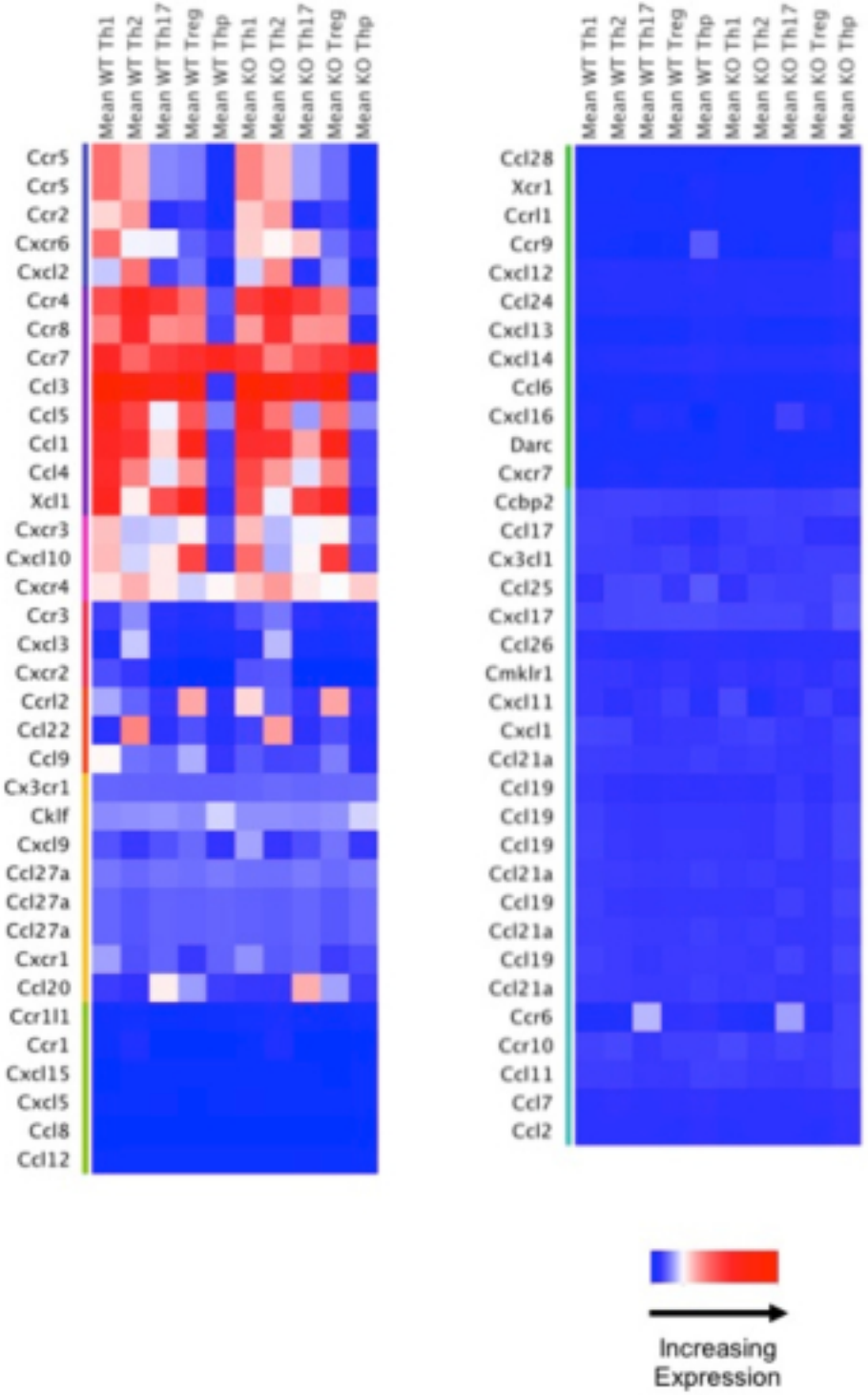

Heatmap showing expression of selected T cell-related chemokines and chemokine receptors. Mean expression is shown for 2 biological replicates.